UNIVERSITY OF CALIFORNIA
SANTA CRUZ

THE ROLE OF RIBOSOMAL SILENCING FACTOR S IN HELICOBACTER PYLORI GROWTH AND LONG-TERM INFECTIONS

A dissertation submitted in partial satisfaction
of the requirements for the degree of

DOCTOR OF PHILOSOPHY in MICROBIOLOGY AND ENVIRONMENTAL TOXICOLOGY

by Yasmine O. Elshenawi

December 2026

The Dissertation of Yasmine O. Elshenawi is approved:

_____
Professor Karen Ottemann, chair

_____
Professor Mee-Ngan Yap

_____
Professor Fitnat Yildiz

_____
Donald Smith
Interim Vice Provost and Dean of Graduate Studies

Contents

Chapter#1→ RsfS a widely conserved ribosomal interaction factor that plays a diverse role in bacterial physiology

Abstract

Ribosomes are essential macromolecules that convert mRNA to polypeptides and functional proteins. Ribosomes can be regulated by multiple mechanisms, including limiting the biogenesis of ribosomal subunits, sequestering 70S ribosomes, dimerizing 70S complexes into translationally inactive 100S ribosome, and "silencing" the 50S subunit to prevent the assembly of active 70S ribosomes. In this review, we focus on the protein that carries out ribosomal silencing, called ribosomal silencing factor S (RsfS), that has been shown in multiple species to bind to the L14 ribosomal protein in the 50S subunit and prevent 50S-to-30S subunit joining. RsfS is a highly conserved small protein found across most bacterial species and in eukaryotes. The direct target of RsfS, L14 (RplN), is one of the most conserved ribosomal proteins. RsfS has been primarily studied for binding interactions with L14 and the downstream effects of preventing 70S ribosome assembly. *rsfS* null mutants exhibit defects in *in vitro* (stationary phase, biofilm, growth, nutrient limitation, oxidative stress) and *in vivo* (macrophage and murine models) conditions in several bacterial species. However, other topics remain underexplored, highlighting areas for future study such as regulation of RsfS and L14 expression, what factors dictate ribosomal interactions, roles in antibiotic tolerance, and whether RsfS has additional physiological roles.

Introduction

Ribosomes are essential macromolecular machine that carry out translation to synthesize the proteins necessary for all aspects of cell function (Bowman et al., 2020; Korostelev, 2011; Moore & Carr, 2022). Ribosomes are the most abundant macromolecules in a cell (Zegarra et al., 2023), and as such represent enormous production cost (Shore & Albert, 2022). Ribosome biogenesis accounts for up to 40% of the total energy needs (Nierhaus, 1991) and ribosomal RNA accounts for approximately 80-90% total RNA in the cell (Johnson et al., 1977). Translation initiation is a key regulatory step (Laursen et al., 2005), with some studies suggesting this step is the rate limiting one in protein synthesis (Gualerzi & Pon, 2015). Ribosome regulation is therefore necessary for the cell to appropriately managed energy conservation. Bacteria have evolved many mechanisms that are believed to preserve existing ribosome populations by placing them in an inactive state. In this review we focus on one such ribosome regulatory protein called ribosomal silencing factor S or A (RsfS or RsfA). We begin with an overview of canonical translation and current understanding of known ribosome regulation mechanisms, before detailing what are the latest developments in RsfS research.

Overview of the Translation Process

The bacterial ribosome is composed of two asymmetrical subunits constituted of protein and ribosomal RNA (rRNA) : the large 50S subunit (referred to as the Large Ribosomal Subunit or LSU) and the small 30S subunit (SSU) (J. R.

Williamson, 2008). These two subunits come together to create the 70S ribosome, which carries out translation in four basic steps: initiation, elongation, termination, and recycling. Canonical ribosome translation has been detailed in several excellent reviews and is just briefly described here (Rodnina, 2018; Samatova et al., 2021; Schmeing & Ramakrishnan, 2009; Tollerson & Ibba, 2020).

Initiation is the first step of active translation. At the start of this step, the 30S subunit associates with Initiation Factor 1 (IF1) and Initiation Factor 3 (IF3) (Nakamoto et al., 2021). These steps allows a component of the 30S subunit, the 16S rRNA, to bind to a complementary region on the mRNA called the Shine-Dalgarno sequence (Tsai et al., 2012). After this event, Initiation Factor 2 (IF-2) recruits an initiator tRNA to the 30S subunit-mRNA complex, and then the 50S subunit associates with the complex to form the 70S ribosome that is ready for the next step of elongation (Milon et al., 2010). During elongation, mRNA is decoded into polypeptides. Elongation occurs via a repeated cycle of three steps: (1) aminoacyl-tRNA binding, (2) transpeptidation and (3) translocation (Agafonov et al., 2001). Once the stop codon enters the A site in the ribosome, the next step of termination starts. Class I release factors (release factor RF1, RF2 and RF3) coordinate peptidyl-tRNA hydrolysis, the ribosome undergoes a conformational change, and releases the newly synthesized polypeptide (Korostelev, 2011; Laurberg et al., 2008). The final step of the translation cycle is recycling. After termination, mRNA and de-acetylated tRNA are freed from the complex as free 50S and 30S subunits by ribosome recycling factor (RRF) and elongation factor-G (EF-G) (Kiel et al., 2003). RRF is similar to

tRNA structurally and is essential for EF-G to allow the dissociation of the ~~70S~~ post-termination 70S ribosome back to 30S and 50S (Zhou et al., 2020). EF-G first hydrolyzes GTP when interacting with a post-termination ribosome which is then followed by RRF binding (Borg et al., 2016; Gao et al., 2007). Inter-subunit bridges that occur between 30S and 50S are disrupted during this stage upon RRF binding (Gao et al., 2005). After dissolution of the 70S, IF3 binds to the 30S subunit to release tRNA and mRNA so it is ready for initiation again (Zavialov et al., 2005).

Overview of Ribosome Regulation and the concept of Ribosomal Dormancy

It has long been recognized that bacterial cells regulate their ribosome amounts and profile to adapt to different growth conditions (Byrgazov et al., 2013; Starosta et al., 2014). Bacteria can regulate the synthesis of ribosomal proteins and ribosomal RNA (rRNA), which in turn regulates the amount of each subunit as well as total assembled ribosomes (Pontes et al., 2016). Post- ribosome biogenesis, bacteria have two general ways to regulate translation. The first is by inducing ribosome hibernation by the 70S sequestration or dimerization of 70S ribosomes into 100S dimers (L. I. Chan et al., 2025; Helena-Bueno, Chan, et al., 2024a; Karari Njenga & Koch, 2026; Koli & Shetty, 2024; Prossliner et al., 2018). The second is by ribosome silencing, in which formation of the 70S ribosome is inhibited by blocking proteins required for 70S assembly (Fatkhullin et al., 2022). Ribosome dimerization and silencing both inhibit canonical translation so the ribosomes can be activated at another time without the re-synthesis of the subunits. This form of regulation has been referred to as dormancy, because the ribosomes exist but are in a non-active

state (Koli & Shetty, 2024). Indeed, studies have suggested that a majority of the ribosome population in some growth conditions, e.g. stationary phase, are dormant and not translationally active (Gefen et al., 2014).

Ribosome Hibernation was the first type of ribosomal dormancy discovered

The first discovery of a form of ribosomal dormancy was the finding that ribosomes could "hibernate" by forming dimers that were translationally inactive. In 1958, *E. coli* lysates were observed to contain ribosomes in both the expected 70S size plus an additional 100S size (Tissieres, 1958). Sucrose sedimentation gradients and chemical analysis confirmed that these 100S particles were composed of two conjoined or dimerized 70S ribosomes. Later research led to the discovery that 100S ribosomes were translationally inactive, but could revert to active 70S ribosomes that were able to synthesize proteins (Gunsalus et al., 1959). Subsequent work identified proteins that facilitated the 70S-to-100S dimerization or direct 70S inactivation, termed ribosome hibernation factors (Table 1). During 70S dimerization, the 30S subunits of the two 70S ribosomes interact with each other via hibernation factors and ribosomal proteins, such as S2, S3 or S4 proteins to form 100S dimers (Kato et al., 2010; Matzov et al., 2019). Many of these hibernation factors were required for survival in stationary phase (Rowe & Summers, 1999; Wada, 1998; Wada et al., 1990; Yamagishi et al., 1993). The formation of 100S ribosome dimers was reported in both model and clinical *E. coli* strains, supporting that hibernation might be widespread (Wada et al., 2000). Studies have suggest that a majority of the ribosome population in stationary phase cultures are not translationally active due to ribosome

hibernation (Reier et al., 2023). Aside from importance in stationary phase (Karari Njenga & Koch, 2026), ribosome dimerization has been found to promote survival when exposed to antibiotic stress (McKay & Portnoy, 2015; Schmid et al., 2026; K. S. Williamson et al., 2012), during host colonization (Basu et al., 2018; Kline et al., 2015; Schmid et al., 2026) and for biofilm formation (Akiyama et al., 2017; K. S. Williamson et al., 2012). This body of work thus established that the translation activity of 70S ribosomes could be suppressed by promoting ribosome dimers under particular conditions, and benefit bacteria in a variety of ways (Gohara & Yap, 2018; Helena-Bueno, Chan, et al., 2024a).

The conditions and proteins that dimerize 70S ribosomes and dissociate the resulting 100S dimers have been well studied in multiple bacterial species (L. I. Chan et al., 2025; Helena-Bueno, Chan, et al., 2024a; Koli & Shetty, 2024; Prossliner et al., 2018). Ribosome dimerization is regulated by stress cues such as ppGpp (Izutsu et al., 2001; Song & Wood, 2020) when bacterial cultures undergo challenging conditions such as stationary phase (Izutsu et al., 2001; Matzov et al., 2019; Yoshida & Wada, 2014). The 100S dimers can be reversed once bacterial cultures are transferred back to favorable conditions (Basu & Yap, 2017). Three types of proteins that promote hibernation have been identified, called ribosome modulation factor (RMF), hibernation-promoting factor (HPF) and ribosome associated inhibitor A (RaiA, or YfiA) (L. I. Chan et al., 2025; Gohara & Yap, 2018; Helena-Bueno, Chan, et al., 2024a; Karari Njenga & Koch, 2026; Koli & Shetty, 2024; Matzov et al., 2019; Prossliner et al., 2018; Yoshida & Wada, 2014; Zegarra et al., 2023). Each of these

proteins play different roles in 100S dimerization and 70S sequestration (L. I. Chan et al., 2025; Helena-Bueno, Chan, et al., 2024a; Koli & Shetty, 2024; Prossliner et al., 2018). RMF proteins induce conformational changes in the 30S subunit within the 70S assembled ribosome to facilitate the dimerization of two 70S ribosomes (Yoshida et al., 2021). *Staphylococcus aureus* HPF proteins facilitate the dimers between the CTD region of two assembled ribosomes to form 100S ribosome dimers (Khusainov et al., 2017; Matzov et al., 2017). RaiA/YfiA proteins share overlapping binding sites with HPF and thus occlude HPF from 70S ribosome dimerization (Polikanov et al., 2012; Puri et al., 2014). Homologues of these proteins are conserved in many bacterial species (L. I. Chan et al., 2025; Helena-Bueno, Chan, et al., 2024a; Koli & Shetty, 2024; Prossliner et al., 2018), and ribosome dimerization has been experimentally validated in *Pseudomonas aeruginosa* (Akiyama et al., 2017), *Lactococcus lactis* (Franken et al., 2017; Puri et al., 2014), *Listeria monocytogenes* (Kline et al., 2015), *Escherichia coli* (Maki & Yoshida, 2021), *Thermus thermophilus* (Flygaard et al., 2018; Polikanov et al., 2012; Ueta et al., 2013), *Legionella pneumophila* (Schmid et al., 2026), *Bacillus subtilis* (Beckert et al., 2017), *Staphylococcus aureus* (Basu & Yap, 2016; Khusainov et al., 2017; Matzov et al., 2017; Ueta et al., 2010) and *Vibrio cholerae* (De Bari & Berry, 2013). Species can have both RMF and HPF, or lack RMF and encode a long form of HPF (Matzov et al., 2019). These studies established that many types of bacteria create hibernating ribosomes (L. I. Chan et al., 2025), using a conserved set of protein factors (Table 1).

Three additional factors have been recently found to hibernate 70S ribosomes as an alternative to 100S dimerization: Balon factor (Helena-Bueno, Rybak, et al., 2024), actinobacteria-specific ribosome tunnel occlusion factor (RTOF) (Majumdar et al., 2024) and YgjD/ElaB/YgaM (Njenga et al., 2024) (Table 1). Balon Factor was found to be recruited by EF-Tu to bind to the A-site of a 70S assembled ribosomes in *Psychrobacter urativorans*, pausing polypeptide synthesis during stress (Helena-Bueno, Rybak, et al., 2024). RTOF has been found in *Mycobacterium tuberculosis* to bind to the nascent polypeptide exit tunnel and the peptidyl transferase center to hibernate 70S assembled ribosomes by inhibiting the binding of initiation tRNAs (Majumdar et al., 2024). C-terminal membrane associated proteins, YgjD/ElaB/YgaM, have been found in *E. coli* to bind to 50S subunit at the exit tunnel to hibernate 70S ribosomes (Njenga et al., 2024).

As mentioned above, early work showed that dimerized ribosomes can be converted back to the active, 70S form. This reaction was found to be carried out by either RRF/EF-G (Basu et al., 2020) or a universally conserved GTPase called HflX that binds to the peptidyl transferase center of 50S ribosome (Basu & Yap, 2017; Blombach et al., 2011; Caldon et al., 2001; Dey et al., 2018; Y. Zhang et al., 2015).

Ribosome dimers have been primarily studied in bacteria but have also been observed in eukaryotic cells, including microsporidian 100S dimers, and rRNA-driven 110S ribosomes in rat hippocampal neurons (W. Huang et al., 2018; Krokowski et al., 2011; McLaren et al., 2023; Schwarz et al., 2026). In addition, certain archaeal species can dimerize 30S subunits (Hassan et al., 2025) and 50S

subunits (Fordjour et al., 2025). Hibernation factors and ribosome dimers were initially thought to be limited to γ-proteobacteria (Ueta et al., 2008), although hibernation factors and ribosome dimers have been observed in Firmicutes species (*B. subtilis, S. aureus, L. lactis, L. monocytogenes*) (Boone et al., 2001) and a *Deinococcota* species (*T. thermophilus*) (Battista & Rainey, 2015). There is variety in the presence and activity of dimerization factors. Some groups, e.g. *Mycobacteria* and *Actinomycetota*, contain species that encode HPF homologues but do not form dimers (Hashim et al., 2026; Kumar et al., 2024; Mishra et al., 2018; Sawyer et al., 2021). while a majority of bacterial species contain ribosome hibernation factor homologues that facilitate 100S dimerization (L. I. Chan et al., 2025), other microbes, e.g. *Campylobacterota* species such as *Helicobacter pylori* contain no RMF-like and HPF-like homologues due to evolutionary loss (L. I. Chan et al., 2025) although whether they can produce ribosome dimers has not been experimentally validated. Overall, ribosome dimerization is widespread but not ubiquitous in bacteria.

Hibernation Factor	Role
HPF	N-terminus blocks the tRNA binding and mRNA channel while C-terminus interacts with another HPF-bound ribosome to facilitate 100S dimerization
RMF	Causes conformational changes when bound to the 30S subunit to facilitate formation of 90S, HPF binds and further stabilizes the 100S complex.
RaiA/YfiA	Binds to vacant 70S ribosome blocking aminoacyl-tRNA binding to prevent translation.
Balon	A factor recruited by EF-Tu to bind to the ribosomal A-site to induce 70S ribosome hibernation.
RTOF	Binds to the nascent polypeptide exit tunnel and peptidyl transferase center to prevent protein synthesis.

YqjD/ElaB/YgaM	Anchors ribosomes to the membranes and blocks the ribosomal exit tunnel

Table 1. Ribosome Hibernation Factors. Ribosome 100S dimerization can be facilitated (HPF/RMF), inhibited (RaiA/YfiA) and dissociated (HflX). Hibernation factors (Balon, RTOF, YqjD/ElaB/YgaM) can also hibernate 70S ribosomes alternative to forming 100S dimers.

Ribosomal silencing is a distinct form of ribosomal dormancy

Another form of ribosome regulation is silencing. In this reaction, ribosome subunits are prevented from assembling into the actively translating 70S form. This type of dormancy is conferred by proteins called Ribosomal Silencing Factors, either RsfA or RsfS. RsfS is the more common annotation in published bacterial genomes, so we will mostly use the RsfS abbreviation going forward. Genes encoding RsfS are highly conserved, with sequence analyses finding them in nearly all Bacteria and Eukarya species, but not in Archaea (Häuser et al., 2012). Ribosome silencing factor homologues are part of the Iojap protein family that was initially identified as a gene involved in maize chloroplast development (Han et al., 1992). In bacteria, ribosome silencing factor homologues were first thought to be associated with cell morphology as an *rsfA* mutant from an *E. coli* transposon pool exhibited loss of normal rod-shape, although this was later found to be due to polar effects (Bernhardt & De Boer, 2004; Häuser et al., 2012). Subsequent work identified *E. coli* RsfA interacting with a 50S subunit protein called L14 (Butland et al., 2005; Jiang et al., 2007). Crystallography and sucrose gradient analysis found that RsfS bound to the 50S subunit protein L14,

and this interaction prevented the 50S from associating with the 30S (Häuser et al., 2012; Khusainov et al., 2020; X. Li et al., 2016). The ability of RsfS to cause translation repression was additionally verified in *E. coli* using a β-galactosidase and oligo(Phe) translation assay (Häuser et al., 2012), and in *M. tuberculosis* using GFP translation (Li et al., 2016). Although ribosome silencing factors have been mainly studied in the context of ribosome dormancy, some evidence has indicated that they may potentially have a role in ribosome biogenesis (Fatkhullin et al., 2022). Phylogenetic analysis indicates that the distribution of RsfS homologs may be independent of the evolutionary loss of classical ribosome dimerization factors (L. I. Chan et al., 2025). RsfS homologues of species like *Helicobacter* that lack ribosome dimerization factors are closely related to RsfS homologues of their cousin *Campylobacter* (Figure 1), a species that does retain ribosome hibernation factors (L. I. Chan et al., 2025). For the rest of this review, we focus on ribosome silencing factor or RsfS, and its roles in bacterial biology.

Figure 1. RsfS homologues are widespread across Bacterial and Eukaryotic Lineages. Parsimony Tree for p-distance with 1000 bootstrap of 20,382 RsfS homologues (Pfam#PF02410). Sequences were aligned with MAFFT, gaps and ambiguous sequences removed with TrimAI, and the tree was constructed using IQtree3 and visualized with ITOL. RsfS from Eukaryotic species are indicated in black. Bacterial species previously shown to form dimers are named: *Deinococcus-Thermus* (light yellow), *Staphylococcus* (dark green), *Listeria* and *Lactococcus* (brown), *Bacillus* (dark blue), *Legionella* (red), *Pseudomonas* (dark pink), *Escherichia* (light orange) and *Vibrio* (light green). *Mycobacterium* (dark yellow) contains ribosome hibernation factors but does not form ribosome dimers. *Helicobacter* contains no classical hibernation factors, although its close relative *Campylobacter* does (light blue). Additional bacterial species lacking HPF that are not closely related to *Helicobacter* and *Mycobacterium* are annotated as well: *Balttobacterium* (light pink) and *Chlamydia* (light brown).

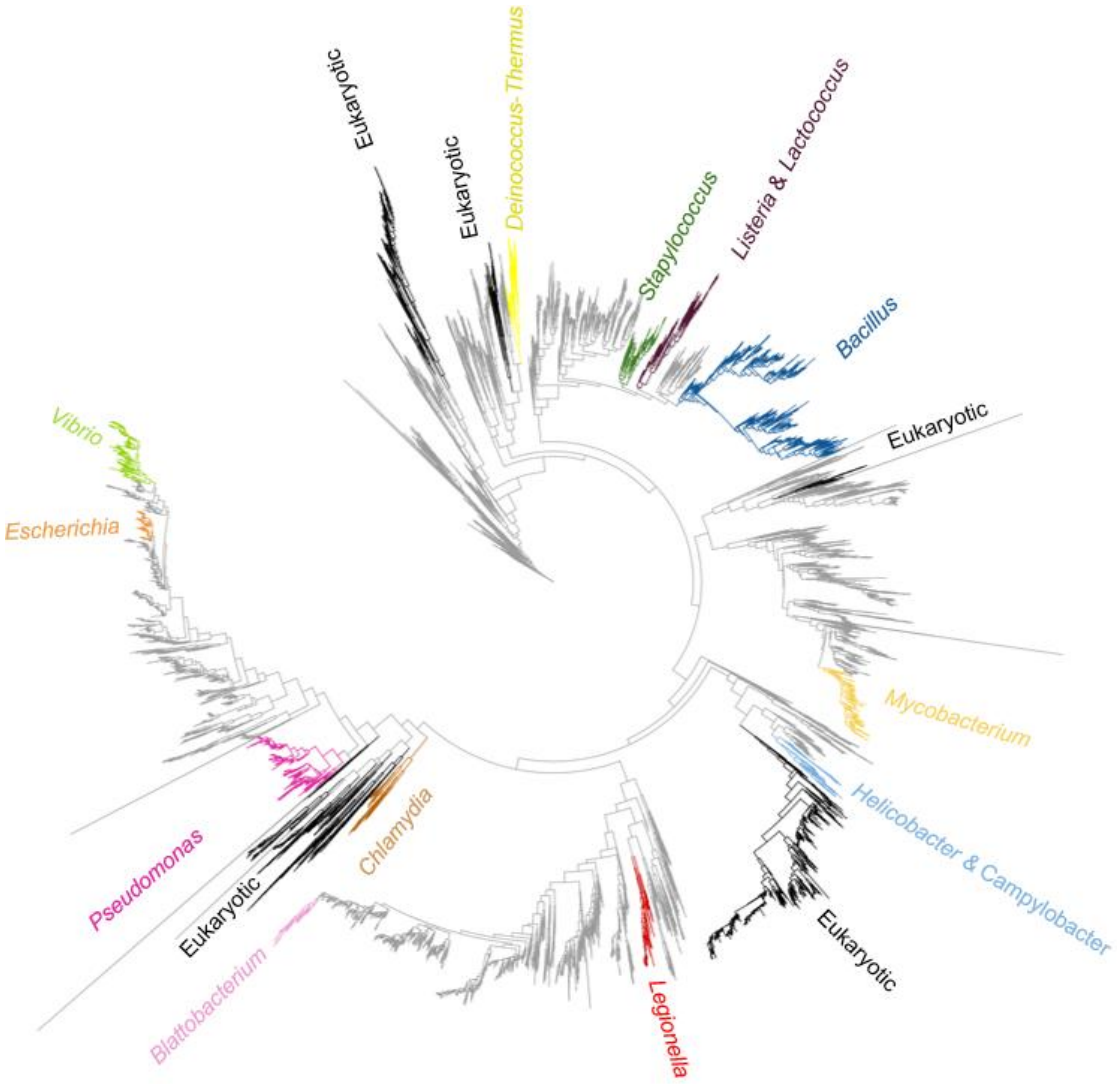

RsfS is a small protein that binds to L14

RsfS from several bacterial species has been studied in a variety of ways. The initial analysis was done in *E. coli*, and this seminal work included structural predictions, protein-protein interaction studies, and phenotypic analysis (Häuser et al., 2012). After that study, two publications focused strictly on RsfS structure and role in

dissociating ribosomal subunits. In this section, these structural studies are summarized.

Residues for RsfS and L14 binding are Conserved in Different Bacterial Species

The structure of RsfS proteins in *E. coli, M. tuberculosis, and S. aureus* have been characterized using in silico analyses (Häuser et al., 2012), crystallography, and cryo-electron microscopy (Cryo-EM) (Khusainov et al., 2020; X. Li et al., 2016). The RsfS structure was solved in isolation (X. Li et al., 2016) and bound to L14 on the 50S subunit (Khusainov et al., 2020; X. Li et al., 2016). Together, the picture that emerged is that RsfS is a ~15 kD protein that is dimeric in solution. It forms a 5-stranded β-sheet, flanked by two long and one short α-helices, a well conserved domain that has been referred to as DUF143 (Häuser et al., 2012; X. Li et al., 2016). In the context of the ribosome, RsfS binds to the large ribosomal subunit protein L14 (Häuser et al., 2012; Khusainov et al., 2020; X. Li et al., 2016). Although RsfS can form homodimers in solution (X. Li et al., 2016), RsfS is in a monomeric form when bound to L14 (Khusainov et al., 2020; X. Li et al., 2016). L14 is one of the most conserved proteins in the ribosome, and is essential for viability (Shoji et al., 2011). L14 is located between the peptidyl transferase center and a GTPase, ObgE, and binds to the 23S rRNA (Davies et al., 1996). The GTPase in proximity to L14, ObgE, is involved in the late assembly stages of the 50S subunit within the same biogenesis network as RsfS (Nikolay et al., 2021). L14 is critical for forming inter-subunit bridges between the 50S and 30S, and thus binding it would be expected to block 70S formation (Q. Liu & Fredrick, 2017).

The RsfS residues that interact with L14 have been identified in studies that used crystallography and Cryo-EM methods to solve the RsfS-L14 structure (Khusainov et al., 2020; X. Li et al., 2016). RsfS bound in a monomeric form, and it was proposed that RsfS dimers dissociated to make the RsfS interface available to interact with L14 (X. Li et al., 2016). This idea was derived from the observation that RsfS β sheet3 and 4 are needed for RsfS to form homodimers and interact with L14 C-terminal (X. Li et al., 2016). Although Khusainov et al., reported that Glu70, Asp81, Tyr98 were conserved in all RsfS homologues (Khusainov et al., 2020), analyzing sequences in other species with crystalized structures and suggest this conservation pattern may not be universal (Figure 2). The interactions between RsfS and L14 appear to include hydrogen bonds as well as complementary electrostatic surface potentials (Khusainov et al., 2020; X. Li et al., 2016). Subsequent co-crystallization of RsfS and L14 show differences in critical residues that facilitate RsfS and L14 interactions between *M. tuberculosis* and *S. aureus,* however some residues are conserved: Glu70, Asp81, Arg95 (Khusainov et al., 2020; X. Li et al., 2016). In *S. aureus,* RsfS occupied the same position as Inter subunit bridge 8, a protein that normally keeps the 50S from joining the initiating 30S before the right time (Khusainov et al., 2020). In summary, the interacting surface and certain residues that facilitate RsfS-L14 binding are conserved, but there may be some species specificity.

RsfS's binding partner, L14 is similar in size at ~13 kD, with a structure consisting of a five stranded β-barrel, a two β-strand ribbon that extends from the barrel, and two α-helices, based on crystal structures from *Bacillus stearothermophilus* (Davies et al., 1996). Mutational analysis of *E. coli* L14 identified Thr97, Arg98, Lys114, and Ser117 residues as critical for RsfS binding (Häuser et al., 2012), with Thr97 and Arg98 containing a secondary role interacting with 16S rRNA to form the B8 inter-subunit bridge (Q. Liu & Fredrick, 2017). *M. tuberculosis* crystal structures found that both L14 α-helices (Glu106-Glu109 and Met113-Leu118) interact with RsfS (X. Li et al., 2016). The study in *S. aureus*, using crystal structures, noted that the L14 residue Arg97 not only binds with RsfS (Khusainov et al., 2020), but has a dual function in interacting with 16S rRNA to form a B8 subunit bridge (Q. Liu & Fredrick, 2017). The *E. coli* RsfS homologues has been shown to bind to L14 independent of a late stage biogenesis checkpoint H68 (Hassan et al., 2026), providing further evidence that RsfS can bind to premature 50S subunits, consistent with a possible role in ribosome biogenesis (Fatkhullin et al., 2022).

These studies thus established that RsfS interacts with the ribosomal protein L14, defining residues in both proteins that are key for the interactions. The structural studies also indicate that RsfS might exist as a dimer prior to interacting with L14 but is found associated with the 50S as a monomer. These studies thus suggested some possible regulatory points, e.g. in dissociating the RsfS dimer and in removing the RsfS from L14, but to date these knowledge gaps have not been filled.

Figure 2. RsfS binds to L14 on the 50S subunit using critical residues. RsfS (red) bound to L14 (blue) on the 50S subunit (grey) using specific residues (yellow). The

top panel shows RsfS (red) bound to L14 (blue) on the 50S ribosomal subunit (grey). The bottom panel shows RsfS (red) bound to L14 (blue) with conserved residues (yellow) found critical for binding in prior crystallography studies. The models were constructed using ChimeraX to visualize published Cryo-EM structures and Alphafold predictions. RsfS-50S subunit crystal structures *S. aureus* (PDB ID: 6SJ6) and *E. coli* (9SS4) have been previously published. *M. tuberculosis* 50S subunit (PDB ID: 7f0d) and RsfS (O86327) predicted structures were aligned to *S. aureus* RsfS-50S Cryo-EM structure (PDB ID: 6SJ6). Due to the absence of existing Cryo-EM structures for *H. pylori* and *Legionella* 50S subunits, their RsfS (O25960, Q5ZVR3) and L14 (P56039, Q5WZK2) homologues were superimposed on *S. aureus* 50S subunit (PDB ID: 6SJ6).

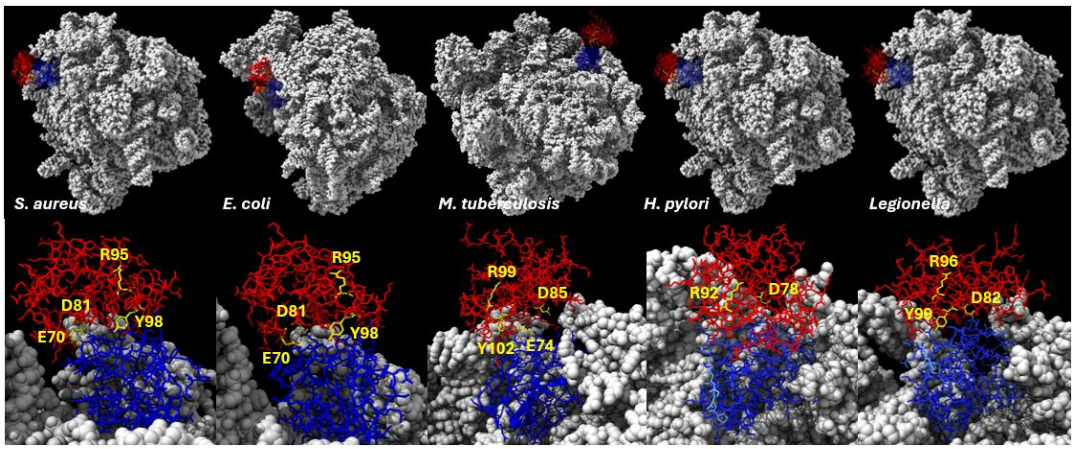

RsfS prevents the 50S from interacting with the 30S but does not split pre-formed 70S ribosomes

The effect of ribosome silencing and hibernation factor on ribosomes has been determined by analyzing ribosome populations using sucrose gradients that separate 30S, 50S, 70S, 100S and polysomes by density (Qin & Fredrick, 2013). These types of sucrose gradient analysis have been conducted vis a vis RsfS on *E. coli* (Häuser et al., 2012), *S. aureus* (Khusainov et al., 2020) and *M. tuberculosis* (X. Li et al., 2016). In these species, RsfS changed the relative abundance of the 30S, 50S and 70S, shifting the population equilibrium away from 70S. These sucrose gradients were

carried out by adding purified RsfS to isolated ribosomes in cell-free assays. This method required RsfS to be at an high molar concentration relative to the 50S (20-fold) and 30S (36-fold) subunits to detect changes in profiles for *E. coli* (Häuser et al., 2012). In other microbes, RsfS was also needed at a high molar amount to change the ribosomal population profile: *S. aureus* required 2-5 molar concentration of RsfS relative to 70S (X. Li et al., 2016), while *M. tuberculosis* required 15 times the molar concentration of RsfS to 50S and 30S subunits (X. Li et al., 2016). One study reported profiling cell lysates, comparing wild type (WT) to *rsfS* null mutants in *Legionella pneumonia*; however, this approach could not detect a difference in the ribosome profiles relative the WT (Schmid et al., 2026). Overall, these studies suggest that *in vitro*, RsfS needs to be in excess concentration so its interactions with the 50S subunit can have a detectable effect, and in that case, RsfS shifts the population equilibrium from 70S to individual 50S and 30S.

RsfS is widespread and likely has a conserved L14 binding mode

The initial landmark work on RsfS by Häuser and colleagues determined that RsfS was widespread and found in nearly all bacteria and eukaryotes (Häuser et al., 2012). Interactions were documented structurally as described in the above work for *M. tuberculosis* and *S. aureus*, and documented using two-hybrid type analyses for *E. coli*, *Treponema pallidum*, *Streptococcus pneumonia*, and *Synechocystis*, as well as human mitochondrial and corn chloroplasts RsfS homologs (Häuser et al., 2012). The interactions were expanded using a bioinformatic approach that combined residue

coevolution and protein structural information to predict all protein-protein interactions within a set of 19 pathogenic bacteria (Humphreys et al., 2024). This report identified a strong likelihood that RsfS and L14 interactions are conserved in both previously experimentally validated microbes, e.g. *M. tuberculosis* (X. Li et al., 2016), as well as several new ones including *H. pylori*, *L. monocytogenes,* and *P. aeruginosa* (Humphreys et al., 2024). Overall, these results strongly suggest that proteins annotated as RsfS homologs have the ability to bind to the ribosomal protein L14.

RsfS promotes viability in low nutrient and starvation conditions in several bacterial species

Genetic elimination of *rsfS*, complementation of the mutant, and studies of associated phenotypes have been demonstrated in *E. coli* (Häuser et al., 2012; Jiang et al., 2007)*, Legionella pneumophila* (Schmid et al., 2026) and *H. pylori* (Y. O. Elshenawi et al., 2026). Overall, the studies support the model that RsfS is required for optimal growth and survival in all of these species, and more so when the bacteria are conditions that might be considered stressful, e.g. nutrient limitation (Starosta et al., 2014). In this section, we described the phenotypes associated with deleting *rsfS*.

The first *rsfS* null mutant to be studied was in *E. coli*, from the *E. coli* Keio collection containing a pool of single gene deletions (Jiang et al., 2007). Initial growth, serial passaging, and spot plating in rich media did not detect that the *rsfS* mutant had a significant growth defect (Jiang et al., 2007). A subsequent study generated an independent *rsfS* null mutation, and characterized the phenotype across

additional conditions and using competition-style growth curves (Häuser et al., 2012). This work found that these *rsfS* mutants had impaired viability in stationary phase and nutrient-poor conditions (Häuser et al., 2012). The *rsfS* mutant could be partially complemented, supporting that *rsfS* is responsible for these phenotypes, but complementation only occurred when the gene was expressed under a strong promoter (Häuser et al., 2012). Indeed, the authors concluded there was some as-yet-unknown transcriptional regulation mechanisms in play. In addition to growth phenotypes, the Häuser et al. authors also evaluated whether loss of *rsfS* affected translation. For this analysis, the authors measured β-galactosidase levels after transcriptional induction and found that there was no difference between the *rsfS* mutant and wild-type (WT) parent when in exponential phase growth. In stationary phase, however, there was a difference, specifically that the WT exhibited a decrease in β-galactosidase activity after the transcriptional halt, while the *rsfS* null mutant had less of a decrease, suggesting *rsfS* mutants did not limit translation like the WT (Häuser et al., 2012). The idea that RsfS normally lessened translation was supported additionally by the finding, described above, that RsfS *in vitro* shifted ribosome populations away from full 70S and toward 30S and 50S. A study investigating the role 30S subunit biogenesis gene, *rimM,* in *E. coli* recovering from growth arrests found that Δ*rimM* knockouts had more RsfS bound to mature and premature 50S subunits to compensate for defective 30S biogenesis (Hassan et al., 2026). Deletion of the *rsfS* gene from the Δ*rimM* mutant to generate a double knockout (Δ*rimM* Δ*rsfS*) retained a defective phenotype during the recovery phase after growth arrest, further

supporting the model that functional RsfS is need by bacteria to adapt to stressful growth conditions (Hassan et al., 2026). Overall, this work provided evidence that bacterial RsfS proteins interact with ribosomal L14 to prevent 70S formation and play key roles in bacterial physiology. Specifically, the loss of *rsfS* created strains that fared poorly in stationary phase, low nutrient conditions and recovery from growth arrest, conditions under which ribosome would be expected to be dormant.

Two other bacteria have had the phenotypes associated with *rsfS* deletion characterized, both done recently. These are *L. pneumophila* and *H. pylori*, which are both pathogens so the phenotypes *in vitro* plus *in vivo* were characterized.

L. pneumophila infections are a significant clinical issue (Viasus et al., 2022). *L. pneumophila* infections causes Legionnaires disease, a fatal form of pneumonia, by colonizing the lung epithelial cells and replicating in macrophages (Iliadi et al., 2022). Clinical isolates of *L. pneumophila* from patients with recurring Legionella infections have the ability to form persister populations (Adams-Ward et al., 2023). To maintain colonization *L. pneumophila* needs to overcome oxidative stress (Ngwaga et al., 2023), nutrient starvation (Fonseca & Swanson, 2014), and macrophage acidification (Fortier et al., 2009). *L. pneumophila* encodes both ribosome hibernation/dimerization factors and a RsfS homologue (Schmid et al., 2026) (Fig. 1). *L. pneumophila* Δ*rsfS* strains were found to have impaired growth during specific conditions, including heat shock and nutrient stress, but not others such as normal nutrient rich and poor media (Schmid et al., 2026). The *rsfS* deletion mutant had defects during long-term starvation and took longer to recover when it

was re-cultured in rich media; the *rsfS* deletion mutant defects could be partially corrected via complementation (Schmid et al., 2026). The deletion of *rsfS* also caused a defect in intracellular macrophage colonization levels, with the replication rate within the macrophage delayed compared to wild type (Schmid et al., 2026). Overall, these studies supported that *L. pneumophila rsfS* is required for survival and growth under specific conditions including in the *in vivo* conditions of macrophages.

The third microbe for which the *rsfS* physiological role has been studied is *H. pylori*. *H. pylori* infections are widespread, chronic stomach infections that lead to the development of gastric ulcers and cancers (Chen et al., 2024; Malfertheiner et al., 2023). *H. pylori* needs to overcome the acidic pH of the stomach, immune factors, scarce nutrients, and penetrate the mucus barrier (Talebi Bezmin Abadi, 2017). The work surrounding *H. pylori rsfS* began with the observation that *rsfS* was upregulated at the transcriptional level when the microbe was grown biofilms as compared to planktonic states (Hathroubi et al., 2018). There are no known regulatory mechanisms for *rsfS* expression, and indeed, *rsfS* mRNA levels in *E. coli* and *M. tuberculosis* remained consistent throughout all the growth phases (X. Li et al., 2016). Following up on this observation, Elshenawi and colleagues deleted *rsfS*. They found that the *H. pylori rsfS* mutant had growth defects in stationary phase, low nutrient conditions, and upon exposure to atmospheric oxygen (Y. O. Elshenawi et al., 2026). These phenotypes are similar to those seen in other bacteria, although an interesting difference is that *H. pylori* is not predicted to encode any known ribosome hibernation/dimerization factors (L. I. Chan et al., 2025). This work additionally

expanded the conditions under which RsfS is needed by finding that the *H. pylori rsfS* mutant had biofilm formation defects. Planktonic growth phenotypes and biofilm phenotypes could be corrected by via complementation with the gene under the native promoter, indicating *rsfS* was responsible for the observed phenotypes. *In vivo*, *H. pylori rsfS* null mutants colonized murine stomachs at low numbers initially, and could not maintain long term infections (Y. O. Elshenawi et al., 2026). These studies suggest that *rsfS* is needed in several microbes for optimal growth in low nutrient and other challenging conditions, including growth modes such as biofilm formation and during mammalian colonization.

Connections between RsfS and antibiotic tolerance

An interesting area of research has been the connection between ribosomal dormancy and antibiotic sensitivity. Many classes of clinically prescribed antibiotics target the ribosome (Krawczyk et al., 2024). These fall into five primary categories: macrolides, lincosamides, oxazolidinones, tetracycline and chloramphenicol (Krawczyk et al., 2024). These each target distinct parts of the ribosome or translation, e.g. the 50S subunit near the peptidyl transferase center (Lenz et al., 2021), the A site at the 50S ribosome, 23S rRNA, or 16S rRNA (Fernandes et al., 2023; Krause et al., 2016; Yu & Zeng, 2024), or by acting as structural analogs of tRNA (Spížek & Řezanka, 2017). Currently only one study has investigated the potential influence of RsfS on antibiotic efficacy, using *L. pneumophilia,* a bacterial species that contains both dimerization/hibernation factors and RsfS (Schmid et al.,

2026). *L. pneumophila rsfS* null mutants were more susceptibility to one ribosome targeting antibiotic, tetracycline, and one cell wall targeting antibiotic, ampicillin (Schmid et al., 2026). The mutant was not more susceptible to other specific antibiotics, including ribosome inhibitor erythromycin and transcription inhibitor rifampicin (Schmid et al., 2026). These results hint that RsfS might protect the ribosome from some antibiotics, but it's also possible that the mutants simply increase the population of actively translating cells.

Mutations in L14 were first associated with lincomycin resistance alongside L15 and S7 from the 30S subunit (Hummel et al., 1979). These findings suggest that L14 and RsfS may influence the efficacy of certain ribosome targeting antibiotics, e.g. possibly by steric hindrance. This question has yet to be explored in other bacterial species, including ones with other dormancy factors (Kumar et al., 2024; Mishra et al., 2018; Sawyer et al., 2021) and species like *H. pylori* that do not contain known ribosome hibernation factors (L. I. Chan et al., 2025).

Regulation of *rsfS* and *rplN* (encoding L14) Expression

The prevailing model is that RsfS interacts with the ribosome under specific conditions, suggesting the interactions would be regulated. One possibility is that *rsfS* mRNA or protein expression increases under these conditions. In terms of analysis of mRNA levels, studies in *E. coli* and *M. tuberculosis* found *rsfS* gene expression to be constitutive across a growth curve (Häuser et al., 2012; X. Li et al., 2016). RNA sequencing studies in another microbe, *H. pylori,* showed regulation in the form of an

increase of *rsfS* transcripts in biofilm versus planktonic cells (Hathroubi et al., 2018). While intriguing, further studies are needed to define the transcriptional regulation of *H. pylori* biofilms and relate this to *rsfS*. In terms of protein levels, in *E. coli,* RsfS appears to be strongly upregulated in late stationary phase as assessed using a translational fusion to a C-terminal His-tag and western blotting (Häuser et al., 2012). This finding suggests the protein product is upregulated in stationary phase, as might be expected for the function to limit translation, but it's not yet clear what drives this increase or whether this increase happens at the transcriptional or translational level. This work did find some evidence for transcriptional regulation in that *rsfS* expression from the native promoter could not complement the mutant, but when the complementing copy was expressed from a non-native promotor, the mutant could be complemented. This outcome could be due to some aspect of regulation or perhaps the requirement for a high level of *rsfS* transcripts. RsfS regulation thus remains an exciting area for future research.

L14 regulation has also been investigated. In *E. coli,* L14 has a regulatory mechanism that is dependent on S8 protein of the 30S subunit repressing the translation of L14 by binding to its mRNA so it can be subject to decay (Liang et al., 1999; Mattheakis et al., 1989). The same feedback loop was found in *M. tuberculosis* in which the S8 homologue, RpsH, represses L14 translation by binding the operon transcript (Cortes & Cox, 2015). In *M. tuberculosis*, L14 transcription can be activated by a transcriptional regulator, ResR/McdR, that has been associated with drug resistance, host colonization and translation regulation (Pal et al., 2023).

Although no studies to investigate ribosome dimerization or silencing have been conducted in *Bordetella pertussis*, L14 transcription was found to be upregulated due to a point mutation in its promoter (Novák et al., 2020). L14 expression has not been extensively investigated beyond these findings and whether RsfS expression influences L14 expression and 50S subunit biogenesis has yet to be explored.

RsfS can bind to proteins beyond L14

RsfS was established to interact with L14 in the early studies of this protein, using several different affinity and protein-protein interaction methods (Butland et al., 2005; Jiang et al., 2007). In these same studies, however, *E. coli* RsfS was found to bind other proteins with weaker affinity. Overlapping interacting proteins included multifunctional CCA protein, 50S ribosomal protein L19, YehL, and YehQ (Butland et al., 2005; Jiang et al., 2007). Multifunctional CCA enzyme facilitates the maturation and repair of tRNAs (Kulandaisamy et al., 2023). L19 plays a role in the B8 bridge between the 30S and 50S subunits (Q. Liu & Fredrick, 2017) and also ensures translational fidelity (VanNice et al., 2016). L19 and L14 both interact with 16S rRNA and have been observed to co-evolve compensatory mutations to increase the rate of translation (Maisnier-Patin et al., 2007). YehL is an uncharacterized protein but is annotated as a putative AAA+ MoxR family ATPase that functions as a chaperones by adding metal cofactors to protein complexes to facilitate folding and activation (Snider & Houry, 2006). YehQ is in the same operon on YehL and has not been characterized in *E. coli* but it contains homology with SWIM zinc finger domain

containing proteins that contain zinc chelating domains are predicted to facilitate DNA binding and protein interactions (Makarova et al., 2002). These studies thus suggest that RsfS may have additional interacting partners beyond L14 and potential extra-ribosomal function in *E. coli*.

In the Humphreys et al. bioinformatic analysis of protein-protein interactions across multiple bacteria, RsfS was found to have predicted interactions with several proteins in addition to L14. These included other ribosomal proteins (50S ribosomal proteins L19 and L29), several involved in transcription (anti-sigma-B factor, the transcriptional regulator Fur, response regulator PhoH), and proteins at the bacterial surface or involved in ferric uptake (outer membrane lipoprotein LolB and ferric uptake) (Humphreys et al., 2024). While most of these have not been experimentally validated, one was: PhoH, which regulates the response to inorganic phosphate starvation (Yang et al., 2025). The *P. aeruginosa* RsfS homologue was confirmed the interact with PhoH using bacterial-2-hybrid, co-immunoprecipitation and pull down assays (Humphreys et al., 2024). The validated binding between RsfS and PhoH combined with the observed interactions between RsfS homologues in *E. coli* isobaric tagging (Jiang et al., 2007) and affinity assays (Butland et al., 2005) support the idea that RsfS may have multiple interaction partners, and the idea that RsfS activity is not limited to ribosome silencing (Fatkhullin et al., 2022).

Concluding remarks

RsfS is an important protein found in nearly all bacteria, where the body of evidence supports it interacts with the 50S ribosomal protein L14 to "silence" the ribosome by preventing formation of an actively translating 70S ribosome. It consequentially creates an alternative post-ribosome biogenesis mechanism for ribosomal dormancy that is separate from dimerization. It is unknown when cells benefit from hibernation versus silencing. In several bacterial species, *rsfS* mutants have growth and/or survival defects in conditions of low growth, e.g. stationary phase, nutrient limitation, starvation recovery, and biofilm formation. In addition, *rsfS* is required for normal host colonization in at least two microbes: for stomach colonization by *H. pylori*, and for macrophage multiplication in *L. pneumophila*. However, other than the clinical use of macrolides and fluoroquinolones to treat both bacterial infections, it is not clear why *rsfS* is needed *in vivo*, e.g. if similar slow growth or nutrient limiting states exist in these infections. Although RsfS is viewed as a silencing and L14-interacting protein, it may have other physiological roles. Some authors have pointed out that it has similarities to proteins that are required for ribosome biogenesis, suggesting RsfS may play that role (Fatkhullin et al., 2022). Additionally, RsfS has been found to bind several other proteins, and whether any phenotypes of *rsfS* mutants are due to affects in these pathways is not known. There is some evidence that *rsfS* mutants may have increased susceptibility to antibiotics, but the basis for such a response is not yet clear. Clearly this protein is an important one to multiple bacteria and in myriad ways, with many open questions (Box 1).

Box 1: Open Questions

1. Does RsfS have additional roles associated with ribosomes besides silencing such as a protective chaperone or ribosome biogenesis? Does RsfS operate in other pathways besides the ribosome?
2. Does RsfS have different physiological roles in bacterial species that form 100S ribosome dimers versus bacterial species that do not form 100S dimers?
3. What are the roles of RsfS and L14 in antibiotic efficacy? Are the roles specific, e.g. steric hindrance, or more related to dormancy?
4. What proteins and conditions regulate *rsfS* transcription and translation? What regulates the association/dissociation of RsfS with the ribosome? Does regulation of L14 contribute to RsfS efficacy?
5. Will other bacteria beyond the three characterized show similar phenotypes—e.g. growth defects during stationary phase, low nutrients, heat shock, biofilm formation, and other stressful conditions? Are these phenotypes part of the same need, e.g. requirement to slow growth or conserve ribosomes?
6. Is RsfS required for *in vivo* growth in a broad set of bacterial pathogens, or only those that need to slow growth? What about non-pathogens, e.g. microbes that must survive in the environment?

Acknowledgements

The authors are grateful to members of the Ottemann lab for multiple helpful discussions. This work was supported by National Institute of Allergy and Infectious Diseases and National Institute of General Medical Sciences of the National Institutes of Health under award numbers R01AI164682 (to KMO), F31AI176804 (to YOE), and R01GM121359 and R01AI192692 (to MFY). The funders had no role in study design, data collection, and interpretation, or decision to submit the work for publication.

Chapter#2→The *Helicobacter pylori* ribosomal silencing factor RsfS is required for low-growth states and chronic infection

Abstract

Helicobacter pylori is a prevalent bacterial pathogen that chronically colonizes the human gastric epithelium, but the bacterium's physiological mechanisms that promote this state have been understudied. Dormancy and low growth are known to facilitate other microbial chronic infections, with a key feature being that ribosome translational activity is downregulated via specific regulatory proteins. The *H. pylori* genome is predicted to encode only one ribosome regulation protein, called RsfS (Ribosomal Silencing Factor S). In other bacterial species, RsfS prevents 30S-50S subunit joining by binding to a protein called L14 on the 50S large ribosomal subunit. Although *H. pylori* RsfS has not been experimentally investigated prior to this work, it conserves key residues, suggesting it is a bona fide RsfS homolog. To investigate phenotypes associated with *H. pylori rsfS*, the gene was deleted and mutant phenotypes characterized. *H. pylori rsfS* null mutants had no defects during exponential phase but had viability defects in stationary phase and low growth factor conditions. Additionally, *rsfS* null mutants could not form biofilms, and instead were only able to form monolayers of multicellular aggregates. These defects were corrected by the re-introduction of *rsfS* in a second site on the chromosome. To explore whether *rsfS* is required *in vivo*, a mouse model was employed. *rsfS* mutants initially colonized in low numbers in both the glands and total stomach but were unable to develop robust long-term colonization. This work supports that *H. pylori*

requires RsfS for survival in low growth states and to maintain chronic infections in the host.

Importance

H. pylori chronic infections are difficult to cure in part because *H. pylori* is proposed to adopt low-growth states known to render bacteria tolerant to antibiotics. One key signature of a low growth state includes low translation via ribosome regulation factors. Unlike other bacterial species, *H. pylori* contain only one known ribosome regulation factor called Ribosomal Silencing Factor S (RsfS). This gene was previously found to be transcriptionally upregulated in at least one low growth state, biofilms. In this work, we found that *H. pylori rsfS* is required for this microbe to thrive in low growth states and during infection. This study is one of only two studies that investigates the phenotypes of *rsfS* knockout mutants in any bacterial species and the first to address knowledge gaps in ribosomal regulation by *H. pylori in vivo*.

Introduction

Helicobacter pylori is a gram-negative bacterium that colonizes the human stomach and establishes chronic infections. These infections can lead to gastrointestinal disorders such as peptic ulcers, gastric mucosal lymphoma, and gastric cancer (Chen et al., 2024; Kim et al., 2023; Malfertheiner et al., 2005). *H. pylori* is a globally prevalent pathogen that infects 40% of the population in developed countries and 80%-90% of the population in developing countries (Perez-Perez et al., 2004). In 1994, the World Health Organization classified *H. pylori* as a

Class-1 carcinogen and the microbe has often made lists of priority pathogens due to the severe disease consequences (Wroblewski & Peek, 2013). *H. pylori* is often acquired in childhood, and is able to persist for the lifetime of the host (Czinn, 2005). *H. pylori* infections can be cured with antibiotics but generally require elevated dosages compared to other bacterial infections. For example, current recommendations suggest treatment for 2 weeks with 2-3 antibiotics combined with a proton pump inhibitor (Y.-C. Lee et al., 2022). The American College of Gastroenterology recommends treatment regimens containing a combination of the following antibiotics to treat *H. pylori* clarithromycin, levofloxacin, metronidazole, amoxicillin, or tetracycline (Aldhaleei et al., 2024). These triple therapy treatments have been reported to fail 20-25% of patients treated in the United States (Schoenfeld, 2024; Vakil et al., 2004). The severity of *H. pylori* disease combined with its difficult treatment highlights a need for improved understanding of factors that feed into this challenge.

H. pylori forms chronic infections that last the life-time of a human host (Bruce & Maaroos, 2008). Many other bacterial pathogens also form chronic infections that occur in a variety of organs, including lungs (Cookson et al., 2018), central nervous system (Giovane & Lavender, 2018), gastrointestinal tract (Fantry et al., 2016), urinary tract (Hjelmager et al., 2025), and skin (Ki & Rotstein, 2008). One emerging idea is that these bacteria adopt low-growth states or dormant forms in the host to allow them to limit immune detection and thus facilitate chronic infections (Fisher et al., 2017; Rhen et al., 2003). These low-growth states are well known to

contribute to treatment failures, largely because antibiotics mostly target processes that occur in growing cells, e.g. cell wall creation, translation, transcription (Da Silva et al., 2024; Rittershaus et al., 2013; Young et al., 2002). These low-growth chronic infection states have been well documented in *Mycobacterium tuberculosis* (Sakamoto, 2012), *Pseudomonas aeruginosa* (Garcia-Clemente et al., 2020), *Staphylococcus aureus* (Tuchscherr & Löffler, 2016), *Salmonella* (Ehrhardt et al., 2023), and *Escherichia coli* (Hannan et al., 2012), but studies in *H. pylori* have lagged behind. There is some evidence, however, to suggest that *H. pylori* similarly adopt a low growth state during chronic infection. Gastric biopsy analysis from clinical patients have reported evidence of low-growth states due to the observation of morphological forms of *H. pylori* associated with dormancy (Reshetnyak & Reshetnyak, 2017a) and a growth mode associated with slow growth such as biofilms (Carron et al., 2006; Coticchia et al., 2006). *H. pylori* forms biofilms during *in vitro* conditions, and cells in this state are highly tolerant to antibiotics (Y. Elshenawi et al., 2023; Windham et al., 2018). The fact that *H. pylori* can adopt these low-growth states and exhibits antibiotic tolerance has supported the idea that low-growth states might form *in vivo* and contribute to the difficulty of achieving complete eradication (Reshetnyak & Reshetnyak, 2017b).

Slow bacterial growth is a multifaceted phenotype in which multiple changes lead to low metabolic activity. One such change is ribosomal inactivation. Inactivated ribosomes have been previously associated with bacterial dormancy, older biofilm subpopulations, and states of low metabolic activity in various bacterial species (Chai

et al., 2014; Kaprelyants et al., 1993; Y. Li et al., 2021; K. S. Williamson et al., 2012). Many microbes employ multiple ribosome-inactivating proteins. These include proteins that induce hibernation or silencing by promoting either ribosome dimerization or blocking ribosomal subunits association (Prossliner et al., 2018). *H. pylori*, in contrast, is predicted to encode only one ribosome-inactivating protein, a ribosomal silencing factor called Ribosomal Silencing Factor S (RsfS). RsfS (RsfA in other bacterial species) prevents the joining of 30S subunits to 50S subunits, and thus prevents the formation of active 70S ribosomes (Fatkhullin et al., 2022). RsfS homologues are highly conserved across bacterial species as well as mitochondria (Häuser et al., 2012). RsfS protein homologues and their binding to the 50S subunit protein L14 have been structurally characterized in several bacteria, including *E. coli, S. aureus* and *M. tuberculosis* (Häuser et al., 2012; Khusainov et al., 2020; X. Li et al., 2016). Previous studies have also reported the conservation of RsfS homologues across bacterial and eukaryotic species and have confirmed binding between L14 and RsfS using the yeast two-hybrid method in *E. coli, T. palladium*, and the human mitochondrial homologue (Häuser et al., 2012). Overall, RsfS-type proteins are widespread across all domains of life and appear to conserve interactions with the ribosome.

The two studies that investigated the phenotypes associated with RsfS-type proteins was in *E. coli* (Häuser et al., 2012) and *L. neumophila* (Schmid et al., 2026). *E. coli rsfA (*the *rsfS* homolog*)* null mutants had growth defects in stationary phase and in low-amino acid conditions, consistent with the idea that ribosomal silencing is

important in these low-growth situations (Häuser et al., 2012). Additionally, the authors used a reporter gene assay and ribosome profiling to quantify assembled 70S versus separated 30S and 50S subunits. The findings led the researchers to suggest that *E. coli* RsfA prevents ribosome assembly under growth limiting conditions (Häuser et al., 2012). The *L. neumophila rsfS* gene was found to promote survival during nutrient starvation, antibiotic exposure and regulating growth and motility within macrophage subpopulations (Schmid et al., 2026). These findings established a premise for ribosome silencing mechanistically promoting bacterial survival during low growth states.

To date, no studies have examined the function of ribosome regulation in *H. pylori*. While *rsfS* transcript levels were reported to be elevated in biofilm populations compared to planktonic cells (Hathroubi et al., 2018), ribosome populations and their regulators remain largely understudied in this bacterium. In this study, we investigate the conservation of RsfS and phenotypes associated with it in *H. pylori*. Our analysis confirms that *H. pylori* conserves critical residues in RsfS known to facilitate binding with L14, in agreement with previously reported protein-protein binding predictions (Humphreys et al., 2024). By creating *rsfS* knockout mutants, we determined that the loss of this protein resulted in growth defects under some conditions, including stationary phase, low nutrient conditions, and biofilm formation, but not others such as exponential phase and normal-nutrient media. These defective phenotypes could be corrected via genetic complementation with *rsfS* in a secondary site. In addition, *H. pylori* lacking *rsfS* mutants showed weak growth *in vivo.* These mutants initially

colonized mouse stomachs in low numbers but were not able to maintain robust populations long term. Overall, our results indicate that *rsfS* expression plays a critical role in *H. pylori* low growth states *in vitro* and colonization *in vivo;* these phenotypes provide potential insights into how *H. pylori* regulate its ribosomal population to promote survival and sustain chronic and life-long infections.

Results

H. pylori RsfS conserves important residues.

H. pylori is predicted to encode only one ribosome silencing factor, RsfS, annotated as HP1414 in *H. pylori* 26695 (Tomb et al., 1997) or HPYLSS1_1340 in SS1 (Draper et al., 2017). Because *H. pylori* RsfS has not been previously investigated, we first analyzed the protein sequence of *H. pylori* RsfS compared to homologues including those with validated L14 binding interactions in which key residues were identified (Fatkhullin et al., 2022; Khusainov et al., 2020; X. Li et al., 2016). *H. pylori* RsfS encodes a 113 amino acid protein, predicted to fold into the same structure as characterized RsfS proteins. Amongst the bacterial species with validated RsfS ribosomal silencing (Fatkhullin et al., 2022; Khusainov et al., 2020; X. Li et al., 2016), the *H. pylori* RsfS was 21.5% percent identical (ID) to the homolog in *S. aureus* versus 19.3% percent ID to that in *M. tuberculosis*. Both *M. tuberculosis* and *S. aureus* contain somewhat longer forms of RsfS totaling 119 amino acids and 115 amino acids respectively. Previous studies have shown that particular residues in *S. aureus* and *M. tuberculosis* RsfS homologues drive protein-protein interactions with the ribosomal protein L14 (Fatkhullin et al., 2022; Khusainov et al., 2020; X. Li

et al., 2016). *H. pylori* RsfS homologues contains at the α-helices-coil junction at the C-terminal that slightly differs from homologues in *S. aureus, E. coli* and *M. tuberculosis* (Figure 1A). Several of these *H. pylori* RsfS residues were conserved in *S. aureus* (Lys54, Asp81, Asp78, and Trp74) and *M. tuberculosis* (Ile23, Asp24, Trp74, Leu77, Asp78, His85, Ser26, Leu97) despite the low percent ID (Fig. 1B). Only three residues (K15, D19, R92) were found to be conserved across all three bacterial species that were not identified as critical binding residues (Fig. 1B). Certain L14 residues that are critical for binding to RsfS were conserved on the C-terminal (Fig. 1C). Sequence and structural analysis show that an electrostatic bond between RsfS D81 and L14 R107 is predicted to be conserved in *H. pylori* homologues (Fig. 1D). Thus is seems highly likely that *H. pylori* RsfS conserves the ability to interact with L14 based on this residue conservation, overall conserved secondary structure, and published bioinformatic analysis (Humphreys et al., 2024).

H. pylori Δ*rsfS* mutants have growth defects compared to WT that are exacerbated in low nutrient conditions and with repeated environmental disruptions

Next, we sought to analyze how the loss of *rsfS* would impact *H. pylori*. An *H. pylori* SS1 mutant lacking *rsfS* was created by replacing the full coding sequence of the *rsfS* gene with a chloramphenicol resistance marker (*cat*) to generate the strain SS1 Δ*rsfS*::*cat*, called Δ*rsfS.* This mutation did not result in a polar effect on transcription of the downstream genes as evidenced by analysis of RNA levels using RT-qPCR (Supplemental Fig. 1). We then determined the growth phenotype of the

resultant strain across a growth curve, starting in standard *H. pylori* rich media consisting of brucella broth with 10% heat-inactivated fetal bovine serum (FBS) (BB10). Using a 96-well microplate reader assay and measurements of optical density, the *H. pylori* Δ*rsfS* mutant had initially lower OD_{600} measurements compared to the WT strain, consistent with a somewhat enhanced lag phase (Fig. 2A). After ~ 10 hours, a time point correlating to mid-exponential phase, the Δ*rsfS* mutant growth rate had increased, such that the mutant and WT strains had similar OD_{600} values at the late exponential time point, 20-hours. During the early and late stationary phases (24-36 hours), the OD_{600} values of the Δ*rsfS* strain remained steady, while the OD_{600} of WT increased to a modest degree (Fig. 2A). These results suggest that *H. pylori* can grow relatively well in rich media without *rsfS*.

Carrying out the same experiment but in low nutrient conditions (brucella broth with only 2% FBS, BB2) resulted in an enhanced defect of the *H. pylori* Δ*rsfS* strain (Fig. 2B). Both WT and the mutant strains achieved lower OD_{600} compared to those in BB10 and appeared to reach stationary phase sooner (Fig. 2B). The Δ*rsfS* strain, however, had consistently lower OD_{600} than the WT (Fig. 2B). These results suggest that loss of *rsfS* caused *H. pylori* to have enhanced defects in low serum conditions compared to high serum ones (Fig. 2B).

We next repeated the growth analysis but plated the bacterial samples to examine live bacteria. In this case, the bacteria were grown in tubes shaking in the incubator. A single culture was employed and repeatedly sampled, an approach referred to as continuous growth (Supplemental Fig. 2). Using this approach and rich

medium (BB10), the Δ*rsfS* mutant produced significantly fewer CFU at the 9-hour time point relative to the WT control. This difference became more severe after 12 hours of incubation (Fig. 2C). We noted that this method had disrupted conditions at each time point, with more disruptions accumulating over time. This analysis suggested the *rsfS* mutant might be sensitive to changes in conditions encountered during disruptions associated with sampling.

To evaluate whether the sampling regime was affecting the *rsfS* mutant, we sought a second growth approach that would eliminate repeated sampling and disruptions to conditions. This outcome was accomplished using an endpoint assay, in which the entirety of an individual sample was used (Supplemental Fig. 2). Using the same timepoints as the continuous growth assay (Fig. 2C), no differences in CFU were observed between WT and two distinct Δ*rsfS* mutants (Fig. 2D, Supplemental Fig. 3). The endpoint approach further revealed that the *H. pylori* Δ*rsfS* mutant did not have a defect compared to WT in the first 20 hours of growth, exponential phase (Fig. 2E). However, as the cells transitioned into stationary phase, loss of *rsfS* created *H. pylori* with significant growth defects that became progressively worse as the cells progressed through stationary phase (Fig. 2E).

Continuing the endpoint analysis approach, we repeated the growth analysis of the Δ*rsfS* mutant in BB2. In BB2, the Δ*rsfS* mutant produced less CFU/mL than the WT control across all timepoints, but the difference between the Δ*rsfS* strain and WT did not become statistically significant until stationary phase time points at 20-25h (Fig. 2F). Similar results were observed with an independent Δ*rsfS* mutant

(Supplemental Fig. 3). Compiled, these results suggest that *rsfS* is required for *H. pylori* to withstand repeated disruptions in growth conditions, for growth in low serum media, and for survival in stationary phase.

H. pylori Δ*rsfS* mutants are weak biofilm formers

Previous work showed that *H. pylori rsfS* expression was significantly elevated in biofilms compared to free-floating cells (Hathroubi et al., 2018). It was not known, however whether RsfS was important for *H. pylori* biofilm growth. *H. pylori* SS1 produces robust biofilms under static, microaerobic conditions in BB2 media after three days, before dispersing at four days (Hathroubi et al., 2018). We thus quantified biofilm formation of the *H. pylori* Δ*rsfS* mutant under these conditions, using two distinct *rsfS* mutant alleles. Δ*rsfS* mutants formed significantly less biofilm than the WT strain (Fig. 3A, Supplemental Fig. 3). Specifically, at the 3-day timepoint the mutant had ~3-fold less biofilm as measured by crystal violet staining. To evaluate whether the Δ*rsfS* strain might have delayed biofilm, the samples were incubated for an additional day, but the mutants still displayed approximately 2-fold less biofilm than the WT strain (Fig. 3A). These results suggest that *rsfS* is important for *H. pylori* biofilm formation.

We wondered whether the Δ*rsfS* mutant would retain this significant biofilm defect when grown in alternative media. We hypothesized that the Δ*rsfS* mutant BB2 growth deficit (Fig. 2) might be driving the biofilm defect, so we explored media with higher serum concentrations where the Δ*rsfS* mutant has no exponential phase defect

(Fig. 2). However, even with 10% serum (BB10), the *ΔrsfS* strain retained its biofilm defect (Fig. 3B). Specifically, the mutant formed 4.6-fold less biofilm than the WT at 3 days (Fig. 3B). In addition to BB10, we also explored whether the *rsfS* mutant would display a biofilm defect in media with no serum, based on a report with *S. aureus* defining FBS as a potential biofilm inhibitor (Abraham & Jefferson, 2010). At 3 days, the SS1 WT control produced about 8-fold the amount of biofilm as the *ΔrsfS* strain, a statistically significant difference that reduced to 2-fold at 4 days prior to dispersal at 5 days (Fig. 3C). Taken together, these results provide strong evidence that the *H. pylori ΔrsfS* strains produced significantly less biofilms relative to the WT across all time points and media conditions.

To gain further insight into the biofilm defect associated with loss of *rsfS*, we used scanning electron microscopy (SEM) to visualize *H. pylori* WT and *ΔrsfS* strain biofilms grown for 3-days in BB2. The SS1 WT strain produced robust networks of multilayer aggregates and flagellar filaments, as reported previously (Hathroubi et al., 2018), whereas the Δ*rsfS* mutant strain had fewer aggregate structures, and aggregated cells generally only formed monolayers (Fig. 3D). These findings supported the crystal violet assays, strongly indicating that the *rsfS* is essential for biofilm formation in *H. pylori*.

The Δ*rsfS* mutant phenotypes can be complemented by exogenous expression of *rsfS* in an intergenic locus but not *rdxA*

The above results suggest that *H. pylori* RsfS is critical for biofilm formation, growth in low nutrient and changing conditions, and stationary phase survival (Figs.

2, 3). To confirm these roles of *rsfS*, we sought to complement the mutant by inserting a copy of *rsfS* into a heterologous locus. We initially used the *rdxA* gene, a chromosomal locus commonly used for complementation in *H. pylori* due to its classification as a neutral locus (A. C. K. Chan et al., 2015; Damke et al., 2019; Howitt et al., 2011; D.-H. Kwon et al., 2000; G. W. Liechti & Goldberg, 2013, 2013; A.-N. Liu et al., 2022; McGee et al., 2005; Nguyen et al., 2025; Rader et al., 2007; Rocha et al., 2025; Smeets et al., 2000; Sycuro et al., 2010; Terry et al., 2005; G. Wang et al., 2012; X. Wang et al., 2025; Zimmerman et al., 2024). We created two *rdxA::rsfS* alleles and used them to transform both WT and the Δ*rsfS* mutant (Supplemental Fig. 4). Exogenous expression of *rsfS* via the *rdxA* locus, however, did not complement the Δ*rsfS* planktonic growth or biofilm defects (Supplemental Fig. 5). This led us to question the neutrality of loss of *rdxA* and examined *rdxA* knockout mutants for growth defects. Surprisingly, loss of *rdxA* alone caused defects in both late stationary phase and biofilms (Supplemental Fig. 5). This phenotype is being explored in a separate manuscript, but this outcome suggested that *rdxA* was not a suitable locus for complementing these types of phenotypes.

As an alternative to *rdxA*, we designed a construct that would place a copy of *rsfS* into an intergenic region that has been used previously (Langford et al., 2006) (Supplementary Fig. 4). As with the *rdxA* integrated constructs, a copy of *rsfS* with 200 base pairs upstream was integrated between the coding sequences for HP0203 – HP0204. After verifying the correct integration, we examined whether the defects observed in the Δ*rsfS* knockout mutants would be corrected. Both biofilm formation

and stationary phase defects of the Δ*rsfS* mutant were corrected by placement of a copy of *rsfS* in the intergenic region (Fig. 4). This outcome strongly suggests that these defects were due to the loss of *rsfS*.

rsfS possesses an upstream promoter that contributes to its expression

Because the *rsfS* complementation constructs also included an upstream 200 base pairs and the putative promoter, we evaluated expression of *rsfS* in the context of these various non-native locus constructs. Previous work demonstrated that the *rsfS* is the first gene in a four gene operon (Supplemental Fig. 1A), with a transcriptional start site mapped in *H. pylori* strain 26695 at an A 26 base pairs upstream of the *rsfS* ATG (Bischler et al., 2015). Two constructs possessed this promoter region as part of the 200 bp *rsfS* upstream section and no other known promoter. The construct that placed *rsfS* in the opposite orientation as *rdxA* (Δ*rdxA*::*rsfS* (1p)), and the construct that placed *rsfS* in the intergenic region (*IG::rsfS)* (Supplemental Fig. 4). After making these strains, transcripts levels of *rsfS* were examined using RT-qPCR, normalized to the *gapB* reference gene to calculate ΔCq (Fig. 5). Strains bearing only the 200 bp upstream of *rsfS* expressed *rsfS* to levels that were within 1 cycle of the WT strain (Fig. 5A), and when normalized to *gapB* (Fig. 5B), resulted in ΔCq values that had a difference of ~1.4 from the WT (Fig. 5C). These findings support that an active *rsfS* promoter is indeed directly upstream of *rsfS*.

Overexpression of *rsfS* leads to elevated stationary phase survival

In addition to complementing the *rsfS* mutant, we also created strains that possessed two copies of *rsfS*, the native WT copy plus the complementing copy. Expression of *rsfS* in these backgrounds was analyzed as above by RT-qPCR. With the intergenic *rsfS* construct, we noticed that while the second copy was expressed, combining it with the native *rsfS* did not produce higher expression than the single native copy alone (Fig. 5A). Indeed, having both copies actually resulted in lower expression compared to just one at either the native or intergenic locus.

Strains in which there was an additional *rdxA* promoter (Δ*rdxA*::*rsfS* (2p)) expressed the most *rsfS* transcripts, with about a ~ 2-3 fold increase in *rsfS* expression relative to the WT (Fig. 5C). This *rsfS* double copy strain—with elevated *rsfS*--had significantly less biofilm than the WT parent strain but more than the control Δ*rdxA::kan* and Δ*rdxA::cat* strains (Supplemental Fig. 5D). Overexpression of *rsfS* using the intergenic locus (Supplemental Fig. 4, Fig 5A&C) had a more substantial effect on stationary phase CFU, leading to close to 40% more CFU compared to WT (Fig. 4B). This outcome suggests that *rsfS* expression has an important effect on controlling stationary phase CFU.

The *rsfS* gene is needed to sustain long-term infections

Our results above support that *rsfS* plays an important role in modulating *H. pylori* growth *in vitro* in specific conditions. To evaluate how these phenotypes would translate to stomach colonization, the *in vivo* behavior of the *H. pylori rsfS* mutant was evaluated. 4-6 week old female mice (C57BL/6) were orally infected with equal

amounts of either *H. pylori* WT or *rsfS* mutant, using strains that had additionally been transformed with the GFP-expressing plasmid pTM115 (Fig. 6A) (Keilberg et al., 2016). Female mice are traditionally used to study *H. pylori* infections as they yield more severe symptoms upon *H. pylori* infections (Ge et al., 2018). The mice were left infected for one or four weeks. After that time, stomachs were collected and divided into the two distinct anatomical regions called corpus and antrum. Colonization levels were assessed by plating for CFU and gland populations were analyzed by microscopy with the Bacterial Localization in Glands (BLIG) approach (Keilberg et al., 2016). After one week, both strains were detectable in the glands in both regions of the stomach, as assessed by percent of glands infected and the number of *H. pylori* per gland (Fig. 6B-D). In both regions and by both measures, the WT was found in higher numbers, with significant differences identified in the number of bacteria per gland and in total CFU (6C-E). By four weeks, the difference in the number of glands occupied had also become statistically significant in both regions (Fig 6B). In all measures, the amount of the Δ*rsfS* mutant strain decreased during this period, while the WT mostly increased. Of note, we were unable to recover live Δ*rsfS* mutant bacteria at four weeks, even though we could detect some GFP+ strains. In summary, the *in vivo* results indicate that lacking the *rsfS* gene causes *H. pylori* to have poor ability to initiate and maintain infections.

Discussion

We report here that *H. pylori* require its predicted ribosomal silencing factor, RsfS, for survival and growth in conditions that are associated with low-growth and *in vivo*. Slow growth or dormant states have been proposed to facilitate chronic infections (Bode et al., 1993; Reshetnyak & Reshetnyak, 2017a) and poor responses to antibiotic treatment in several microbes (Kaprelyants et al., 1993) . A common feature in bacterial low growth states is low translation activity (Chai et al., 2014). Ribosome inactivation has been investigated in other species and determined to be an essential physiological mechanism for low growth states (Kaprelyants et al., 1993; Song & Wood, 2020; K. S. Williamson et al., 2012). Before this work, how *H. pylori* might use ribosome inactivation remained largely unstudied. Our analysis supports that the *H. pylori* RsfS conserves certain key residues with other well-studied RsfS homologs that are important for its interactions with the ribosomal L14 protein. Deleting *rsfS* from *H. pylori* decreased the microbe's survival in stationary phase, low serum conditions, and biofilm assays, phenotypes that could be complemented by placement of an *rsfS* gene in an intergenic locus. This complementation also provided support for the prediction that there is a promoter upstream of *rsfS*. Additionally, deleting *rsfS* also caused severe deficits in *H. pylori's* ability to initially colonize mice and impaired the ability of *H. pylori* to achieve the same levels of bacteria after four weeks as WT did. The combined findings in this study lead us to propose the model that *rsfS* is needed for *H. pylori* to survive challenging growth conditions and promote low-growth states that are critical in situations such as the stomach and biofilms.

RsfS operates by binding to the L14 protein on the 50S subunit and preventing the 50S and 30S subunits from assembling into a fully assembled 70S ribosome (Fig. 1A). The interaction of RsfS and L14 is highly conserved in multiple species, as assayed using a yeast two hybrid assay (Häuser et al., 2012; Parrish et al., 2007), and in a couple species using either crystallography or sucrose gradient methods (Fatkhullin et al., 2022; Häuser et al., 2012; Khusainov et al., 2020; X. Li et al., 2016). Our analysis here shows that the *H. pylori* RsfS protein conserves at least 12 residues that have been found in other RsfS homologs to be critical for L14 interactions (Fig. 1B). Additionally, the *C. jejuni* RsfS and L14 homologs have been shown to interact as part of a global yeast two hybrid screen (Parrish et al., 2007), thus supporting that RsfS/L14 binding may be conserved in species closely related to *H. pylori*. Consistent with our analysis, Humphreys *et al.,* 2024 reported the RsfS-L14 interaction is predicted to be conserved in *H. pylori.* as well as many other bacteria including *M. tuberculosis, S. aureus, Listeria monocytogenes* and *P. aeruginosa* (Humphreys et al., 2024). That work also suggests that RsfS proteins can interact with other proteins beyond L14. Specifically, they found that *P. aeruginosa* RsfS bound a PhoH-like protein called YbeZ (Humphreys et al., 2024), although the function of this interaction is not known. Thus, it is highly likely that *H. pylori* RsfS interacts with L14 but possibly has additional targets.

Although genetic knockout and complementation experiments are a common approach to investigate the role of genes in bacteria (Tong et al., 2023), only one study has applied this approach to study *rsfS* or the *E. coli rsfA* (Häuser et al., 2012).

In that work, *E. coli* Δ*rsfA* had defects in stationary phase and nutrient conditions that could only be corrected by complementing with the entire four gene *rsfA* operon but not *rsfA* alone (Häuser et al., 2012). *E. coli rsfA* and *H. pylori rsfS* do not have the same operon structure. Replacing *H. pylori rsfS* with *cat* did not significantly affect the transcription of other genes in the operon, indicating our mutation was not polar as was observed in *E. coli* (Supplemental Fig. 1), and we were able to complement the mutant with only *rsfS* in a non-native locus (Fig. 4).

The first phenotypes we investigated with the *H. pylori rsfS* null mutant were planktonic growth (Fig. 2). Three conditions were initially found to significantly delay the growth of *rsfS* knockout mutants: frequent disruptions in shaking for measurements obtained in a plate reader (Fig. 2A), low serum conditions (Fig. 2B), and repeated exposure to atmospheric conditions using a continuous growth curve approach (Fig. 2C). The growth impairment due to fluctuations in growth conditions matches the conclusions made with *E. coli rsfA* (Häuser et al., 2012), prompting these authors to conclude that RsfA played a role in adaptation to stressful growth conditions. When bacteria are starved for nutrients, they are able to mount a coordinated response that alters transcription, decreased ribosome biogenesis, and other effects (Akiyama & Kim, 2023). One known pathway is the stringent response that depends on a signaling molecule called ppGpp (Brown et al., 2016). Although ppGpp has not been extensively characterized in *H. pylori,* it does contain *spoT* and *relA* homologues that have been associated with response to fluctuating growth conditions including nutrient starvation, acidic conditions, stationary phase and

aerobic shock (Mouery et al., 2006; Wells & Gaynor, 2006). Given that our findings support that *rsfS* is needed by *H. pylori* to mitigate stressful growth conditions, RsfS may be a part of *H. pylori's* stringent response as well. Using the endpoint growth curve approach (Supplemental Fig. 2), we were able to mitigate these limiting growth factors that could complicate our analysis of the *rsfS* null mutant phenotypes (Fig. 2C). Without these additional complexities, it became clear that *H. pylori rsfS* knockout mutants have defects in stationary phase and low serum conditions, similar to phenotypes reported in *E. coli rsfA* mutants. Overall, these data further indicate that *H. pylori* RsfS homologues have a function that is conserved in *E. coli* toward responding to challenging growth conditions.

We report here that *H. pylori rsfS* is required for biofilm formation. Based on our endpoint growth curve experiment, we were able to identify a time point at which the *rsfS* mutant did not have a growth defect compared to WT (Fig. 2D). We used cultures grown to this time point, 20 hours, for biofilm and mouse inoculation to mitigate growth effects in these assays. Previous work had shown that *rsfS* was upregulated in *H. pylori* biofilms cells relative to unadhered cells (Hathroubi et al., 2018). In the work herein, we found that *H. pylori rsfS* mutants had consistent biofilm defects under a variety of conditions that could not be compensated for with longer incubations (Fig. 3), but could be complemented by ectopic *rsfS* expression (Fig. 4). SEM imaging further corroborated that the *rsfS* mutants were unable to form robust multi-layered aggregates as seen in WT. Given that biofilms also contain slow-growing populations, the findings appear consistent with the planktonic growth

phenotype in noting that *H. pylori* needs *rsfS* during slow growth. Whether RsfS homologs are needed for biofilm formation in other bacteria remains to be determined.

Our first approach to complement the Δ*rsfS* mutant was to utilize the *rdxA* locus. This approach failed as, to our surprise, *rdxA* itself is needed for biofilm formation and stationary phase survival (Supplemental Fig. 5). Defective phenotypes that are similar between loss of *rdxA* and *rsfS* suggest that both are needed for challenging growth conditions. We therefore generated a distinct complementing strain, with *rsfS* inserted in a previously used intergenic region (Langford et al., 2006). This approach allowed the *rsfS* mutant phenotypes to be complemented, confirming *rsfS* itself is required for biofilm formation and stationary phase growth (Fig. 4). Overall, these results provide strong support for the idea that the *H. pylori* SS1 mutants described here are defective only for *rsfS*.

Previous work had predicted that *rsfS* was the first gene in a four gene operon (Supplemental Fig. 1A), with a transcriptional start site located 26 basepairs from the first *rsfS* codon, and a presumed promoter about 60 basepairs from the first codon (Bischler et al., 2015). RT-qPCR in this work confirmed that the 200 bp upstream of *rsfS* was sufficient for expression in both the *rdxA* and intergenic loci (Fig. 5). Furthermore, *rsfS* was still expressed when the *rsfS* gene and its upstream region were inverted within the *rdxA* locus (Fig. 5) further supporting the existence of a promoter in this 200 bp region.

To further investigate the role of *rsfS* in *H. pylori* growth *in vivo,* mice were infected with the mutant or WT and analyzed for both CFU and stomach gland populations. By some measures, the mutant was able to initiate a reasonable infection, e.g. the percentage of glands infected at 1-week were similar between the *rsfS* mutant and the WT (Fig. 6B), but at this time the *rsfS* mutant population in the glands and total CFU were significantly less than with WT (Fig. 6D, E). Thus, it can be concluded that the Δ*rsfS* mutant can establish initial colonization but at significantly lower numbers. After four weeks, the Δ*rsfS* mutant could be visualized in the glands (Fig. 6 B,C,D), but the bacteria were not able to be re-cultured from the mice (Fig. 6E). These results suggest that RsfS contributes to *H. pylori* colonization and persistence *in vivo*, consistent with the idea that this protein supports survival in low-growth states and under stressful conditions encountered in the mammalian stomach.

Our study finds that the only known ribosome regulation factor in *H. pylori,* RsfS is required for this bacterium to survive during slow growth and other challenging conditions including murine stomachs. Based on similarity to other well characterized homologues, *H. pylori* RsfS likely interacts with ribosomal L14 and contributes to ribosome silencing. How this process contributes to survival during slow growth is not well understood, with the idea that RsfS slows translation and/or protects ribosomes (Fatkhullin et al., 2022). Regardless, our work suggests that eliminating or blocking RsfS would render *H. pylori* less able to survive low-growth states and chronic infections *in vivo*.

Acknowledgements

The described project was supported by the National Institute of Allergy and Infectious Disease (NIAID) grants R01AI164682 and RO1AI116946 to K.M.O and F31AI176804 to Y.O.E. The authors are grateful to Ottemann lab members Jashwin Sagoo for help with the transcriptional start site mapping, Dr. Jiunn Fong for help with cloning, Dr. Shuai Hu for help with mouse experiments and cloning approaches. In addition, they are grateful to Dr. Frances Yap (Northwestern) for input on ribosomal regulation topics, Dr. Fitnat Yildiz (UC Santa Cruz) for insight on biofilm phenotypes and all members of the Ottemann lab for support and input on this project.

Methods and Materials

Sequence Analysis for *H. pylori* L14 and RsfS

Clustal Omega program (https://www.ebi.ac.uk/jdispatcher/msa/clustalo) was used to generate guide trees that compared the genetic conservation of *rsfS* and *L14* of *H. pylori* relative to species that were investigated in Häuser, Roman, et al. (2012). Protein sequences were obtained via UCSC microbes genome browser (https://toolkit.engineering.ucsc.edu/website-support/maintenance/) and Open Reading Frames sequences using default parameters were obtained for analysis. The Clustal Omega program was also used to align RsfS and L14 protein sequences of *E. coli* (Grenier et al., 2014), *S. aureus* (Kuroda et al., 2001) and *M. tuberculosis* (Lew et al., 2011) to *H. pylori* one by one to identify whether amino acid residues that were previously identified to be critical to RsfS-L14 binding are conserved.

H. pylori Strains and Growth Conditions

H. pylori strain SS1 (A. Lee et al., 1997) was used as a wild type control for all assays and the parent strain to generate mutant strains (Table 1). All *H. pylori* strains were incubated at 37°C under microaerobic conditions with 5% O_2, 10% CO_2, and 85% N_2. All chemicals are from Thermo Fisher or Gold Biotech unless otherwise indicated. Media consisted of Columbia Horse Blood Agar (CHBA) base with the addition of 0.2%-*β* cyclodextrin dissolved in dimethyl sulfoxide, 10 µg of vancomycin per ml, 0.025 µg of cefsulodin per ml, 0.0125 U of polymyxin B per ml, 50µg of cycloheximide ml, 5% (vol/vol) defibrinated horse blood (Hemostat Labs). For antibiotic resistance marker selection, CHBA was supplemented with 15 µg of chloramphenicol (Cm) per ml, 15µg of kanamycin (Kan) per ml or 1 µg of

erythromycin (Erm) per ml. Liquid cultures were grown in Brucella Broth (Fisher Scientific) with 10% heat-inactivated Fetal Bovine Serum (Gibco) resulting in the media abbreviation BB10. For long term storage, strains were stored at -80°C in brain heart infusion media supplemented with 10% heat-inactivated fetal bovine serum, 1% (wt/vol) β-cyclodextrin, 25% glycerol, and 5% dimethyl sulfoxide.

Creation of *H. pylori* Mutants

All *H. pylori* transformations were done using natural transformation protocols, by either adding DNA directly to plate grown *H. pylori* or to *H. pylori* scraped from the plate into BB10 (S. Hu et al., 2023). In all cases, *H. pylori* was incubated on selective media until single colonies were detectable, and then single colonies were colony purified before collecting for storage at -80C. In all cases, genome modifications were analyzed using PCR products from genomic DNA preparations (Promega Wizard Prep) that flanked or were within the region or interest with Q5 High Fidelity 2X Master Mix. PCR products were purified using GFX Gel Band and PCR Purification Kit (Ge28-9034-71) analyzed by both agarose gel electrophoresis and DNA sequencing (Azenta), and in some cases by RT-qPCR for gene expression.

To create *H. pylori* Δ*rsfS* deletion mutants (HP1414, HPYLSS1_1340 in the *H. pylori* 26695 (Tomb et al., 1997) and SS1 genomes (Draper et al., 2017) respectively, a synthetic construct called pTwist *ΔrsfS::kan* (Supplemental Fig. 2), was created that contains a kanamycin resistance gene (*aphA*3, Kan^R) flanked by upstream and downstream regions of *rsfS,* designed to replace the *rsfS* gene (HPYSS1_1340/HP_1414) with the a*phA3* to generate *H. pylori ΔrsfS::kan.* This

plasmid was stored in *E. coli* DH5α using ampicillin selection, and isolated using a miniprep approach with QIAprep Spin Miniprep Kit. The resulting plasmid was used for natural transformation to transform *H. pylori* SS1 WT to Kan^R. To swap the *aphA* gene for chloramphenicol resistance, the *H. pylori* SS1 *ΔrsfS::kan* strain was transformed with a kan2cat plasmid (KO#1579, Table 1) containing a *cat* (Cm^R) gene flanked by *aphA3* sequences and selecting for chloramphenicol resistance resulting in *ΔrsfS::cat* (KO#1830) . Genomic DNA (2µg) from *ΔrsfS::cat* was then used to transform into SS1 pTM115 (KO#529) by adding directly to patches of colonies that previously incubated for 5 hours. Transformations were incubated overnight and then streak plated onto CHBA supplement with Cm to select for colonies containing the *ΔrsfS::cat* allele. Transformants were then visualized under the microscope to check for GFP positive fluorescence to ensure the strain *ΔrsfS::cat* pTM115 (KO#). Transformants were analyzed by PCR using primers that flank the *rsfS* sequence, specifically targeting 263 bp upstream and 335 bp downstream relative to the *rsfS* sequence called *rsfS* flanking Forward and *rsfS* flanking Reverse (Table 2).

To create complementation strains with *rsfS* insertions in the *rdxA* locus, synthetic plasmids (Twist Bioscience) were designed that contained the full *rsfS* gene and its potential promoter according to the annotations in the 26695 genome, an erythromycin resistant gene (*erm*) and sequences from *rdxA* to promote integration at that chromosomal locus (Supplemental Fig. 4). Plasmids were maintained in *E. coli* DH5α using ampicillin. *H. pylori* SS1 WT or *ΔrsfS* strains were used as parent strains for transformation and colonies were selected on CHBA supplemented with Erm to

select for *rsfS-erm* integration in *rdxA*. Chromosomal integration of the *rdxA::rsfS* transformants was confirmed by PCR with primers (1) targeting the upstream region of the *rdxA* locus and the gene using primers "Double Promoter Left *rdxA* flanking-*rsfS"* and "Single Promoter Left *rdxA* flanking-*rsfS"* (Table 2)*;* (2) targeting the *rsfS* gene from the insert and the downstream region of the *rdxA* locus using primers "Double Promoter *rsfS*- Right *rdxA"* and "Single Promoter *rsfS*- Right *rdxA".* Complementation strains were created by inserting *rsfS* in an intergenic region between HP_0203and HP_0203, as used in Langford et al. 2006. Gibson assembly was conducted using the following four fragments: (1) Left intergenic, (2) 200bp upstream region, *rsfS* ORF, 29bp downstream intergenic, (3) *cat* resistance cassette and (4) Right intergenic. The template containing *rsfS* with predicted promoter was obtained from *H. pylori* SS1 genomic DNA by PCR with primers *rsfS* flanking Forward and Reverse (Table 2), and then further amplified to synthesize the second fragment with overhangs for Gibson assembly. The second fragment was synthesized to include the *rsfS* ORF, 200bp upstream the *rsfS* ORF to account for a promoter and 29bp of intergenic region downstream *rsfS* ORF using the Gibson *rsfS* primer set (Table 2). The flanking intergenic regions were synthesized from SS1 WT gDNA using primer set NF023_iSS1 primer set and used as a base template to synthesize first and fourth fragments with Gibson overhangs. The first fragment was synthesized using the primer set Gibson 193 which also added overhanging sequences for Gibson assembly (Table 2). The template for the fourth fragment was initially generated from the purified intergenic region PCR product using primer set HPSS1_0192 (Table 2).

The resulting PCR product was purified so Gibson overhangs could be added using primer set Gibson HPSS1_0192 creating the fourth fragment (Table 2). The third fragment containing the *cat* gene was then generated using purified PCR products generated from Δ*rsfS::cat* gDNA using *rsfS* flanking primer set (Table 2). The purified PCR product from *rsfS* flanking primers were then used to synthesize the *cat* gene template using primer set CAT SOE (Lowenthal et al., 2009). Gibson overhangs were then added to the *cat* gene template with primer set Gibson CAT primer set creating the third fragment (Table 2). All four fragments were synthesized and purified and stored in 4 degrees for no less than 24 hours prior to Gibson assembly with the plasmid backbone.

To construct the backbone to complete the Gibson assembly, pUC-19 plasmids were isolated from KO#137 (SY327 pUC19) using Qiagen miniprep kit (CAT# 27106). The pUC-19 plasmid was then linearized using High Fidelity Restriction Enzyme Hind III (CAT#R3104S) using manufacturer instructions, then immediately purified and used as template to add Gibson overhangs using Gibson Int-pUC-19. The resulting PCR product was purified immediately resulting in a plasmid backbone with Gibson overhangs added. The initial templates generated through PCR from Hp gDNA, the resulting fragments that were synthesized with Gibson overhangs and the linearized pUC-19 plasmid with Gibson overhangs were purified using Genomic DNA Clean & Concentrator™ Kits, Zymo Research CAT# 77001-150 (KT).

All PCR reactions for gibson assembly were conducted with Q5 Master Mix, NEB, Q5 2X Master Mix CAT# M0492S. Gibson assembly was then conducted using

NEBuilder HiFi DNA Assembly Master Mix CAT#E2621L, fragment concentrations were determined by using the NEB HiFi calculator provided and used to make 20 uL reactions of 4 fragments and linearized pUC-19 plasmid with Gibson overhangs combined with 10uL of master mix. The reaction was incubated according to protocol recommendations for 4-6 fragment reactions, 50°C for 1 hour. The resulting plasmid was then transformed into *E. coli* DH5α and colonies that up took the Gibson plasmid were selected by supplement LB agar with Chloramphenicol (20µg/mL). Chloramphenicol resistant colonies were streak plated and plasmids were isolated using the QIAprep Spin Miniprep Kit were sent to AZENTA for whole genome sequencing. Upon the verification of the insert sequence remaining intact without SNPs, mutations or truncations, the resulting DH5α isolate containing the *pIG::rsfS* (KO#2056) was cultured in liquid LB supplemented with Cm and mixed with 80% glycerol and stored in -80°C long term.

H. pylori transformations were then conducted with the plasmid *pIG::rsfS* (KO#2056) isolated via QIAprep Spin Miniprep Kit to insert *rsfS* gene copy in the defined intergenic region (Langford et al., 2006). *H. pylori* strain SS1 WT (A. Lee et al., 1997) was used as a parent strain with transformation of *pIG::rsfS* (KO#2056) plasmid on CHBA supplemented with Cm and confirmed by PCR using primer set NF023_iSS1 primer set (Table 1, 2). To create the complementation construct, this strain was transformed with pTwist *ΔrsfS::kan* (KO# 2052) to delete the native copy of *rsfS*; the resulting transformation was selected on CHBA supplemented with Kan and Cm and verified by PCR using primer set *rsfS* flanking (Table 1, 2).

H. pylori growth assays

For growth assays in the plate reader, *H. pylori* strains were grown initially overnight in BB10 with shaking for 12-15 hours in tubes or flasks. Overnight cultures were normalized to OD_{600} of 0.1 and used to inoculate 96-well flat bottom, non-treated clear polystyrene with low evaporation lid (Corning cat#7200656)to a final volume of 200uL in the desired media (BB10 or BB2). Microplate growth assays were conducted using CLARIOstar^{Plus} Microplate Reader (BMG LABTECH) with microaerobic conditions (double orbital shaking 200 rpm) with 5% O_2, 10% CO_2 and 85% N_2 at 37˚C. OD_{600} was measured hourly throughout the assays.

Overnight BB10 cultures were inoculated from CHBA-plate grown *H. pylori* and incubated for 12-15 hours in BB10, using 3 mL in a 15 mL falcon-style tube. Endpoint and monoculture replicates were normalized to an OD_{600} of 0.1 at the start of the experiment, followed by incubation (shaking) under microaerobic conditions with 5% O_2, 10% CO_2 and 85% N_2 at 37˚C. Samples for optical density (OD_{600}) and colony forming units (CFU/mL) were collected by removing 100uLfor each type of analysis at the desired time point.

Biofilm Assays

Biofilm phenotypes were analyzed using a protocol previously adapted to *H. pylori* (Hathroubi et al., 2018). *H. pylori* strains were grown for 20h with shaking in BB10 using 3 mL in 15 mL falcon-style types. After growth, the cultures were diluted to an OD_{600} of 0.15 using fresh media (BB only, BB2 or BB10). 200uL per well was inoculated in sterile 96-well polystyrene microtiter plates (Costar#3370). Plates were

incubated in static microaerobic conditions (5% O_2, 10% CO_2, 85% N_2) for 72h. Media was removed from the wells via pipetting, and the remaining biofilms were stained with 300uL of crystal violet (0.1% wt/vol) at room temperature for 3 minutes. The crystal violet solution was then removed by pipetting and the wells were washed with 300ul of 1X phosphate-buffered saline (PBS) twice. After these steps, the plates were dried for 20 minutes at room temperature and 300uL of ethanol (95% vol/vol) was added to the wells and incubated at room temperature for 10 minutes. After this period, optical density at 595 nm was measured.

To collect biofilms for SEM imaging, the initial overnight growth and back dilution were the same except the back diluted cultures were inoculated into μ-Slide 8-well glass bottom plates (ibidi, Germany #80826) followed by the placement of 12mm diameter 1/2oz EM cover slips (Electron Microscopy Sciences) in each well diagonal, so biofilms could form on the slide at the liquid-air interface on the acute angle side. The cover slips were static in microaerobic conditions as described above for 72h. The cover slips were then removed and rinsed with PBS before fixation at room temperature for 1h in 2.5% glutaraldehyde. After fixation, serial dehydration steps were conducted by placing the coverslips for 10 minutes, room temperature in progressively higher amounts of ethanol: 25%, 50%, 75%, 90% and 100% (100% step was repeated twice). The coverslips containing the fixed biofilms were then left in the final 100% ethanol solution until SEM imaging was conducted shortly afterwards within the hour.

RNA Extractions

RNA extractions done using the Purelink RNA Minikit (CAT#12183018A) from H. pylori grown as described above. Bacterial cells were collected, suspended in TRIzol, and stored in -80°C until RNA isolation. TRIzol-suspended samples were thawed at room temperature before the addition of chloroform. Samples were shaken by hand until thoroughly mixed prior to being incubated at room temperature for 3 minutes. Samples were centrifuged at 15,000 × g for 15 minutes at 4ºC which caused phase separation of the mixture into a lower pink phenol-chloroform phase, an opaque white interphase, and a clear upper phase containing RNA. The phase containing RNA was transferred to a new tube and an equal volume of 70% ethanol (final concentration ~35%) was added and mixed by vortexing and vigorous inversion to disperse any precipitate. The homogenized mixture was placed in a Purelink RNA Minikit spin cartridge, and manufacturer's instructions followed with an additional on-column DNase treatment using Turbo DNA-Free Kit (Invitrogen ThermoFisher CAT# AM1907) for 15 minutes at room temperature. After this step, the column was washed four times at 4ºC with wash buffer 1 and then wash buffer 2, followed by a repeat of both steps. After washing, the column was dried by centrifugation at 15,000 × g for 1 minute at 4ºC. RNase–Free water was added to the membrane and incubated at room temperature for 1 minute prior to eluting the extracted RNA by centrifuging for 1 minute at 15,000 x g at 4ºC. RNA yield and quality was quantified using a Nanodrop spectrometer. RNA was stored at either -80°C long-term or in4°C for immediate processing into cDNA.

cDNA synthesis

RNA was synthesized into cDNA using High-Capacity cDNA Reverse Transcription Kit with RNase Inhibitor (Applied Biosystems/Thermo Fisher CAT#4374966) using the manufacturer's recommendations. 1ug of RNA for each sample was used for cDNA synthesis and diluted with RNase- Free water to meet the total recommended volume of 10ul. One technical replicate of cDNA synthesis was conducted per biological RNA replicate. A no RNA template control (NTC) and a no-reverse transcriptase control (No RT) were added to assess contamination.

RT-qPCR protocol

RT-qPCR was performed using reagents from the Power SYBR™ Green PCR Master Mix kit (Applied Biosystems#4367659) and a Bio-Rad CFX96 Real Time PCR Detection System. All reactions were carried out with 1µL of the cDNA reaction (synthesized from 1µg of RNA) mixed with 5 µM each of the forward and reverse primers for the target gene, 10 µl of PCR Master Mix, and water for a total volume of 20 µL per reaction a. The thermal cycling conditions were executed as the following: Step#1- 95ºC for 10 minutes, 40 cycles of denaturing at 95ºC for 15 seconds and Annealing/extension at 60ºC for 1 minute with a final melting curve step for 5 seconds. No template and no-reverse transcriptase controls were used as controls. Four to five technical replicates for each primer set were conducted for each biological RNA replicate.

Soft Agar Assays

Soft agar plates that were made using Brucella broth (BB) media, 2.5% heat-inactivated Fetal Bovine Serum and 0.35% (w/v) agar and supplemented with *H. pylori* selective antibiotics: 50µg of cycloheximide per mL, 10µg of vancomycin per ml, 5µg of cefsulodin per ml, 2.5 U of polymyxin B per ml (Thermo Fisher or Gold Biotech). Soft agar plates were inoculated by using a sterile micropipette tip and picking bacteria from CHBA plates and inserting the tip containing bacteria into the soft agar. The soft agar plates were incubated in microaerobic conditions at 37°C for 6 days prior to measurement.

Ethics Statement

The University of California Santa Cruz Institutional Animal Care and Use Committee approved all animal protocols and experiments (protocol OTTEK2405). All animal procedures used were in strict accordance with the Guide for the Care and Use of Laboratory Animals. Female C57BL/6N mice (Helicobacter free; Charles River), ages 4-6 weeks, were housed at the University of California Santa Cruz animal facility

Mouse Infections

Prior to infection, *H. pylori* strains were grown overnight for 16-20h hours in BB10, collected by centrifugation, normalized to an optical density at 600 nm of ~ 1, and then 500 µl was used via gavage. Infection cultures from *H. pylori* SS1 pTM115 or its isogenic Δ*rsfS*::*cat* derivative were serially diluted and plated to assure similar amounts of CFU between both strains were used in the infectious dose. Mice were

sacrificed at 1 and 4 weeks. using CO_2 narcosis followed by cervical dislocation to confirm death prior to dissection to extract the stomach for both infection methods.

Stomach Extraction

The stomach was extracted by severing the stomach-esophageal junction and the antrum-duodenum sphincter using scissors. The stomach was then opened along the lesser curvature from antrum to for stomach and then the contents of the stomach (food and debris) were removed by rinsing the internal side of the stomach in 1X phosphate-buffered saline (PBS). The stomach was then spread out using pins and the forestomach was removed. The stomach was sectioned into corpus and antrum based on the anatomical orientation of the stomach and tissue coloration, with the corpus identified as pink versus the antrum as translucent/white.

Stomach Bacterial Numbers

The tissue collected for total bacteria number was weighed then homogenized using the Bullet Blender (Next Advance) with 1.0-mm zirconium silicate beads. The resulting homogenate was serially diluted and plated on CHBA supplemented with 10ug/ml nalidixic acid, 20ug/ml bacitracin and 1000X HP (5 µg/ml trimethoprim and 8 µg/ml amphotericin B) to select for *H. pylori*.

Gland isolation

The gland isolation protocol utilized in this study was a protocol from a previous study (Keilberg et al., 2016). Dissected gastric tissue from both regions was cut into approximately 6 X 4 mm rectangles, which were then incubated at 4°C for 3-4 hours with slight shaking in Dulbecco's phosphate-buffered saline (DPBS) supplemented

with 5 mM EDTA. Tissue samples were transferred to DPBS supplemented with 1% sucrose and 1.5% sorbitol then subsequently stained with 2uL of Hoechst DNA stain (Life Technologies). The tissue suspensions were put on ice to settle. A total of 100 glands were counted for gavage infection and 200 glands were counted for micro-pipette infection. Bacteria per gland (sample size for gavage: 100 glands) were counted in each region to calculate how many glands were infected and the average bacteria per gland.

Figures and Legends

Fig. 1.

Fig. 1. *H. pylori* contains RsfS Homologues. (A) Model for how the RsfS ribosomal silencing protein functions by binding to L14 protein on the large ribosomal subunit 50S, preventing assembly with the 30S subunit and formation of a 70S ribosome that can translate mRNA to polypeptides. **(A)** *H. pylori* RsfS **(**O25960) homologue was aligned with RsfS homologues from *S. aureus* (W8TVV3), *E. coli* (P0AAT6) and *M. tuberculosis* (A0A045I766) colored using C-alpha (Cα) RMSD analysis. Dark blue indicates low RSMD score/high structural alignment. Light blue indicates moderate RSMD score/slight variances in structural alignment. Yellow, orange and red indicate high RSMD/distinct structural difference with yellow representing the lower end of the spectrum, orange representing the middle and red representing the highest. **(B)** RsfS and **(C)** L14 protein alignment for *H. pylori*, *S. aureus*, *E. coli* and *M. tuberculosis*. Secondary structures as predicted by alpha fold are color coded as the following: α-helices (pink), β-sheet (green) and coils (blue). RsfS residues that were found to be critical for binding to L14 via crystallography structures that are conserved in *H. pylori* are annotated in highlighted text beneath the sequence alignment. Residues that were not identified in previous studies but conserved in all three species are annotated as such (*). **(D)** Predicted electrostatic bond for *H. pylori* RsfS (Red) and L14 (Blue) homologues based on published Cyro-EM structure in *S. aureus* (PBD: 6SJ5).

A.

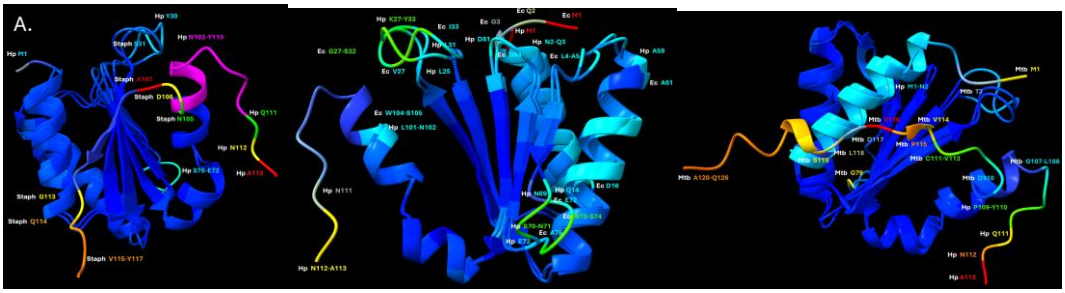

B.

```
H. pylori            M  NQRI------ETITALLDE KKA FDITHID    LSKTPYLVE DVIIATT LA NKHALSLLDALKNTL    57
S. aureus       ----MN  SQELLAIAVDAID      NKKG EDTISLE    MKGISDMTD YFVVTHG NN ERQVQAIARAVKEVANE  61
M. tuberculosis  MTAN  REAIDMARVAAGAAAA     KLA DDVVVID     VSGQLVITD CFVIASG SN ERQVNAIVDEVEEKMRQ  65
                                           *K*  *D*I23,D24  S26        I37,A38              K54

H. pylori          KPLGEVFY- QID  ESNEE  WILLD LGD LMIHLFT EECRKKF D LEGFLNAYK RGLPYQNT   113
S. aureus          QNIEVK    RME  GYNEAR WILID LAD VVVHVFH KDERNYY N IEKL      YQDAPL-ESY   SQV AY 115
M. tuberculosis    AGYRPA    RREG AREGR WILLD YRD IVVGHIQH QDDRNFY A LDRL      WGDCPV-VPVDLSANSAGAQ     119
                             W74,L77,D78 D81   H85    *R*    L97
```

C.

```
                                                                                  ******X**:*.X.****:**
E. coli          MIQEQTMLNVADNSGARRVMCIKVLGGSHRRYAGVGDIIKITIKEAIPRGKVKKGDVLKAVVVRTKKGVRRPDGSVIRFDGNACVLLNNNSEQPIGTRIFGPVTREL-SERFMKIISLAPEVL 123
H. pylori        MIQSFTRLNVADNSGAKEIMCIKVLGGSHKRYASVGSVIVASVKKAIPNGKVKRGQVVKAVVVRTKKEIQRKNGSLVRFDDNAAVILDA-KKDPVGTRIFGPVSREVVNYDNFKMIISLAPEVV 122
S. aureus        MIQQETRLKVADNSGAREVLTIKVLGGSGRKTANIGDVIVCTVKNATPGGVVKKGDVVKAVIVRTKSGVRRNDGSYIKFDENACVIIRD-DKGPRGTRIFGPVTRELMDNFKMIVSLAPEVL 122
M. tuberculosis  MIQQESRLKVADNTGAKEILCIRVLGGSSRRYAGIGDVIVATVKDAIPGGNVKRGDVVKAVVVRTVKERRPDGSYIKFDENAAVIIKP-DNDPRGTRIFGPVTRELMDRFKMIISLAPEVL 122
                                                                                  Arg97   Arg107 Lys111
```

D.

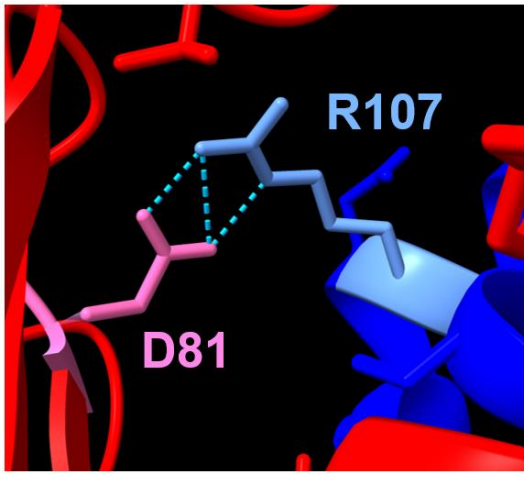

Fig. 2.

Fig. 2. Growth analysis of *H. pylori* Δ*rsfS* mutant. Growth analysis of *H. pylori* SS1 WT (blue and light blue) and its isogenic *ΔrsfS* strains (red and light red) grown in either BB10 or BB2. **(A-B)** Growth analysis carried out in 96-well microtiter dishes. Biological replicates (n=4) and technical replicates for each timepoint (n=30-75). **(C-F).** Growth analysis carried out using flasks in the incubator (biological replicates n= 4-6) with measurements of colony-forming units at the indicated times. **(C)** Continuous growth approach in BB10. **(D-F)** Endpoint growth approach in **(D)** BB10 or **(E)** BB2. Pairwise T- test analysis was used to compare WT to mutant at matched times, with P values indicated as <0.001 (***) and <0.0001 (****).

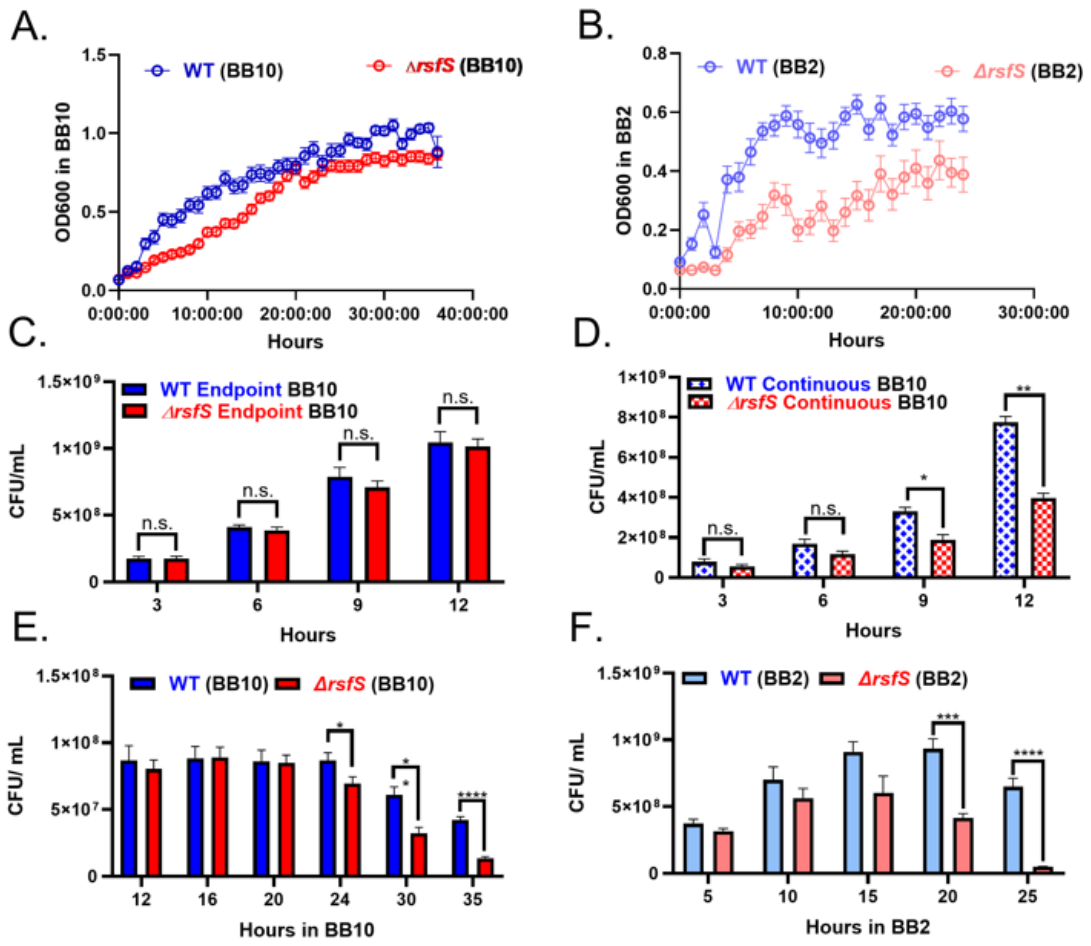

Fig. 3.

Fig. 3. *H. pylori* Δ*rsfS* mutants are weak biofilm formers. Temporal analysis of biofilm formation in various media. Four biological replicates of the WT control (blue) and *ΔrsfS* (red) biofilms were grown in 96-well plates, stained with crystal violet and OD_{595} was measured at the indicated times. **(A)** BB2 (technical replicates 105-252). **(B)** BB10 (technical replicates 35-115). **(C)** No serum (BB only) (technical replicates 38-136). Statistical analysis comparing WT and mutant using T test. **(D)** Biofilms and their flagellar filaments in BB2 were formed on glass cover slips for 3 days and imaged using scanning electron microscopy **(**SEM) for both *H. pylori* WT and Δ*rsfS.* Pairwise T- test analysis was used to compare WT to mutant, with P values indicated as <0.0001 (****).

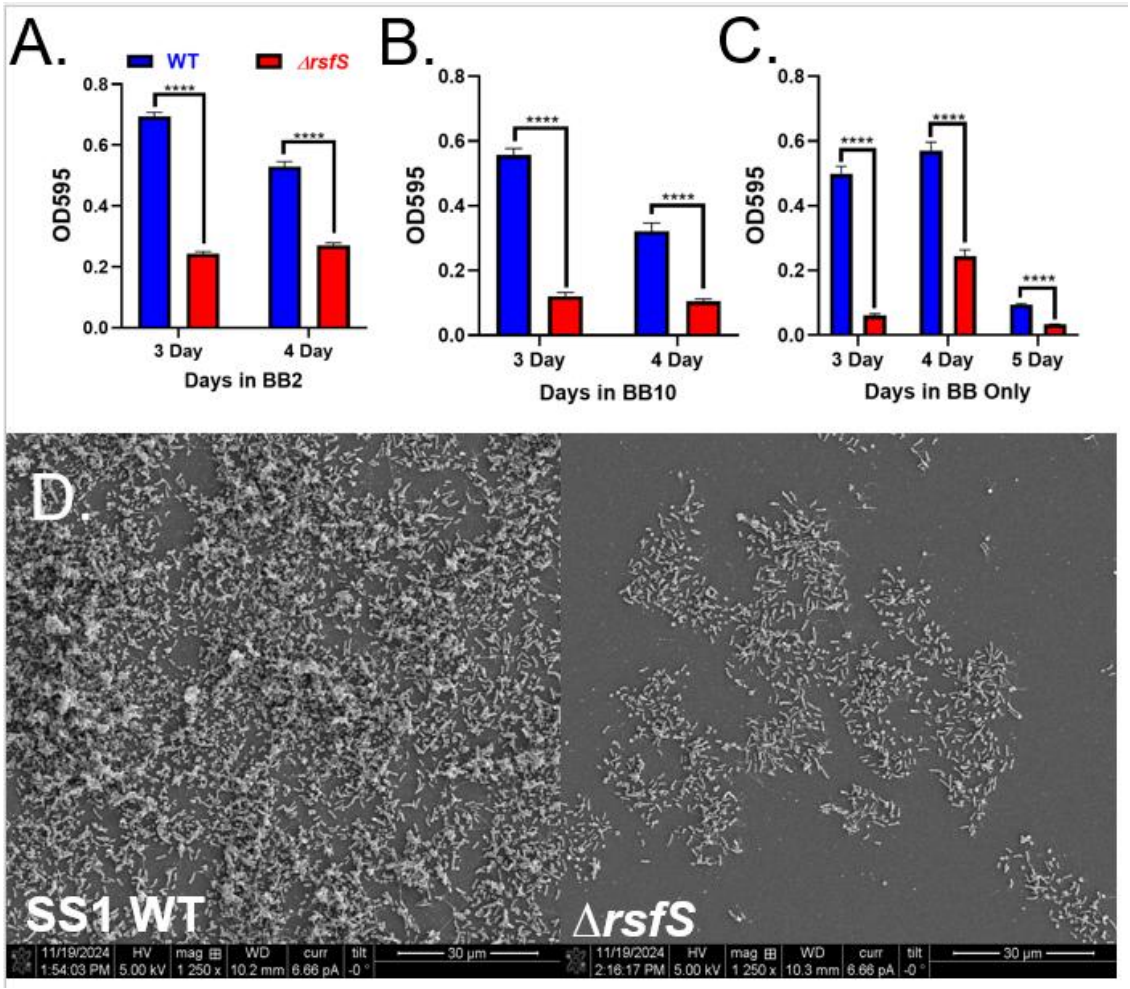

Fig. 4.

Fig. 4. *rsfS* mutants are complemented by insertion of an exogenous copy of *rsfS*. *rsfS* with 200 bp upstream and a chloramphenicol resistance marker (*cat*) was integrated into the intergenic region between HP0203 and HP0204 in either the Δ*rsfS* mutant (1X *rsfS*) or WT (called 2X *rsfS).* **(A)** Biofilms were grown in BB2 for the 3 days and analyzed by crystal violet staining (OD_{595}). 4 biological replicates per strain, with technical replicates of WT, 20; *ΔrsfS::cat*, 21; 1X *rsfS*, 84; and 2X *rsfS,* 100. Students T test analysis was conducted comparing each strain to WT, p value <0.0001, ****. **(B)** The endpoint growth approach was used to compare CFU yields during exponential (t=20h) and stationary (t= 24h) phase growth in BB10. T- test analysis was used to compare each strain to WT (P-value <0.01, **).

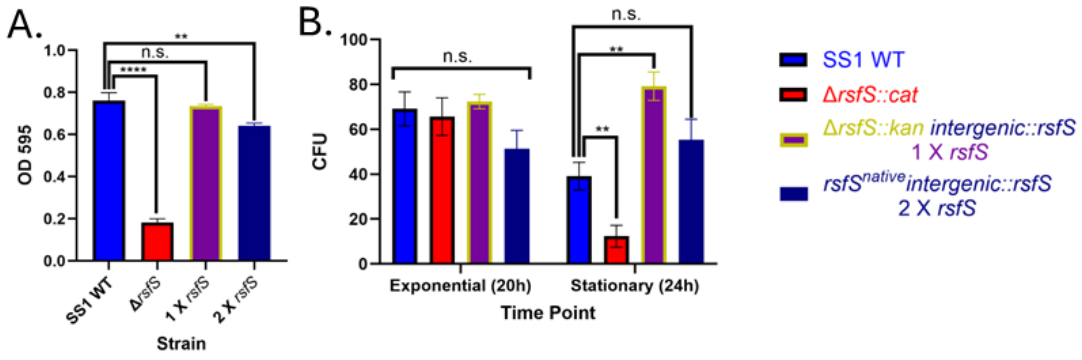

Fig. 5.

Fig. 5. *rsfS* possesses an upstream promoter that contributes to its expression. RT-qPCR was conducted on RNA isolated form 4-6 biological replicates to determine the expression **(A)** target *rsfS* gene **(B)** reference *gapB* gene to assure RNA quality. Cq Values are plotted with mean and standard deviations values of ~0.3 to ensure qPCR and RNA quality within strains. Single promoter and double promoter constructs are indicated as (1p) and (2p) respectively. Technical replicates are annotated at the top of the bars whereas means are annotated at the bottom on the bars. **(C)** ΔCt was calculated by subtracting the target gene Cq value (*rsfS*) by the reference gene Cq value (*gapB*).

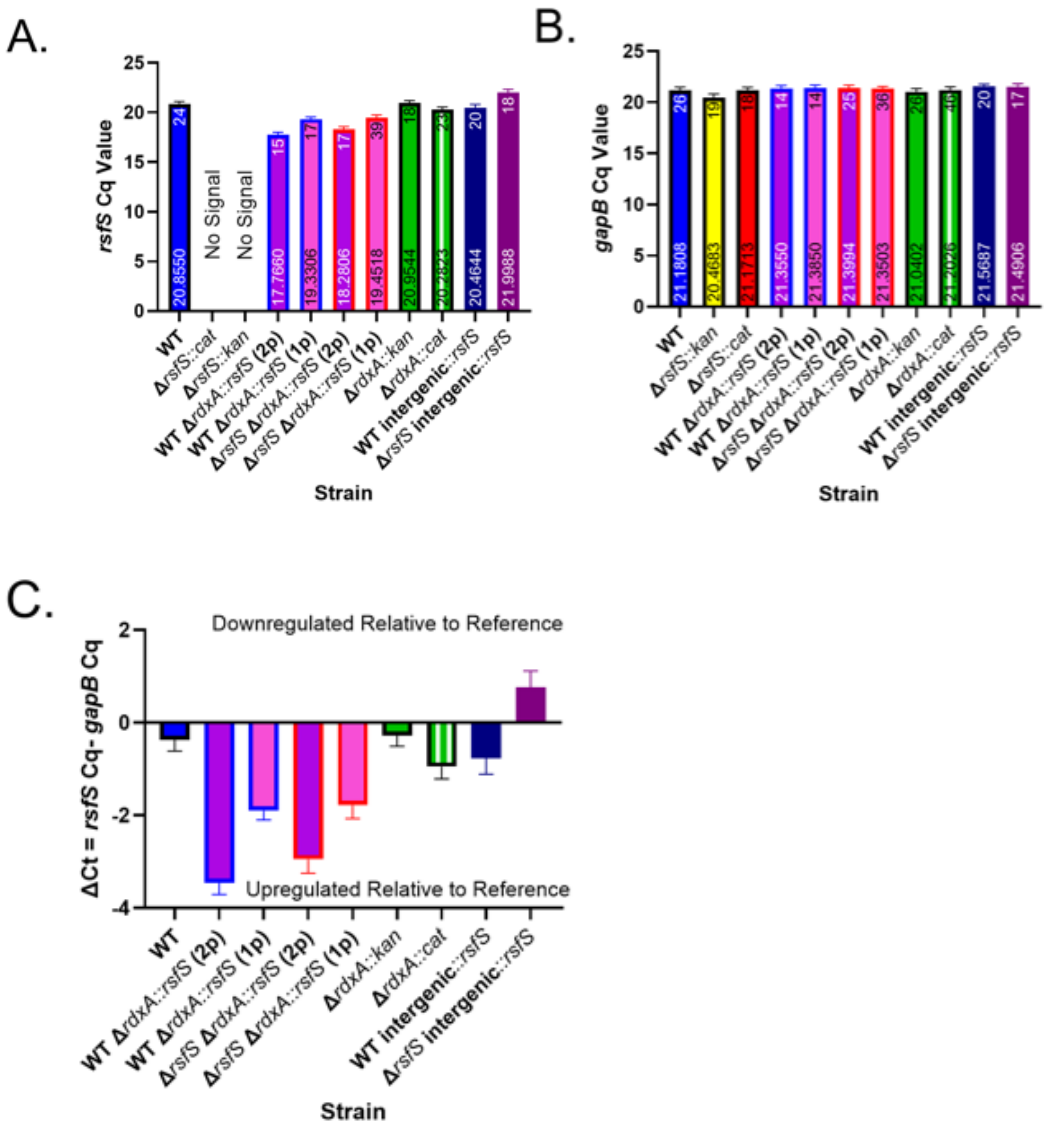

Fig. 6.

Fig. 6. Δ*rsfS* mutant colonizes mice initially but fails to sustain long-term infections. Two sections of the stomach (antrum and corpus) from n=20 mice were used to compare the phenotypes of Δ*rsfS* and the control SS1. **(A)** Six technical replicates were serially diluted and plated to assure similar amounts of inoculums were used. Using BILG, 100 gastric glands (both occupied and unoccupied) from each stomach section were analyzed to calculate **(B)** the percentage of glands infected by *H. pylori,* the population of *H. pylori* per gland in the **(C)** antrum and **(D)** corpus. **(E)** Stomach tissue was then homogenized to culture live *H. pylori*. Statistical analysis was done using t-test p<0.1(*), p<0.001 (***), and p<0.0001 (****)**.**

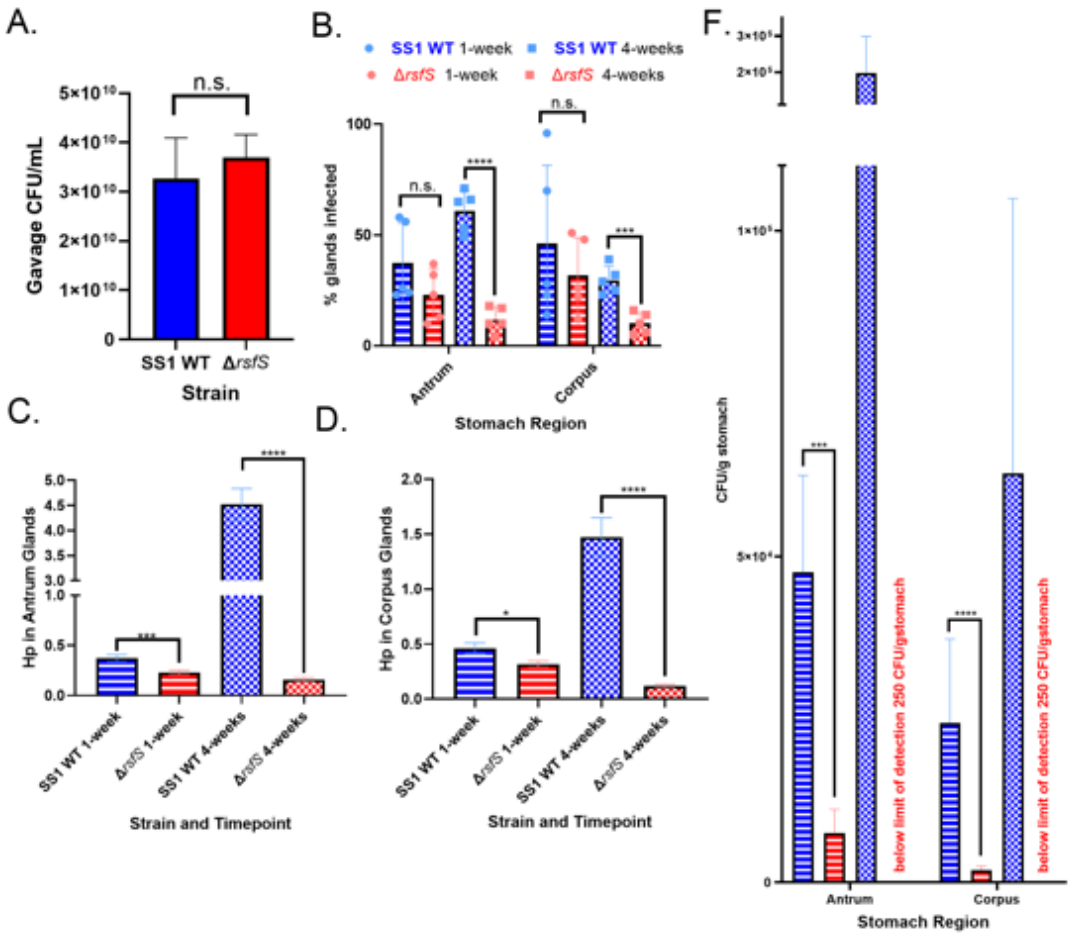

Table 1. Strains and plasmids used in this study.

Strain	KO#	Description
SS1	399	WT SS1 strain.
SS1 pTM115	529	WT SS1 strain with pTM115 containing a GFP plasmid to allow for visualization in glands for microscopy.
ΔrsfS::kan	1674	WT SS1 parent strain (KO#399) that was transformed with pTwist ΔrsfS::kan to delete chromosomal *rsfS* gene and replace with AphaA3 (KanR)
ΔrsfS::cat	1830	Parent strain ΔrsfS::kan (KO#1674) that was transformed with kan2cat plasmid to swap AphaA3 (KanR) for cat (CmR)
ΔrsfS::cat pTM115	2211	Parent strain SS1 pTM115 (KO#529) transformed with genomic DNA from ΔrsfS::cat (KO#1830)
ΔrsfS::cat ΔrdxA::rsfS 2 X promoter	2033	Parent strain ΔrsfS::cat (KO#1830) that was transformed with pTwist ΔrdxA::rsfS 2 X promoter to add a copy of *rsfS* in the *rdxA* locus under the influence of it's predicted promoter and the *rdxA* promoter
ΔrdxA::rsfS 2 X promoter	2031	WT SS1 parent strain (KO#399) that was transformed pTwist ΔrdxA::rsfS 2 X promoter to add a copy of rsfS in the rdxA locus under the influence of it's predicted promoter and the rdxA promoter
ΔrsfS::cat ΔrdxA::rsfS 1 X promoter	2034	Parent strain ΔrsfS::cat (KO#1830) that was transformed with pTwist ΔrdxA::rsfS 1 X promoter to add a copy of *rsfS* in the *rdxA* locus under the influence of it's predicted promoter only
ΔrdxA::rsfS 1 X promoter	2032	WT SS1 parent strain (KO#399) that was transformed pTwist ΔrdxA::rsfS 1 X promoter to add a copy of rsfS in the rdxA locus under the influence of it's predicted promoter only
Kan2cat	1579	plasmid to swap AphaA3 (KanR) for cat (CmR)
ΔrdxA::kan	1018	*rdxA* knockout with AphaA3 (KanR) strain previously used and published in Terry et al., 2005
ΔrdxA::cat	1019	rdxA knockout with cat (CmR) strain previously used and published in Terry et al., 2005
pTwist ΔrsfS::kan	2052	plasmid containing AphaA3 (KanR) flanked by upstream and downstream regions of the *rsfS* to delete it
pTwist ΔrdxA::rsfS 2 X promoter	2035	plasmid containing *rsfS* flanked with upstream and downstream regions of the *rdxA* to knockout. *rsfS* is in the same transcirptional oreintations of the *rdxA* promoter in addition to being under the influence of its native promoter.
pTwist ΔrdxA::rsfS 1 X promoter	2036	plasmid containing *rsfS* flanked with upstream and downstream regions of the *rdxA* to knockout. *rsfS* is in the opposite transcirptional oreintations of the *rdxA* promoter so it is only under the influence of its native promoter.
Gibson Intergenic region *rsfS*	2056	plasmid constructed via gibson assembly that contains *rsfS* flanked with intergenic regions HPYSS1_0192 and HPYSS1_0193 for *rsfS* insertion
rsfS^{native}*Δintergenic::rsfS* 2X *rsfS*	2212	WT SS1 parent strain (KO#399) that was transformed with Gibson Intergenic Region *rsfS* plasmid (KO#2056) to add a copy of *rsfS* 200bp upstream region with it's predicted promoter.
ΔrsfS::kanΔintergenic::rsfS 1X *rsfS*	2213	*rsfS*^{native}*Δintergenic::rsfS* 2X *rsfS (*KO#) that was transformed with pTwist ΔrsfS::kan to delete chromosomal *rsfS* gene and replace with AphaA3 (KanR)

Table 2. Primers used in this study.

Primer Set	Purpose	Forward	Reverse
rsfS flanking	confirm *rsfS* gene deletion	CCCCTAGAGGCAAAATCCCC	TGGCGTATCGCTCAAACTT
rdxA flanking	preliminary confirming *rdxA* insert	ATGAAATTTTTGGATCAAGAAAAAAGAAG	CAACCAAGTAATCGCATCAACTTTTGATTT
Double Promoter Left *rdxA* flanking-*rsfS*	Targets Region Upstream *rdxA* and *rsfS* insert	Cgcttcgtatctttatagccgt	TTACGGCATTCTTCGGTGAA
Double Promoter *rsfS*-Right *rdxA*	Targets *rsfS* insert and Region Downstream *rdxA*	Tggggtttgggttagggaaa	Aaagtcgcttgctcaatccc
Single Promote Left *rdxA* flanking-*rsfS*	Targets Region Upstream *rdxA* and *rsfS* insert	Tgcgttatcccagccaattg	Tggggtttgggttagggaaa
Single Promoter *rsfS*- Right *rdxA*	Targets *rsfS* insert and Region Downstream *rdxA*	AAAGGGCATGCTTATTCGCT	Aggttttcaacgctcgcttt
SOE Cat KO	Synthesize *cat* gene fragment from *rsfS::cat* strain	GATATAGATTGAAAAGTGGAT	TTATCAGTGCGACAAACTGGG
NF023_iSS1	Synthesize 1kb of intergenic region between HPSS1_0192 and HPSS1_0193 from SS1 WT gDNA Also Used to verify *rsfS* insertion in intergenic region	TATGAAGAGGGGCGCTTGAA	GCTGGATTATCGTGCGACTG
HPSS1_0192	Synthesize Left Side of McGee Fragment	TAATGGTGTTGGGGGGGTTAAA	GGGATAAGTGCCTAGAATGGTTAG
Template and Gibson HPSS1_0193	Synthesize Right Side of McGee Fragment With Overlap Additions for Gibson Assembly to generate double copy mutant using *rsfS* native locus	CTGATAAAACGAATAATTTCGGTATTTATAGGCATATTTTTC	CAGCTATGACTGGGGAAAATGACGGACTC
Gibson *rsfS*	Add overlapping fragments for gibson assembly to generate complement and double *rsfS* mutant using McGee Intergenic Region	atgaaccaacTGTAAATTCCTTGCATTCTAGAGTGATTAG	ttaggtgtttCTCCCGCTAGGCCCTAAAAG
Intergenic *cat*	Add overlapping fragments to *cat* gene for gibson assembly to generate complement and double *rsfS* mutant using McGee Intergenic Region	AAACACCTAAGATATAGATTGAAAAGTGGATAGATTTATG	GAAATTATTCGTTTTATCAGTGCGACAAAC
Gibson HPSS1_0192	Add overlapping nucleotides to Left McGee fragment for gibson assembly to generate complement and double *rsfS* mutant using McGee Intergenic Region	GACGGCCAGTTAATGGTGTTGGGGGGGTTAAAG	GTTGGTTCATCTAACCATTCTAGGCACTTATCC
Intergenic pUC-19	Add overlapping fragments for gibson assembly to syntheisze plasmid with desired insert to generate complement and double *rsfS* mutants using McGee's intergenic region	ATTTTCCCCAGTCATAGCTGTTTCCTGTGTG	AACACCATTAACTGGCCGTCGTTTTACAAC

Supplemental Materials.

Supplemental Fig 1.

Supplemental Figure 1. *rsfS* operon and downstream gene expression in Δ*rsfS* mutants. (1) The *rsfS* operon contains a total of four genes in following order: *rsfS* (HPYSS1_1340), *miaA* (HPYSS1_1341), *rfaG* (HPSS1_1342) and *Hp PEA* (HPYSS1_1343). **(2)** Transcriptional expression of *rsfS* operon genes in Δ*rsfS::cat* mutant strain suggest the *rsfS* deletion/insertion is not a polar mutation. RNA was extracted from plate grown bacteria. Cq values between Δ*rsfS::cat* and SS1 WT control produce a standard deviation of approximately 0.3 which is indicative that there is no differential transcription of the operon genes due to a polar effect caused by the *rsfS* deletion.

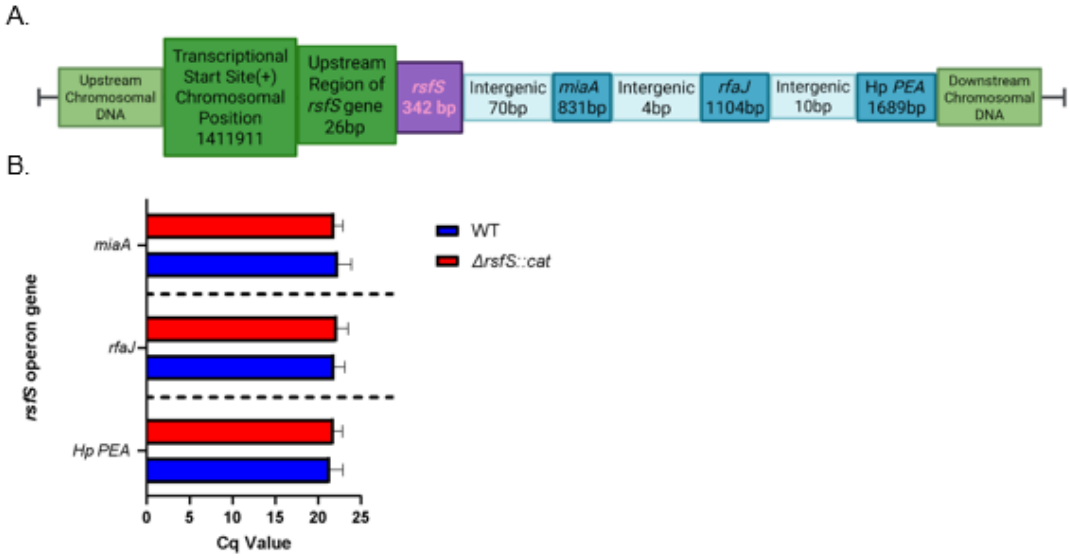

Supplemental Fig 2.

Supplemental Figure 2. Endpoint versus Continuous Growth Curve Experiments. Two approaches to growth curves were used to fully define potential growth defects in the Δ*rsfS* strain: endpoint and continuous growth. For the endpoint approach, multiple samples were created from the same initial starting culture, and one removed at each time point. For the continuous approach, a single initial starting culture was created and sampled repeatedly

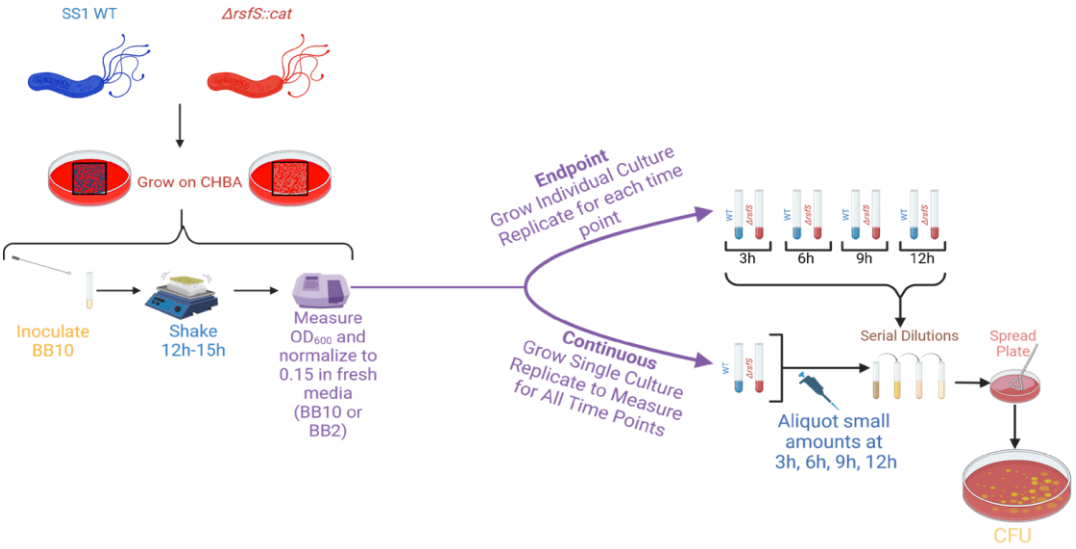

Supplemental Fig 3.

Supplemental Figure 3. Phenotypic verification of a second Δ*rsfS* strain. *In vitro* assays were conducted with the Δ*rsfS::kan* strain to confirm that the defective phenotypes observed in the Δ*rsfS::cat* strain are inherently due to the genetic deletion of *rsfS.* **(A)** Three biological replicates of the positive control, SS1 WT (mean= 0.905, technical replicates=71), and the negative control, Δ*rsfS::cat* (mean= 0.359, technical replicates= 70), were grown to compare to six biological replicates of the parent Δ*rsfS::kan* strain (mean=0.358, technical replicates= 152). T-test analysis with Welch's correction revealed a statistically significant defect p value <0.0001, ****, between the WT and the Δ*rsfS::kan* but no significant differences between Δ*rsfS::kan* and Δ*rsfS::cat* **(B)** Strains were grown in BB10 and statistically significant differences were not observed between WT and the Δ*rsfS::kan* until the stationary phase timepoints t= 24h, 30h and 35h with T-test analysis revealing p value <0.0001, ***,*,**** respectively but no significant differences between Δ*rsfS::kan* and Δ*rsfS::cat.* **(C)** Strains were grown in BB2 and statistically significant differences were not observed between WT and the Δ*rsfS::kan* until the later timepoints t= 20h and 25h with T-test analysis revealing p value <0.0001, **,*** respectively but no significant differences between Δ*rsfS::kan* and Δ*rsfS::cat.*

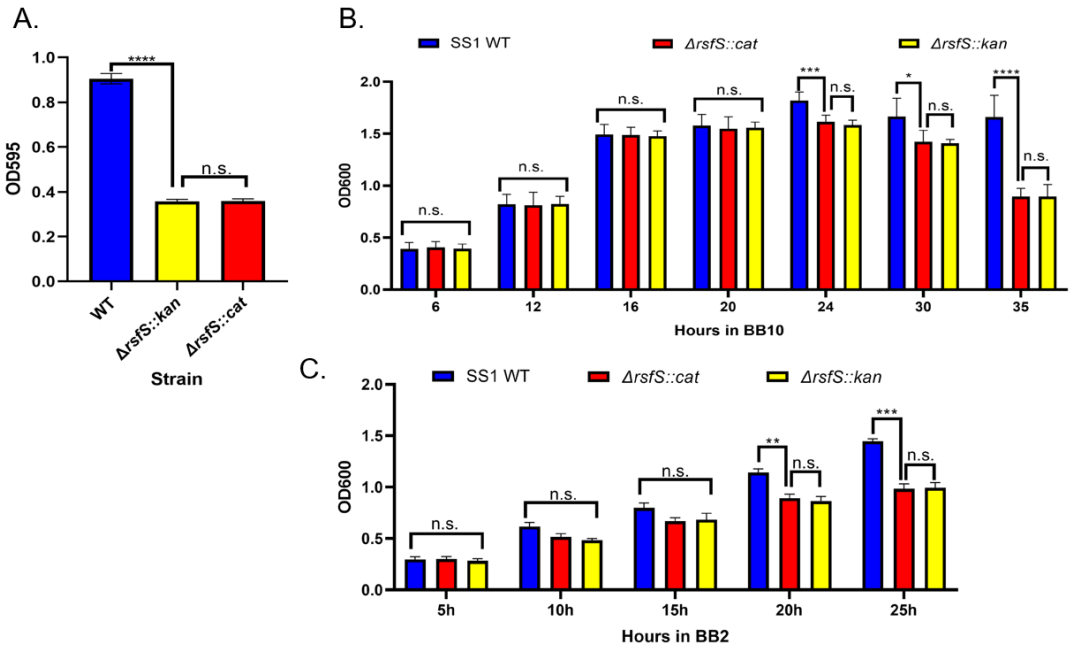

Supplemental Fig 4.

Supplemental Figure 4. Designs for *rsfS* complementation constructs. Plasmid inserts were designed with 200 bp upstream of the *rsfS* gene to include the predicted transcriptional start site, potential promoters (arrowheads), and any regulatory sequences. This segment along with a selectable marker, either erythromycin resistance gene (*erm*) or chloramphenicol resistance gene (*cat*) for selection and flanking with either *rdxA* or intergenic (IG) loci sequences to promote integration of the *rsfS* gene at those sites. For the *rdxA* integrated constructs, there are two versions. One has *rsfS* oriented in the same direction as *rdxA*, and thus may be transcribed from both promoters (2p). The other has *rsfS* oriented in the opposite direction as *rdxA*, and thus is predicted to be transcribed only from its own promoter (1p).

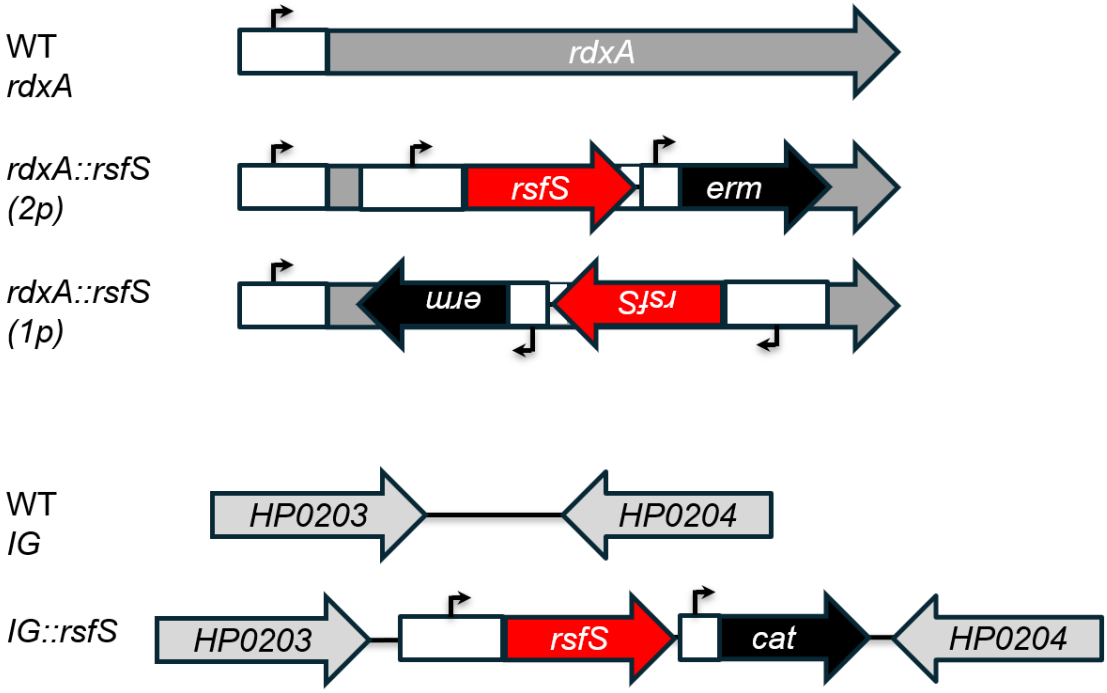

Supplemental Fig 5.

Supplemental Figure 5. Phenotypes associated with *rsfS* expression and complementation in *rdxA*. *rsfS* was integrated in the *rdxA* locus in either the WT or ΔrsfS background in two independent transformations, T#1 and T#2. Two variants of the *rdxA*:: *rsfS* mutants were assessed (Supplemental Fig. 5): 2P with both the rdxA and rsfS promoters, and 1P with only the *rsfS* promoter. **(A)** Soft agar assays were conducted with 12 biological replicates with 45 and 60 technical replicates respectively. Students T test was used to compare diameters to that of WT (p value <0.0001, ****). **(B)** Exponential phase growth was examined at the 20h time point, using the endpoint approach. No significant statistical difference was found across all strains relative to the SS1 WT control using Students T test. Four-five biological replicates were used. **(C)** Stationary phase OD_{600} values were examined after 35h of growth. (p value <0.0001, *, **, ***). Double copy mutants were compared to WT (Blue Bracket) and Δ*rdxA* mutants (Green Bracket) because the phenotypes were partially rescued by the *rsfS* insertion despite the loss of function mutations. **(D)** Biofilms were grown in BB2 and analyzed by crystal violet staining. Three-four biological replicates per strain with 164-246 technical replicates were used. Students T test was used to compare the indicated strains (p value <0.0001, *, ****). Control strains WT and Δ*rdxA* mutants (Teal Bracket) were. WT strains were compared to double copy mutants containing single or double promoters (Blue Bracket). Δ*rsfS* mutant was compared to Δ*rsfS* Δ*rdxA::rsfS* (1 X *rsfS*) mutants containing single or double promoters (Red Bracket).

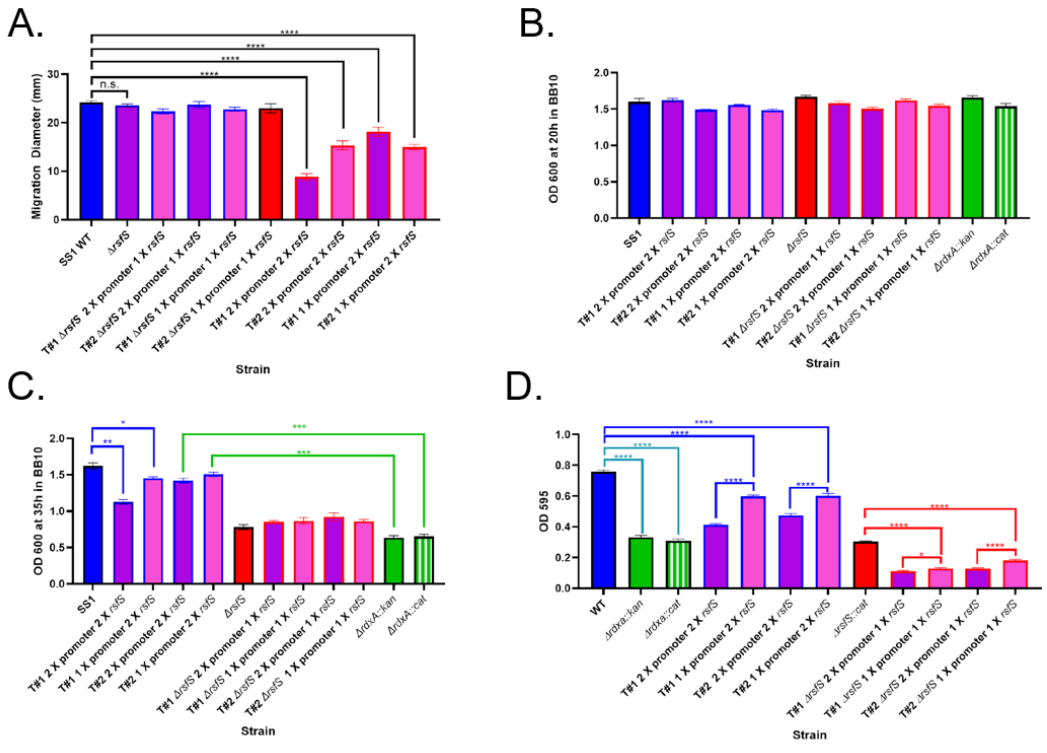

Chapter#3→*rdxA* in *Helicobacter pylori* is required for specific growth modes and resistance to nitro-group compounds

Abstract

Molecular biology relies on the use of mutations and complementation to explore the mechanistic roles of genes. In *Helicobacter pylori,* a chromosomal locus called *rdxA* is commonly used for genetic complementation. This site was chosen originally due to findings that null mutations did not confer detectable loss of fitness and additionally conferred metronidazole resistance, as the gene product is required to activate metronidazole to the active form. *rdxA* has been successfully applied as a genetic complementation locus for genes involved in numerous processes, including natural transformation, chemotaxis, cell shape, DNA damage, and model rodent colonization. The full appropriateness of *rdxA* was called into question, however, in recent reports that found *rdxA* inactivation, during use for complementation, resulted in some growth defects. In this work, we explored whether there are other as-yet-known defects associated with loss of *rdxA*. Loss of *rdxA* resulted *H. pylori* that were normal for as expected for phenotypes such as soft agar migration and exponential phase growth, but had defects in stationary phase and biofilm growth, across multiple strains. Furthermore, loss of *rdxA* resulted in growth defects upon 2-nitroethanol exposure. Our results suggest that caution should be used when selecting *rdxA* as a site for complementation. Functional RdxA appears to modulate *H. pylori* growth in different *in vitro* conditions, possibly related to its role as preventing harm from nitro compounds.

Importance

The *rdxA* chromosomal locus was first established as a locus for *H. pylori* genetic complementation in Smeets *et al.* 2000. It was chosen due to the high prevalence of mutations in clinical isolates that were associated with metronidazole resistance, suggesting that loss of *rdxA* would not affect *H. pylori* physiology. *rdxA* has been successfully applied as a genetic complementation locus for genes involved in multiple processes. A recent study attempted to complement a ribosomal silencing factor gene in the *rdxA* locus but reported that the loss of *rdxA* itself failed to correct defects in stationary phase and biofilm growth, a finding we confirmed in this work. *H. pylori rdxA* is required furthermore for growth in the presence of nitro group containing compounds. This work presents the first identification of a role for RdxA beyond metronidazole resistance and suggests that it should be used with caution as a site for complementation.

Introduction

Genetic knockout and complementation are essential tools for studying gene function in microbiology (Tong et al., 2023). During complementation, a copy of the disrupted gene or genes is placed back at a heterologous locus (Moore & Carr, 2022). For the heterologous locus, scientists can use plasmids or a location on the chromosome (Crépin et al., 2012). A variety of approaches are used, depending on the genetic properties of the microbe in question. In all cases, the underlying assumption is the

modifications used for the complementation restore wild-type phenotypes (Baron, 1996).

Helicobacter pylori is an important pathogen and a common subject for molecular genetics studies. *H. pylori* infects nearly half the global population and can lead to gastric ulcers and cancers (Malfertheiner et al., 2023). The transmission route of *H. pylori* infection from person to person is not completely characterized but epidemiological evidence support an oral-oral or fecal-oral transmission route (Kayali et al., 2018). Once ingested, *H. pylori* use motility and chemotaxis to colonize the gastric epithelium and maintain chronic infections that cause disease (Mu et al., 2023). Numerous studies have reported the identification and analysis of virulence factors (Malfertheiner et al., 2023). To identify the molecular underpinnings of these virulence factors, the genes are commonly mutated and then complemented. *H. pylori* is naturally competent and can recombine DNA from several sources—linear PCR products, circular plasmids, or chromosomal DNA—into the chromosome (Noto & Peek, 2012).

In *H. pylori,* a chromosomal gene called *rdxA* (HP0954) has been established as a commonly used locus for complementation (Smeets et al., 2000). RdxA is an oxygen-insensitive NADPH nitro reductase, required to reduce the pro-antibiotic metronidazole to its active, antibacterial form. RdxA mutations are highly prevalent in clinical isolates from the North America (Eng et al., 2015; D. H. Kwon, 2000;

Nezami et al., 2019), Latin America (Cabrera et al., 2024; Contreras et al., 2024; Mannion et al., 2021), Europe (Gómez-Ruiz De Arbulo et al., 2023; Marques et al., 2019; Saracino et al., 2020; Tankovic et al., 2000), Africa (Jaka et al., 2018; Secka et al., 2013; Tanih et al., 2011), and Asia (Butlop et al., 2016; Gong et al., 2023; Perez Aldana et al., 2005; Teh et al., 2014). The parameters in which *rdxA* was designated as an appropriate locus for genetic complementation was in part due to the high prevalence of mutations in clinical isolates that did not impair cell viability (Smeets et al., 2000). The initial report of *rdxA* as a complementation locus used it to complement a mutation in *comH*, and effectively demonstrated that the gene is required for DNA uptake (Smeets et al., 2000). Subsequently, numerous studies have reported using *rdxA* as a locus for complementation to confirm the roles of genes in motility/chemotaxis (McGee et al., 2005; Terry et al., 2005; X. Wang et al., 2025), liposaccharide synthesis (A.-N. Liu et al., 2022; Nguyen et al., 2025), natural transformation competency (Damke et al., 2019; Smeets et al., 2000), metronidazole resistance (Jeong et al., 2000; D.-H. Kwon et al., 2000), nucleotide synthesis (G. Liechti & Goldberg, 2012; G. W. Liechti & Goldberg, 2013), cell shape (A. C. K. Chan et al., 2015; Sycuro et al., 2010), DNA damage (G. Wang et al., 2012), quorum sensing (Rader et al., 2007), acid induced responses (Zimmerman et al., 2024) and rodent colonization (McGee et al., 2005; Sycuro et al., 2010; Terry et al., 2005; G. Wang et al., 2012). In our own earlier work, we employed the *rdxA* locus to genetically complement ribosomal silencing factor gene (*rsfS,* HP1414) mutants, which had stationary phase and biofilm defects. For the complementation, a copy of

rsfS was inserted into the *rdxA* locus, creating an *rdxA* null mutant. Instead of complementation, however, this approach failed to rescue growth defects associated with loss of *rsfS,* and indeed, uncovered evidence that loss of *rdxA* itself conferred growth phenotypes (Y. O. Elshenawi et al., 2026). Together, this body of work suggested that loss of *rdxA* is tolerated by *H. pylori* for many conditions but may lead to specific growth defects.

H. pylori RdxA is part of class of cytosolic enzymes (Bryant & DeLuca, 1991) called nitroreductases that are widespread amongst bacteria and used to reduce nitroaromatic compounds (Boddu et al., 2020). One such nitroaromatic compound is metronidazole, a 5-nitroimidazole prodrug used clinically to treat *H. pylori* and other microbial infections (Goodwin et al., 1998). Metronidazole enters the bacterial cell by passive diffusion (Smith & Edwards, 1995) and RdxA uses NAD(P)H as an electron donor to anaerobically catalyzes a four electron reduction of metronidazole's 5-nitro groups to a hydroxylamine group (Olekhnovich et al., 2009). This reductase activity involves a cysteine and flavin mononucleotide and is specific to *H. pylori* and its related species (Martínez-Júlvez et al., 2012). The reduction of the 5-nitro group results in mutagenic nitroso and hydroxylamine products that damage DNA (Sisson et al., 2000). One way *H. pylori* becomes resistant to metronidazole is via genetic mutations in the *rdxA* gene (Jenks et al., 1999; Jeong et al., 2000; Marais et al., 2003) causing a loss in the microbe's ability to reduce metronidazole (Valada et al., 2025). *rdxA* mutations that lead to metronidazole resistance have also been observed in the food-borne pathogen

called *Campylobacter jejuni* (Ribardo et al., 2010). *C. jejuni* is a close relative of *H. pylori* (Kelly, 2001) from raw poultry meat has been reported to have significant levels of metronidazole resistance (Andersen et al., 2006). The *rdxA* chromosomal gene was proposed to be an appropriate locus for genetic complementation for *C. jejuni* similar to *H. pylori* (Ribardo et al., 2010) and was additionally verified for genes involved in flagellar biosynthesis (Faber et al., 2016; Hendrixson, 2008) and Cas9 nucleases (Dugar et al., 2018).

Metronidazole resistance has been strongly associated with *rdxA* mutations since 1999 (Jenks et al., 1999). A high diversity of *rdxA* mutations in clinical isolates have been documented to be associated to high tolerance to antibiotics (Gong et al., 2023; J. Huang et al., 2024; Subsomwong et al., 2022). This topic remains clinically relevant, as *H. pylori* with *rdxA* mutations that confer metronidazole resistance are still documented in isolates from patients who developed either gastric cancer or peptic ulcers (Phuc et al., 2023) and experienced treatment failures (Guo et al., 2022). In addition to *rdxA* mutations, several other mutations have been reported that confer metronidazole resistance. Some are in a S-nitroso glutathione reductase gene called *frxA* (HP0642) (Jeong et al., 2000, 2001; S. M. Lee et al., 2018; Marais et al., 2003) and an efflux pump called HefA (HP0605) (S. M. Lee et al., 2018). Despite the high occurrence of *rdxA* mutations, a survey of clinical isolates found only 51.8% of *rdxA* mutations could experimentally validated for loss of ability to reduce metronidazole (J. Huang et al., 2024). This finding elucidates a confounding variable to interpreting *rdxA* mutations as ‘loss of function’ mutations that cause metronidazole resistance or

phylogenetic differences due to strain origin (J. Huang et al., 2024; S. Zhang et al., 2020).

In this study, we characterized the phenotypes of *H. pylori* strains that contain *rdxA* deletions to investigate the role of RdxA in *H. pylori* growth. Loss of function mutations in the *rdxA* locus did not affect chemotaxis and motility, as evidenced by normal soft agar migration, consistent with prior studies that used *rdxA* insertions for complementation constructs (McGee et al., 2005; Terry et al., 2005; X. Wang et al., 2025). In contrast, *rdxA* mutants in multiple *H. pylori* strains have biofilm defects, as initially observed with strain SS1 (Y. O. Elshenawi et al., 2026). Analyzing *H. pylori rdxA* mutant growth in detail, we found that these mutants have viability defects in stationary phase but not exponential phase. Interestingly, transcripts of *rdxA, frxA* and *hefA* are less abundant in stationary phase relative to exponential phase. *rdxA* deletion resulted in the upregulation of *frxA* and *hefA* transcripts, supporting the model that RdxA, FrxA and HefA are in a shared regulatory pathway. Finally, we evaluated whether *H. pylori* RdxA promotes growth upon exposure to a model nitro group ($-NO_2$) compounds. *rdxA* mutants in multiple strains had significantly exacerbated growth defects to 2-nitroethanol compared to their parent WT strains. Sequence analysis of published *H. pylori* genomes from clinical isolates reveal that amino acid substitutions associated with metronidazole resistance reported in prior publications to are conserved in model laboratory strains with no known Metronidazole resistance. This highlights an open question in field regarding whether of *rdxA* genetic diversity between strains truly results in metronidazole resistance or is due to phylogenetic

origin. Whether certain amino acid substitutions result in either increased or decreased nitroreductase activity is a potential phenotype that has not been explored In conclusion our results show that RdxA has additional roles that modulate *H. pylori* growth aside from its role in metronidazole resistance and should be used with caution as a complementation locus.

Results

RdxA is not required for growth and migration on soft agar media

The work that laid the foundation for this study found that insertion into *H. pylori rdxA* for complementation purposes resulted in several physiological defects (Y. O. Elshenawi et al., 2026). However, numerous studies have reported that insertions into *rdxA* for complementation have been successful for 18 other genes and correcting 10 different phenotypes (Supplemental Table 1). We therefore embarked on an analysis to carefully evaluate phenotypes associated with loss of *rdxA*. We initially explored soft agar motility, because this phenotype has been analyzed in several complementation-related publications (Table 1). These studies, however, only measured the final diameter of the migrating colonies at ~ 5 days (McGee et al., 2005; Terry et al., 2005; X. Wang et al., 2025). Recent work has shown that *H. pylori* can pause initial soft agar migration but can recover, giving the appearance that mutants may be similar to WT (Sagoo et al., 2024). We therefore analyzed soft agar migration of *rdxA* mutants in detail. Measuring soft agar migration daily for six days revealed that two independent *rdxA* null mutants, *H. pylori* SS1 Δ*rdxA::kan* and Δ*rdxA::cat*, had identical phenotypes to the wild type (Figure 1). The media used for

soft agar assays contains brucella broth (BB) supplemented with heat-inactivated fetal bovine serum (FBS) (Supplemental Table 2), so this observation preliminarily indicated that *rdxA* deletions did not result in defects in growth in this type of media, or the other phenotypes required for this assay, chemotaxis and motility. Overall, these data agree with the many complementation studies, that rdxA mutants do not have general growth defects.

Loss of *rdxA* creates strains with biofilm defects

Prior studies suggested that *rdxA* deletions in the *H. pylori* SS1 strain caused defects in biofilm formation (Y. O. Elshenawi et al., 2026). Additionally, prior RNA-sequencing analysis reported that *rdxA* transcripts were upregulated two-fold in G27 biofilm cells (Hathroubi et al., 2020). To further investigate the role of RdxA in biofilms, biofilm formation was compared between SS1 WT and isogenic Δ*rdxA::kan* and Δ*rdxA::cat* mutants. The WT produced about ~2.4 fold more biofilm than both the mutants (Figure 2). To confirm this defect applied to other strains, H. pylori G27 and LSH100 *rdxA* null strains were analyzed. Similar trends were observed in these strains: WT G27 and LSH100 made 1.6-fold or 2-fold more biofilm than their isogenic Δ*rdxA* strains (Figure 2). The defects were retained regardless of whether *rdxA* was replaced by an antibiotic marker or fluorescent marker. These results thus support the conclusion that functional RdxA plays a critical role in *H. pylori* biofilms *in vitro.*

RdxA is required during stationary phase

We next performed a detailed analysis of *H. pylori rdxA* mutant planktonic growth phenotypes. Two independent *H. pylori rdxA* mutant cultures were grown to across growth phases and the number of live cells analyzed by plating for colony forming units (CFU). In exponential phase time points (12h and 20h), both Δ*rdxA* mutants produced similar CFU as the WT (Figure 3A). Starting in early stationary phase, the Δ*rdxA* mutants displayed lower CFU numbers. At 24 hours, they produced 5.5-fold less CFU than the WT control (Figure 3A). This defect continued into late stationary phase (35h), during which time the WT and mutant CFU decreased such that there were 4-fold fewer CFU of mutant than WT (Figure 3A). These findings suggest that *rdxA* mutants grow fine in exponential phase but have defects in stationary phase.

***rdxA* is a highly expressed gene that displays decreased expression in stationary phase and connections to other metronidazole resistance genes**

Our results above show that *rdxA* plays an important role in biofilm and stationary phase conditions. It is not yet known whether *rdxA* is expressed under all these growth states. We therefore examined the transcriptional expression of *rdxA* across a growth curve using RT-qPCR. *rdxA* was generally expressed to a high level, with Ct values of ranging from 15-17, similar to other highly expressed genes. ΔCt levels for *rdxA* transcript decreased in late stationary phase, compared to early exponential phase (6h), by 71% (Fig. 3B). We also evaluated whether other genes related to metronidazole resistance, *frxA* (HP0642, HPYLSS1_00849) and *hefA* (HP0605,

HPYLSS1_00812) would show similar trends. ΔCt analysis revealed all three genes were expressed to lower levels in late stationary phase compared to exponential, with some variation on whether the decrease was apparent in early or late stationary phase (Figure 3B-D). We also evaluated how loss of *rdxA* would impact *frxA* and *hefA* expression. Transcripts for both genes produced higher ΔCq values in *rdxA* mutants compared to the WT (Figure 3E). These increased ΔCq values indicate that loss of function mutations in *rdxA* lead to an upregulation in *hefA* and *frxA* expression. The upregulation of *frxA* and *hefA,* indicate that there may be some kind of regulatory circuit that connects these genes and allow them to play compensatory roles in *H. pylori* growth when loss of function mutations in *rdxA* occur.

RdxA Confers a Growth Benefit Upon Exposure to Compounds with Nitro Groups

rdxA mutants displayed growth defects under biofilm and stationary phase conditions (Fig. 2, 3). This finding suggests the activity of RdxA might be important under these conditions, perhaps related to slow growth, high density growth, or build up of particular compounds. Nitroreductases like RdxA have been studied for reducing harmful nitroaromatic compounds, and have been reported to reduce other related chemicals including nitroalkanes (Russo et al., 2025). A prior study investigating growth effects of short chain nitro compounds tested a nitroalkane called 2-nitroethanol in *Campylobacter* (Horrocks et al., 2007). These authors found that 2-nitroethanol had inhibitory effects on two Campylobacter species (Horrocks et al., 2007). To extend this assay to *H. pylori*, we first determined the dose response to this

compound, using three *H. pylori* strains. *H. pylori* was grown overnight in BB10, diluted into fresh BB10 supplemented with the desired concentrations of 2-nitroethanol and grown for 20 hours, followed by evaluating growth amount by measurement of OD_{600}. WT isolates of all three *H. pylori* strains were inhibited by 5μM and 10μM 2-nitroethanol but were able to grow at lower concentrations of 1μM, 0.5μM or 0.1 μM (Figure 4). The *rdxA* mutants were then evaluated. In each case, they were more sensitive to the 2-nitroethanol than their isogenic WT strains, displaying statistically significantly lower CFU numbers after 20 hours of 2-nitroethanol exposure. SS1 Δ*rdxA* mutants had decreased growth at all concentrations (Figure 4A), G27 *rdxA* mutants showed statistically significant defects at the three highest amounts but not defects at 0.5μM and 0.1 μM (Figure 4B), and LSH100 *rdxA* mutants had defects at all concentrations except the lowest (Fig. 4C). Taken together, these results show that *H. pylori rdxA* mutants are significantly more sensitive to nitroalkane compounds than strains with intact *rdxA*, supporting the idea that *H. pylori* uses RdxA to detoxify harmful compounds.

Model *H. pylori* strains contain RdxA Residues Found in Clinical Isolates That Are Resistant to Metronidazole

Multiple studies have analyzed the genetic diversity across global clinical samples of *H. pylori rdxA* and amino acid substitutions associated with metronidazole resistance (Gong et al., 2023; J. Huang et al., 2024; D. H. Kwon, 2000; D. H. Kwon et al., 2001; Secka et al., 2013; Tankovic et al., 2000). The primary parameters for RdxA sequence analysis used in these studies to identify distinct

residues is to compare clinical isolates to the reference genome 26695 or to compare metronidazole resistant strains to susceptible ones. There remains a gap, however, in our understanding of whether these differences lead to metronidazole resistance, and how connected these changes are to strain origin (S. Zhang et al., 2020). To fill this gap, we first analyzed RdxA sequences in 15 *H. pylori* strains from different geographical regions with publicly available genomes (Figure 5A) to construct a guide tree using Clustal Omega program (Figure 5B).

Although RdxA sequences are traditionally compared to the 26695 strain as a reference genome, RdxA sequences are diverse from each other despite having similar continental origin (Figure 5A, B). A total of 11 amino acid substitutions (Gln6→His, Leu62→Val, Ser88→Pro, Arg90→Lys, Gly98→Ser, Arg131→Lys, Val172→Ile, Glu175→Gln, Ala183→Val, Gln197→Lys, Val204→Ile) previously reported in both Metronidazole susceptible and resistant *H. pylori* clinical isolates (Gong et al., 2023; D. H. Kwon, 2000; Secka et al., 2013; S. Zhang et al., 2020) were observed in our sequence alignment (Figure 5C). Three amino acids substitutions were also observed in both metronidazole resistant/susceptible populations (Thr31→Ala, His97→Thr, Gly122→Ser), (Gong et al., 2023; D. H. Kwon, 2000; Secka et al., 2013; S. Zhang et al., 2020) were distinct in the strains we surveyed as we observed the following amino acid substitution: Thre31→Glu (9/15 strains), His97→Thr (3/15 strains), His97→Tyr (5/15 strains), Gly122→Asp (SouthAfrica7) (Figure5C). The presence of these amino acid substitutions in model laboratory

strains that are susceptible to metronidazole, supports the model that the high genetic diversity in the RdxA gene is due to phylogenetic origin.

Three amino acids (Thr58→Ala, Ala80→Ile/Thr, Asp205→Ala) were strictly observed in metronidazole resistant clinical isolates (D. H. Kwon, 2000; Secka et al., 2013; Tankovic et al., 2000) were observed in strains we surveyed with unknown Metronidazole susceptibilities/resistance (Figure 5A)**.** SouthAfrica7 contains Thr58→Ala and Ala80→Val substitutions (Figure 5C). PeCan4 contains a Ala80→Val (Figure 5C) which is distinct from either the isoleucine or threonine polymorphism previously reported in Metronidazole resistant clinical isolates (D. H. Kwon, 2000; Secka et al., 2013; Tankovic et al., 2000)**.** Strain v225d contains a Ala80→Val amino acid substitution. Determining if these strains are resistant to Metronidazole would support the assertion that these residues are markers of Metronidazole resistance that can be applied clinically.

Our sequence analysis revealed that the strains we surveyed contain amino acid substitutions in regiones required for nitroreductase activity. RdxA nitrorecutase acvitiy requires the recruitment of a flavin mononucleotide (FMN) (Martínez-Júlvez et al., 2012) . Arg16→His was previously associated with FMN cofactor affinity that is needed for RdxA to reduce Metronidazole (Gong et al., 2023; D. H. Kwon, 2000; Secka et al., 2013; Tankovic et al., 2000). Polymorphisms were found in a 15 amino acid region that is highly conserved in oxygen insensitive nitroreductases from gram-negative bacteria (Goodwin et al., 1998). Two strains without known Metronidazole resistance (F16 and PeCan4) contain the Arg16→His amino acid substitution (Figure

5D). Two residue polymorphisms (Pro44→Leu, His53→Arg) were found in strains (Gong et al., 2023; Secka et al., 2013; S. Zhang et al., 2020) located in coil#3 and β-sheet#1, a highly conserved region of oxygen-insensitive nitroreductase from gram negative bacteria (Tankovic et al., 2000). ELS37 containing Pro44→Ser and two strains (F16, v225d) contain His53→Arg (Figure 5D). All these strains have unknown Metronidazole susceptibilities (Figure 5A), but contain a Cys159 (Figure 5D) which was previously reported to be essential for metronidazole reduction in a study that solved RdxA's crystal structure (Martínez-Júlvez et al., 2012). Whether the observed polymorphisms are due to phylogenetic origin, result in complete loss of function or create phenotypic variability in nitro-compound reduction is unknown.

In Huang et al., 2024, mutations observed in clinical isolates were recapitulated in *E. coli* and screened for RdxA to losing its ability to reduce Metronidazole resulting in resistant populations (J. Huang et al., 2024). D59N has been reported in both metronidazole susceptible and resistant *H. pylori* clinical isolates (Gong et al., 2023; Secka et al., 2013; S. Zhang et al., 2020), however has been produced sole metronidazole resistant *E. coli* populations (J. Huang et al., 2024). Strain 26695 is the only strain that does not contain a the D59N substitution as model research strains without (Figure 5D) indicating that this substitution alone is not sufficient to cause metronidazole resistance. Although *E. coli* contains nitro reductases that are being explored as gene therapies (Valiauga et al., 2024), it does not contain a direct homologue of *H. pylori* RdxA in its genome which potentially limits it efficacy as a model system to identify mutations that lead to resistance. All

strains including strains with unknown and known Metronidazole susceptibilities (Figure 5A) contained a phenotypes Summary Sentence Here. Whether certain residues confer a fitness benefit in *H. pylori* by being more efficient at reducing toxic nitro aromatic compounds remains an open question.

Discussion

Genetic complementation and knockout approaches are commonly used methodologies in microbiology (Tong et al., 2023). In the *H. pylori* field, the *rdxA* gene (HP0954) is commonly used as a chromosomal locus for genetic complementation due the assumption that it does not affect *H. pylori* physiology outside of metronidazole resistance (Smeets et al., 2000). Despite the success of this locus to complement a diversity of genes (Table 1), the work that led to this study found that complementation in this locus failed to complement phenotypes associated with stationary phase growth and biofilm formation defects (Y. O. Elshenawi et al., 2026). In this paper, we confirm that *rdxA* deletions do not affect several aspects of *H. pylori* physiology, as expected by its widespread use, but functional RdxA is needed for stationary phase growth and *in vitro* biofilm formation. Transcripts of *rdxA, frxA* and *hefA* are more abundant in exponential phase, before decreasing in stationary phase during planktonic growth. Interestingly, deleting the *rdxA* gene results in the upregulation of *frxA* and *hefA* transcripts which supports prior metronidazole resistance studies that identified these two genes play compensatory roles when loss of function mutations occur in *rdxA* (S. M. Lee et al., 2018). Functional RdxA confers a growth benefit upon exposure to short-chain nitro-

compound, 2-nitroethanol, which suggests that RdxA is a flexible nitro reductase that has multiple substrates other than nitroaromatic compounds. Across strains, there was heterogeneity in the susceptibility in the Δ*rdxA* mutants leading us to hypothesize the RdxA nitro reductase activity could vary between strains. RdxA homologues across 15 select strains had 46 distinct amino acid variations. Amino acid variations previously associated with metronidazole resistance are present in model strains used for research that are not resistant to metronidazole. This reveals a gap in the fields understanding about whether RdxA amino acid substitutions amongst strains result in metronidazole resistance, strain origin or variances in nitroreductase efficiency. Our combined findings suggest that functional RdxA is needed to modulate *H. pylori* growth, therefore it is not truly a neutral locus for genetic complementation.

RdxA is needed by *H. pylori* for several *in vitro* growth assays such as soft agar assays, biofilm and planktonic growth assays. Soft agar assays is a routine method in microbiology to study the motility (Tittsler & Sandholzer, 1936), an essential mechanism for *H. pylori* infection (O'Toole et al., 2000). Deleting *rdxA* did not cause defects or pausing phenotypes in soft agar migration (Figure 1). Our findings support prior studies reporting that loss of function mutations in *rdxA* did not inherently affect motility (McGee et al., 2005; Terry et al., 2005; X. Wang et al., 2025). It could be presumed that downstream behaviors influenced by motility phenotypes such as biofilm formation (X. Liu et al., 2024), would also remain unaffected. Prior work not only reported an upregulation of *rdxA* transcripts in G27 biofilms (Hathroubi et al., 2020) but SS1 *rdxA* knockouts had biofilm formation

defects (Y. O. Elshenawi et al., 2026). Indeed, we found that multiple strains have biofilm defects due to *rdxA* mutations (Figure 2). This led us to further explore the planktonic phenotypes of the *rdxA* mutants because planktonic growth assays also use the same base components in shaking conditions. Δ*rdxA* mutants presented severe defects in stationary phase (Figure 3A), indicating that functional RdxA is needed to sustain high population densities under these conditions (Navarro Llorens et al., 2010). In contrast, *rdxA* is not required *in vivo*. *rdxA* mutations are prevalent in clinical isolates and loss of function mutations do not to impair *H. pylori's* ability for rodent model colonization (McGee et al., 2005; Sycuro et al., 2010; Terry et al., 2005; G. Wang et al., 2012). Overall, these results suggest that *H. pylori* require RdxA for *in vitro* growth conditions.

Although SS1 Δ*rdxA* mutants presented defects in stationary phase, *rdxA* transcripts were more abundant during exponential to mid-stationary phase and decreased in late stationary phase (Figure 3B). *frxA* transcripts followed the same expression trends (Figure 3C) providing further evidence for the idea that *H. pylori* elevate nitroreductase expression in exponential phase, even media that does not contain known nitro aromatic compounds. Like *rdxA* and *frxA, hefA* transcripts decreased in abundance in stationary phase (Figure 3D), presenting the possibility that the three genes might be part of the same transcriptional pathways. In agreement with this idea, *H. pylori* Δ*rdxA* mutants showed elevated abundance of *frxA* and *hefA* gene transcripts compared to WT (Figure 4). This finding indicates that FrxA and

HefA may play a compensatory role in the event of loss of RdxA, a trend that has been previously reported in *H. pylori* (Kuo & Kao, 2025). Thus, our data suggests that *rdxA* is co-regulated with *frxA* and *hefA* whose products play roles in similar resistance pathways.

RdxA has long been appreciated to reduce metronidazole, and our results suggest it also plays roles in resistance to other types of nitro-containing compounds in *H. pylori* (Fig. 4). One can speculate that *H. pylori* does not normally encounter lethal levels of nitroaromatic compound *in vivo,* based on the observation that *rdxA* loss of function mutations do not cause rodent-stomach colonization defects (McGee et al., 2005; Sycuro et al., 2010; Terry et al., 2005; G. Wang et al., 2012) and *H. pylori* clinical isolates often have mutations that are thought to be *rdxA* null as they result in inability to reduce metronidazole. However, humans can be exposed to various harmful nitroaromatic compounds via inhalation or diet (Rafil et al., 1991). *H. pylori* does get directly exposed to nitroaromatic compounds during metronidazole treatment (Schoenfeld, 2024; Shah et al., 2021). Prior to this work, *H. pylori* RdxA was not known to reduce other nitro compounds, although nitro reductases from other species such as *E. coli* have been reported to have a range of substrates (Valiauga et al., 2024). We tested the role of RdxA in 2-nitroethanol management, due to its prior use in *C. jejuni,* a close relative of *H. pylori* (Ribardo et al., 2010). *H. pylori* Δ*rdxA* mutants were more susceptible to 2-nitroethanol at concentrations where the WT strain could grow exponentially, across three strains (Figure 4). Higher concentrations of 2-nitroethanol do not inhibit *H. pylori* growth, however the *rdxA* gene is needed for

H. pylori to promote survival in media containing 2-nitroethanol. These phenotypes indicate that RdxA has a range of substrates beyond metronidazole and other nitroaromatic compounds and it is needed by *H. pylori* to reduce harmful nitro-compounds it might encounter.

Considering the heterogeneity of Δ*rdxA* mutant phenotypes, suggested that nitro reductase activity and susceptibilities to nitro compounds might be strain specific. Meta-analysis studies document a continuing high frequency of *rdxA* mutations and genetic diversity in clinical isolates from symptomatic patients (Hong et al., 2024; Zou et al., 2020). We next decided to analyze published *rdxA* gene sequences to identify critical amino acids that might contribute to the heterogeneity of nitro reductase activity within strains to provide further insight into these phenotypes. RdxA mutations have been primarily studied in the context of metronidazole resistance (Gong et al., 2023; J. Huang et al., 2024; Jeong et al., 2001; S. M. Lee et al., 2018; Ribardo et al., 2010, 2010; S. Zhang et al., 2020). Variation in fourteen residues from the 15 strains that were surveyed were found to be due to be due to phylogenetic origin (Figure 5) as what was previously reported in prior publications (Gong et al., 2023; D. H. Kwon, 2000; Secka et al., 2013; S. Zhang et al., 2020). Additionally we found three amino acids found in only in metronidazole resistant isolates (D. H. Kwon, 2000; Secka et al., 2013; Tankovic et al., 2000) and four polymorphisms in residues critical for nitroreductases acvittiy (Gong et al., 2023; Secka et al., 2013; S. Zhang et al., 2020) located in strains with unconfirmed metronidazole susceptibility/resistance phenotypes. Some of these specific mutations,

have been directly tested for conferring loss of metronidazole reduction (S. Zhang et al., 2020), such as D95 (J. Huang et al., 2024) and C159 (Martínez-Júlvez et al., 2012) and however many are just correlations and lack functional validation (J. Huang et al., 2024; S. Zhang et al., 2020). Most notably D95N that were functionally validated to confer resistance in *E. coli* (J. Huang et al., 2024) were present in model research strains that are known to not be resistant to metronidazole (Figure 5). Although metronidazole is used to treat abdominal parasitic (Cohen, 1996) and bacterial infections (Galante et al., 2025; Mikamo et al., 2016) which in some cases can be due to *E. colli* infections (Onderdonk et al., 1979). a limitation to using *E. coli* as a model system for *H. pylori* RdxA functionality is that not only does *E. coli* not contain RdxA homologues. Further functional analysis of RdxA, RdxB and FrxA is needed to fully deduce the essential components required by these nitro reductases to promote *H. pylori* growth.

In summary, our findings suggest caution should be used when employing the *rdxA* locus (HP0954) in the *H. pylori* genome as a genetic complementation locus and provide some of the first ideas of the roles that RdxA might play. RdxA is needed under specific growth conditions, such that deletion of this gene results in stationary phase planktonic and biofilm defects. The media used, Brucella Broth and Fetal Bovine Serum, do not contain nitro aromatic compounds. However, when known nitro group chemicals were added to bacterial media, RdxA conferred a growth benefit to all strains, suggesting there may be some kind of compound in the media created by *H. pylori* that RdxA helps to detoxify. *rdxA* is highly expressed by *H.*

pylori, although more abundant in exponential phase versus stationary phase. The other genes whose produces have been associated with metronidazole resistance are expressed similarly, and are upregulated when *rdxA* was deleted, suggesting the idea that they are part of a coordinated transcription network. RdxA sequence analysis identified key distinct amino acid substitutions that might contribute to the heterogeneity of nitro reductase activity within strains. Additionally, certain amino acid variances RdxA observed in clinical isolates and associated with metronidazole resistance are conserved in research model strains that are susceptible to metronidazole, suggesting whether a strain is resistant or sensitive is more nuanced than just the RdxA sequence, and may relate to RdxA expression or the other genes in the network. In conclusion, RdxA plays a newly appreciated role in *H. pylori* biology, suggesting it should be used for complementation with these caveats in mind.

Acknowledgements

This project was supported by the National Institute of Allergy and Infectious Disease (NIAID) R01AI164682 and RO1AI116946 to K.M.O. and 5F31AI176804-02 to Y.O.E. The authors are grateful to Ottemann Lab members Dr. Skander Hathroubi for discussions and input.

Methods

H. pylori Strains and Growth Conditions

H. pylori strains (Supplemental Table 3) were incubated at 37°C under microaerobic conditions with (5% O_2, 10% CO_2, and 85% N_2) for 48-72 hours on Columbia Horse Blood Agar (CHBA) plates. CHBA plates were made with Columbia Horse Blood

Agar powdered base (Fisher CAT#279240), 0.2%-β cyclodextrin (TCI America CAT#C0900) dissolved in dimethyl sulfoxide (Fisher CAT#D1281), 5% (vol/vol) defibrinated horse blood (Hemostat Labs CAT#DHB500) and selective antibiotics with following components: 10µg of vancomycin (Gold Bio CAT#V-200-5) per ml, 0.025 µg of cefsulodin (Gold Bio CAT#C-114-1) per ml, 0.0125 U of polymyxin B sulfate (Sigma Aldrich CAT#P1004) per ml, and 50µg of cycloheximide (Sigma Aldrich CAT#501784369) per ml. Liquid media (BB10) consists of Brucella Broth (Fisher Scientific CAT# B11088) with 10% heat-inactivated Fetal Bovine Serum (Gibco CAT# 10437028). Strains were stored at -80°C long term in freeze media made up of the following ingredients: brain heart infusion media (Fischer CAT#DF0037-17-8), 25% glycerol (Fisher CAT# G33-1), 10% fetal bovine serum, 1% (wt/vol) β-cyclodextrin dissolved in 5% dimethyl sulfoxide.

Soft Agar Motility Assays

Soft agar motility media contained Brucella broth (BB), 2.5% heat-inactivated Fetal Bovine Serum (FBS), 0.35% (w/v) agar (BD Difco CAT#214010) with the selective antibiotics described above. *H. pylori* strains were initially grown on CHBA for 2-3 days prior to collecting a small sample with a sterile micropipette tip, and then stabbing this sample ¾ into the depth of the agar plate. Soft agar plates were incubated in microaerobic conditions at 37°C between 1-6 days. Replicates were imaged daily using Biorad Chemidoc MP Imaging System (Hercules, CA, USA) with the UV Transilluminator set to White Epi Illumination and then measured using ImageJ software.

Planktonic bacterial Growth

Bacteria were grown on CHBA for 2-3 days and used to inoculate 3 ml. cultures of BB10 media in a 15mL falcon tube. Tubes were incubated with shaking in microaerobic conditions at 200rpm for 15-17 hours. The optical density was then measured and cultures diluted to an OD_{600} of 0.1 using fresh BB10 and placed in individual tubes, one per time point. Replicates were grown using an endpoint approach for 12-35 hours. At the desired time point, the optical density of culture was measured and serially diluted in phosphate buffered saline (PBS, NaCl, KCl, Na_2HPO_4, $KH_2\ PO_4$) for plating on CHBA to count CFU. Plates were incubated in microaerobic conditions for 6 days before counting colonies.

Biofilm Assays

Biofilm phenotypes were analyzed using an *H. pylori* adapted protocol (Hathroubi et al., 2018). Overnight cultures were made by inoculating 3ml of BB10 in a 15ml falcon tube with a few loops of plate grown *H. pylori* strains. Tubes were incubated with shaking at 200rpm for 12-17 hours, measured for optical density using a spectrophotometer, then diluted with fresh media (BB10 for G27 and LSH100, BB2 for SS1) to an OD_{600} of 0.15. These diluted cultures where then used to inoculate sterile 96-well polystyrene microtiter plates (Costar#3370) with a volume of 200uL per well. Biofilms plates were incubated in static microaerobic conditions for 72h prior to crystal violet staining. For staining, liquid media was aspirated from the wells using a multichannel pipette, and each well was washed by adding 200 µl of PBS and gently removing, two times. Biofilms adhered to the polystyrene were stained with

300uL of crystal violet solution (0.1% wt/vol) and incubated at room temperature for 3 minutes. The crystal violet solution was removed by pipetting, following by washing with 200 µl PBS twice. After these staining steps, the plates were air dried for 20 minutes at room temperature and 300uL of room temperature ethanol (95% vol/vol) was added to the wells and incubated at room temperature for 10 minutes to resuspend the dried crystal violet. After this incubation period, optical density of the crystal violet in ethanol solution was measured at 595 nm.

RNA preparation

RNA extractions were done using the Purelink RNA Minikit (CAT#12183018A) from *H. pylori* strains grown in either liquid media or CHBA plates, following the manufacturers protocols. Bacterial samples were resuspended in 1mL of TRIzol (Thermo Fisher Scientific CAT#15596018) and stored at -80°C until needed. For preparation, the frozen TRIzol-suspended replicates were thawed at room temperature for 5-8 minutes. For each sample, 200µL of chloroform (Fischer Scientific CAT#BP1145-1) was added and then shaken by hand at room temperature for 3 minutes. Thoroughly shaken samples were then centrifuged at 15,000 × g for 15 minutes at 4ºC to separate the mixture into three phases: a lower phase of pink phenol-chloroform, a white interphase, and an upper clear phase that contains RNA. The upper phase was moved to a fresh sterile tube and mixed with an equal volume of 70% ethanol, inverted by hand vigorously, and then transferred to a Purelink RNA Minikit spin cartridge. The spin column was centrifuged at 15,000 *g* and then washed

with Wash Buffer I prior to DNase treatment using Turbo DNA-Free Kit (Invitrogen ThermoFisher CAT# AM1907) for 15 minutes at room temperature according to the manufacturer's protocol. After this step, the column was washed at room temperature with wash buffer 1 then wash buffer 2. These wash steps were repeated a second time. The column was then dried by centrifuging at 15,000 × g for 1 minute at room temperature. Nuclease-Free Water (Invitrogen CAT#AM9937) was added to the membrane and incubated at room temperature for 1 minute. RNA was eluted immediately afterwards by centrifuging for 1 minute at 15,000 x g at 4°C. RNA elutions were kept on ice and yields were quantified with a Nanodrop spectrometer. RNA elutions were either stored at -80°C long-term or kept on ice to immediately convert to cDNA.

cDNA synthesis and qPCR analysis

RNA was converted to cDNA using High-Capacity cDNA Reverse Transcription Kit with RNase Inhibitor (Applied Biosystems/Thermo Fisher CAT#4374966). The manufacturer's protocol was followed and with each replicate reaction containing 1ug of RNA diluted with Nuclease- Free water to a final volume of 10ul. RT-qPCR was conducting with the resulting cDNA product using Power SYBR™ Green PCR Master Mix kit (Applied Biosystems#4367659) and a Bio-Rad CFX96 Real Time PCR Detection System. qPCR reaction mixtures were composed of 1µL of the cDNA, 10 µl of PCR Master Mix and 5 µM each of the forward and reverse primers in Supplemental table 3 and water for a total volume of 20 µL per reaction. The

thermal cycling protocol was conducted in following steps.: Step#1- 95ºC (10 minutes), 40 cycles of denaturing and annealing/extension at 95ºC (15 seconds) and 60ºC (1 minute) respectively, with a final melting curve (5 seconds).

Growth Curves with 2-nitroethanol

Growth curves were conducted with liquid media supplemented with 2-nitroethanol (Sigma Aldrich CAT#146633) as done previously with *C. jejuni* (Horrocks et al., 2007). H. pylori was grown overnight in BB10 with shaking for 12-15 hours, then diluted with fresh BB10 supplemented with variable final concentrations of 2-nitroethanol: 10mM, 5mM, 1mM, 0.5 mM and 0.1 mM, followed by growth for 12 hours under microaerobic conditions with shaking. After the incubation, OD_{600} was measured to evaluate growth.

Sequence Analysis of *H. pylori* RdxA

Model research strains and clinical isolates from various global origins with RdxA sequences available in (https://biocyc.org/) annotated as "Open Reading Frames" were used to obtained the RdxA protein sequences. Strains selected were: 26995 (Tomb et al., 1997), B8 (Farnbacher et al., 2010), B38 (Bernarde et al., 2010), CCUG (Porwollik et al., 1999), ELS37 (García-Zea et al., 2019), F16 (Furuta et al., 2011), G27 (Dong et al., 2009), GAM100Ai (Estibariz, n.d.), J99 (Israel et al., 2001), Lithuania75 (Boyanova et al., 2010), PeCan4 (Kersulyte et al., 2002), PMSS1 (Dyer et al., 2018), South Africa 7 (Duncan et al., 2013), SS1 (A. Lee et al., 1997) and v225d (Hashi et al., 2014). Sequences were aligned using Clustal Omega

(https://www.ebi.ac.uk/jdispatcher/msa/clustalo) using default parameters. Amino acids that varied between sequences were identified visually.

Figures

Figure 1.

Figure 1. *rdxA* mutants perform like WT for in soft agar migration over 6 days. Migration distance of SS1 WT and two *rdxA* knockout mutants (*rdxA::kan* and *rdxA::cat*) was measured daily for 6 days and no statistically significant defects as analyzed using a Student T-test comparing each strain to WT at each time point.

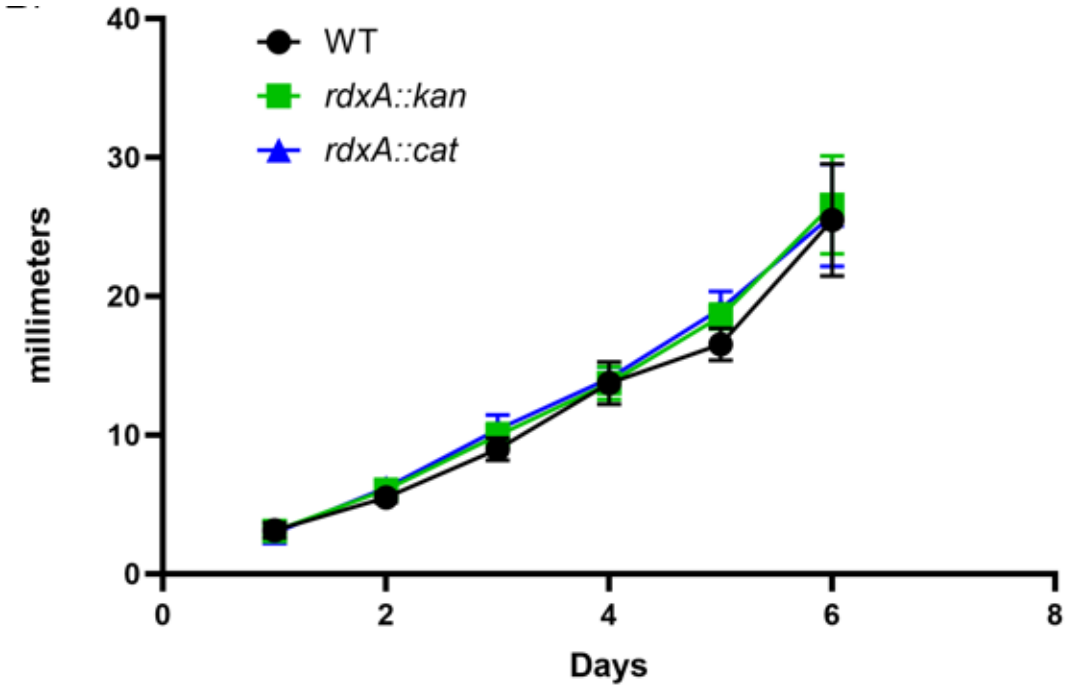

Figure 2.

Figure 2. *rdxA* null mutants have biofilm defects. Biofilms were grown statically in 96 well plates for 3 days in either BB2 (SS1 strains) or BB10 (G27 and LSH100 strains) and quantified using crystal violet staining at Optical Density of 595 nm (OD595). Statistical analysis was carried out using Students t-test with Welch's correction, comparing each WT to its isogenic mutant strains; p-value <0.0001, ****. Three biological replicates were conducted for each strain, with 55-63 technical replicates each. Error bars represent standard error of the mean.

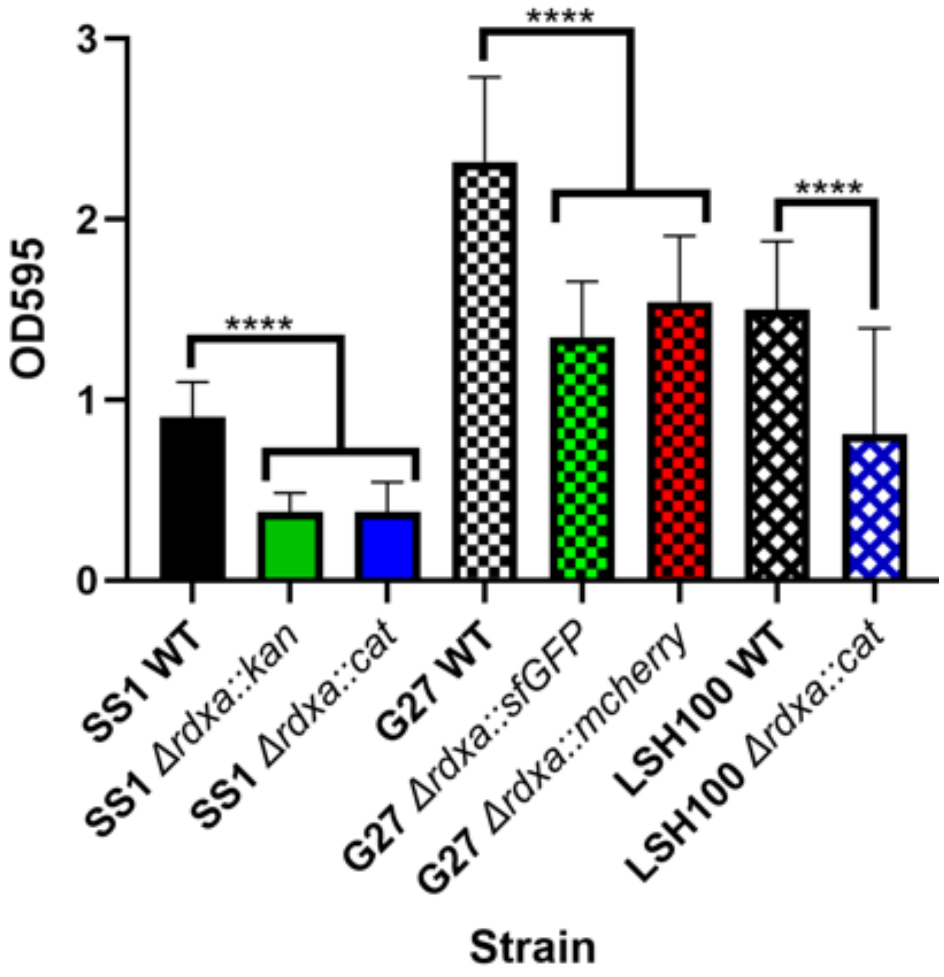

Figure 3.

Figure 3. *rdxA* mutants have growth defects in stationary phase (A) SS1 WT and Δ*rdxA* mutant were grown in BB10, and individual samples collected for endpoint analysis in which the samples were serially diluted and plated. Each bar represents four to five biological replicates. Students T- test was conducted to compare each mutant to WT at the same time with statistically significant differences observed in early stationary (P-value <0.005, **) and late stationary phase (P-value <0.05, *). RT qPCR was conducted on SS1 WT strain (n=6) grown using endpoint approach in BB10 to quantify **(B)** *rdxA* **(C)** *frxA* **(D)** *hefA.* and normalized to a constitutively expressed gene *imaA* to obtain ΔCt.. **(E)** qPCR was conducted for four to five biological replicates from plate grown bacteria quantify transcription for *frxA* and *hefA* in *rdxA* knockout mutants relative to SS1 WT. Standard deviation was calculated from raw Cq values are ~0.3 value to ensure RNA quality and three primer sets were used for each gene.. ΔCt was calculated by subtracting the target gene Cq value (*frxA* or *hefA*) by the reference gene Cq value (*gapB*).

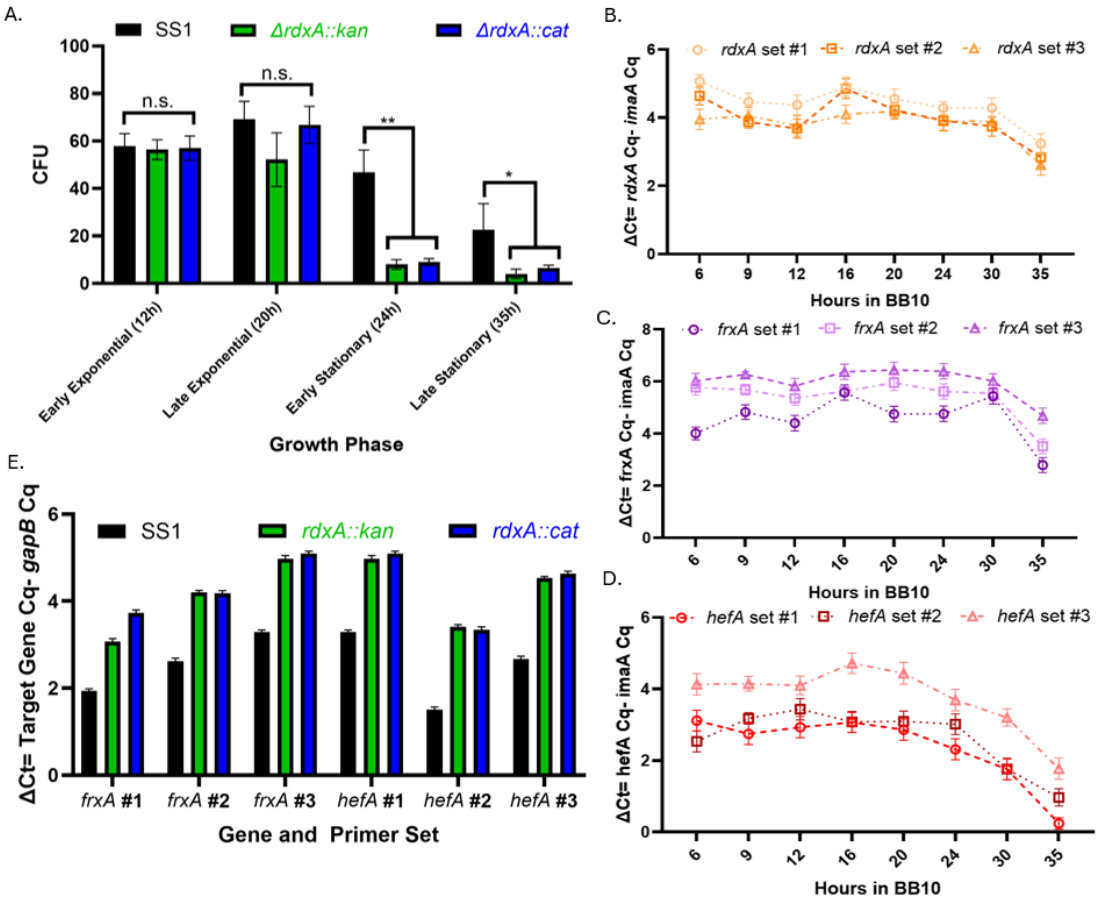

Figure 4.

Figure 4. Loss of function *H. pylori rdxA* mutations cause growth defects upon exposure to 2-nitroethanol. *H. pylori* strains were grown for 20 hours in BB10 media supplemented with 2-nitroethanol. OD_{600} was measured for three to five biological replicates per strain for **(A)** SS1 WT was compared to isogenic Δ*rdxA::kan* and Δ*rdxA::cat.* **(B)** G27 WT was compared to isogenic Δ*rdxA::sfGFP* and *ΔrdxA::mcherry* mutants. **(C)** LSH100 WT was compared to LSH Δ*rdxA::cat*. Students T-test was used to compare each mutant to WT at the specific concentration with the following significant differences: p-value <0.05 (*), p-value <0.005 (**), p-value <0.0005 (***) and p-value <0.00005 (****).

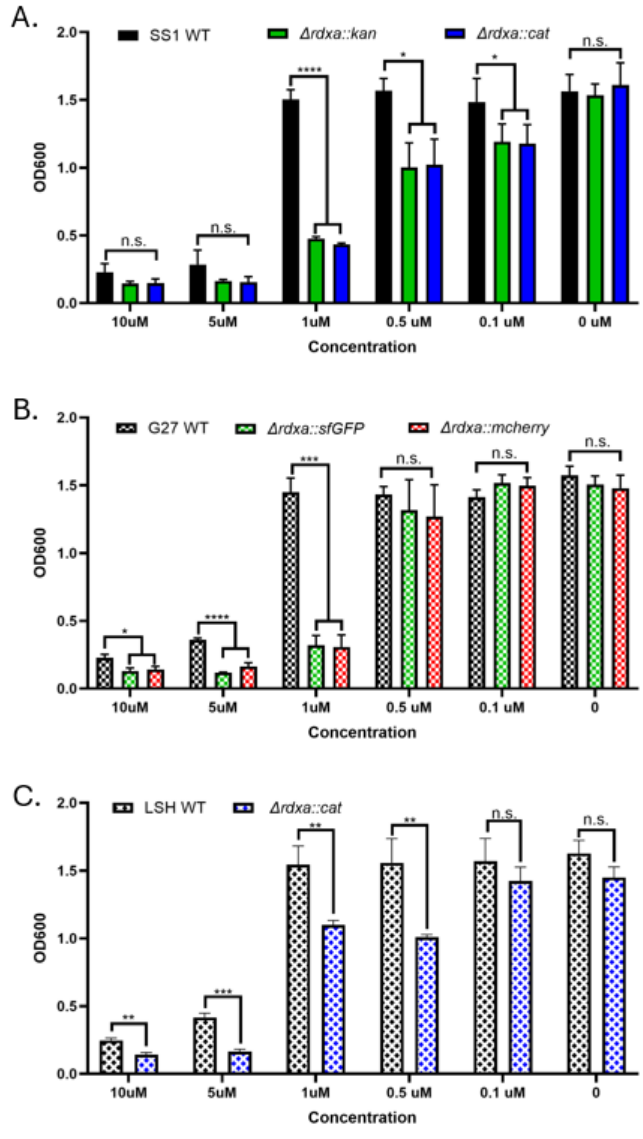

Figure 5.

Figure 5. RdxA Guide Tree from Global *H. pylori* strains. (A) Guide tree based on RdxA sequences with branch distances are listed next to strains indicating amino acid differences. (B) Region of origin for strains, disease outcomes and status of metronidazole resistance. (C) Alphafold Model of RdxA (O25608) in ChimeraX, α-helices (pink), coils (blue) and β–sheets (green). Residues found in clinical isolates that metronidazole resistant and susceptible are highlighted in white. Residues that are involved in FMN cofactor affinity are highlighted in purple. Residues found in metronidazole resistant clinical isolates only are highlighted in yellow. Residues that are part of the highly conserved regions in nitroreductases from gram negative bacteria are highlighted in blue. Residues found in metronidazole resistant clinical isolates only are highlighted in yellow. Residues that are part of the highly conserved regions in nitroreductases from gram negative bacteria are highlighted in blue. Residues that have been functionally validated to lose its ability to reduce metronidazole are highlighted in red. Residue involved in cysteine rich redox active center is highlighted in orange. Catalytic pocket residue is in grey. (D) Sequence alignment of RdxA protein sequence from different strains with amino acid variances annotated. Secondary structure containing the primary cysteine required for the rich redox active center is boxed in orange. Secondary structure involved in catalytic pocket is boxed in grey. Secondary structures involved in FMN cofactor binding are boxed in purple. Amino acid substitutions observed in clinical isolates that metronidazole resistant and susceptible are highlighted in black. Amino acid substitutions that are in sites involved in FMN cofactor affinity are highlighted in purple. Amino acid substitutions in sites only found only in metronidazole resistant clinical isolates are highlighted in yellow. Amino acid substitutions that are part of the highly conserved regions in nitroreductases from gram negative bacteria are highlighted in blue. Amino acid substitutions in sites that have been functionally validated to lose their ability to reduce metronidazole are highlighted in red.

A.

Strain	Region of Origin	Disease Outcome	Metronidazole Resistance
South Africa7	Strain Isolated within Indigenous South African Population	Low incidence of severe gastrointestinal disease	Unknown
PeCan4	Peru	Patients were diagnosed with gastric cancer	Unknown
v225d	Venezuelan Piarca Amerindian Person	Gastritis and peptic ulcers	Unknown
F16	Japan	Gastritis	Unknown
GAM100Ai	Gambia	Unknown	Unknown
SS1	Australia	Mouse adapted Gastritis and Ulcers	No
PMSS1	Parent strain of SS1	Gastric ulcers	No
B38	France	MALT lymphoma	Unknown
26695	United Kingdom	Gastritis	Unknown
B8	Adapted to infect gerbils from European patient	Gastric Ulcer	Unknown
G27	Italy	Gastritis and Ulcers	No
CCUG	Sweden	Gastric ulcer	Unknown
ELS37	El Salvador	Gastric Cancer	Unknown
Lithuania75	Lithuania	Chronic Gastritis and Duodenal Ulcers	Unknown
J99	Tennessee	Duodenal Ulcers	No

B.

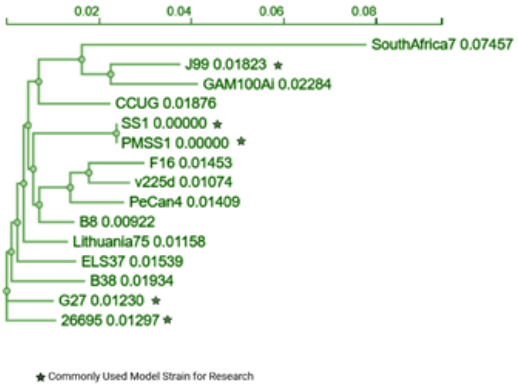

C.

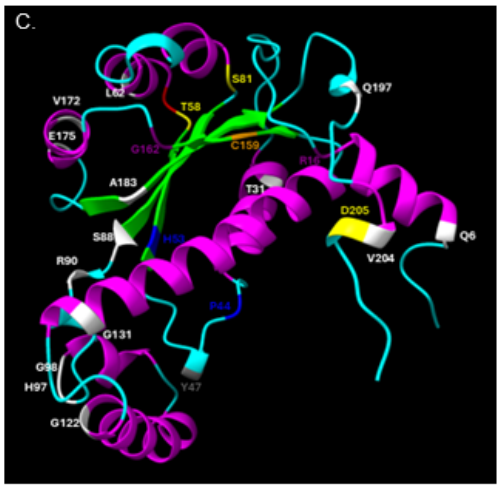

D.

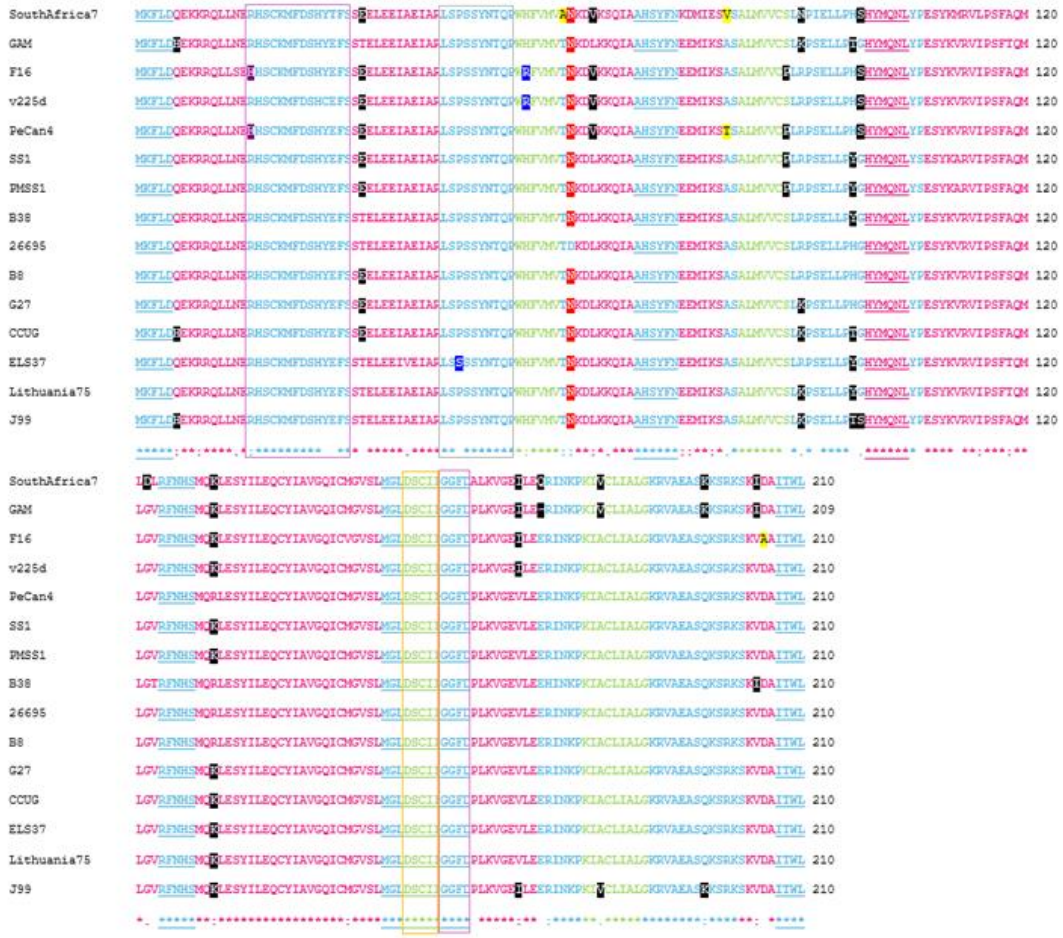
SouthAfrica7
GAM
F16
v225d
PeCan4
SS1
PMSS1
B38
26695
B8
G27
CCUG
ELS37
Lithuania75
J99

Supplemental Figures

Supplemental Table 1. List of Genes Complementation Approaches in *rdxA* locus

Research Topic	Genes and Publications
Natural Transformation Competency	HP1527- Smeets et al., 2000 and Dambke et al. 2019
Chemotaxis	**HP1067- Terry et al., 2005 and McGee et al., 2005** HP0099- Wang et al., 2025
Metronidazole Resistance	HP0642- Jeong et al., 2001 HP0954 and HP1417 Kwon et al., 2000
Nucleotide Synthesis	HP0829, HP0854, HP0572 Shaffer et al. 2012, HP0323 Nikolaitchik et al. 2016
Cell shape	**HP1543- Sycuro et al., 2010** HP1075- Chan et al., 2014
DNA Damage	**HP0835- Wang et al., 2012**
Rodent Colonization	**HP1067- Terry et al., 2005 and McGee et al., 2005, HP1543- Sycuro et al., 2010, HP0835- Wang et al., 2012**
Liposaccharide Synthesis	HP0858- Nguyen et al., 2025, HP0044 and HP1275 Liu et al., 2022
Acid Induced Response	HP0463- Zimmerman et al., 2024
Quorum Sensing	HP0105 Rader et al., 2007

Supplemental Table 2. Media Ingredients Lack Known Nitroaromatic Compounds

CHBA Component	Amount	Nitrated Compounds
Pancreatic digest of Casein	10g/L	No
Proteose Peptone No. 3	3 5g/L	No
Yeast extract	5g/L	No
Beef heart infusion from 500 g	3g/L	No
Corn Starch	1g/L	No
Sodium Chloride	5g/L	No
Agar	15g/L	No
Defrinalated Horse Blood	50mL/L	No
Vancomycin	10µg/mL	No
Cycloheximide	50µg/mL	No
Polymyxin B	0.0125 U/mL	No
Cefsulodin	0.025 µg/mL	No
β cyclodextrin in dimethyl sulfoxide	0.2%/mL	No

BB10 Components	Amount	Nitrated Compounds
Pancreatic digest of Casein	10g/L	No
Peptic Digest of Animal Tissues	10g/L	No
Yeast extract	2g/L	No
Dextrose	1g/L	No
Sodium Bisulfate	0.1g/L	No
Sodium Chloride	5g/L	No
Fetal Bovine Serum	10%/L	No

BB10 Components	Amount	Nitrated Compounds
Pancreatic digest of Casein	10g/L	No
Peptic Digest of Animal Tissues	10g/L	No
Yeast extract	2g/L	No
Dextrose	1g/L	No
Sodium Bisulfate	0.1g/L	No
Sodium Chloride	5g/L	No
Fetal Bovine Serum	2.5%/L	No
Vancomycin	10µg/mL	No
Cycloheximide	50µg/mL	No
Polymyxin B	0.0125 U/mL	No
Cefsulodin	0.025 µg/mL	No
Agar	3.5g/L	No

Supplemental Table 3. Strains Used In this Study

Strain	KO#
SS1 WT	399
SS1 Δ*rdxA::kan*	1018
SS1 Δ*rdxA::cat*	1019
G27 WT	379
G27 Δ*rdxA::sfGFP*	1564
G27 Δ*rdxA::mCherry*	1563
LSH100	1275
LSH100 Δ*rdxA::cat*	1403

Supplemental Table 4. Primers Used In this Study

Primer Set	Forward	Reverse
rdxA #1	CCAAGCTCTTACAACACGCA	ACTCGCTGGGTCTTAAAGGG
rdxA #2	TGCTTGGCGTGAGATTCAAC	ACGCTCTTCTAAAACTTCGCC
rdxA #3	ATCGCTGTGGGGCAAATTTG	CTGCCACCCTCTTACCCAAA
frxA #1	GCTTTGGTTGAAGTGGGGAG	ATGACAAAATGGCTCGCTCC
frxA #2	GGCGTTACTTATGACAGCGA	GCCATCATCATGTTCGCCAT
frxA #3	CGGGCTTGAACCATGGAAAA	TCGCTGTCATAAGTAACGCC
hefA #1	CTCATTGATCCGCCGACAAG	ACACTGAGTTCTTGCGCTTG
hefA #2	CAAGGCTAGTTTGGATGCGG	ATGCCCGCTGTTGAAAATGT
hefA #3	CCTAAAGAAACGGCGACCAC	TGTGGTTCTTCATCGCTTGC
imaA	GCAACATAACGCCGGAATCT	ATCGCCGCTGAATTGGTAAC
gapB	GCCTCTTGCACGACTAACGC	CTTTGCTCACGCCGGTGCTT

Chapter#4→ The *Helicobacter pylori* predicted Ribosome silencing factor S (HP1414) is required for transcription of ribosomal protein genes and to promote tolerance to ribosome targeting antibiotics

Abstract

In 2016, the WHO categorized clarithromycin- resistant *Helicobacter pylori* as a high priority research pathogen, due to the rise of resistant clinical isolates and decreased efficacy of current treatments. *H. pylori* can maintain life-long infections that are not eradicated by the immune system nor by antibiotic treatments. The failure to eradicate *H. pylori* in patients leads to the significant risk of developing gastric cancers as *H. pylori* infections are associated with the majority to stomach cancer diagnoses. Ribosome Silencing Factor S, RsfS, is essential for *H. pylori* to survive challenging growth conditions and to form biofilms, a protective growth mechanism that allows *H. pylori* to form multicellular aggregates that are tolerant to environmental stress and high amounts of antibiotics. In this study, we analyze the transcriptional expression of *rsfS* and genes that code for ribosomal proteins in planktonic growth to begin defining the influence of RsfS on the ribosomal population. Prior studies reported that the *rsfS* gene is needed for viability in stationary phase, but surprisingly *rsfS* transcripts were more abundant in exponential phase than stationary phase. Quantifying the transcripts of RsfS's binding partner, L14 (*rplN*), in plate grown strains revealed that the deletion of the *rsfS* gene caused differential levels of *rplN* transcripts. The *rsfS* mutant similarly upregulated transcripts for other genes that code for 50S and 30S proteins, more so in exponential

phase than stationary. *rsfS* null mutants had significantly higher susceptibility to ribosome targeting antibiotics, suggesting a role for *rsfS* in protecting ribosomal populations. In summary, these findings provide evidence that *H. pylori* RsfS influences the ribosomal population and may confer a protective role for ribosomal components.

Introduction

Helicobacter pylori is pathogen that has infected nearly half the world population (Malfertheiner et al., 2023). Chronic *H. pylori* infections induce the formation of gastric lymphomas (Perez-Perez et al., 2004) and adenocarcinomas which make up a prominent portion of worldwide cancers (Park et al., 2025). In 1994, the World Health Organization (WHO) classified *H. pylori* as a Class-1 Carcinogen, which are definite carcinogens (Wroblewski et al., 2010). *H. pylori* persists against stomach acid to adhere to gastric epithelial cells (Aguilar et al., 2022). After cell adherence, *H. pylori* survives the host immune response (Fan et al., 2024), but upon the development of symptoms and a clinical diagnosis, *H. pylori* infections are typically treated with antibiotics and proton pump inhibitors (Matthews & Alexander, 2026; Schoenfeld, 2024; Vakil et al., 2004). Despite the WHO health organization recently removing Clarithromycin-resistant *H. pylori* strains from the high priority research list (*WHO Bacterial Priority Pathogens List 2024*, 2024), *H. pylori* clinical isolate have continued to be reported to have increasing resistance to currently used antibiotics (Menbari et al., 2025; Schulz et al., 2025).

H. pylori infections are commonly treated with antibiotics that include metronidazole, levofloxacin, amoxicillin, tetracycline, and clarithromycin (Matthews & Alexander, 2026; Schoenfeld, 2024; Vakil et al., 2004). However, treatment failures are currently reported due to the rise in antibiotic-resistant *H. pylori* (Aumpan et al., 2023). Of the commonly used antibiotics, tetracycline targets to the smaller 30S subunit of the ribosome (Sun et al., 2022) and clarithromycin targets the large 50S subunit of the ribosome (Kocsmár et al., 2021). *H. pylori* has been documented to resist clarithromycin by developing 23S rRNA mutations (Benigno et al., 2022; Bogiel et al., 2025; Serena et al., 2025; Xia, 1999), whereas 16S rRNA mutations are observed in tetracycline resistant *H. pylori* (Argueta et al., 2022; Gerrits et al., 2002; Lin et al., 2023; J. Y. Wu et al., 2005; W. Wu et al., 2012). Two limitations to the use of current ribosome targeting antibiotics is: (1) the efficacy of these antibiotics is greatest in exponential phase bacteria (Greulich et al., 2015) when ribosomes are assembled and active (Akiyama & Kim, 2023) and (2) *H. pylori* may have inhibitors or regulation factors that may reduce their efficacy under some conditions.

The ribosome is a common target of antibiotics, and highly abundant in the cell to carry out its function of protein synthesis. Protein synthesis is energetically costly (X.-P. Hu et al., 2020), as ribosomes make up 45% of bacterial cell mass (Pavlou et al., 2025). The bacterial 70S ribosome is composed of a small 30S subunit and a large 50S subunit (Green & Hall, 1961). The ribosome translates mRNA to polypeptides in three phases: initiation, elongation, and termination (Laursen et al., 2005). Ribosomes during these canonical steps have a well-studied dynamic, but

mechanisms that regulate ribosomes after they are produced in response to stressful conditions are only partially understood (Prossliner et al., 2018). In bacteria, protein synthesis can be regulated using mechanisms called ribosome hibernation and ribosome silencing (Helena-Bueno, Chan, et al., 2024b; Karari Njenga & Koch, 2026). Ribosome hibernation prevents translation by dimerizing two 70S ribosomes into a translationally inactive 100S dimer (Franken et al., 2017). Ribosome silencing inhibits 70S ribosome assembly by binding to a 50S protein called L14, preventing the 30S subunit from joining (Fatkhullin et al., 2022). *H. pylori* lacks known ribosome hibernation factors, but does contain a ribosomal silencing factor homologue (HP1414, *rsfS*) (Y. O. Elshenawi et al., 2026).

A common methodology used to quantify gene expression in bacterial cells is Reverse Transcription-quantitative Polymerase Chain Reaction (RT-qPCR) (Zhu et al., 2020). Traditionally, 16S rRNA is used as a reference gene to normalize target genes (Carrillo-Casas et al., 2008); however, 16S rRNA has been reported to be an inadequate reference gene in some bacteria, e.g. *Clostridium perfringens* due to non-constitutive expression in test conditions (Williams & Ghanem, 2022). The Minimum Information for Publication of Quantitative Real-Time PCR Experiment **(**MIQE) reports that to detect differential gene expression reliably with RT-qPCR, a reference gene must be validated for constitutive expression within the experiment (Bustin & Wittwer, 2017). MIQE standards for a reference gene has been applied in various bacterial species to verify the constitutive expression of alternative genes for normalization in RT-qPCR (De Oliveira et al., 2024; Gomes et al., 2023; Patole et al.,

2021). A primary application of qPCR in *H. pylori* research is to characterize the expression of virulence factors (Binmaeil et al., 2021; De La Cruz et al., 2017; Deng et al., 2020; Oktem-Okullu et al., 2015; Sasichai Kangsadalampai, 2021; Thompson et al., 2003; Wen et al., 2007). A limitation to using 16S rRNA as a reference gene during *H. pylori* planktonic growth curves is that gene transcripts for products involved in translation decrease in stationary phase (Thompson et al., 2003). Several genes in the same study were identified as potential reference genes that are constitutively expressed in exponential and stationary phase growth (Thompson et al., 2003). In this study, we screen 12 homologues (Thompson et al., 2003) and another previously used alternative gene, *gapB* (HP1346) (Collins et al., 2018), for constitutive expression in exponential and stationary phase growth. These alternative gene candidates were analyzed in planktonically grown SS1 wild type (WT) and an Δ*rsfS* knockout mutant (Ribosomal Silencing Factor S, HP1414). Our rationale for additionally verifying these genes in the Δ*rsfS* mutant was to find a gene that met two main criteria: (1) its expression does not change in stationary phase, or (2) its expression is not affected by the loss of a gene needed for stationary phase. We found that *imaA* was the only gene that was constitutively in the WT strain during exponential and stationary phase. However, constitutive expression of *imaA* in the Δ*rsfS* mutant was observed at all timepoints except for late stationary phase.

Prior work reported that *H. pylori rsfS* knockout mutants have growth defects upon exposure to atmospheric conditions, during stationary phase growth, in low serum conditions, in biofilm assays, and *in vivo* (Y. O. Elshenawi et al., 2026); these

defects could be corrected with the re-introduction of the *rsfS* gene and its native promoter in a neutral locus (Y. O. Elshenawi et al., 2026). To gain more insight into the nature of the function of RsfS, we analyzed the transcription of the *rsfS*, *rplN (*encodes L14), and several additional genes that encode proteins for the ribosomal 50S subunit (L1, L2) and 30S subunit (S4, S20) and 16S rRNA modifying enzyme (*rsmD*). These proteins were chosen for their critical roles in 70S ribosome assembly to gain further insight in the influence of RsfS on the ribosome population. L1 (Nevskaya et al., 2006) and L2 (Willumeit et al., 2001) are part of the 50S subunit and are essential for 70S ribosome assembly (Diedrich et al., 2000; Seffouh et al., 2024). S4 is critical for 70S assembly at multiple stages, (Mayerle & Woodson, 2013) and S20 promotes 70S assembly efficiency via mRNA binding (Tobin et al., 2010). The third gene we included in this screen is *rsmD,* a small rRNA methyltransferase (Sergeeva et al., 2012) that was predicted to be constitutively expressed in exponential and stationary phase growth (Thompson et al., 2003). Because *rsfS* was needed in stationary phase, we hypothesized it would be expressed maximally there. Contrary to our expectations, we found that *rsfS* transcripts are more abundant in exponential phase than stationary phase. Additionally, we found that *rsfS* knockout, complement and double copy mutants differentially transcribed L14. Interestingly, the *rsfS* deletion causes L14 (*rplN*), L1 (*rplA*) and L2 (*rplB*) transcripts to be similarly upregulated during exponential phase, but each were differentially expressed in stationary phase. Genes for 30S subunit proteins were found to have differential mRNA levels the *rsfS* knockout mutant as well, relative to the WT. Notably we find

that the *rsfS* knockout mutants are more susceptible to ribosome targeting antibiotics such as tetracycline, which targets the 30S subunit (Sun et al., 2022), and chloramphenicol, which targets the 50S subunit (Long, 2003). These findings suggest that *rsfS* expression is related to transcription of other genes that code for ribosomal proteins, and that loss of *rsfS* creates cells that are more susceptible to antibiotics, suggesting its inhibition would be a good target to enhance antibiotic efficacy.

Results

Identification of a constitutively expressed gene to be used as a reference gene

Our first goal was to evaluate expression of *rsfS* across a bacterial growth curve. However, preliminary experiments found that several genes previously used for normalization were downregulated during stationary phase, complicating our ability to define *rsfS* expression patterns. We therefore analyzed the literature for *H. pylori* genes that might not differ between exponential and stationary phase conditions (Thompson et al., 2003). This previous microarray study identified thirteen candidate genes that could be organized into five categories by function: metabolism (*hypE, ppK, dgkA, narK* and *gapB*), DNA modification (*cinA*, *uvrC*), synthesis pathways (*bioV*, *pseI*), and membrane proteins (*horD, β-OMP, imaA*, putative *abc* transporter) (Supplemental Table 1). RNA was isolated from WT and the *rsfS* null mutant and equal amounts of RNA were converted to cDNA to obtain Cq values via qPCR to quantify gene transcripts. Many of the target genes were down regulated in stationary phase and produced standard deviations greater than 0.3, the MIQE standard (Bustin

& Wittwer, 2017), and also varied between WT and *rsfS* mutant (Figure 1). Conversely, *imaA* was constitutively expressed in the WT strain across all time points with standard deviations below 0.3 (Figure 1D). In the Δ*rsfS* mutant, *imaA* was found to generally also be constitutively expressed with the exception of the late stationary phase time point (35h). Of all the gene transcripts that were analyzed, *imaA* most fit our criteria for a reference gene as its mRNA levels did not change in stationary phase and was least affected by the Δ*rsfS* mutant stationary phase defects.

rsfS transcripts are more abundant in exponential phase and less abundant in stationary phase

Prior work has shown that the deletion of *H. pylori rsfS* caused stationary phase defects that could be complemented by the re-introduction of *rsfS* in a neutral locus (Y. O. Elshenawi et al., 2026). We sought to analyze the expression of *rsfS* under these same conditions using a previously used a *rsfS* primer set referred to as #1 that targets +28 to +366 of the transcript (Y. O. Elshenawi et al., 2026), *rsfS* primer set#2 targets +31 to +147 of the transcript and *rsfS* primer set#3 targets +120 to +268 of the transcript (Supplemental Table 2). *rsfS* transcripts were normalized to *imaA* transcripts that are constitutively expressed in SS1 WT growth curve. Due to the loss of the *rsfS* gene resulting in stationary phase viability defects, we hypothesized that *rsfS* transcripts would be abundant in stationary phase. However, all three primer sets revealed the opposite: the highest amount of *rsfS* transcripts occurred in early exponential phase (Figure 2). *rsfS* transcript abundance steadily declined as growth progressed (Figure 2). By early stationary phase at 24h, all three primer sets detected

a decline in *rsfS* transcripts that continued to mid-stationary phase at 30h, with the lowest abundance at 35 hours (Figure 2). At late stationary phase (35h), all three primer sets demonstrated less *rsfS* transcript abundance than any of exponential phase time points, although there was some variation in the extent between them (Figure 2). In summary, all three primer sets consistently presented that *rsfS* transcripts were more abundant in exponential phase versus stationary phase.

rplN (L14) transcripts are upregulated upon the deletion of *rsfS*

We next explored whether *rsfS* could influence the transcription of its binding partner, L14 encoded by *rplN*. Several isogenic strains were analyzed due to their varying profiles of RsfS expression (Y. O. Elshenawi et al., 2026) including WT, two *rsfS* deletion strains (Δ*rsfS::kan* and Δ*rsfS::cat*), strains with two copies of *rsfS* (WT Δ*rdxA::rsfS* (2p), WT Δ*rdxA::rsfS* (1p), WT *Δintergenic::rsfS*), and complemented mutants (Δ*rsfS* Δ*rdxA::rsfS* (2p), Δ*rsfS* Δ*rdxA::rsfS* (1p), Δ*rsfS::Δintergenic::rsfS*) (Supplemental Table 3, Supplemental Figure 1). Five primer sets targeting *rplN* transcripts (Supplemental Table 2) were used to obtain Cq values (Supplemental Figure 2). RNA was isolated from each strain that was plate grown as was done with the *rsfS* primer set#1 in Elshenawi et al., 2026. Both Δ*rsfS* mutants caused had an increase in the ΔCq relative to the wildtype which indicated a 6.3-fold and 1.7-fold upregulation of *rplN* transcripts in Δ*rsfS::kan* and Δ*rsfS::cat* relative to the WT parent strain (Figure 3). *rsfS* complementation did not restore *rplN* expression to WT levels, even using the complementation strain that correct the *rsfS* growth phenotypes (Figure 3). Strains with

two copies of *rsfS*, using either the *rdxA* locus or the intergenic locus, produced *rplN* transcripts similar to the *rsfS* mutant (Figure 3). The intergenic double copy mutant (WT *Δintergenic::rsfS*) is the only strain that produced less transcripts than Δ*rsfS::cat* but still had elevated amounts relative to the WT (Figure 3). All in all, the data suggests deletions of *rsfS* and the *rdxA* gene causes differential *rplN* mRNA levels, but it is not clear whether differential *rlpN* transcription is a direct effect caused by *rsfS* expression.

ΔrsfS::cat produces more abundant *rplN* (encodes L14) transcripts in exponential phase and mid-stationary phrase growth

The above results suggest that the absence and overexpression of *rsfS* influences *rplN* (L14) transcript abundance, but this approach was limited to plate grown *H. pylori*. We therefore quantified *rplN* transcripts across a growth curve, using endpoint sample preparation to minimize effects of condition changes as previously described in Elshenawi *et al.,* 2026. The same five primer sets mentioned in the above paragraph were used to obtain Cq values (Supplemental Figure 3). *rplN* transcripts were in lower amounts at the first exponential phase time point (6h) as the Δ*rsfS::cat* mutant only produced an average of 0.22-fold less *rplN* transcripts than the WT across all the primer sets (Figure 4). Interestingly, Δ*rsfS::cat* upregulated *rplN* transcripts by 1.7-fold and 2.3-fold at exponential phase timepoint at 9h and 12h respectively (Figure 4). A slight variance in upregulation was observed at the exponential phase point 16h, as a majority of primer sets reported a range (2.6-3.8 fold) (Figure 4). At the late exponential phase time point (20h), there was generally not a change in *rplN* transcript amounts, a phenotype that persisted into the later time points (Figure 4). The higher abundance of

rplN transcripts at exponential phase in the Δ*rsfS::cat* mutant (Figure 4) is an interesting finding as the WT strain exhibits a higher amount of *rsfS* transcripts in exponential phase. These findings indicate that the complete absence of *rsfS* expression causes an increase in *rplN* transcripts under certain growth conditions.

ΔrsfS::cat upregulates the transcription of genes that code for 50S subunit proteins in a similar trend as *rplN* (L14) during exponential phase

The above finding that *H. pylori rsfS* mutants have differential expression of *rplN* (L14) transcripts, led us to wonder whether other components of the 50S subunit would be expressed differently due to the loss of *rsfS*. We decided to screen genes that code for L1 (*rplA*) and L2 (*rplB*) (Supplemental Figure 5), 50S proteins that are critical for 70S ribosome assembly (Seffouh et al., 2024; Willumeit et al., 2001). The Δ*rsfS::cat* mutant had nearly half the amount of transcripts for *rplA* in early exponential phase (6h) and mid stationary phase (30h) (Figure 5); however, *rplA* was upregulated at all the timepoints in between with its peak abundance being observed to be increased 73% relative to the WT at the exponential phase time point 16h (Figure 5). L2 on other hand did not follow the same expression trend as *rplB* transcripts were less abundant at early exponential phase (6h), late exponential phase (20h) and early stationary phase (24h) by 40%, and 20% and 19% respectively (Figure 5). *rplB* transcripts had less dramatic increase than *rplA* (L1), but its peak abundance was observed at 16h by 51% (Figure 5). Although these expression patterns are variable from each other, *rplA* and *rplB* transcript expression during exponential phase (9h,12h,16h) seem to follow the same progressive trend as *rplN.*

The similarities in these expression trends indicate that *rsfS* expression during exponential phase is critical for the wild-type expression of genes that encode 50S proteins.

ΔrsfS::cat differentially transcribes genes that code for 30S subunit proteins in a similar during planktonic growth

To further explore the impact of loss of *rsfS* on expression of other ribosomal genes, we further examined transcription of genes for 30S proteins. The genes we included in this analysis code for S4 (*rspD*) which is needed for 70S assembly at multiple stages (Mayerle & Woodson, 2013), S20 (*rspT*) which promotes 70S assembly efficiency (Tobin et al., 2010), and a small rRNA methyl transferase *rsmD* (Sergeeva et al., 2012) that was predicted to be constitutively expressed during *H. pylori* planktonic growth (Thompson et al., 2003) (Supplemental Figure 5). The Δ*rsfS::cat* mutant downregulated *rspD* for most the exponential phase timepoints except for the 16h time point where the transcripts increased by 85% (Figure 6). *rspD* transcripts were also slightly more abundant in early-mid stationary phase by 10-15% (Figure 6). *rspT* transcripts were less abundant at early (6h) and late (20h) exponential phase time points by 20% and 16% respectively, as well as early stationary phase (24h) by 30% (Figure 6). *rspT* transcripts were significantly more abundant between exponential phase time points (9h-16h) upwards of 70%-105% and at mid stationary phase (30h) by 84% (Figure 6). *rsmD* transcripts were more abundant at the beginning of exponential phase (6h,9h) by 57% and 14%, but between mid-exponential (12h) and mid-stationary (30h) phase, the Δ*rsfS::cat* mutant produced

approximately 10%-15% less of *rsmD* transcripts (Figure 6). The transcription of genes that encode proteins for the 30S subunit did not have an expression trend that is empiric to what was observed with genes for the 50S subunit, but it was still differential to WT expression. Our results indicate that a lack of *rsfS* transcription causes the differential transcription of genes for the 30S subunit.

ΔrsfS::cat have more abundant *rplA* (L1), *rplB* (L2) and *rpsD* (S4) transcripts at late stationary phase

A limiting factor to using *imaA* as a reference gene for the latest stationary phase timepoint is reported above, specifically the Δ*rsfS::cat* mutant did not produce an equivalent Cq value for *imaA* transcripts as the WT. Alternatively we opted to use *rdxA* as a reference gene solely for the late stationary phase time point as it was the only gene transcript that we observed in the Δ*rsfS::cat* to have near equivalent Cq values to the WT (Supplemental Figure 7A). ΔCq values were obtained for each gene by normalizing RT-qPCR results for *rlpN* (L14), *rlpA* (L1), *rlpB* (L2), *rspD* (S4), *rspT* (S20) and *rsmD* to *rdxA* (Supplemental Figure 7B) so that $2^{-\Delta\Delta Cq}$ analysis could be conducted to calculate fold change in the Δ*rsfS::cat* mutant relative to the WT (Supplemental Figure 7C). Of the primer sets that were designed for *rlpN*, all primer sets indicated that the Δ*rsfS::cat* mutant expresses only 22-32% of transcripts relative to the WT, whereas primer set# 4 was the only primer set that reported a 137% increase in transcripts (Figure 7). *rplA* and *rplB* both had more transcript abundance at 75% and 523% respectively (Figure 7). *rspD* was the only 30S ribosome gene that was upregulated in the Δ*rsfS::cat* mutant by 109%, whereas *rspT* and *rsmD* was

decreased by 36% and 50% respectively (Figure 7). In conclusion at late stationary phase, the Δ*rsfS::cat* mutant dramatically upregulates *rlpB* transcripts and slightly upregulates *rlpA* and *rspD* genes while transcripts of RsfS's binding partner L14 (*rplN*) are significantly downregulated. Further work at the protein level is needed to determine the translation effects of these transcription trends, but these combined transcriptional trends indicate that *rsfS* expression is needed for the normal expression of genes that code for multiple ribosomal proteins.

***ΔrsfS::cat* mutant has a higher susceptibility to ribosome targeting antibiotics**

To explore the role of RsfS in antibiotic sensitivity, E-test strips were used to determine how loss of *rsfS* affected *H. pylori's* susceptibility to antibiotics. The two antibiotics we tested were tetracycline, which targets the 30S ribosome (Sun et al., 2022), and clarithromycin, which targets the larger 50S subunit of the ribosome (Kocsmár et al., 2021). The Δ*rsfS::cat* strain MIC for tetracycline and clarithromycin were 8-fold and 7.8-fold lower than the WT respectively (Table 1). Additional antibiotics that target other cell components were also examined, including levofloxacin, a fluoroquinolone that target DNA gyrase to inhibit cell growth (Cao et al., 2020), and amoxicillin, a beta-lactams antibiotic that disrupts cell wall synthesis (Huttner et al., 2020). The Δ*rsfS::cat* strain MIC for levofloxacin and amoxicillin were 1-fold and 2.4-fold lower than the WT respectively (Table 1). Although the deletion of *rsfS* generally lowered its MIC towards all the antibiotics that were screened, the fold difference in susceptibility to ribosome targeting antibiotics was

significantly more. Our results provide a preliminary indication that functional RsfS provide a protective role to the ribosomal subunits that protect them from being targeted by antibiotics therefore promoting their tolerance.

Discussion

RsfS is primarily categorized as a ribosome silencing factor with an ability to bind to pre-mature 50S ribosome indicating biogenesis (can we preprint mini review so I can reference it here?). Our work provides preliminary evidence that *H. pylori* RsfS has potential roles in ribosome biogenesis and protecting the 50S ribosome from degradation due to its influence on ribosome gene transcript abundance and promoting tolerance to ribosome targeting antibiotic (Figure 8). We report that *H. pylori rsfS* transcripts are more abundant during exponential phase and decreases in stationary phase. We were able to reach this conclusion by screening potential reference genes and identifying that the *imaA* gene as one that did not change over the *H. pylori* growth curve. We also determined that deletion of the *rsfS* gene caused an increase in *rplN* transcripts that encode L14. This effect was most pronounced at certain timepoints, specifically exponential phase. In addition to L14, we screened additional genes for proteins in the 50S and 30S subunit and found the *rsfS* null mutant also differentially transcribed these genes at certain growth phases. The *rsfS* knockout mutants were more susceptible to ribosome targeting antibiotics such as tetracycline and chloramphenicol.

H. pylori transcriptomes are not well characterized (Sharma et al., 2010) and the field lacks studies that validate the constitutive expression of reference genes for

RT-qPCR analysis. A typical practice in RT-qPCR is to select reference genes that are in a different biological pathway than the target gene (Jacobsen et al., 2014). Although 16S rRNA is a commonly used reference gene in bacterial qPCR, it has been reported to have variable expression in test conditions (Williams & Ghanem, 2022) and is not a suitable choice when studying ribosome regulation factors such RsfS. In this study, we screened genes in the following pathways for constitutive expression in exponential and stationary phase growth: metabolism, DNA modification, synthesis, outer membrane proteins and transport proteins. Only one gene, *imaA* (HP0289)*,* was determined to be a constitutively expressed gene *in vitro* in the SS1 WT and *rsfS* mutant strain, in nearly all timepoints except for the late stationary phase. Interestingly, differential expression trends were observed in the Δ*rsfS* in *pseI* transcripts which could possibly indicate that ribosomal silencing and flagella glycosylation are co-regulated pathways. Although metabolic genes were reported to be downregulated in stationary phase (Thompson et al., 2003), genes involved in hydrogen, inorganic polyphosphates, fatty acids phospholipids, and nitrogen metabolism were predicted to be constitutively expressed. Additionally, *gapB* has been used previously as references gene for *H. pylori* qPCR for *in vivo* conditions (Collins et al., 2018)*;* however our results indicate that due to *gapB's* role in glycolysis, it is not a suitable choice as a reference gene for exponential and stationary phase growth as it is downregulated in stationary phase when nutrients are limited (Wells & Gaynor, 2006). In summary, candidate genes involved in metabolic pathways presumably are not ideal choices for qPCR on *H. pylori* cells in stationary

phase growth. Due to *H. pylori's* high mutation rates (Suerbaum & Ailloud, 2023), it could be presumed that DNA modification enzymes would be actively transcribed during *H. pylori* growth. Instead, we found variable expression of DNA modification genes in both strains regardless of growth phase. Interestingly, genes in synthesis pathways were downregulated in stationary phase in both strains despite being in different pathways: *bioV* is a gene involved in biotin synthesis (Bi et al., 2016) and *pseI,* a gene involved in flagellin glycosylation (Schoenhofen et al., 2006). While no clear trend could be observed with the DNA modification enzymes in either strain, biosynthetic pathways particularly flagellin glycosylation were significantly downregulated in the Δ*rsfS* mutant. This could indicate that genes in biosynthetic pathways are not optimal choices for reference genes in qPCR when studying genes involved in ribosomal regulation. *H. pylori* outer membrane proteins are known for their role in pathogenesis as they can serve several functions including adherence to stomach tissue and transporting molecules such as nutrients or antibiotics across the cell membrane (You et al., 2025). The β-barrel OMP (Outer membrane protein) gene in this study has not been previously studied but its downregulation in stationary phase is consistent with expression trends of other metabolic genes. These similar expression trends potentially indicate that this β-barrel OMP has a role in metabolite uptake. Conversely, *horD,* is known to belong to a family of proteins that facilitate *H. pylori* adhesion to the gastric epithelium had variable expression with no definitive expression trend. The putative osmo-protective ABC transporter has not been previously studied, but variable expression phenotypes were observed between the

WT and Δ*rsfS* mutant. Expression trends indicate that elevated expression of the ABC transporter in the Δ*rsfS* mutant mid-late stationary phase growth might potentially be a compensatory effect. The *imaA* gene was the only gene that showed constitutive expression in the WT strain across all timepoints. Previous work had shown that *imaA* is upregulated *in vivo* and in response to acid (Sause et al., 2012), but under the conditions used here, its expression is not affected in planktonic conditions except in the Δ*rsfS* mutant as it is not constitutively expressed at late stationary phase. Considering all candidate reference genes screened in the Δ*rsfS* mutant had significantly higher expression at the late stationary phase timepoint combined with its stationary phase defect (Y. O. Elshenawi et al., 2026), it is possible that these phenotypes indicate that the Δ*rsfS* mutant is in death phase at 35h. Further testing using a bioanalyzer on RNA samples could detect lack of prominent 16s rRNA and 23S rRNA in the Δ*rsfS* mutant at 35h of growth relative to the WT would determine if these afore mentioned phenotypes are due to death phase.

Contrary to our original hypothesis, *rsfS* transcripts were less abundant in stationary phase (Figure 2). This finding contrasts to the small-scale expression study in *E. coli,* which showed its RsfS protein (called RsfA) was greatly increased in stationary phase. A potential reason could be that *H. pylori rsfS* transcription is co-regulated with expression of genes involved in translation as prior transcriptome studies reported these genes to be downregulated in stationary phase (Thompson et al., 2003). This finding aligns with our observations that the WT strain exhibited a lower

abundance of all the ribosomal gene transcripts we screened in stationary phase (Supplement Figure 3,4,5). This led us to hypothesize a common regulatory pathway for the transcription of *rsfS* and genes that code for proteins in the 50S subunit. In Elshenawi et al., 2026, a multitude of *rsfS* mutants was generated with a diverse range of *rsfS* transcriptional expression (Supplement Figure 2) (Y. O. Elshenawi et al., 2026). Although the initial *rsfS* deletion to generate the *rsfS::kan* mutant consequentially resulted in a significant upregulation in *rplN* (L14) transcripts that was slightly decreased in the *rsfS::kan* (Figure 3), One could eliminate the Kan^R cassette as the contributor for the elevated *rplN* transcripts due to the observation that *rdxA::cat* mutants had more elevated *rplN* transcripts than *rdxA::kan*. These combined findings indicate that *rplN* transcript expression is independent of the antibiotic cassette but can be elevated by the deletion of either the *rsfS* or *rdxA* gene. Since no definitive conclusions could be made about *rsfS* transcriptional expression and its possible relationship with *rplN* transcript abundance from this assay using plate grown bacteria, this led us to investigate *rplN* expression in the *rsfS::cat* mutant planktonic growth.

When the expression of *rplN* (L14), *rplA* (L1) and *rplB* (L2) were analyzed over the planktonic growth, *rsfS::cat* mutant and the WT strain exhibited similar expression trends in exponential phase. The *rsfS::cat* mutant increased *rplN*, *rplA* and *rlpB* transcripts progressively throughout exponential phase (Figures 4,5). Heterogeneity in the increase of these transcripts was observed throughout stationary phase except for

the late stationary phase-time point where all 50S genes transcripts were observed to be upregulated (Figure 7). Interestingly, *rplN* and *rplB* followed similar expression trends as both transcripts increased in mid stationary phase (30h), but *rplB* was less abundant at other stationary phase timepoints whereas *rplN* was not impacted relative to the wild-type (Figures 4 & 5). Other than binding to RsfS, L14 is one of the most conserved ribosomal proteins and that binds to the 23S rRNA to stabilize the structure of the 50S subunit, specifically the area between the peptidyl transferase and the GTPase (Davies et al., 1996). The *rsfS::cat* mutant might be upregulating L14 during exponential phase when ribosomes are actively translating to increase 50S stability in the absence of the RsfS during exponential phase and mid stationary phase. The decrease in *rplN* transcripts at early and late exponential phase and early to late stationary phase suggests that the *rsfS::cat* mutant does not require or has sufficient 50S subunit stability do the increase of *rplN* transcripts at other timepoints. L1 has two known roles as a binding protein for 23S rRNA and is its own translation repressor, (Tishchenko et al., 2007) indicating that the increased transcript abundance is required to compensate for lack of *rsfS* expression for exponential phase and early and late stationary phase. The decreased abundance of *rplA* transcripts in early exponential phase and mid-stationary phase indicates that *rplA* represses its expression at these timepoints as the *rsfS* mutant does not require 70S ribosome assembly. L2 is also a 23S rRNA binding protein that is essential for ribosome assembly and for the functionality of the peptidyl transferase center (PTC) and tRNA binding (Diedrich et al., 2000); so it's upregulation due to the deletion of *rsfS* indicates excessive *rplB* at exponential

phase and exponential phase, early and late stationary phase indicate the heterogeneity of transcript abundance relative to *rplN* and *rplA* is due the *rsfS* mutant requiring its ribosomes to undergo translation at certain timepoints. In summary, transcripts of *rplN*, *rplA* and *rplB* indicate that 50S stability, 70S assembly and translation activity is upregulated by the *rsfS* mutant during exponential phase whereas these functions are selectively needed for different stages in stationary phase. The fluctuating levels of 50S protein gene transcripts suggests that *rsfS* transcription is needed for the transcription of genes for 50S proteins, and the absence of *rsfS* results in differential expression of these genes.

We also explored whether genes for 30S proteins S4 (*rspD*) and S20 (*rspT*) were affected by *rsfS*. *rspD* was the most impacted gene transcript by the *rsfS* deletion as its abundance progressively increased throughout both the exponential and a stationary phase (Figure 6, 7). Given that S4 is needed for multiple stages of 70S ribosome assembly, the presumable shift in 50S gene transcription would alter S4 transcription (Mayerle & Woodson, 2013). S20 regulates 70S assembly efficiency (Tobin et al., 2010) and therefore less impacted by the *rsfS* deletion relative to S20 (Figure 6, 7). *rsmD* transcripts were predicted to be constitutively expressed throughout planktonic growth curves (Thompson et al., 2003), however due to its role in translation (Sergeeva et al., 2012), the Δ*rsfS::cat* mutant was observed that more abundant *rsmD* transcripts in exponential phase that decreased in stationary phase (Figure 6, 7). The gene transcripts that encode proteins for the 30S subunit did not have an expression trend that is empiric to what was observed with genes for the 50S subunit, but it was

still differential to WT expression. Our observation supports a model in which the absence of *rsfS* causes the differential expression of 50S genes that causes a downstream effect on the transcription of genes for the 30S subunit.

H. pylori strains are typically treated with triple therapies consisting of a proton pump inhibitor plus two antibiotics, clarithromycin plus amoxicillin or metronidazole (Matthews & Alexander, 2026; Schoenfeld, 2024). However, clarithromycin resistance *H. pylori* has gained global recognition (Kocsmár et al., 2021) for leading to treatment failures that require second-line approaches (Shih et al., 2023; Sun et al., 2022). The absence of the *rsfS* gene caused *H. pylori* to be more susceptible to ribosome targeting antibiotics (Table 1). One possibility is that RsfS binding to the 50S subunit offers a protective role from targeting via antibiotics, as proposed by others. Potential mechanisms for ribosome hibernation factors, including RsfS, to decrease the efficacy of ribosome targeting antibiotics has not been extensively explored. L14 is not in proximity to clarithromycin's binding site, the nascent polypeptide exit tunnel on the 50S (Dinos, 2002), or tetracycline's binding site on the 16S rRNA (Brodersen et al., 2000). However, the efficacy of ribosome targeting antibiotics has been primarily assessed in exponential phase bacteria where ribosomes are assembled and actively translating (Greulich et al., 2015). The efficacy of antibiotics binding to silenced RsfS-50S subunits that are not assembled to actively translating ribosomes to induce cell death remains an open question. Regardless of the mechanism, the results suggest that eliminating RsfS or decreasing its expression

might create *H. pylori* that are more treatable by currently used therapeutics. Given the difficulty curing *H. pylori* infections, these insights might provide important interventions that help prevent gastric disease.

In conclusion, our study preliminary supports a model that *H. pylori* RsfS has additional roles as a ribosome biogenesis factor and a protective chaperone (Figure 8). Our findings suggest that loss of the *rsfS* gene effects the transcript abundance of genes in multiple physiological pathways including genes that code for ribosomal proteins. Candidate reference genes that were screened during planktonic growth for constitutive expression led to the identification of the *imaA* gene as the most suitable reference for analyzing target transcripts in this growth. Although the *rsfS* gene is required for stationary phase growth (Y. O. Elshenawi et al., 2026), *rsfS* transcripts were found to be less abundant in stationary phase unlike what was observed in *E .coli* (Häuser et al., 2012); this indicates that regulatory mechanisms for RsfS expression is species specific and that protein work is needed to characterize *H. pylori* RsfS expression. The absence of the *rsfS* gene causes differential mRNA levels of *rplN* (L14) in both plate grown and planktonic growth conditions indicating that *rsfS* and L14 transcription is co-regulated. Genes that code for 50S and 30S proteins and are essential for 70S assembly are differentially transcribed by the *rsfS* null mutant during planktonic growth. This suggests that RsfS influences the abundance of assembled 70S ribosomes and free 50S and 30S subunits, but further protein work is needed to definitively conclude this. Given that the presence of the *rsfS* gene promotes tolerance to ribosome targeting antibiotics additionally indicates that RsfS plays a protective role for ribosomal

subunits and should be investigated as potential drug targets. Further investigation into *H. pylori* RsfS's potential role as a protective chaperone would provide insight into the dynamics of ribosome degradation during stationary phase and other growth-limiting conditions to promote bacterial survival (Piir et al., 2011). All in all, additional methods are needed to characterize the potential roles of *H. pylori* RsfS in silencing the 50S subunit, regulating 50S subunit biogenesis and protecting the 50S from degradation.

Methods and Materials

H. pylori strains and growth conditions

H. pylori strains SS1, G27 and 22695 were incubated at 37°C with 5% O_2, 10% CO_2, and 85% N_2. Cultures were on grown using Columbia Horse Blood Agar (Difco) plates supplemented with 5% defibrinated horse blood (Hemostat Labs, Davis, CA) and 0.2% β-cyclodextrin, 50 μg/ml cycloheximide, 10 μg/ml vancomycin, 5 μg/ml cefsulodin, 2.5 U/ml polymyxin B. For planktonic growth curves and biofilm assays, liquid cultures were inoculated using bacteria grown for 72h on agar plates and were shaken for 12h-15h in brucella broth (Becton, Dickinson and Company) with 10% fetal bovine serum (FBS; Gibco). Plate grown bacteria were scraped using a sterile loop and added directly to 1mL of TriZol and immediately stored in -80°C for RNA extraction

Planktonic growth curves

For planktonic growth curves, liquid cultures were back diluted with fresh BB10 or BB2 (2% FBS) and normalized to OD_{600} of .1, planktonic cultures were grown shaking for singular time points where OD_{600} was measured and a small volume was used serial dilutions were plated on agar to calculate CFU. The remaining culture was centrifuged at 16,000g to pellet bacterial cells and separate from liquid media. Liquid media was removed by pipetting and cell pellets were resuspended in 1mL of TriZol and immediately stored in -80°C for RNA extraction and qPCR work.

RNA Extraction

RNA extractions were conducted using the Purelink RNA Minikit (CAT#12183018A). Samples suspended in TriZol were incubated at room temperature for 5 minutes. Chloroform was then added to samples and shaken vigorously by hand for 15 seconds. Mixture was then incubated at room temperature for 3 minutes. Samples were centrifuged at 15,000 × g for 15 minutes at 4°C which separated the mixture into a lower pink phenol-chloroform phase, an opaque white interphase, and a clear upper phase containing RNA. The upper phase was transferred to a new RNase–free tube. Equal volume of 70% ethanol (final concentration ~35%) was added and then mixed by vortexing and inverted to disperse any precipitate. The homogenized mixture was then added to spin cartridge and centrifuged at 15,000 × g for 1 minute at 4°C. Wash Buffer I to the Spin Cartridge and centrifuged at 15,000 × g for 15 seconds at 4°C. The flow-through was discarded and the column was treated DNase mixture from Turbo DNA-Free Kit (Invitrogen ThermoFisher CAT#

AM1907) at room temperature for 15 minutes. Insert the Spin Cartridge into a new Collection Tube. Wash Buffer I was then added to the Spin Cartridge and Centrifuge at 15,000 x g for 15 seconds at 4ºC. The flow-through was discarded and then Wash Buffer II with ethanol was added to the Spin Cartridge and centrifuge at 15,000 x g for 15 seconds at 4ºC. Wash Buffer I and II steps were repeated once. The membrane was dried by centrifuging the Spin Cartridge at 15,000 × g for 1 minute at 4ºC. RNase–Free Water was added to the membrane of the Spin Cartridge and incubated at room temperature for 1 minute. RNA was eluted by centrifuging the Spin Cartridge in a fresh RNase free tube for 1 minute at 15,000 x g at 4ºC. RNA yields were quantified using a ThermoScientific Nanodrop 2000 Spectrometer. Protein and reagent contamination was assessed using the 260/280 and 260/230 ratios respectively. Exponential phase RNA was frozen immediately with dry ice and stored in -80ºC in aliquots for single usage that were only thawed once for cDNA synthesis. For stationary phase, biofilm and *in vivo* samples, RNA was immediately processed into cDNA and stored in -80ºC to prevent degradation from constant freeze/thawing.

cDNA synthesis

cDNA was synthesized using High-Capacity cDNA Reverse Transcription Kit with RNase Inhibitor (Thermo Fischer CAT#4374966) using the recommended master mix for a 20ul total reaction volume (10ul of Master Mix to 10ul of RNA Samples) and the recommended PCR incubation steps: Step#1- 25ºC for 10 minutes, Step#2- 37ºC for 120 minutes, Step#3: 85ºC for 5 minutes, and Step#4- 4ºC hold. A total of 1ug of RNA for each sample was used for cDNA synthesis and diluted with RNase- Free

water to generate samples with a total volume of 10ul. Four technical replicates for cDNA synthesis were conducted for each biological RNA replicate. A no RNA template control (NTC) was included to ensure no reagents were contaminated and a no-reverse transcriptase control (No RT) was added to assess for genomic DNA contamination in qPCR reactions as well.

qPCR protocol

Power SYBR™ Green PCR Master Mix (CAT#4367659) was used for all qPCR reactions executed on Bio-Rad CFX96 Real Time PCR Detection System. A total of 1uL of cDNA reaction was combined with forward and reverse primers for target genes (5uM), 10ul of PCR Master Mix and diluted with water for a total volume of 20uL per reaction according to the Applied Biosystems recommended guidelines. The thermal cycling conditions were conducted as following: Step#1- 95ºC for 10 minutes, 40 cycles of denaturing at 95ºC for 15 seconds and Annealing/extension at 60ºC for 1 minute with a final melting curve step for 5 seconds at T_m specific to the primer set. No template and no-reverse transcriptase controls were used to screen for genomic DNA and reagent contamination that could conflate fluorescence detection. Six technical replicates were conducted for each biological replicate per primer set. Upon completion of the thermal cycling steps to obtain Cq values, the resulting reactions underwent gel electrophoresis using an 1% agarose gel to verify target gene specificity by size.

Antibiotics ETEST

H. pylori strains used to determine antibiotic minimum inhibitory concentration (MIC) were grown overnight in BB10. Overnight cultures were diluted to an OD_{600} of 0.5 and 200uL were plated on CHBA. Antibiotic susceptibility was tested in triplicates using ETEST strips (bioMérieux) for the following antibiotics: amoxicillin, clarithromycin, levofloxacin and tetracycline. ETEST strips were applied to plates and incubated under microaerobic conditions for five days. MICs were determined to be at concentrations on the strip bordered by bacterial growth.

Figures and Legends

Fig. 1.

Figure 1. Cq values for candidate reference genes for planktonic growth. Expression of the indicated target genes were analyzed in *H. pylori* SS1 strains WT (blue) and Δ*rsfS* (red), at exponential (6h-20h) and stationary phases (24h-35h). Transcripts were quantified using qRT-PCR on cDNA produced from equal amount of RNA of RNA were converted to cDNA to obtain Cq values for genes involved in (A) metabolism (orange axis), (B) DNA modification (pink axis), (C) synthesis pathways (green axis), and (D) membrane proteins (purple axis). Standard deviations (STD) were calculated across all timepoints with means annotated at the bottom of the bars and technical replicates are annotated at the top.

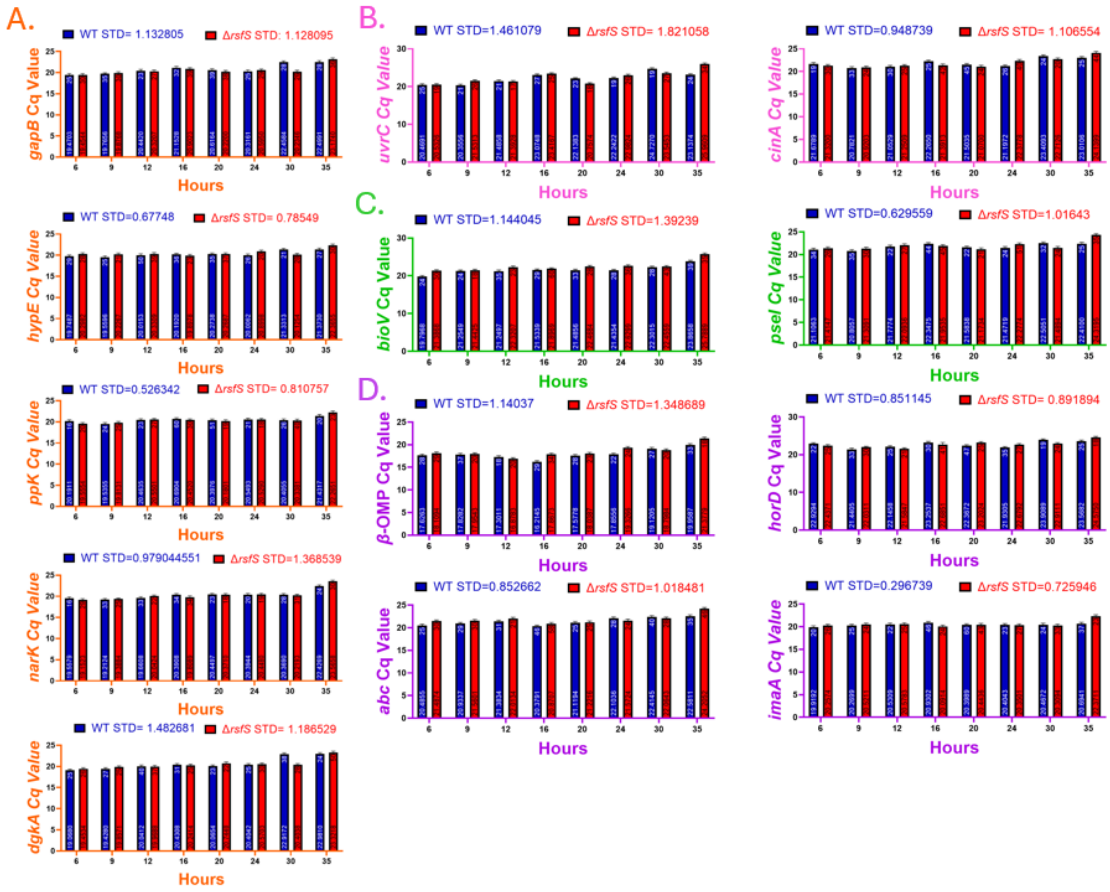

Fig. 2.

Figure 2. *rsfS* transcripts are more abundant in exponential phase versus stationary phase. (A) RT-qPCR analysis was conducted on SS1 WT grown planktonically (3-6 biological replicates) to compare *rsfS* transcript abundance using three primer sets in exponential phase (6h-20h) and stationary phase (24h-35h). ΔCq was obtained by normalizing *rsfS* transcripts to *imaA*. **(B)** Primer binding sites on the *rsfS* operon for primer set#1 (blue), primer set#2 (purple) and primer set#3 (pink) annotated with the start codon (green) and stop codon (red).

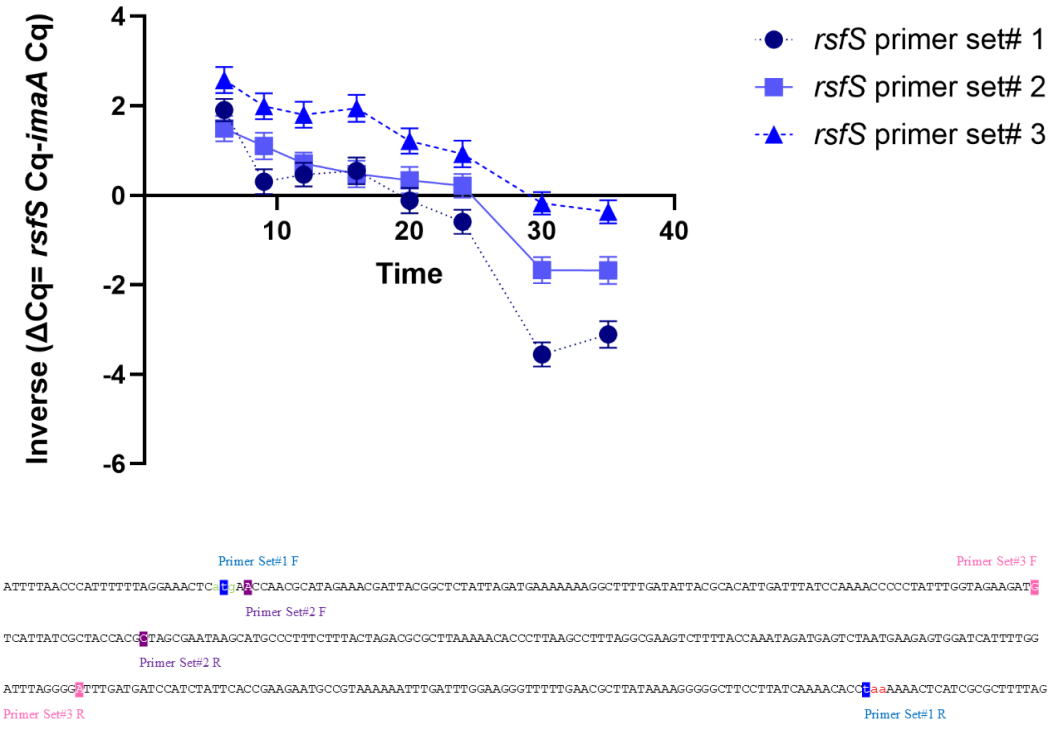

Fig. 3.

Figure 3. *rplN* (L14) Transcripts in Plate Grown Bacteria. RT-qPCR was isolated from 4-6 biological replicates for *rsfS* knockout (Δ*rsfS::kan* and Δ*rsfS::cat*), complement (Δ*rsfS* Δ*rdxA::rsfS* (2p), Δ*rsfS* Δ*rdxA::rsfS* (1p), Δ*rsfS::Δintergenic::rsfS*), and double copy mutants (WT Δ*rdxA::rsfS* (2p), WT Δ*rdxA::rsfS* (1p), WT *Δintergenic::rsfS*) mutants to quantify L14 transcripts using five primer sets: **(A)** *rplN* primer set#1, **(B)** *rplN* primer set#2, **(C)** *rplN* primer set#3, **(D)** *rplN* primer set#4 and **(E)** *rplN* primer set#5. All *rplN* (L14) Cq values were normalized to reference *gapB* gene to obtain ΔCq values plotted with mean and SEM. 1p indicates a single promoter construct and 2p indicates a double promoter construct.

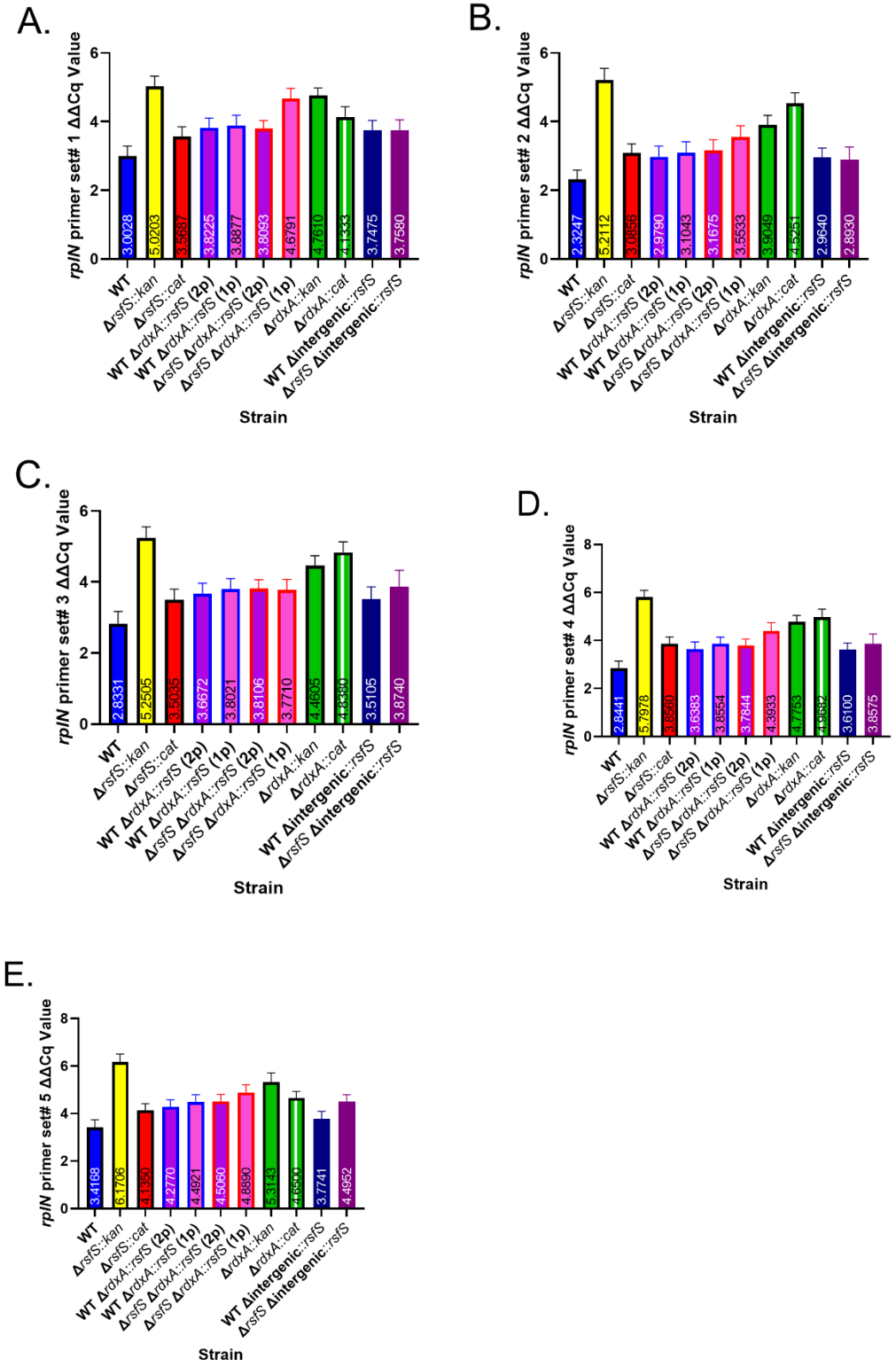
A.
rplN primer set# 1 ΔΔCq Value
3.0028
5.0203
3.5687
3.8225
3.8877
3.8093
4.6791
4.7610
4.1333
3.7475
3.7580
B.
rplN primer set# 2 ΔΔCq Value
2.3247
5.2112
3.0856
2.9750
3.1043
3.1675
3.5533
3.9049
4.5251
2.9640
2.8930
C.
rplN primer set# 3 ΔΔCq Value
2.8331
5.2505
3.5035
3.6672
3.8021
3.8106
3.7710
4.4605
4.8480
3.5105
3.8740
D.
rplN primer set# 4 ΔΔCq Value
2.8441
5.7978
3.8560
3.6383
3.8554
3.7844
4.3933
4.7763
4.9584
3.6100
3.8575
E.
rplN primer set# 5 ΔΔCq Value
3.4168
6.1706
4.1350
4.2770
4.4921
4.5060
4.8890
5.3143
4.6500
3.7741
4.4952
WT
ΔrsfS::kan
ΔrsfS::cat
WT ΔrdxA::rsfS (2p)
WT ΔrdxA::rsfS (1p)
ΔrsfS ΔrdxA::rsfS (2p)
ΔrsfS ΔrdxA::rsfS (1p)
ΔrdxA::kan
ΔrdxA::cat
WT Δintergenic::rsfS
ΔrsfS Δintergenic::rsfS
Strain

Fig. 4.

Figure 4. *rplN* (L14 encoding gene) $2^{-\Delta\Delta Cq}$ Δ*rsfS* normalized to WT in planktonic growth. RT-qPCR was performed on RNA isolated from 4-6 biological replicates of *H. pylori* SS1 WT and Δ*rsfS* grown planktonically using an end point approach. ΔCq values were obtained by normalizing L14 transcripts to *imaA* transcripts. ΔΔCq values were obtained by normalizing Δ*rsfS* ΔCq values to WT ΔCq values. $2^{-\Delta\Delta Cq}$ values were obtained to determine fold expression in the Δ*rsfS* mutant relative to the WT. Values found to be above 1 indicate upregulation, values that are equal to one indicate no change in expression, values below 1 are considered downregulation.

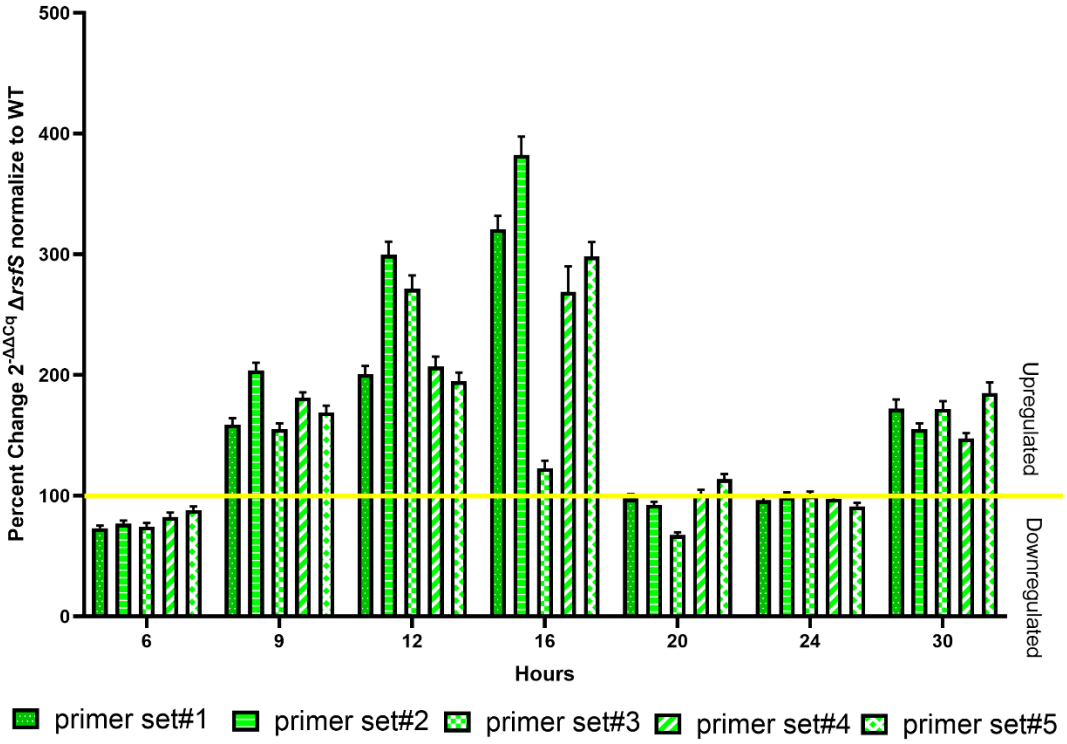

Fig. 5.

Figure 5. *rplA* (L1) and *rplB* (L2) $2^{-\Delta\Delta Cq}$ Δ*rsfS* normalized to WT in planktonic growth. RT-qPCR was conducted on RNA isolated from 4-6 biological replicates from WT and Δ*rsfS* grown planktonically using end point approach. Primers that target genes that code for 50S subunit genes L1 and L2 were used to obtain Cq values that could be normalized to the *imaA* gene to obtain ΔCq values. ΔΔCq values were obtained by normalizing Δ*rsfS* ΔCq values to WT ΔCq values. $2^{-\Delta\Delta Cq}$ values were obtained to determine fold expression in the Δ*rsfS* mutant relative to the WT. Fold expression was then converted to percentages. Values found to be above 100% indicate upregulation, values that are equal to 100% indicate no change in expression, values below 100% are considered downregulation.

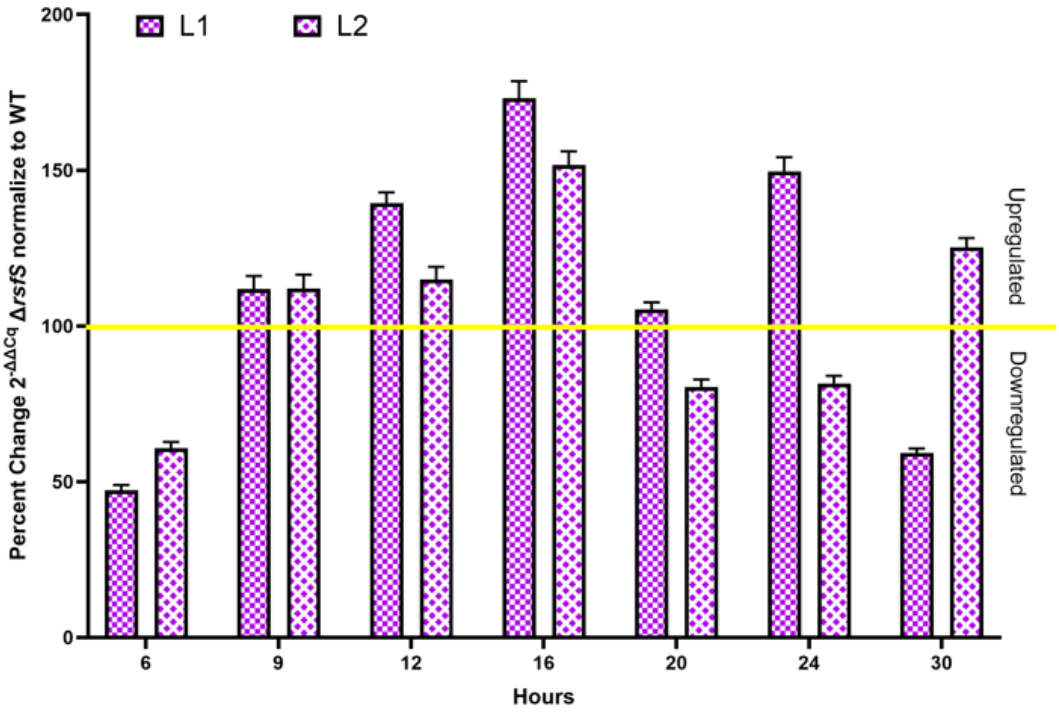

Fig. 6.

Figure 6. *rpsD* (S4), *rpsT* (S20) and *rsmD* $2^{-\Delta\Delta Cq}$ Δ*rsfS* normalized to WT in planktonic growth. RT-qPCR was conducted on RNA from 4-6 biological replicates from WT and Δ*rsfS* grown planktonically using end point approach. Primers that target genes that code for 30S subunit genes S4, S20 and *rsmD* were used to obtain Cq values that could be normalized to the *imaA* gene to obtain ΔCq values. ΔΔCq values were obtained by normalizing Δ*rsfS* ΔCq values to WT ΔCq values. $2^{-\Delta\Delta Cq}$ values were obtained to determine fold expression in the Δ*rsfS* mutant relative to the WT. Fold expression was then converted to percentages. Values found to be above 100% indicate upregulation, values that are equal to 100% indicate no change in expression, values below 100% are considered downregulation.

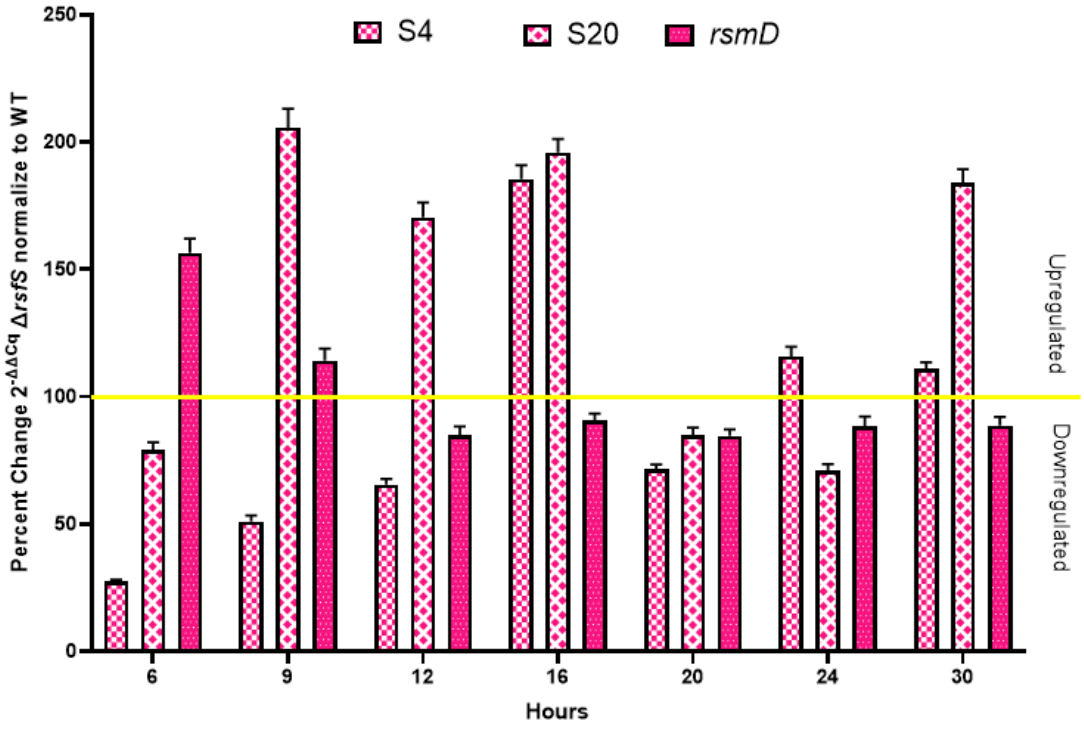

Fig. 7.

Figure 7. Genes for ribosomal proteins $2^{-\Delta\Delta Cq}$ Δ*rsfS* normalized to WT in late stationary phase. RT-qPCR was conducted on RNA isolated from 4-6 biological replicates from WT and Δ*rsfS* grown to late stationary phase (35h) using the endpoint approach. Primers that target genes that encode proteins for the 50S subunit (L14, L1, L2) and for 30S subunit genes (S4, S20 and *rsmD*) were used to obtain Cq values that could be normalized to the *rdxA* gene to obtain ΔCq values. ΔΔCq values were obtained by normalizing Δ*rsfS* ΔCq values to WT ΔCq values. $2^{-\Delta\Delta Cq}$ values were obtained to determine fold expression in the Δ*rsfS* mutant relative to the WT. Fold expression was then converted to percentages. Values found to be above 100% indicate upregulation, values that are equal to 100% indicate no change in expression, values below 100% are considered downregulation.

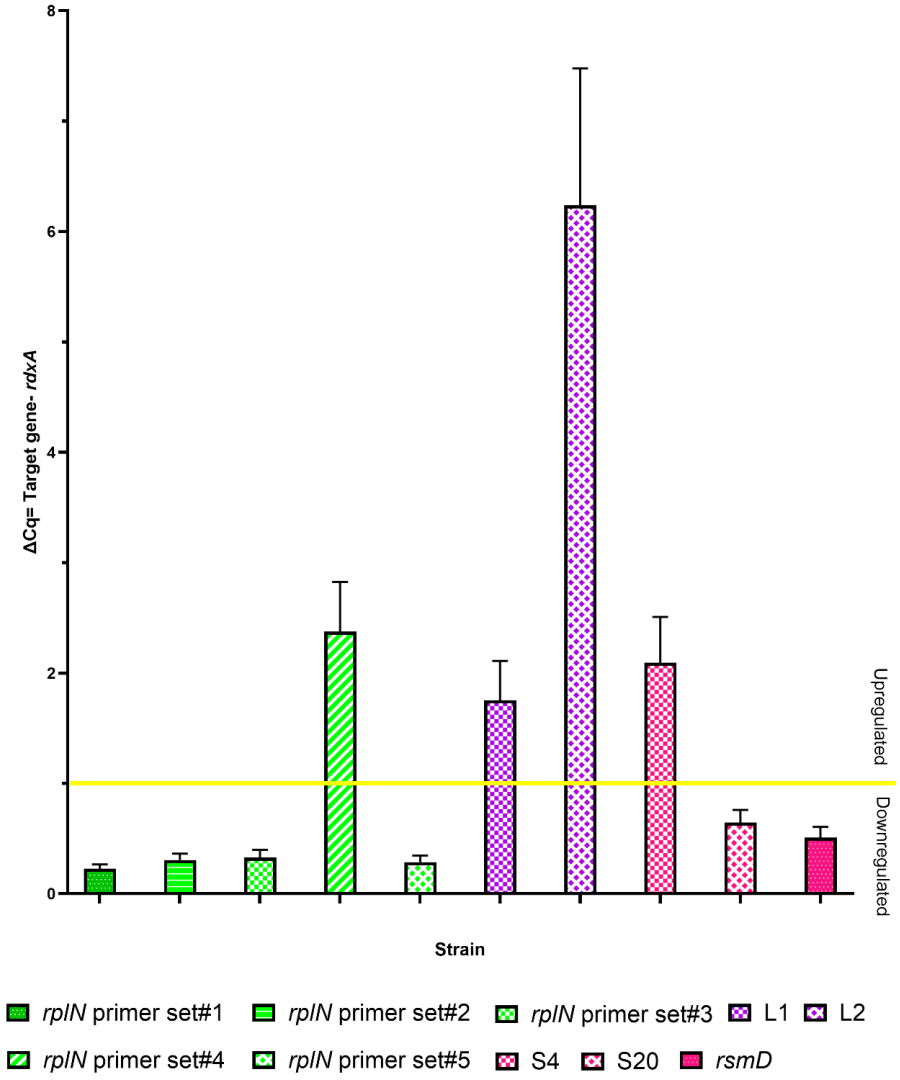

Fig. 8.

Figure 8. Proposed Model for *H. pylori* RsfS homologue with multiple roles as a silencing factor, biogenesis factor and protective chaperone. RsfS bind to L14 on the 50S subunit to prevent it from interacting with the 30S subunit to assemble 70S ribosomes that can translate mRNA to polypeptides. RsfS may bind to the 50S subunit to repress translation in stationary phase when growth factors and mRNA levels are low. RsfS may participate in 50S maturation to produce more 50S subunits because mRNA bound 30S subunits are abundant. RsfS may protect the 50S subunit from degradation in conditions like stationary phase where ribosomes can be degraded to provide essential amino acids for survival. RsfS may potentially reduce the amount of 50S subunits assembled in 70S ribosomes that are susceptible to clarithromycin.

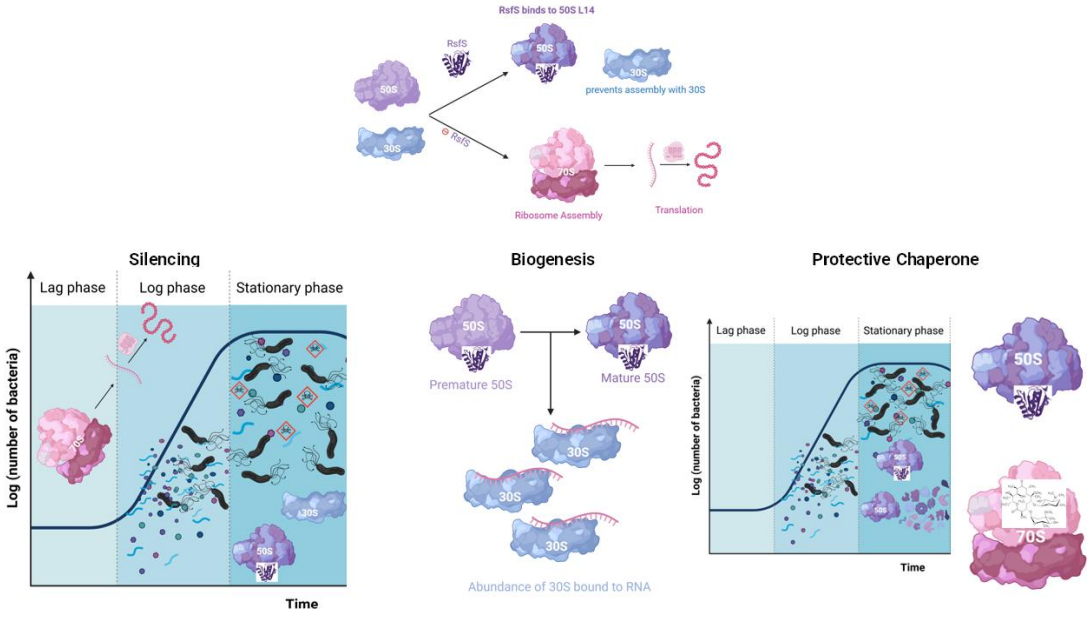

Table 1. E-test strips for levofloxacin, clarithromycin, amoxicillin and tetracycline were used to compare MIC (4-biological replicates) of the Δ*rsfS* mutant to the WT.

Antibiotic (ug/mL)	SS1 WT	SS1 Δ*rsfS::cat*	Fold Difference
Levofloxacin	0.25	0.23	**X1**
Clarithromycin	**0.125**	**0.016**	**X7.8**
Amoxicillin	1.0	0.41	**X2.4**
Tetracycline	**0.75**	**0.094**	**X8**

Supplementary Figures and Legends

Supplemental Table 1. Candidate Reference Genes for qPCR analysis

26695	SS1	Gene	Function
HP0178	HPYLSS1_00169	*neuB*	Sialic acid synthase required involved in flagellin glycosylation.
HP0289	HPYLSS1_00278	*imaA*	Immune modulator A is an outer membrane autotransporter.
HP0047	HPYLSS1_00047	*hypE*	Nickle hydrogenase maturation protein metabolizes hydrogen for urease activity.
HP1010	HPYLSS1_00421	*ppK*	An enzyme polyphosphate kinase used to metabolize inorganic polyphosphates.
HP0821	HPYLSS1_00514	*uvrC*	Subunit C for an excision nuclease.
HP0700	HPYLSS1_00903	*dgkA*	Diacylglycerol kinase used to metabolize fatty acids and phospholipids.
HP0313	HPYLSS1_00304	*nark*	Nitrate and nitrite antiporter used to metabolize nitrogen.
HP0818	HPYLSS1_00517	*abc*	Putative ABC transporter.
HP0952	HPYLSS1_00934	*cinA*	Competence/damage inducible nicotinamide-nucleotide amidohydrolase protein
HP1066	HPYLSS1_00364	*horD*	Outer membrane protein.
HP0287	HPYLSS1_00276	*bioV*	Pimeloyl-ACP methyl ester esterase enzyme that synthesis biotin.
HP0608	HPYLSS1_00815	β-OMP	Putative outer membrane β barrel protein.
HP1346	HPYLSS1_01294	*gapB*	Glyceraldehyde-3-phosphate dehydrogenase involved in glycolysis.

Supplemental Table 2. Primers Candidate Reference Genes for qPCR analysis

Gene	Forward	Reverse
neuB	CCCAGCCAAATAGAAGACGC	CGCTGTCTGGGGTTTGTAAG
imaA	GCAACATAACGCCGGAATCT	ATCGCCGCTGAATTGGTAAC
Hype	AACCCTACACGCTAGCCAAT	TCCTTTCAAAACCCCATGCG
ppK	CAAATCGCCCAATTTCACGC	TGCTTGCCCACACGATAAAG
uvrC	TAGAGCGTTGTAAAGCCCCA	AGGGCTTCTTCAAAACGCAA
dgkA	GAGCGCGTTCAGGCAAATT	CGGTGCCAGTAAAATCCACA
Nark	GGTATTGCGGTGCTAATGGG	AAGGTAAAGAGAGAGGGGCG
Abc	CGCTATTGGGCTAGGGTGTA	AAACTGCCCGCCACTAAAAG
cinA	CAATGAAGAGGTTAAGCGCGA	GCGCCAATGTAAATTGTGCC
horD	GGGGTGGGAGGGGATTTTAT	AACTGCACCCCAAATTTCCC
bioV	ACGCTTGCAACTTTCTTCGT	GGGCTTGAATGTCAGTGATCC
β-OMP	TTTTGGCTTTATGGGTGGGC	TTAATCGTGTGCAATGCGGT
gapB	GCCTCTTGCACGACTAACGC	CTTTGCTCACGCCGGTGCTT
rsfS#1	TGAACCAACGCATAGAAACGA	AGGTGTTTTGATAAGGAAGCCC
rsfS#2	ACCAACGCATAGAAACGATTAC	GCGTGGTAGCGATAATGACA
rsfS#3	GTCATTATCGCTACCACGCTAG	TCCCCTAAATCCAAAATGATCCA
L14#1	GTCAAGTCGTCAAAGCCGTT	TATACAACCTCCGGCGCTAG
L14#2	AGGAGGCAGTCATAAACGCT	AGCGTCCAAAATCACTGCTG
L14#3	GATCGTGGCTTCCGTGAAAA	TAACGCACTTCTCGGCTCA
L14#4	AAGGTGTTAGGAGGCAGTCA	TCAAAACGCACCAAAGAACCA
L14#5	AGGCAGTCATAAACGCTATGC	TCACTGCTGCATTGTCATCA
rdxA # 2	TGCTTGGCGTGAGATTCAAC	ACGCTCTTCTAAAACTTCGCC

Supplemental Table 3. Strains used in this study.

Strain	KO#	Description
SS1	399	WT SS1 strain from Lee et al., 1997
ΔrsfS::kan	1674	WT SS1 parent strain (KO#399) that was transformed with pTwist ΔrsfS::kan to delet chromosomal rsfS gene and replace with AphaA3 (KanR)
ΔrsfS::cat	1830	Parent strain ΔrsfS::kan (KO#1674) that was transformed with kan2cat plasmid to swap AphaA3 (KanR) for cat (CmR)
ΔrsfS::cat ΔrdxA::rsfS 2 X promoter	2033	Parent strain ΔrsfS::cat (KO#1830) that was transformed with pTwist ΔrdxA::rsfS 2 X promoter to add a copy of rsfS in the rdxA locus under the influence of it's predicted promoter and the rdxA promoter
ΔrdxA::rsfS 2 X promoter	2031	WT SS1 parent strain (KO#399) that was transformed pTwist ΔrdxA::rsfS 2 X promoter to add a copy of rsfS in the rdxA locus under the influence of it's predicted promoter and the rdxA promoter
ΔrsfS::cat ΔrdxA::rsfS 1 X promoter	2034	Parent strain ΔrsfS::cat (KO#1830) that was transformed with pTwist ΔrdxA::rsfS 1 X promoter to add a copy of rsfS in the rdxA locus under the influence of it's predicted promoter only
ΔrdxA::rsfS 1 X promoter	2032	WT SS1 parent strain (KO#399) that was transformed pTwist ΔrdxA::rsfS 1 X promoter to add a copy of rsfS in the rdxA locus under the influence of it's predicted promoter only
ΔrdxA::kan	1018	rdxA knockout with AphaA3 (KanR) strain previously used and published in Terry et al., 2005
ΔrdxA::cat	1019	rdxA knockout with cat (CmR) strain previously used and published in Terry et al., 2005

Supplemental Figure 1.

Supplemental Figure 1. Cq values obtained from plate grown strains using (A) *rsfS* primer set#2 and (B) *rsfS* primer set#3. ΔCq values were obtained by normalizing *rsfS* Cq values to *gapB* Cq values for (C) *rsfS* primer set#2 and (D) *rsfS* primer set#3.

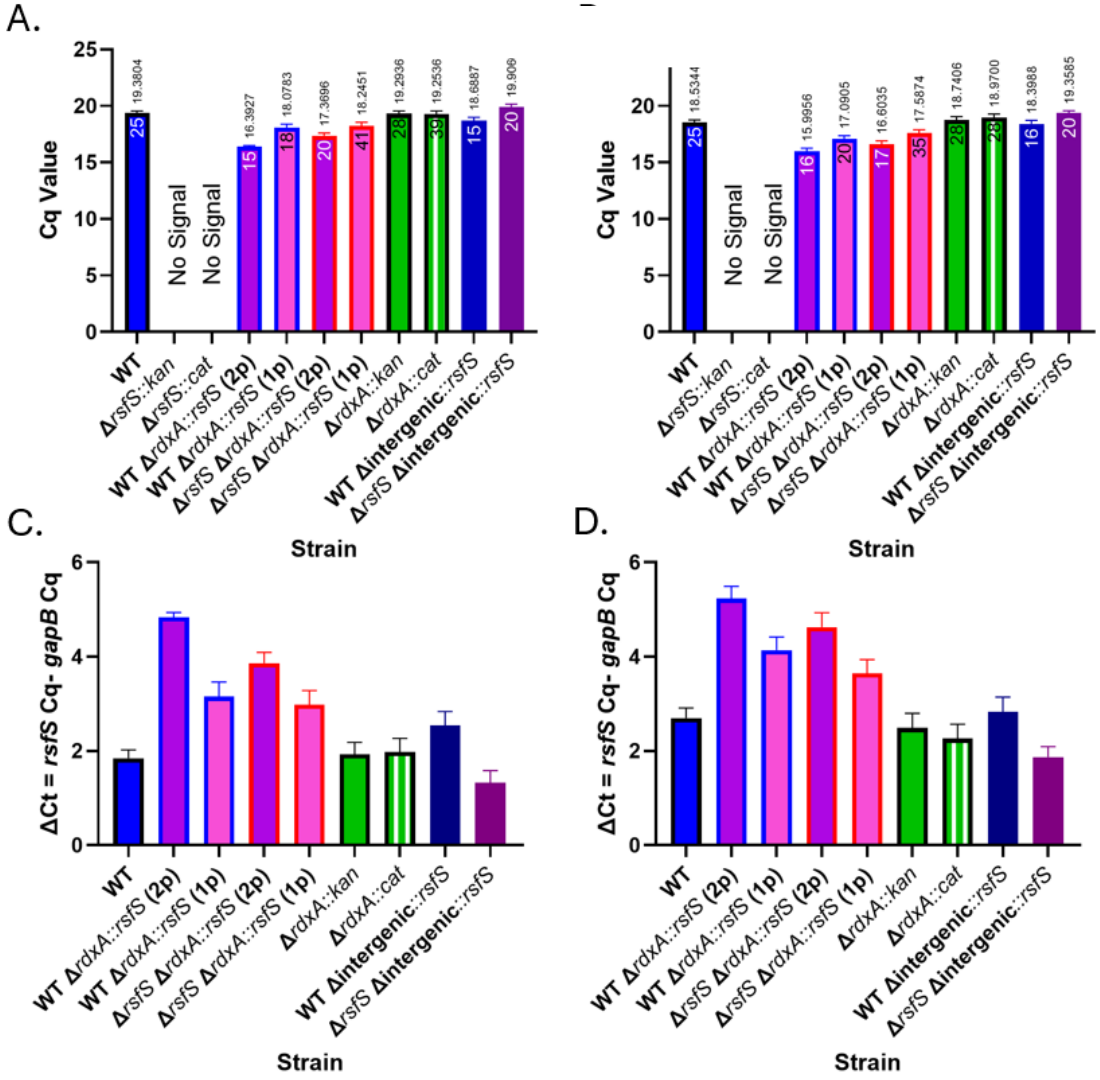

Supplemental Figure 2.

Supplemental Figure 2. Cq values obtained from plate grown strains using (A) *rplN* primer set#1, (B) *rplN* primer set#2, (C) *rplN* primer set#3, (D) *rplN* primer set#4, and (E) *rplN* primer set#5.

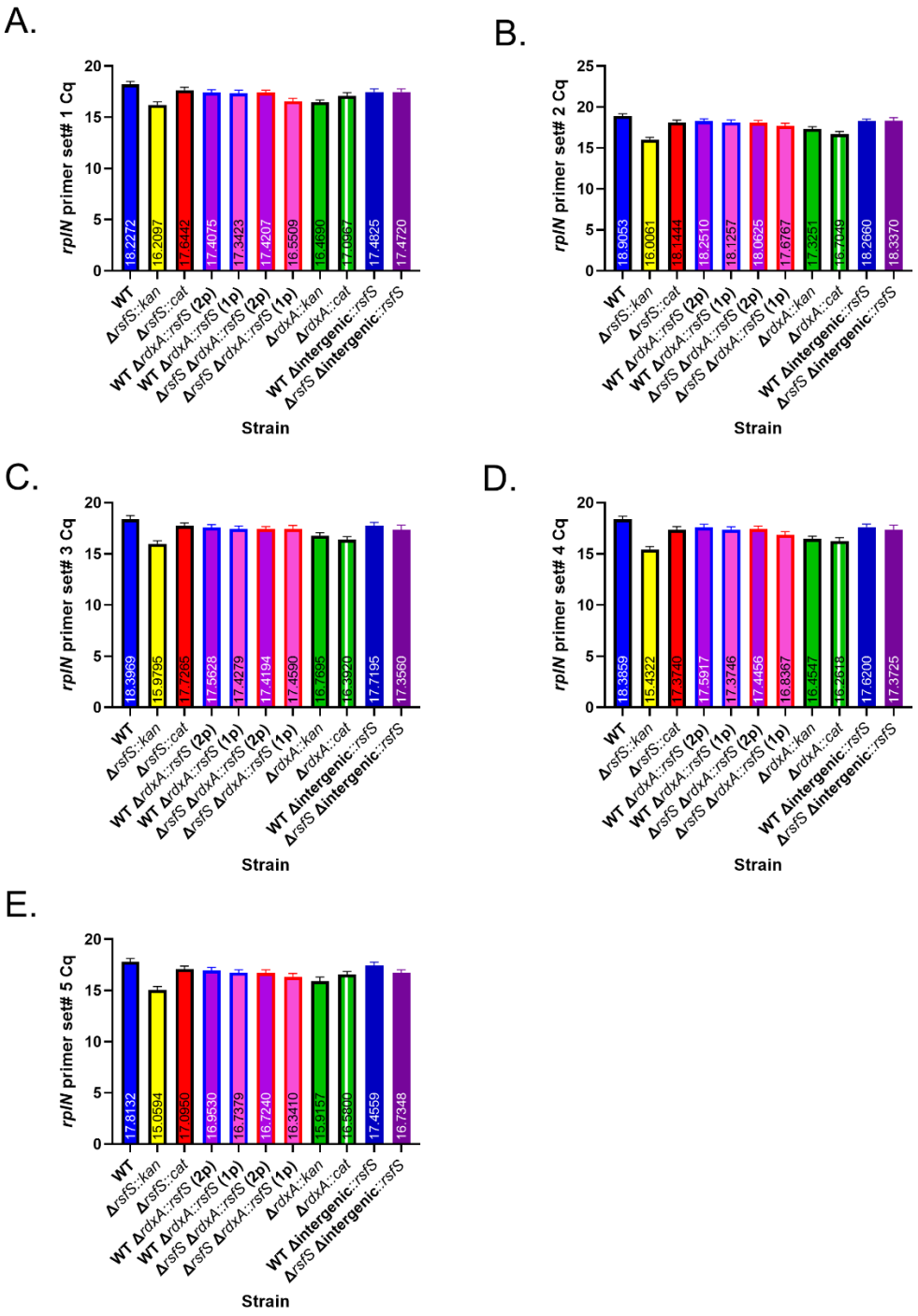

Supplemental Figure 3.

Supplemental Figure 3. Cq values obtained from SS1 WT and Δ*rsfS* mutant across the growth curve using primers that target *rplN* (L14) with the following primer sets: (A) L14 primer set#1, (B) L14 primer set#2, (C) L14 primer set#3, (D) L14 primer set#4, and (E) L14 primer set#5.

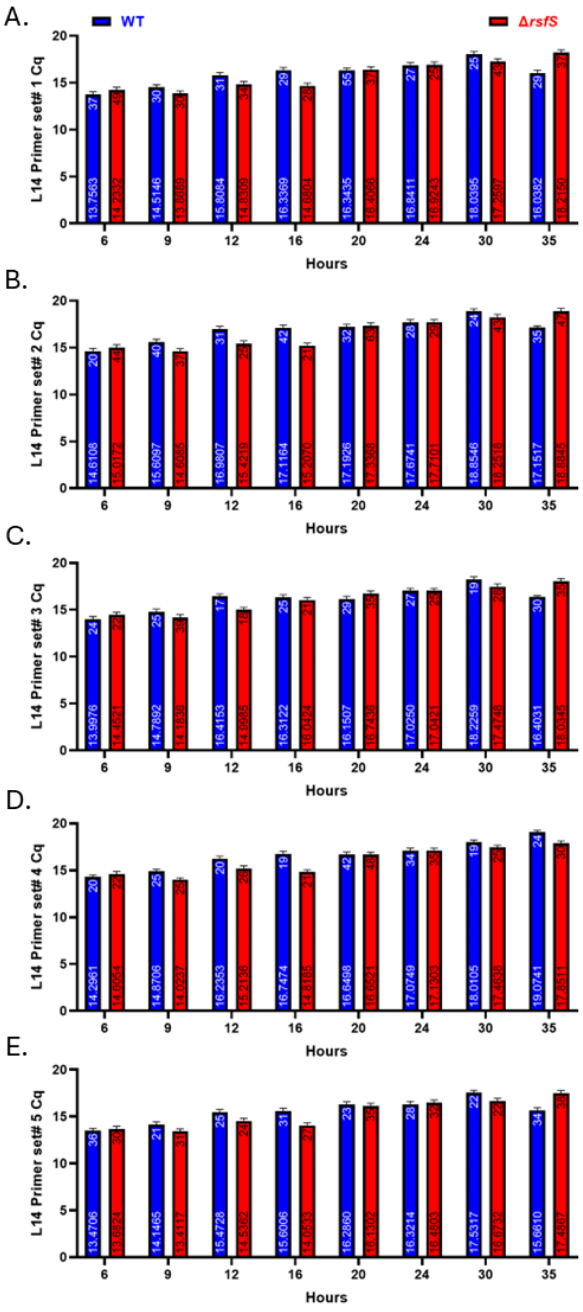

Supplemental Figure 4.

Supplemental Figure 4. Cq values obtained from SS1 WT and Δ*rsfS* mutant across the growth curve using primer sets for 50S genes (A) *rplA* (L1) and (B) *rplB* (L2).

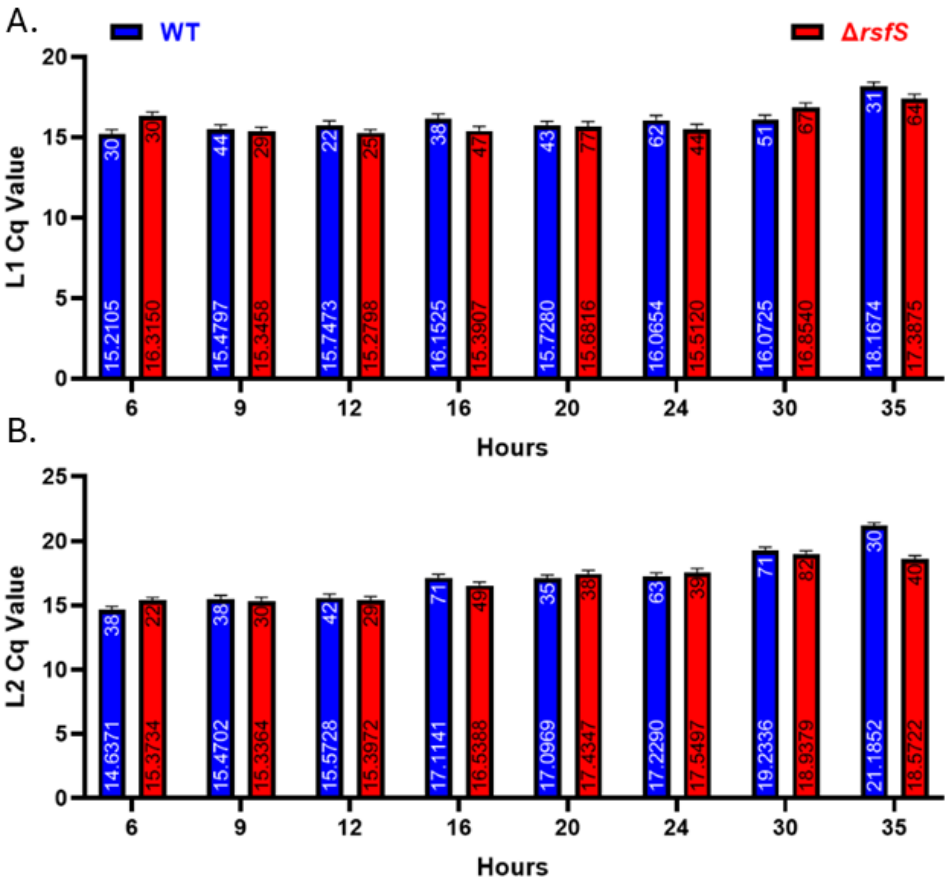

Supplemental Figure 5.

Supplemental Figure 5. Cq values obtained from SS1 WT and Δ*rsfS* mutant across the growth curve using primer sets for 30S genes (A) *rspD* (S4), (B) *rspT* (S20) and (C) *rsmD*.

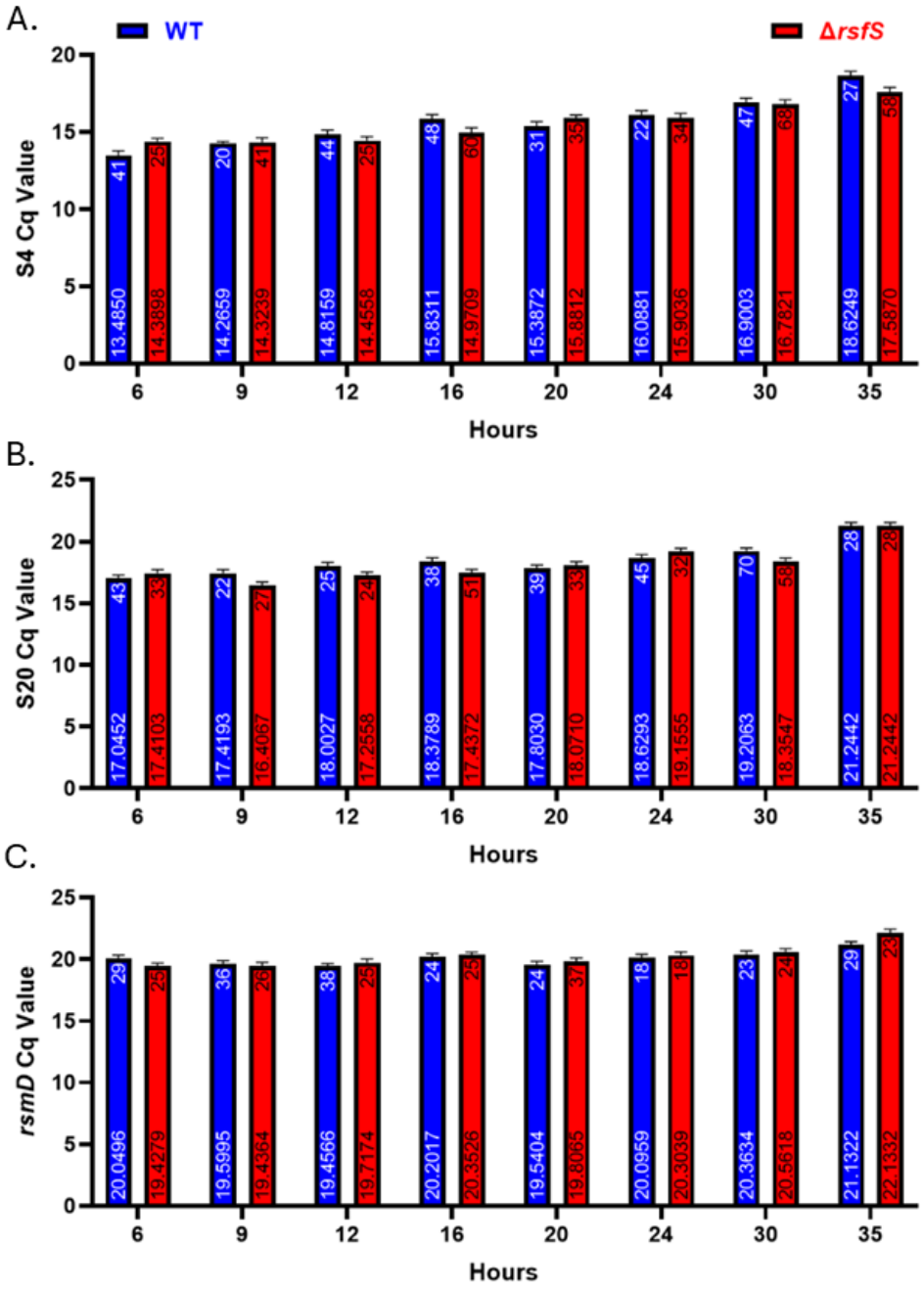

Supplemental Figure 6.

Supplemental Figure 6. (A) *rdxA* Cq values obtained from SS1 WT and Δ*rsfS* mutant at late stationary phase at 35h in BB10 **(B)** Δ Cq values were obtained by normalizing target gene Cq values to *rdxA* Cq values. **(C)** $2^{-\Delta\Delta Cq}$ analysis normalizing Δ*rsfS* mutant transcripts to WT transcripts

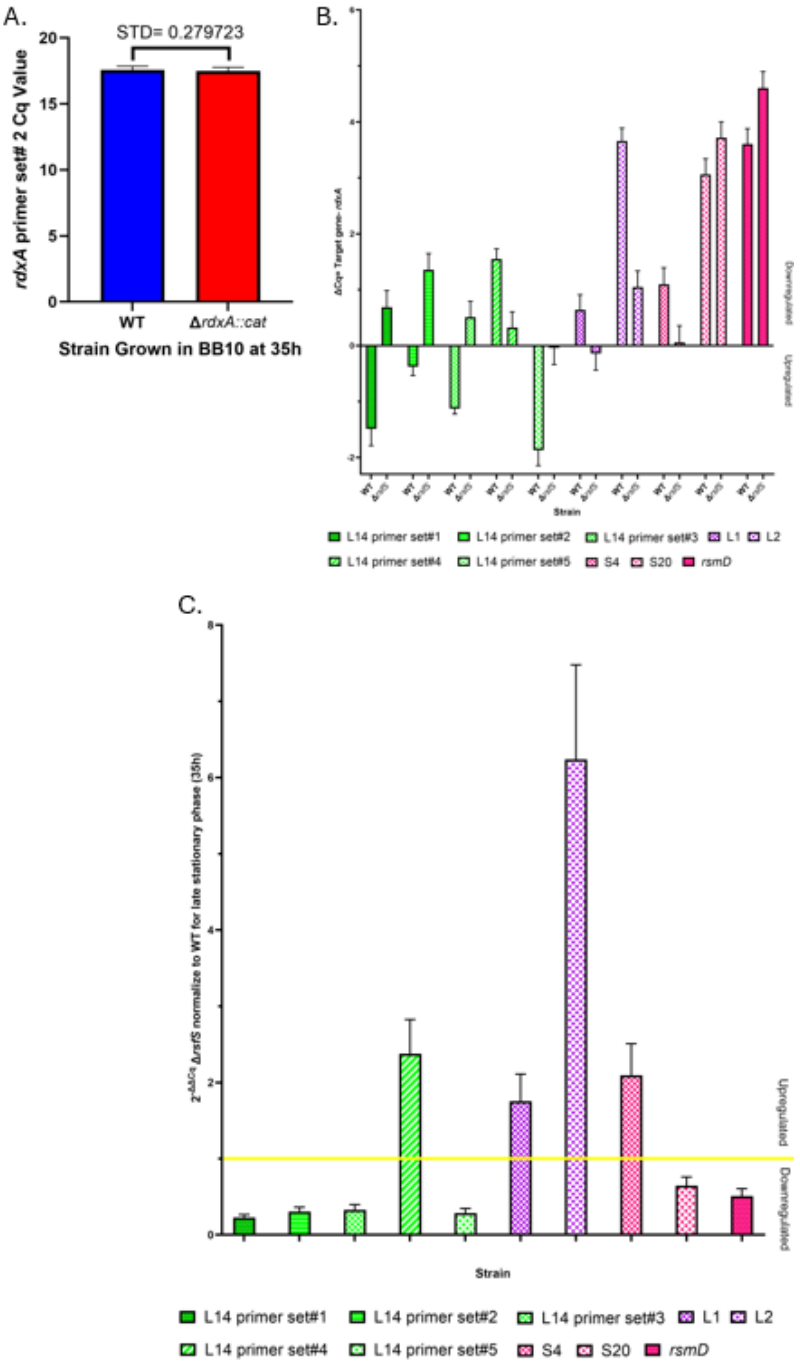

Reference

Abraham, N. M., & Jefferson, K. K. (2010). A low molecular weight component of serum inhibits biofilm formation in *Staphylococcus aureus*. *Microbial Pathogenesis*, *49*(6), 388–391. https://doi.org/10.1016/j.micpath.2010.07.005

Adams-Ward, X., Chapalain, A., Ginevra, C., Jarraud, S., Doublet, P., & Gilbert, C. (2023). Bacterial persistence in Legionella pneumophila clinical isolates from patients with recurring legionellosis. *Frontiers in Cellular and Infection Microbiology*, *13*, 1219233. https://doi.org/10.3389/fcimb.2023.1219233

Agafonov, D. E., Kolb, V. A., & Spirin, A. S. (2001). Ribosome-associated protein that inhibits translation at the aminoacyl-tRNA binding stage. *EMBO Reports*, *2*(5), 399–402. https://doi.org/10.1093/embo-reports/kve091

Aguilar, C., Pauzuolis, M., Pompaiah, M., Vafadarnejad, E., Arampatzi, P., Fischer, M., Narres, D., Neyazi, M., Kayisoglu, Ö., Sell, T., Blüthgen, N., Morkel, M., Wiegering, A., Germer, C.-T., Kircher, S., Rosenwald, A., Saliba, A.-E., & Bartfeld, S. (2022). Helicobacter pylori shows tropism to gastric differentiated pit cells dependent on urea chemotaxis. *Nature Communications*, *13*(1), 5878. https://doi.org/10.1038/s41467-022-33165-4

Akiyama, T., & Kim, M. (2023). Bet-hedging: Bacterial ribosome dynamics during growth transitions. *Current Biology*, *33*(22), R1186–R1188. https://doi.org/10.1016/j.cub.2023.10.007

Akiyama, T., Williamson, K. S., Schaefer, R., Pratt, S., Chang, C. B., & Franklin, M. J. (2017). Resuscitation of *Pseudomonas aeruginosa* from dormancy requires hibernation promoting factor (PA4463) for ribosome preservation. *Proceedings of the National Academy of Sciences*, *114*(12), 3204–3209. https://doi.org/10.1073/pnas.1700695114

Aldhaleei, W. A., Wallace, M. B., Harris, D. M., & Bi, Y. (2024). *Helicobacter pylori*: A concise review of the latest treatments against an old foe. *Cleveland Clinic Journal of Medicine*, *91*(8), 481–487. https://doi.org/10.3949/ccjm.91a.24031

Andersen, S. R., Shukri, N. M., Boel, J., & Saadbye, P. (2006). Metronidazole Resistance in Campylobacter jejuni from Poultry Meat. *Journal of Food Protection*, *69*(4), 932–934. https://doi.org/10.4315/0362-028X-69.4.932

Argueta, E. A., Ho, J. J. C., Elfanagely, Y., D'Agata, E., & Moss, S. F. (2022). Clinical Implication of Drug Resistance for H. pylori Management. *Antibiotics*, *11*(12), 1684. https://doi.org/10.3390/antibiotics11121684

Aumpan, N., Issariyakulkarn, N., Mahachai, V., Graham, D., Yamaoka, Y., & Vilaichone, R. (2023). Management of Helicobacter pylori treatment failures: A large population-based study (HP treatment failures trial). *PLOS ONE*, *18*(11), e0294403. https://doi.org/10.1371/journal.pone.0294403

Baron, S. (1996). *Medical Microbiology* (4th edition). Galveston (TX): University of Texas Medical Branch at Galveston. https://www.ncbi.nlm.nih.gov/books/NBK7627/

Basu, A., Shields, K. E., Eickhoff, C. S., Hoft, D. F., & Yap, M.-N. F. (2018). Thermal and Nutritional Regulation of Ribosome Hibernation in Staphylococcus aureus. *Journal of Bacteriology*, *200*(24). https://doi.org/10.1128/JB.00426-18

Basu, A., Shields, K. E., & Yap, M.-N. F. (2020). The hibernating 100S complex is a target of ribosome-recycling factor and elongation factor G in Staphylococcus aureus. *Journal of Biological Chemistry*, *295*(18), 6053–6063. https://doi.org/10.1074/jbc.RA119.012307

Basu, A., & Yap, M.-N. F. (2016). Ribosome hibernation factor promotes *Staphylococcal* survival and differentially represses translation. *Nucleic Acids Research*, *44*(10), 4881–4893. https://doi.org/10.1093/nar/gkw180

Basu, A., & Yap, M.-N. F. (2017). Disassembly of the *Staphylococcus aureus* hibernating 100S ribosome by an evolutionarily conserved GTPase. *Proceedings of the National Academy of Sciences*, *114*(39). https://doi.org/10.1073/pnas.1709588114

Battista, J. R., & Rainey, F. A. (2015). *Deinococcus*. In M. E. Trujillo, S. Dedysh, P. DeVos, B. Hedlund, P. Kämpfer, F. A. Rainey, & W. B. Whitman (Eds.), *Bergey's Manual of Systematics of Archaea and Bacteria* (1st ed., pp. 1–13). Wiley. https://doi.org/10.1002/9781118960608.gbm00475

Beckert, B., Abdelshahid, M., Schäfer, H., Steinchen, W., Arenz, S., Berninghausen, O., Beckmann, R., Bange, G., Turgay, K., & Wilson, D. N. (2017). Structure of the Bacillus subtilis hibernating 100S ribosome reveals the basis for 70S

dimerization. *The EMBO Journal*, *36*(14), 2061–2072. https://doi.org/10.15252/embj.201696189

Benigno, T. G. D. S., Ribeiro Junior, H. L., Azevedo, O. G. R. D., Pinheiro, R. F., Oliveira, R. T. G. D., Maciel, F. S., Oliveira, E. L. D., Queiroz, D. M. M., & Braga, L. L. B. C. (2022). Clarithromycin-resistant H. pylori primary strains and virulence genotypes in the Northeastern region of Brazil. *Revista Do Instituto de Medicina Tropical de São Paulo*, *64*, e47. https://doi.org/10.1590/s1678-9946202264047

Bernarde, C., Lehours, P., Lasserre, J.-P., Castroviejo, M., Bonneu, M., Mégraud, F., & Ménard, A. (2010). Complexomics Study of Two Helicobacter pylori Strains of Two Pathological Origins. *Molecular & Cellular Proteomics*, *9*(12), 2796–2826. https://doi.org/10.1074/mcp.M110.001065

Bernhardt, T. G., & De Boer, P. A. J. (2004). Screening for synthetic lethal mutants in *Escherichia coli* and identification of EnvC (YibP) as a periplasmic septal ring factor with murein hydrolase activity. *Molecular Microbiology*, *52*(5), 1255–1269. https://doi.org/10.1111/j.1365-2958.2004.04063.x

Bi, H., Zhu, L., Jia, J., & Cronan, J. E. (2016). A Biotin Biosynthesis Gene Restricted to Helicobacter. *Scientific Reports*, *6*(1), 21162. https://doi.org/10.1038/srep21162

Binmaeil, H., Hanafiah, A., Mohamed Rose, I., & Raja Ali, R. A. (2021). Development and Validation of Multiplex Quantitative PCR Assay for Detection of Helicobacter pylori and Mutations Conferring Resistance to

Clarithromycin and Levofloxacin in Gastric Biopsy. *Infection and Drug Resistance*, *Volume 14*, 4129–4145. https://doi.org/10.2147/IDR.S325056

Bischler, T., Tan, H. S., Nieselt, K., & Sharma, C. M. (2015). Differential RNA-seq (dRNA-seq) for annotation of transcriptional start sites and small RNAs in Helicobacter pylori. *Methods*, *86*, 89–101. https://doi.org/10.1016/j.ymeth.2015.06.012

Blombach, F., Launay, H., Zorraquino, V., Swarts, D. C., Cabrita, L. D., Benelli, D., Christodoulou, J., Londei, P., & Van Der Oost, J. (2011). An HflX-Type GTPase from Sulfolobus solfataricus Binds to the 50S Ribosomal Subunit in All Nucleotide-Bound States. *Journal of Bacteriology*, *193*(11), 2861–2867. https://doi.org/10.1128/JB.01552-10

Boddu, R. S., Perumal, O., & K, D. (2020). Microbial nitroreductases: A versatile tool for biomedical and environmental applications. *Biotechnology and Applied Biochemistry*, bab.2073. https://doi.org/10.1002/bab.2073

Bode, G., Mauch, F., & Malfertheiner, P. (1993). The coccoid forms of *Helicobacter pylori*. Criteria for their viability. *Epidemiology and Infection*, *111*(3), 483–490. https://doi.org/10.1017/S0950268800057216

Bogiel, T., Szaflarska-Popławska, A., & Krawczyk, A. (2025). Prevalence and Variability of Helicobacter pylori Clarithromycin Resistance Mutations in Pediatric Patients in Poland: A Genotypic Analysis Using the Bosphore Genotyping Kit. *Antibiotics*, *14*(4), 352. https://doi.org/10.3390/antibiotics14040352

Boone, D. R., Castenholz, R. W., & Garrity, G. M. (Eds.). (2001). *Bergey's manual of systematic bacteriology* (2nd ed). Springer.

Borg, A., Pavlov, M., & Ehrenberg, M. (2016). Complete kinetic mechanism for recycling of the bacterial ribosome. *RNA*, *22*(1), 10–21. https://doi.org/10.1261/rna.053157.115

Bowman, J. C., Petrov, A. S., Frenkel-Pinter, M., Penev, P. I., & Williams, L. D. (2020). Root of the Tree: The Significance, Evolution, and Origins of the Ribosome. *Chemical Reviews*, *120*(11), 4848–4878. https://doi.org/10.1021/acs.chemrev.9b00742

Boyanova, L., Yordanov, D., Gergova, G., Markovska, R., & Mitov, I. (2010). Association of iceA and babA genotypes in Helicobacter pylori strains with patient and strain characteristics. *Antonie van Leeuwenhoek*, *98*(3), 343–350. https://doi.org/10.1007/s10482-010-9448-y

Brodersen, D. E., Clemons, W. M., Carter, A. P., Morgan-Warren, R. J., Wimberly, B. T., & Ramakrishnan, V. (2000). The Structural Basis for the Action of the Antibiotics Tetracycline, Pactamycin, and Hygromycin B on the 30S Ribosomal Subunit. *Cell*, *103*(7), 1143–1154. https://doi.org/10.1016/S0092-8674(00)00216-6

Brown, A., Fernández, I. S., Gordiyenko, Y., & Ramakrishnan, V. (2016). Ribosome-dependent activation of stringent control. *Nature*, *534*(7606), 277–280. https://doi.org/10.1038/nature17675

Bruce, M. G., & Maaroos, H. I. (2008). Epidemiology of *Helicobacter pylori* Infection. *Helicobacter*, *13*(s1), 1–6. https://doi.org/10.1111/j.1523-5378.2008.00631.x

Bryant, C., & DeLuca, M. (1991). Purification and characterization of an oxygen-insensitive NAD(P)H nitroreductase from Enterobacter cloacae. *Journal of Biological Chemistry*, *266*(7), 4119–4125. https://doi.org/10.1016/S0021-9258(20)64294-6

Bustin, S. A., & Wittwer, C. T. (2017). MIQE: A Step Toward More Robust and Reproducible Quantitative PCR. *Clinical Chemistry*, *63*(9), 1537–1538. https://doi.org/10.1373/clinchem.2016.268953

Butland, G., Peregrín-Alvarez, J. M., Li, J., Yang, W., Yang, X., Canadien, V., Starostine, A., Richards, D., Beattie, B., Krogan, N., Davey, M., Parkinson, J., Greenblatt, J., & Emili, A. (2005). Interaction network containing conserved and essential protein complexes in Escherichia coli. *Nature*, *433*(7025), 531–537. https://doi.org/10.1038/nature03239

Butlop, T. R. P., Mungkote, N. T. N., & Chaichanawongsaroj, N. T. R. (2016). Analysis of allelic variants of rdxA associated with metronidazole resistance in Helicobacter pylori: Detection of common genotypes in rdxA by multiplex allele-specific polymerase chain reaction. *Genetics and Molecular Research*, *15*(3). https://doi.org/10.4238/gmr.15038674

Byrgazov, K., Vesper, O., & Moll, I. (2013). Ribosome heterogeneity: Another level of complexity in bacterial translation regulation. *Current Opinion in Microbiology*, *16*(2), 133–139. https://doi.org/10.1016/j.mib.2013.01.009

Cabrera, C., Torres, J., Serrano, C. A., Gallardo, P., Orellana, V., George, S., O'Ryan, M., & Lucero, Y. (2024). Antimicrobial Resistance of *Helicobacter pylori* Isolated From Latin American Children and Adolescents (2008–2023): A Systematic Review. *Helicobacter*, *29*(4), e13101. https://doi.org/10.1111/hel.13101

Caldon, C. E., Yoong, P., & March, P. E. (2001). Evolution of a molecular switch: Universal bacterial GTPases regulate ribosome function. *Molecular Microbiology*, *41*(2), 289–297. https://doi.org/10.1046/j.1365-2958.2001.02536.x

Cao, G., Zhu, Y., Xie, X., Chen, Y., Yu, J., Zhang, J., Chen, Z., Pang, L., Zhang, Y., & Shi, Y. (2020). Pharmacokinetics and pharmacodynamics of levofloxacin in bronchial mucosa and lung tissue of patients undergoing pulmonary operation. *Experimental and Therapeutic Medicine*, *20*(1), 607–616. https://doi.org/10.3892/etm.2020.8715

Carrillo-Casas, E. M., Hernández-Castro, R., Suárez-Güemes, F., & De La Peña-Moctezuma, A. (2008). Selection of the Internal Control Gene for Real-Time Quantitative RT-PCR Assays in Temperature Treated Leptospira. *Current Microbiology*, *56*(6), 539–546. https://doi.org/10.1007/s00284-008-9096-x

Carron, M. A., Tran, V. R., Sugawa, C., & Coticchia, J. M. (2006). Identification of *Helicobacter pylori* Biofilms in Human Gastric Mucosa. *Journal of Gastrointestinal Surgery*, *10*(5), 712–717. https://doi.org/10.1016/j.gassur.2005.10.019

Chai, Q., Singh, B., Peisker, K., Metzendorf, N., Ge, X., Dasgupta, S., & Sanyal, S. (2014). Organization of Ribosomes and Nucleoids in *Escherichia coli* Cells during Growth and in Quiescence. *Journal of Biological Chemistry*, *289*(16), 11342–11352. https://doi.org/10.1074/jbc.M114.557348

Chan, A. C. K., Blair, K. M., Liu, Y., Frirdich, E., Gaynor, E. C., Tanner, M. E., Salama, N. R., & Murphy, M. E. P. (2015). Helical Shape of *Helicobacter pylori* Requires an Atypical Glutamine as a Zinc Ligand in the Carboxypeptidase Csd4. *Journal of Biological Chemistry*, *290*(6), 3622–3638. https://doi.org/10.1074/jbc.M114.624734

Chan, L. I., Omae, K., Brown, C. R., Amikura, K., Ekemezie, C. L., Clark, J., Nishide, K., Helena-Bueno, K., Palmowski, P., Porter, A., Suzuki, S., & Melnikov, S. V. (2025). *The evolutionary lifecycle of ribosome hibernation factors*. Microbiology. https://doi.org/10.1101/2025.11.04.686544

Chen, Y.-C., Malfertheiner, P., Yu, H.-T., Kuo, C.-L., Chang, Y.-Y., Meng, F.-T., Wu, Y.-X., Hsiao, J.-L., Chen, M.-J., Lin, K.-P., Wu, C.-Y., Lin, J.-T., O'Morain, C., Megraud, F., Lee, W.-C., El-Omar, E. M., Wu, M.-S., & Liou, J.-M. (2024). Global Prevalence of *Helicobacter pylori* Infection and Incidence of

Gastric Cancer Between 1980 and 2022. *Gastroenterology*, *166*(4), 605–619. https://doi.org/10.1053/j.gastro.2023.12.022

Cohen, J. (1996). Metronidazole to clear intestinal parasites. *The Lancet*, *348*(9022), 273. https://doi.org/10.1016/S0140-6736(05)65588-2

Collins, K. D., Hu, S., Grasberger, H., Kao, J. Y., & Ottemann, K. M. (2018). Chemotaxis Allows Bacteria To Overcome Host-Generated Reactive Oxygen Species That Constrain Gland Colonization. *Infection and Immunity*, *86*(5), e00878-17. https://doi.org/10.1128/IAI.00878-17

Contreras, M., Mujica, H., & García-Amado, M. A. (2024). Molecular tools of antibiotic resistance for Helicobacter pylori: An overview in Latin America. *Frontiers in Gastroenterology*, *3*, 1410816. https://doi.org/10.3389/fgstr.2024.1410816

Cookson, W. O. C. M., Cox, M. J., & Moffatt, M. F. (2018). New opportunities for managing acute and chronic lung infections. *Nature Reviews Microbiology*, *16*(2), 111–120. https://doi.org/10.1038/nrmicro.2017.122

Cortes, T., & Cox, R. A. (2015). Transcription and translation of the rpsJ, rplN and rRNA operons of the tubercle bacillus. *Microbiology*, *161*(4), 719–728. https://doi.org/10.1099/mic.0.000037

Coticchia, J. M., Sugawa, C., Tran, V. R., Gurrola, J., Kowalski, E., & Carron, M. A. (2006). Presence and Density of *Helicobacter pylori* Biofilms in Human Gastric Mucosa in Patients With Peptic Ulcer Disease. *Journal of*

Gastrointestinal Surgery, *10*(6), 883–889. https://doi.org/10.1016/j.gassur.2005.12.009

Crépin, S., Harel, J., & Dozois, C. M. (2012). Chromosomal Complementation Using Tn *7* Transposon Vectors in Enterobacteriaceae. *Applied and Environmental Microbiology*, *78*(17), 6001–6008. https://doi.org/10.1128/AEM.00986-12

Czinn, S. J. (2005). *Helicobacter pylori* infection: Detection, investigation, and management. *The Journal of Pediatrics*, *146*(3), S21–S26. https://doi.org/10.1016/j.jpeds.2004.11.037

Da Silva, C. V., Velikkakam, T., De Oliveira, E. C. M., Silveira, A. C. A., De Lima Júnior, J. P., Uombe, N. P. I., Da Silva, P. H. R., & Borges, B. C. (2024). Cellular dormancy: A widespread phenomenon that perpetuates infectious diseases. *Journal of Basic Microbiology*, *64*(5), 2300389. https://doi.org/10.1002/jobm.202300389

Damke, P. P., Di Guilmi, A. M., Varela, P. F., Velours, C., Marsin, S., Veaute, X., Machouri, M., Gunjal, G. V., Rao, D. N., Charbonnier, J.-B., & Radicella, J. P. (2019). Identification of the periplasmic DNA receptor for natural transformation of *Helicobacter pylori*. *Nature Communications*, *10*(1), 5357. https://doi.org/10.1038/s41467-019-13352-6

Davies, C., White, S. W., & Ramakrishnan, V. (1996). The crystal structure of ribosomal protein L14 reveals an important organizational component of the translational apparatus. *Structure*, *4*(1), 55–66. https://doi.org/10.1016/S0969-2126(96)00009-3

De Bari, H., & Berry, E. A. (2013). Structure of *Vibrio cholerae* ribosome hibernation promoting factor. *Acta Crystallographica Section F Structural Biology and Crystallization Communications*, *69*(3), 228–236. https://doi.org/10.1107/S1744309113000961

De La Cruz, M. A., Ares, M. A., Von Bargen, K., Panunzi, L. G., Martínez-Cruz, J., Valdez-Salazar, H. A., Jiménez-Galicia, C., & Torres, J. (2017). Gene Expression Profiling of Transcription Factors of Helicobacter pylori under Different Environmental Conditions. *Frontiers in Microbiology*, *8*. https://doi.org/10.3389/fmicb.2017.00615

De Oliveira, P. A. A., Baboghlian, J., Ramos, C. O. A., Mançano, A. S. F., Porcari, A. D. M., Girardello, R., & Ferraz, L. F. C. (2024). Selection and validation of reference genes suitable for gene expression analysis by Reverse Transcription Quantitative real-time PCR in Acinetobacter baumannii. *Scientific Reports*, *14*(1), 3830. https://doi.org/10.1038/s41598-024-51499-5

Deng, L., He, X.-Y., Tang, B., Xiang, Y., & Yue, J.-J. (2020). An improved quantitative real-time polymerase chain reaction technology for Helicobacter pylori detection in stomach tissue and its application value in clinical precision testing. *BMC Biotechnology*, *20*(1), 33. https://doi.org/10.1186/s12896-020-00624-z

Dey, S., Biswas, C., & Sengupta, J. (2018). The universally conserved GTPase HflX is an RNA helicase that restores heat-damaged *Escherichia coli* ribosomes.

Journal of Cell Biology, *217*(7), 2519–2529. https://doi.org/10.1083/jcb.201711131

Diedrich, G., Spahn, C. M. T., Stelzl, U., Schäfer, M. A., Wooten, T., Bochkariov, D. E., Cooperman, B. S., Traut, R. R., & Nierhaus, K. H. (2000). Ribosomal protein L2 is involved in the association of the ribosomal subunits, tRNA binding to A and P sites and peptidyl transfer. *The EMBO Journal*, *19*(19), 5241–5250. https://doi.org/10.1093/emboj/19.19.5241

Dinos, G. P. (2002). *Erythromycin, Roxithromycin, and Clarithromycin: Use of Slow-Binding Kinetics to Compare Their in Vitro Interaction with a Bacterial Ribosomal Complex Active in Peptide Bond Formation*.

Dong, Q.-J., Wang, Q., Xin, Y.-N., Li, N., & Xuan, S.-Y. (2009). Comparative genomics of Helicobacter pylori. *World Journal of Gastroenterology*, *15*(32), 3984. https://doi.org/10.3748/wjg.15.3984

Draper, J. L., Hansen, L. M., Bernick, D. L., Abedrabbo, S., Underwood, J. G., Kong, N., Huang, B. C., Weis, A. M., Weimer, B. C., Van Vliet, A. H. M., Pourmand, N., Solnick, J. V., Karplus, K., & Ottemann, K. M. (2017). Fallacy of the Unique Genome: Sequence Diversity within Single *Helicobacter pylori* Strains. *mBio*, *8*(1), e02321-16. https://doi.org/10.1128/mBio.02321-16

Dugar, G., Leenay, R. T., Eisenbart, S. K., Bischler, T., Aul, B. U., Beisel, C. L., & Sharma, C. M. (2018). CRISPR RNA-Dependent Binding and Cleavage of Endogenous RNAs by the Campylobacter jejuni Cas9. *Molecular Cell*, *69*(5), 893-905.e7. https://doi.org/10.1016/j.molcel.2018.01.032

Duncan, S. S., Bertoli, M. T., Kersulyte, D., Valk, P. L., Tamma, S., Segal, I., McClain, M. S., Cover, T. L., & Berg, D. E. (2013). Genome Sequences of Three hpAfrica2 Strains of Helicobacter pylori. *Genome Announcements*, *1*(5), e00729-13. https://doi.org/10.1128/genomeA.00729-13

Dyer, V., Brüggemann, H., Sörensen, M., Kühl, A. A., Hoffman, K., Brinkmann, V., Reines, M. D. M., Zimmerman, S., Meyer, T. F., & Koch, M. (2018). Genomic features of the *Helicobacter pylori* strain PMSS1 and its virulence attributes as deduced from its *in vivo* colonisation patterns. *Molecular Microbiology*, *110*(5), 761–776. https://doi.org/10.1111/mmi.14123

Ehrhardt, K., Becker, A.-L., & Grassl, G. A. (2023). Determinants of persistent *Salmonella* infections. *Current Opinion in Immunology*, *82*, 102306. https://doi.org/10.1016/j.coi.2023.102306

Elshenawi, Y., Hu, S., & Hathroubi, S. (2023). Biofilm of Helicobacter pylori: Life Cycle, Features, and Treatment Options. *Antibiotics*, *12*(8), 1260. https://doi.org/10.3390/antibiotics12081260

Elshenawi, Y. O., Hathroubi, S., Lane, A. E., Hetzel, M., & Ottemann, K. M. (2026). *The Helicobacter pylori ribosomal silencing factor RsfS is required for low-growth states and chronic infection*.

Eng, N. F., Ybazeta, G., Chapman, K., Fraleigh, N. L., Letto, R., Altman, E., & Diaz-Mitoma, F. (2015). Antimicrobial Susceptibility of Canadian Isolates of *Helicobacter pylori* in Northeastern Ontario. *Canadian Journal of Infectious*

Diseases and Medical Microbiology, *26*(3), 137–144. https://doi.org/10.1155/2015/853287

Estibariz, I. (n.d.). *Genomic evolution and epigenetic DNA modification in Helicobacter pylori phenotypic adaptation and transcriptional regulation*.

Faber, E., Gripp, E., Maurischat, S., Kaspers, B., Tedin, K., Menz, S., Zuraw, A., Kershaw, O., Yang, I., Rautenschlein, S., & Josenhans, C. (2016). Novel Immunomodulatory Flagellin-Like Protein FlaC in Campylobacter jejuni and Other *Campylobacterales*. *mSphere*, *1*(1), e00028-15. https://doi.org/10.1128/mSphere.00028-15

Fan, J., Zhu, J., & Xu, H. (2024). Strategies of Helicobacter pylori in evading host innate and adaptive immunity: Insights and prospects for therapeutic targeting. *Frontiers in Cellular and Infection Microbiology*, *14*, 1342913. https://doi.org/10.3389/fcimb.2024.1342913

Fantry, G. T., Fantry, L. E., James, S. P., & Alpers, D. H. (2016). Chronic Infections of the Small Intestine. In D. K. Podolsky, M. Camilleri, J. G. Fitz, A. N. Kalloo, F. Shanahan, & T. C. Wang (Eds.), *Yamada's Atlas of Gastroenterology* (1st ed., pp. 177–183). Wiley. https://doi.org/10.1002/9781118512104.ch23

Farnbacher, M., Jahns, T., Willrodt, D., Daniel, R., Haas, R., Goesmann, A., Kurtz, S., & Rieder, G. (2010). Sequencing, annotation, and comparative genome analysis of the gerbil-adapted Helicobacter pylori strain B8. *BMC Genomics*, *11*(1), 335. https://doi.org/10.1186/1471-2164-11-335

Fatkhullin, B. F., Gabdulkhakov, A. G., & Yusupov, M. M. (2022). Is RsfS a Hibernation Factor or a Ribosome Biogenesis Factor? *Biochemistry (Moscow)*, *87*(6), 500–510. https://doi.org/10.1134/S0006297922060025

Fernandes, G. F. S., Scarim, C. B., Kim, S.-H., Wu, J., & Castagnolo, D. (2023). Oxazolidinones as versatile scaffolds in medicinal chemistry. *RSC Medicinal Chemistry*, *14*(5), 823–847. https://doi.org/10.1039/D2MD00415A

Fisher, R. A., Gollan, B., & Helaine, S. (2017). Persistent bacterial infections and persister cells. *Nature Reviews Microbiology*, *15*(8), 453–464. https://doi.org/10.1038/nrmicro.2017.42

Flygaard, R. K., Boegholm, N., Yusupov, M., & Jenner, L. B. (2018). Cryo-EM structure of the hibernating Thermus thermophilus 100S ribosome reveals a protein-mediated dimerization mechanism. *Nature Communications*, *9*(1), 4179. https://doi.org/10.1038/s41467-018-06724-x

Fonseca, M. V., & Swanson, M. S. (2014). Nutrient salvaging and metabolism by the intracellular pathogen Legionella pneumophila. *Frontiers in Cellular and Infection Microbiology*, *4*. https://doi.org/10.3389/fcimb.2014.00012

Fordjour, G. N. R., Ghosh, A., Ferry, J. G., Armache, J.-P., Bevilacqua, P. C., & Murakami, K. S. (2025). Cryo-EM study and in vivo chemical mapping of the Methanosarcina acetivorans ribosome and its dimerization via a repurposed enzyme and translation factor. *Journal of Biological Chemistry*, *301*(11), 110686. https://doi.org/10.1016/j.jbc.2025.110686

Fortier, A., Doiron, K., Saleh, M., Grinstein, S., & Gros, P. (2009). Restriction of *L egionella pneumophila* Replication in Macrophages Requires Concerted Action of the Transcriptional Regulators Irf1 and Irf8 and Nod-Like Receptors Naip5 and Nlrc4. *Infection and Immunity*, *77*(11), 4794–4805. https://doi.org/10.1128/IAI.01546-08

Franken, L. E., Oostergetel, G. T., Pijning, T., Puri, P., Arkhipova, V., Boekema, E. J., Poolman, B., & Guskov, A. (2017). A general mechanism of ribosome dimerization revealed by single-particle cryo-electron microscopy. *Nature Communications*, *8*(1), 722. https://doi.org/10.1038/s41467-017-00718-x

Furuta, Y., Kawai, M., Yahara, K., Takahashi, N., Handa, N., Tsuru, T., Oshima, K., Yoshida, M., Azuma, T., Hattori, M., Uchiyama, I., & Kobayashi, I. (2011). Birth and death of genes linked to chromosomal inversion. *Proceedings of the National Academy of Sciences*, *108*(4), 1501–1506. https://doi.org/10.1073/pnas.1012579108

Galante, S., Castillo, R., Price, T., Tran, M., & Stramel-Stafford, S. (2025). Assessing Clinical Outcomes of Metronidazole for Intra-Abdominal Infections When Dosed Every 12 h Versus Every 8 h in a Multi-Center Health System. *Antibiotics*, *14*(7), 688. https://doi.org/10.3390/antibiotics14070688

Gao, N., Zavialov, A. V., Ehrenberg, M., & Frank, J. (2007). Specific Interaction between EF-G and RRF and Its Implication for GTP-Dependent Ribosome Splitting into Subunits. *Journal of Molecular Biology*, *374*(5), 1345–1358. https://doi.org/10.1016/j.jmb.2007.10.021

Gao, N., Zavialov, A. V., Li, W., Sengupta, J., Valle, M., Gursky, R. P., Ehrenberg, M., & Frank, J. (2005). Mechanism for the Disassembly of the Posttermination Complex Inferred from Cryo-EM Studies. *Molecular Cell*, *18*(6), 663–674. https://doi.org/10.1016/j.molcel.2005.05.005

Garcia-Clemente, M., De La Rosa, D., Máiz, L., Girón, R., Blanco, M., Olveira, C., Canton, R., & Martinez-García, M. A. (2020). Impact of *Pseudomonas aeruginosa* Infection on Patients with Chronic Inflammatory Airway Diseases. *Journal of Clinical Medicine*, *9*(12), 3800. https://doi.org/10.3390/jcm9123800

García-Zea, J. A., De La Herrán, R., Robles Rodríguez, F., Navajas-Pérez, R., & Ruiz Rejón, C. (2019). Detection and variability analyses of CRISPR-like loci in the *H. pylori* genome. *PeerJ*, *7*, e6221. https://doi.org/10.7717/peerj.6221

Ge, Z., Sheh, A., Feng, Y., Muthupalani, S., Ge, L., Wang, C., Kurnick, S., Mannion, A., Whary, M. T., & Fox, J. G. (2018). Helicobacter pylori-infected C57BL/6 mice with different gastrointestinal microbiota have contrasting gastric pathology, microbial and host immune responses. *Scientific Reports*, *8*(1), 8014. https://doi.org/10.1038/s41598-018-25927-2

Gefen, O., Fridman, O., Ronin, I., & Balaban, N. Q. (2014). Direct observation of single stationary-phase bacteria reveals a surprisingly long period of constant protein production activity. *Proceedings of the National Academy of Sciences*, *111*(1), 556–561. https://doi.org/10.1073/pnas.1314114111

Gerrits, M. M., De Zoete, M. R., Arents, N. L. A., Kuipers, E. J., & Kusters, J. G. (2002). 16S rRNA Mutation-Mediated Tetracycline Resistance in *Helicobacter pylori*. *Antimicrobial Agents and Chemotherapy*, *46*(9), 2996–3000. https://doi.org/10.1128/AAC.46.9.2996-3000.2002

Giovane, R. A., & Lavender, P. D. (2018). Central Nervous System Infections. *Primary Care: Clinics in Office Practice*, *45*(3), 505–518. https://doi.org/10.1016/j.pop.2018.05.007

Gohara, D. W., & Yap, M.-N. F. (2018). Survival of the drowsiest: The hibernating 100S ribosome in bacterial stress management. *Current Genetics*, *64*(4), 753–760. https://doi.org/10.1007/s00294-017-0796-2

Gomes, T. G., De Assis Fonseca, F. C., Alves, G. S. C., De Siqueira, F. G., & Miller, R. N. G. (2023). Development of reference genes for RT-qPCR analysis of gene expression in Pleurotus pulmonarius for biotechnological applications. *Scientific Reports*, *13*(1), 12296. https://doi.org/10.1038/s41598-023-39115-4

Gómez-Ruiz De Arbulo, M., Tamayo, E., Bujanda, L., Mendibil, L., Mendiola, J., Cilla, G., & Montes, M. (2023). Surveillance of Helicobacter pylori resistance over 22 Years (2000-2021) in Northern Spain. *Journal of Global Antimicrobial Resistance*, *34*, 127–133. https://doi.org/10.1016/j.jgar.2023.07.002

Gong, Y., Zhai, K., Sun, L., He, L., Wang, H., Guo, Y., & Zhang, J. (2023). RdxA Diversity and Mutations Associated with Metronidazole Resistance of

Helicobacter pylori. *Microbiology Spectrum*, *11*(2), e03903-22. https://doi.org/10.1128/spectrum.03903-22

Goodwin, A., Kersulyte, D., Sisson, G., Veldhuyzen Van Zanten, S. J. O., Berg, D. E., & Hoffman, P. S. (1998). Metronidazole resistance in *Helicobacter pylori* is due to null mutations in a gene (*rdxA*) that encodes an oxygen-insensitive NADPH nitroreductase. *Molecular Microbiology*, *28*(2), 383–393. https://doi.org/10.1046/j.1365-2958.1998.00806.x

Green, M. H., & Hall, B. D. (1961). A Comparison of the Native and Derived 30S and 50S Ribosomes of Escherichia coli. *Biophysical Journal*, *1*(6), 517–523. https://doi.org/10.1016/S0006-3495(61)86905-1

Grenier, F., Matteau, D., Baby, V., & Rodrigue, S. (2014). Complete Genome Sequence of Escherichia coli BW25113. *Genome Announcements*, *2*(5), e01038-14. https://doi.org/10.1128/genomeA.01038-14

Greulich, P., Scott, M., Evans, M. R., & Allen, R. J. (2015). Growth-dependent bacterial susceptibility to ribosome-targeting antibiotics. *Molecular Systems Biology*, *11*(3), 796. https://doi.org/10.15252/msb.20145949

Gualerzi, C. O., & Pon, C. L. (2015). Initiation of mRNA translation in bacteria: Structural and dynamic aspects. *Cellular and Molecular Life Sciences*, *72*(22), 4341–4367. https://doi.org/10.1007/s00018-015-2010-3

Gunsalus, I. C., Goulden, C. H., Swingle, K. E., Axelrod, A. E., Elvehjem, C. A., Wolfe, E. C., & Ball, E. G. (1959). SHORT COMMUNICATIONS 563. *Biochim. Biophys. Acta*. https://doi.org/10.1016/0006-3002(60)90221-3

Guo, Z., Tian, S., Wang, W., Zhang, Y., Li, J., & Lin, R. (2022). Correlation Analysis Among Genotype Resistance, Phenotype Resistance, and Eradication Effect After Resistance-Guided Quadruple Therapies in Refractory *Helicobacter pylori* Infections. *Frontiers in Microbiology*, *13*, 861626. https://doi.org/10.3389/fmicb.2022.861626

Han, C. D., Coe, E. H., & Martienssen, R. A. (1992). Molecular cloning and characterization of iojap (ij), a pattern striping gene of maize. *The EMBO Journal*, *11*(11), 4037–4046. https://doi.org/10.1002/j.1460-2075.1992.tb05497.x

Hannan, T. J., Totsika, M., Mansfield, K. J., Moore, K. H., Schembri, M. A., & Hultgren, S. J. (2012). Host–pathogen checkpoints and population bottlenecks in persistent and intracellular uropathogenic *Escherichia coli* bladder infection. *FEMS Microbiology Reviews*, *36*(3), 616–648. https://doi.org/10.1111/j.1574-6976.2012.00339.x

Hashi, K., Murata-Kamiya, N., Varon, C., Mégraud, F., Dominguez-Bello, M. G., & Hatakeyama, M. (2014). Natural variant of the *Helicobacter pylori* CagA oncoprotein that lost the ability to interact with PAR 1. *Cancer Science*, *105*(3), 245–251. https://doi.org/10.1111/cas.12342

Hashim, H. S., Zayan, M. M., Mohamed, A. A., & El Rahman Abulila, H. I. A. (2026). Actinomycetes in the spotlight: Biodiversity and their role in bioremediation. *World Journal of Microbiology and Biotechnology*, *42*(2), 44. https://doi.org/10.1007/s11274-025-04610-5

Hassan, A. H., Nakano, Y., Gamper, H., Masuda, I., Vesela, L., Pinkas, M., Nagarajan, S. N., Dworkin, J., Blaha, G., Hou, Y.-M., & Demo, G. (2026). Mechanistic insights into E. coli recovery from growth arrest. *Nature Communications*, *17*(1), 5124. https://doi.org/10.1038/s41467-026-71781-6

Hassan, A. H., Pinkas, M., Yaeshima, C., Ishino, S., Uchiumi, T., Ito, K., & Demo, G. (2025). Novel archaeal ribosome dimerization factor facilitating unique 30S–30S dimerization. *Nucleic Acids Research*, *53*(2), gkae1324. https://doi.org/10.1093/nar/gkae1324

Hathroubi, S., Hu, S., & Ottemann, K. M. (2020). Genetic requirements and transcriptomics of *Helicobacter pylori* biofilm formation on abiotic and biotic surfaces. *Npj Biofilms and Microbiomes*, *6*(1), 56. https://doi.org/10.1038/s41522-020-00167-3

Hathroubi, S., Zerebinski, J., & Ottemann, K. M. (2018). Helicobacter pylori Biofilm Involves a Multigene Stress-Biased Response, Including a Structural Role for Flagella. *mBio*, *9*(5), e01973-18. https://doi.org/10.1128/mBio.01973-18

Häuser, R., Pech, M., Kijek, J., Yamamoto, H., Titz, B., Naeve, F., Tovchigrechko, A., Yamamoto, K., Szaflarski, W., Takeuchi, N., Stellberger, T., Diefenbacher, M. E., Nierhaus, K. H., & Uetz, P. (2012). RsfA (YbeB) Proteins Are Conserved Ribosomal Silencing Factors. *PLoS Genetics*, *8*(7), e1002815. https://doi.org/10.1371/journal.pgen.1002815

Helena-Bueno, K., Chan, L. I., & Melnikov, S. V. (2024a). Rippling life on a dormant planet: Hibernation of ribosomes, RNA polymerases, and other essential

enzymes. *Frontiers in Microbiology*, *15*, 1386179. https://doi.org/10.3389/fmicb.2024.1386179

Helena-Bueno, K., Chan, L. I., & Melnikov, S. V. (2024b). Rippling life on a dormant planet: Hibernation of ribosomes, RNA polymerases, and other essential enzymes. *Frontiers in Microbiology*, *15*, 1386179. https://doi.org/10.3389/fmicb.2024.1386179

Helena-Bueno, K., Rybak, M. Yu., Ekemezie, C. L., Sullivan, R., Brown, C. R., Dingwall, C., Baslé, A., Schneider, C., Connolly, J. P. R., Blaza, J. N., Csörgő, B., Moynihan, P. J., Gagnon, M. G., Hill, C. H., & Melnikov, S. V. (2024). A new family of bacterial ribosome hibernation factors. *Nature*, *626*(8001), 1125–1132. https://doi.org/10.1038/s41586-024-07041-8

Hendrixson, D. R. (2008). Restoration of flagellar biosynthesis by varied mutational events in *Campylobacter jejuni*. *Molecular Microbiology*, *70*(2), 519–536. https://doi.org/10.1111/j.1365-2958.2008.06428.x

Hjelmager, J. S., Andersen, K., Andersen, T. E., & Stærk, K. (2025). What is chronic urinary tract infection? A systematic review. *BJU International*, *136*(1), 12–18. https://doi.org/10.1111/bju.16764

Hong, T.-C., El-Omar, E. M., Kuo, Y.-T., Wu, J.-Y., Chen, M.-J., Chen, C.-C., Fang, Y.-J., Leow, A. H. R., Lu, H., Lin, J.-T., Tu, Y.-K., Yamaoka, Y., Wu, M.-S., Liou, J.-M., Hong, T.-C., El-Omar, E. M., Kuo, Y.-T., Wu, J.-Y., Chen, M.-J., … Chang, Y.-Y. (2024). Primary antibiotic resistance of *Helicobacter pylori* in the Asia-Pacific region between 1990 and 2022: An updated systematic review

and meta-analysis. *The Lancet Gastroenterology & Hepatology*, *9*(1), 56–67. https://doi.org/10.1016/S2468-1253(23)00281-9

Horrocks, S. M., Jung, Y. S., Huwe, J. K., Harvey, R. B., Ricke, S. C., Carstens, G. E., Callaway, T. R., Anderson, R. C., Ramlachan, N., & Nisbet, D. J. (2007). Effects of Short-Chain Nitrocompounds against *Campylobacter jejuni* and *Campylobacter coli* in vitro. *Journal of Food Science*, *72*(2). https://doi.org/10.1111/j.1750-3841.2006.00255.x

Howitt, M. R., Lee, J. Y., Lertsethtakarn, P., Vogelmann, R., Joubert, L.-M., Ottemann, K. M., & Amieva, M. R. (2011). ChePep Controls *Helicobacter pylori* Infection of the Gastric Glands and Chemotaxis in the *Epsilonproteobacteria*. *mBio*, *2*(4), e00098-11. https://doi.org/10.1128/mBio.00098-11

Hu, S., Giacopazzi, S., Modlin, R., Karplus, K., Bernick, D. L., & Ottemann, K. M. (2023). Altering under-represented DNA sequences elevates bacterial transformation efficiency. *mBio*, *14*(6), e02105-23. https://doi.org/10.1128/mbio.02105-23

Hu, X.-P., Dourado, H., Schubert, P., & Lercher, M. J. (2020). The protein translation machinery is expressed for maximal efficiency in Escherichia coli. *Nature Communications*, *11*(1), 5260. https://doi.org/10.1038/s41467-020-18948-x

Huang, J., Li, Z., Ge, F., Sun, C., Deng, Z., Yao, W., & He, X. (2024). Functional determination of site-mutations in *rdxA* involved in metronidazole resistance

of *Helicobacter pylori*. *Frontiers in Cell and Developmental Biology*, *12*, 1435064. https://doi.org/10.3389/fcell.2024.1435064

Huang, W., Krokowski, D., Hatzoglou, M., & Taylor, D. (2018). Eukaryotic Hibernating Ribosome Dimers are Maintained by a Kissing Loop Formed by Ribosomal RNA. *Microscopy and Microanalysis*, *24*(S1), 1234–1235. https://doi.org/10.1017/S1431927618006657

Humphreys, I. R., Zhang, J., Baek, M., Wang, Y., Krishnakumar, A., Pei, J., Anishchenko, I., Tower, C. A., Jackson, B. A., Warrier, T., Hung, D. T., Peterson, S. B., Mougous, J. D., Cong, Q., & Baker, D. (2024). Protein interactions in human pathogens revealed through deep learning. *Nature Microbiology*, *9*(10), 2642–2652. https://doi.org/10.1038/s41564-024-01791-x

Huttner, A., Bielicki, J., Clements, M. N., Frimodt-Møller, N., Muller, A. E., Paccaud, J.-P., & Mouton, J. W. (2020). Oral amoxicillin and amoxicillin–clavulanic acid: Properties, indications and usage. *Clinical Microbiology and Infection*, *26*(7), 871–879. https://doi.org/10.1016/j.cmi.2019.11.028

Iliadi, V., Staykova, J., Iliadis, S., Konstantinidou, I., Sivykh, P., Romanidou, G., Vardikov, D. F., Cassimos, D., & Konstantinidis, T. G. (2022). Legionella pneumophila: The Journey from the Environment to the Blood. *Journal of Clinical Medicine*, *11*(20), 6126. https://doi.org/10.3390/jcm11206126

Israel, D. A., Salama, N., Krishna, U., Rieger, U. M., Atherton, J. C., Falkow, S., & Peek, R. M. (2001). *Helicobacter pylori* genetic diversity within the gastric

niche of a single human host. *Proceedings of the National Academy of Sciences*, *98*(25), 14625–14630. https://doi.org/10.1073/pnas.251551698

Izutsu, K., Wada, A., & Wada, C. (2001). Expression of ribosome modulation factor (RMF) in *Escherichia coli* requires ppGpp. *Genes to Cells*, *6*(8), 665–676. https://doi.org/10.1046/j.1365-2443.2001.00457.x

Jacobsen, A. V., Yemaneab, B. T., Jass, J., & Scherbak, N. (2014). Reference Gene Selection for qPCR Is Dependent on Cell Type Rather than Treatment in Colonic and Vaginal Human Epithelial Cell Lines. *PLoS ONE*, *9*(12), e115592. https://doi.org/10.1371/journal.pone.0115592

Jaka, H., Rhee, J. Ah., Östlundh, L., Smart, L., Peck, R., Mueller, A., Kasang, C., & Mshana, S. E. (2018). The magnitude of antibiotic resistance to Helicobacter pylori in Africa and identified mutations which confer resistance to antibiotics: Systematic review and meta-analysis. *BMC Infectious Diseases*, *18*(1), 193. https://doi.org/10.1186/s12879-018-3099-4

Jenks, P. J., Ferrero, R. L., & Labigne, A. (1999). The role of the rdxA gene in the evolution of metronidazole resistance in *Helicobacter pylori*. *Journal of Antimicrobial Chemotherapy*.

Jeong, J.-Y., Mukhopadhyay, A. K., Akada, J. K., Dailidiene, D., Hoffman, P. S., & Berg, D. E. (2001). Roles of FrxA and RdxA Nitroreductases of *Helicobacter pylori* in Susceptibility and Resistance to Metronidazole. *Journal of Bacteriology*, *183*(17), 5155–5162. https://doi.org/10.1128/JB.183.17.5155-5162.2001

Jeong, J.-Y., Mukhopadhyay, A. K., Dailidiene, D., Wang, Y., Velapatiño, B., Gilman, R. H., Parkinson, A. J., Nair, G. B., Wong, B. C. Y., Lam, S. K., Mistry, R., Segal, I., Yuan, Y., Gao, H., Alarcon, T., Brea, M. L., Ito, Y., Kersulyte, D., Lee, H.-K., … Berg, D. E. (2000). Sequential Inactivation of *rdxA* (HP0954) and *frxA* (HP0642) Nitroreductase Genes Causes Moderate and High-Level Metronidazole Resistance in *Helicobacter pylori*. *Journal of Bacteriology*, *182*(18), 5082–5090. https://doi.org/10.1128/JB.182.18.5082-5090.2000

Jiang, M., Sullivan, S. M., Walker, A. K., Strahler, J. R., Andrews, P. C., & Maddock, J. R. (2007). Identification of Novel *Escherichia coli* Ribosome-Associated Proteins Using Isobaric Tags and Multidimensional Protein Identification Techniques. *Journal of Bacteriology*, *189*(9), 3434–3444. https://doi.org/10.1128/JB.00090-07

Johnson, L. F., Abelson, H. T., Penman, S., & Green, H. (1977). The relative amounts of the cytoplasmic RNA species in normal, transformed and senescent cultured cell lines. *Journal of Cellular Physiology*, *90*(3), 465–470. https://doi.org/10.1002/jcp.1040900310

Kaprelyants, A. S., Gottschal, J. C., & Kell, D. B. (1993). Dormancy in non-sporulating bacteria. *FEMS Microbiology Letters*, *104*(3–4), 271–286. https://doi.org/10.1111/j.1574-6968.1993.tb05871.x

Karari Njenga, R., & Koch, H.-G. (2026). Falling asleep: The importance of ribosome hibernation in bacteria. *Microbiology and Molecular Biology Reviews*, e00159-25. https://doi.org/10.1128/mmbr.00159-25

Kato, T., Yoshida, H., Miyata, T., Maki, Y., Wada, A., & Namba, K. (2010). Structure of the 100S Ribosome in the Hibernation Stage Revealed by Electron Cryomicroscopy. *Structure*, *18*(6), 719–724. https://doi.org/10.1016/j.str.2010.02.017

Kayali, S., Manfredi, M., Gaiani, F., Bianchi, L., Bizzarri, B., Leandro, G., Di Mario, F., & de' Angelis, G. L. (2018). Helicobacter pylori, transmission routes and recurrence of infection: State of the art. *Acta Bio Medica Atenei Parmensis*, *89*(8-S), 72–76. https://doi.org/10.23750/abm.v89i8-S.7947

Keilberg, D., Zavros, Y., Shepherd, B., Salama, N. R., & Ottemann, K. M. (2016). Spatial and Temporal Shifts in Bacterial Biogeography and Gland Occupation during the Development of a Chronic Infection. *mBio*, *7*(5), e01705-16. https://doi.org/10.1128/mBio.01705-16

Kelly, D. J. (2001). The physiology and metabolism of Campylobacter jejuni and Helicobacter pylori. *Journal of Applied Microbiology*, *90*(S6), 16S-24S. https://doi.org/10.1046/j.1365-2672.2001.01350.x

Kersulyte, D., Velapatiño, B., Dailide, G., Mukhopadhyay, A. K., Ito, Y., Cahuayme, L., Parkinson, A. J., Gilman, R. H., & Berg, D. E. (2002). Transposable Element IS *Hp608* of *Helicobacter pylori*: Nonrandom Geographic Distribution, Functional Organization, and Insertion Specificity. *Journal of Bacteriology*, *184*(4), 992–1002. https://doi.org/10.1128/jb.184.4.992-1002.2002

Khusainov, I., Fatkhullin, B., Pellegrino, S., Bikmullin, A., Liu, W., Gabdulkhakov, A., Shebel, A. A., Golubev, A., Zeyer, D., Trachtmann, N., Sprenger, G. A., Validov, S., Usachev, K., Yusupova, G., & Yusupov, M. (2020). Mechanism of ribosome shutdown by RsfS in *Staphylococcus aureus* revealed by integrative structural biology approach. *Nature Communications*, *11*(1), 1656. https://doi.org/10.1038/s41467-020-15517-0

Khusainov, I., Vicens, Q., Ayupov, R., Usachev, K., Myasnikov, A., Simonetti, A., Validov, S., Kieffer, B., Yusupova, G., Yusupov, M., & Hashem, Y. (2017). Structures and dynamics of hibernating ribosomes from *Staphylococcus aureus* mediated by intermolecular interactions of HPF. *The EMBO Journal*, *36*(14), 2073–2087. https://doi.org/10.15252/embj.201696105

Ki, V., & Rotstein, C. (2008). Bacterial Skin and Soft Tissue Infections in Adults: A Review of Their Epidemiology, Pathogenesis, Diagnosis, Treatment and Site Of Care. *Canadian Journal of Infectious Diseases and Medical Microbiology*, *19*(2), 173–184. https://doi.org/10.1155/2008/846453

Kiel, M. C., Raj, V. S., Kaji, H., & Kaji, A. (2003). Release of Ribosome-bound Ribosome Recycling Factor by Elongation Factor G. *Journal of Biological Chemistry*, *278*(48), 48041–48050. https://doi.org/10.1074/jbc.M304834200

Kim, S. H., Soliman, Y., Chitnavis, V. N., & Chitnavis, M. V. (2023). *Helicobacter pylori*-Negative MALT Lymphoma: A Series of Two Cases Presenting with Life-Threatening Upper Gastrointestinal Bleeding. *Case Reports in Gastrointestinal Medicine*, *2023*, 1–4. https://doi.org/10.1155/2023/8244696

Kline, B. C., McKay, S. L., Tang, W. W., & Portnoy, D. A. (2015). The Listeria monocytogenes Hibernation-Promoting Factor Is Required for the Formation of 100S Ribosomes, Optimal Fitness, and Pathogenesis. *Journal of Bacteriology*, *197*(3), 581–591. https://doi.org/10.1128/JB.02223-14

Kocsmár, É., Buzás, G. M., Szirtes, I., Kocsmár, I., Kramer, Z., Szijártó, A., Fadgyas-Freyler, P., Szénás, K., Rugge, M., Fassan, M., Kiss, A., Schaff, Z., Röst, G., & Lotz, G. (2021). Primary and secondary clarithromycin resistance in Helicobacter pylori and mathematical modeling of the role of macrolides. *Nature Communications*, *12*(1), 2255. https://doi.org/10.1038/s41467-021-22557-7

Koli, S., & Shetty, S. (2024). Ribosomal dormancy at the nexus of ribosome homeostasis and protein synthesis. *BioEssays*, *46*(7), 2300247. https://doi.org/10.1002/bies.202300247

Korostelev, A. A. (2011). Structural aspects of translation termination on the ribosome. *RNA*, *17*(8), 1409–1421. https://doi.org/10.1261/rna.2733411

Krause, K. M., Serio, A. W., Kane, T. R., & Connolly, L. E. (2016). Aminoglycosides: An Overview. *Cold Spring Harbor Perspectives in Medicine*, *6*(6), a027029. https://doi.org/10.1101/cshperspect.a027029

Krawczyk, S. J., Leśniczak-Staszak, M., Gowin, E., & Szaflarski, W. (2024). Mechanistic Insights into Clinically Relevant Ribosome-Targeting Antibiotics. *Biomolecules*, *14*(10), 1263. https://doi.org/10.3390/biom14101263

Krokowski, D., Gaccioli, F., Majumder, M., Mullins, M. R., Yuan, C. L., Papadopoulou, B., Merrick, W. C., Komar, A. A., Taylor, D. J., & Hatzoglou, M. (2011). Characterization of hibernating ribosomes in mammalian cells. *Cell Cycle*, *10*(16), 2691–2702. https://doi.org/10.4161/cc.10.16.16844

Kulandaisamy, R., Velpula, K. K., & Inampudi, K. K. (2023). New biochemical insights of CCA enzyme role in tRNA maturation and an efficient method to synthesize the 3′-amino-tailed tRNA. *Biochimie*, *209*, 95–102. https://doi.org/10.1016/j.biochi.2023.01.007

Kumar, N., Sharma, S., & Kaushal, P. S. (2024). Cryo- EM structure of the mycobacterial 70S ribosome in complex with ribosome hibernation promotion factor RafH. *Nature Communications*, *15*(1), 638. https://doi.org/10.1038/s41467-024-44879-y

Kuo, P.-Y., & Kao, C.-Y. (2025). Regulatory Networks in Helicobacter pylori: The Roles of Two-Component Systems and CsrA in Stress Adaptation. *Journal of Microbiology, Immunology and Infection*, *58*(6), 632–640. https://doi.org/10.1016/j.jmii.2025.06.009

Kuroda, M., Ohta, T., Uchiyama, I., Baba, T., Yuzawa, H., Kobayashi, I., Cui, L., Oguchi, A., Aoki, K., Nagai, Y., Lian, J., Ito, T., Kanamori, M., Matsumaru, H., Maruyama, A., Murakami, H., Hosoyama, A., Mizutani-Ui, Y., Takahashi, N. K., … Hiramatsu, K. (2001). Whole genome sequencing of meticillin-resistant Staphylococcus aureus. *The Lancet*, *357*(9264), 1225–1240. https://doi.org/10.1016/S0140-6736(00)04403-2

Kwon, D. H. (2000). Frameshift mutations in rdxA and metronidazole resistance in North American Helicobacter pylori isolates. *Journal of Antimicrobial Chemotherapy*, *46*(5), 793–796. https://doi.org/10.1093/jac/46.5.793

Kwon, D. H., Hulten, K., Kato, M., Kim, J. J., Lee, M., El-Zaatari, F. A. K., Osato, M. S., & Graham, D. Y. (2001). DNA Sequence Analysis of *rdxA* and *frxA* from 12 Pairs of Metronidazole-Sensitive and -Resistant Clinical *Helicobacter pylori* Isolates. *Antimicrobial Agents and Chemotherapy*, *45*(9), 2609–2615. https://doi.org/10.1128/AAC.45.9.2609-2615.2001

Kwon, D.-H., El-Zaatari, F. A. K., Kato, M., Osato, M. S., Reddy, R., Yamaoka, Y., & Graham, D. Y. (2000). Analysis of *rdxA* and Involvement of Additional Genes Encoding NAD(P)H Flavin Oxidoreductase (FrxA) and Ferredoxin-Like Protein (FdxB) in Metronidazole Resistance of *Helicobacter pylori*. *Antimicrobial Agents and Chemotherapy*, *44*(8), 2133–2142. https://doi.org/10.1128/AAC.44.8.2133-2142.2000

Langford, M. L., Zabaleta, J., Ochoa, A. C., Testerman, T. L., & McGee, D. J. (2006). *In Vitro* and *In Vivo* Complementation of the *Helicobacter pylori* Arginase Mutant Using an Intergenic Chromosomal Site. *Helicobacter*, *11*(5), 477–493. https://doi.org/10.1111/j.1523-5378.2006.00441.x

Laurberg, M., Asahara, H., Korostelev, A., Zhu, J., Trakhanov, S., & Noller, H. F. (2008). Structural basis for translation termination on the 70S ribosome. *Nature*, *454*(7206), 852–857. https://doi.org/10.1038/nature07115

Laursen, B. S., Sørensen, H. P., Mortensen, K. K., & Sperling-Petersen, H. U. (2005). Initiation of Protein Synthesis in Bacteria. *Microbiology and Molecular Biology Reviews*, *69*(1), 101–123. https://doi.org/10.1128/MMBR.69.1.101-123.2005

Lee, A., O'Rourke, J., De Ungria, M., Robertson, B., Daskalopoulos, G., & Dixon, M. (1997). A standardized mouse model of *Helicobacter pylori* infection: Introducing the Sydney strain. *Gastroenterology*, *112*(4), 1386–1397. https://doi.org/10.1016/S0016-5085(97)70155-0

Lee, S. M., Kim, N., Kwon, Y. H., Nam, R. H., Kim, J. M., Park, J. Y., Lee, Y. S., & Lee, D. H. (2018). *rdxA, frxA* , and efflux pump in metronidazole-resistant *Helicobacter pylori*: Their relation to clinical outcomes. *Journal of Gastroenterology and Hepatology*, *33*(3), 681–688. https://doi.org/10.1111/jgh.13906

Lee, Y.-C., Dore, M. P., & Graham, D. Y. (2022). *Diagnosis and Treatment of* Helicobacter pylori *Infection*.

Lenz, K. D., Klosterman, K. E., Mukundan, H., & Kubicek-Sutherland, J. Z. (2021). Macrolides: From Toxins to Therapeutics. *Toxins*, *13*(5), 347. https://doi.org/10.3390/toxins13050347

Lew, J. M., Kapopoulou, A., Jones, L. M., & Cole, S. T. (2011). TubercuList – 10 years after. *Tuberculosis*, *91*(1), 1–7. https://doi.org/10.1016/j.tube.2010.09.008

Li, X., Sun, Q., Jiang, C., Yang, K., Hung, L.-W., Zhang, J., & Sacchettini, J. C. (2016). *Structure of Ribosomal Silencing Factor Bound to* Mycobacterium tuberculosis *Ribosome*.

Li, Y., Sharma, M. R., Koripella, R. K., Banavali, N. K., Agrawal, R. K., & Ojha, A. K. (2021). Ribosome hibernation: A new molecular framework for targeting nonreplicating persisters of mycobacteria. *Microbiology*, *167*(2). https://doi.org/10.1099/mic.0.001035

Liang, S.-T., Ehrenberg, M., Dennis, P., & Bremer, H. (1999). Decay of rplN and lacZ mRNA in Escherichia coli 1 1Edited by D. E. Draper. *Journal of Molecular Biology*, *288*(4), 521–538. https://doi.org/10.1006/jmbi.1999.2710

Liechti, G., & Goldberg, J. B. (2012). *Helicobacter pylori* Relies Primarily on the Purine Salvage Pathway for Purine Nucleotide Biosynthesis. *Journal of Bacteriology*, *194*(4), 839–854. https://doi.org/10.1128/JB.05757-11

Liechti, G. W., & Goldberg, J. B. (2013). *Helicobacter pylori* Salvages Purines from Extracellular Host Cell DNA Utilizing the Outer Membrane-Associated Nuclease NucT. *Journal of Bacteriology*, *195*(19), 4387–4398. https://doi.org/10.1128/JB.00388-13

Lin, Y., Shao, Y., Yan, J., & Ye, G. (2023). Antibiotic resistance in *Helicobacter pylori*: From potential biomolecular mechanisms to clinical practice. *Journal of Clinical Laboratory Analysis*, *37*(7), e24885. https://doi.org/10.1002/jcla.24885

Liu, A.-N., Teng, K.-W., Chew, Y., Wang, P.-C., Nguyen, T. T. H., & Kao, M.-C. (2022). The Effects of HP0044 and HP1275 Knockout Mutations on the Structure and Function of Lipopolysaccharide in *Helicobacter pylori* Strain 26695. *Biomedicines*, *10*(1), 145. https://doi.org/10.3390/biomedicines10010145

Liu, Q., & Fredrick, K. (2017). *Intersubunit bridges of the bacterial ribosome*.

Liu, X., Lertsethtakarn, P., Mariscal, V. T., Yildiz, F., & Ottemann, K. M. (2024). Counterclockwise rotation of the flagellum promotes biofilm initiation in *Helicobacter pylori*. *mBio*, *15*(6), e00440-24. https://doi.org/10.1128/mbio.00440-24

Long, K. S. (2003). A conserved chloramphenicol binding site at the entrance to the ribosomal peptide exit tunnel. *Nucleic Acids Research*, *31*(24), 7208–7215. https://doi.org/10.1093/nar/gkg945

Lowenthal, A. C., Hill, M., Sycuro, L. K., Mehmood, K., Salama, N. R., & Ottemann, K. M. (2009). Functional Analysis of the *Helicobacter pylori* Flagellar Switch Proteins. *Journal of Bacteriology*, *191*(23), 7147–7156. https://doi.org/10.1128/JB.00749-09

Majumdar, S., Li, Y., Manjari, S. R., Gamper, H. B., Hou, Y.-M., Banavali, N. K., Ojha, A. K., & Agrawal, R. K. (2024). *A Novel Actinobacteria-Specific Ribosome Hibernation Factor in* Mycobacterium tuberculosis. Microbiology. https://doi.org/10.1101/2024.11.25.625233

Makarova, K. S., Aravind, L., & Koonin, E. V. (2002). SWIM, a novel Zn-chelating domain present in bacteria, archaea and eukaryotes. *Trends in Biochemical Sciences*, *27*(8), 384–386. https://doi.org/10.1016/S0968-0004(02)02140-0

Maki, Y., & Yoshida, H. (2021). Ribosomal Hibernation-Associated Factors in Escherichia coli. *Microorganisms*, *10*(1), 33. https://doi.org/10.3390/microorganisms10010033

Malfertheiner, P., Camargo, M. C., El-Omar, E., Liou, J.-M., Peek, R., Schulz, C., Smith, S. I., & Suerbaum, S. (2023). Helicobacter pylori infection. *Nature Reviews Disease Primers*, *9*(1), 19. https://doi.org/10.1038/s41572-023-00431-8

Malfertheiner, P., Sipponen, P., Naumann, M., Moayyedi, P., Megraud, F., Xiao, S.-D., Sugano, K., Nyren, O., & the Lejondal H. pylori-Gastric Cancer Task Force. (2005). Helicobacter pylori Eradication Has the Potential to Prevent Gastric Cancer: A State-of-the-Art Critique. *The American Journal of Gastroenterology*, *100*(9), 2100–2115. https://doi.org/10.1111/j.1572-0241.2005.41688.x

Mannion, A., Dzink-Fox, J., Shen, Z., Piazuelo, M. B., Wilson, K. T., Correa, P., Peek, R. M., Camargo, M. C., & Fox, J. G. (2021). Helicobacter pylori Antimicrobial Resistance and Gene Variants in High- and Low-Gastric-Cancer-Risk Populations. *Journal of Clinical Microbiology*, *59*(5), e03203-20. https://doi.org/10.1128/JCM.03203-20

Marais, A., Bilardi, C., Cantet, F., Mendz, G. L., & Mégraud, F. (2003). Characterization of the genes *rdxA* and *frxA* involved in metronidazole resistance in *Helicobacter pylori*. *Research in Microbiology*, *154*(2), 137–144. https://doi.org/10.1016/S0923-2508(03)00030-5

Marques, B., Donato, M. M., Cardoso, O., Luxo, C., Martinho, A., & Almeida, N. (2019). Study of rdxA and frxA genes mutations in metronidazole-resistant and -susceptible Helicobacter pylori clinical isolates from the central region of Portugal. *Journal of Global Antimicrobial Resistance*, *17*, 300–304. https://doi.org/10.1016/j.jgar.2019.01.008

Martínez-Júlvez, M., Rojas, A. L., Olekhnovich, I., Angarica, V. E., Hoffman, P. S., & Sancho, J. (2012). Structure of R dx A – an oxygen-insensitive nitroreductase essential for metronidazole activation in *H elicobacter pylori* . *The FEBS Journal*, *279*(23), 4306–4317. https://doi.org/10.1111/febs.12020

Mattheakis, L., Vu, L., Sor, F., & Nomura, M. (1989). Retroregulation of the synthesis of ribosomal proteins L14 and L24 by feedback repressor S8 in Escherichia coli. *Proceedings of the National Academy of Sciences*, *86*(2), 448–452. https://doi.org/10.1073/pnas.86.2.448

Matthews, H. C., & Alexander, J. T. (2026). *Treatment of HelicobacterpyloriInfection*.

Matzov, D., Aibara, S., Basu, A., Zimmerman, E., Bashan, A., Yap, M.-N. F., Amunts, A., & Yonath, A. E. (2017). The cryo-EM structure of hibernating 100S ribosome dimer from pathogenic Staphylococcus aureus. *Nature Communications*, *8*(1), 723. https://doi.org/10.1038/s41467-017-00753-8

Matzov, D., Bashan, A., Yap, M. F., & Yonath, A. (2019). Stress response as implemented by hibernating ribosomes: A structural overview. *The FEBS Journal*, *286*(18), 3558–3565. https://doi.org/10.1111/febs.14968

Mayerle, M., & Woodson, S. A. (2013). Specific contacts between protein S4 and ribosomal RNA are required at multiple stages of ribosome assembly. *RNA*, *19*(4), 574–585. https://doi.org/10.1261/rna.037028.112

McGee, D. J., Langford, M. L., Watson, E. L., Carter, J. E., Chen, Y.-T., & Ottemann, K. M. (2005). Colonization and Inflammation Deficiencies in Mongolian Gerbils Infected by *Helicobacter pylori* Chemotaxis Mutants. *Infection and Immunity*, *73*(3), 1820–1827. https://doi.org/10.1128/IAI.73.3.1820-1827.2005

McKay, S. L., & Portnoy, D. A. (2015). Ribosome Hibernation Facilitates Tolerance of Stationary-Phase Bacteria to Aminoglycosides. *Antimicrobial Agents and Chemotherapy*, *59*(11), 6992–6999. https://doi.org/10.1128/AAC.01532-15

McLaren, M., Conners, R., Isupov, M. N., Gil-Díez, P., Gambelli, L., Gold, V. A. M., Walter, A., Connell, S. R., Williams, B., & Daum, B. (2023). CryoEM reveals that ribosomes in microsporidian spores are locked in a dimeric hibernating state. *Nature Microbiology*, *8*(10), 1834–1845. https://doi.org/10.1038/s41564-023-01469-w

Menbari, S., Shahsavar, S. K., Keikha, M., & Karbalaei, M. (2025). Global Profile of Drug Resistance Related to *Helicobacter pylori* Infection in Children: A

Systematic Review and Meta-Analysis. *Health Science Reports*, *8*(9), e71238. https://doi.org/10.1002/hsr2.71238

Mikamo, H., Yuasa, A., Wada, K., Crawford, B., & Sugimoto, N. (2016). Optimal Treatment for Complicated Intra-abdominal Infections in the Era of Antibiotic Resistance: A Systematic Review and Meta-Analysis of the Efficacy and Safety of Combined Therapy With Metronidazole. *Open Forum Infectious Diseases*, *3*(3), ofw143. https://doi.org/10.1093/ofid/ofw143

Milon, P., Carotti, M., Konevega, A. L., Wintermeyer, W., Rodnina, M. V., & Gualerzi, C. O. (2010). The ribosome-bound initiation factor 2 recruits initiator tRNA to the 30S initiation complex. *EMBO Reports*, *11*(4), 312–316. https://doi.org/10.1038/embor.2010.12

Mishra, S., Ahmed, T., Tyagi, A., Shi, J., & Bhushan, S. (2018). Structures of Mycobacterium smegmatis 70S ribosomes in complex with HPF, tmRNA, and P-tRNA. *Scientific Reports*, *8*(1), 13587. https://doi.org/10.1038/s41598-018-31850-3

Moore, R. A., & Carr, C. E. (2022). Snyder and Champness Molecular Genetics of Bacteria, 5th Edition. *Emerging Infectious Diseases*, *28*(1), 266–266. https://doi.org/10.3201/eid2801.211628

Mouery, K., Rader, B. A., Gaynor, E. C., & Guillemin, K. (2006). The Stringent Response Is Required for *Helicobacter pylori* Survival of Stationary Phase, Exposure to Acid, and Aerobic Shock. *Journal of Bacteriology*, *188*(15), 5494–5500. https://doi.org/10.1128/JB.00366-06

Mu, T., Lu, Z.-M., Wang, W.-W., Feng, H., Jin, Y., Ding, Q., & Wang, L.-F. (2023). *Helicobacter pylori* intragastric colonization and migration: Endoscopic manifestations and potential mechanisms. *World Journal of Gastroenterology*, *29*(30), 4616–4627. https://doi.org/10.3748/wjg.v29.i30.4616

Nakamoto, J. A., Evangelista, W., Vinogradova, D. S., Konevega, A. L., Spurio, R., Fabbretti, A., & Milón, P. (2021). The dynamic cycle of bacterial translation initiation factor IF3. *Nucleic Acids Research*, *49*(12), 6958–6970. https://doi.org/10.1093/nar/gkab522

Navarro Llorens, J. M., Tormo, A., & Martínez-García, E. (2010). Stationary phase in gram-negative bacteria. *FEMS Microbiology Reviews*, *34*(4), 476–495. https://doi.org/10.1111/j.1574-6976.2010.00213.x

Nevskaya, N., Tishchenko, S., Volchkov, S., Kljashtorny, V., Nikonova, E., Nikonov, O., Nikulin, A., Köhrer, C., Piendl, W., Zimmermann, R., Stockley, P., Garber, M., & Nikonov, S. (2006). New Insights into the Interaction of Ribosomal Protein L1 with RNA. *Journal of Molecular Biology*, *355*(4), 747–759. https://doi.org/10.1016/j.jmb.2005.10.084

Nezami, B. G., Jani, M., Alouani, D., Rhoads, D. D., & Sadri, N. (2019). Helicobacter pylori Mutations Detected by Next-Generation Sequencing in Formalin-Fixed, Paraffin-Embedded Gastric Biopsy Specimens Are Associated with Treatment Failure. *Journal of Clinical Microbiology*, *57*(7), e01834-18. https://doi.org/10.1128/JCM.01834-18

Nguyen, T. T. H., Chen, P.-C., Wang, P.-C., Wang, W.-H., Lan, C.-Y., Backert, S., & Kao, M.-C. (2025). Roles of the lipopolysaccharide biosynthesis-related gene *HP0858* in the fitness of *Helicobacter pylori* and its virulence in *Galleria mellonella*. *Virulence*, *16*(1), 2548620. https://doi.org/10.1080/21505594.2025.2548620

Ngwaga, T., Chauhan, D., Salberg, A. G., & Shames, S. R. (2023). Effector-mediated subversion of proteasome activator (PA)28αβ enhances host defense against Legionella pneumophila under inflammatory and oxidative stress conditions. *PLOS Pathogens*, *19*(6), e1011473. https://doi.org/10.1371/journal.ppat.1011473

Nierhaus, K. H. (1991). The assembly of prokaryotic ribosomes. *Biochimie*, *73*(6), 739–755. https://doi.org/10.1016/0300-9084(91)90054-5

Nikolay, R., Hilal, T., Schmidt, S., Qin, B., Schwefel, D., Vieira-Vieira, C. H., Mielke, T., Bürger, J., Loerke, J., Amikura, K., Flügel, T., Ueda, T., Selbach, M., Deuerling, E., & Spahn, C. M. T. (2021). Snapshots of native pre-50S ribosomes reveal a biogenesis factor network and evolutionary specialization. *Molecular Cell*, *81*(6), 1200-1215.e9. https://doi.org/10.1016/j.molcel.2021.02.006

Njenga, R. K., Boele, J., Drepper, F., Sinha, K., Marouda, E., Huesgen, P. F., Blaby-Haas, C., & Koch, H.-G. (2024). Ribosome-inactivation by a class of widely distributed C-tail anchored membrane proteins. *Structure*, *32*(12), 2259-2275.e6. https://doi.org/10.1016/j.str.2024.09.019

Noto, J. M., & Peek, R. M. (2012). Genetic Manipulation of a Naturally Competent Bacterium, Helicobacter pylori. In J. Houghton (Ed.), *Helicobacter Species* (Vol. 921, pp. 51–59). Humana Press. https://doi.org/10.1007/978-1-62703-005-2_8

Novák, J., Jurnečka, D., Linhartová, I., Holubová, J., Staněk, O., Štipl, D., Dienstbier, A., Večerek, B., Azevedo, N., Provazník, J., Beneš, V., & Šebo, P. (2020). A Mutation Upstream of the *rplN-rpsD* Ribosomal Operon Downregulates Bordetella pertussis Virulence Factor Production without Compromising Bacterial Survival within Human Macrophages. *mSystems*, *5*(6), e00612-20. https://doi.org/10.1128/mSystems.00612-20

Oktem-Okullu, S., Tiftikci, A., Saruc, M., Cicek, B., Vardareli, E., Tozun, N., Kocagoz, T., Sezerman, U., Yavuz, A. S., & Sayi-Yazgan, A. (2015). Multiplex-PCR-Based Screening and Computational Modeling of Virulence Factors and T-Cell Mediated Immunity in Helicobacter pylori Infections for Accurate Clinical Diagnosis. *PLOS ONE*, *10*(8), e0136212. https://doi.org/10.1371/journal.pone.0136212

Olekhnovich, I. N., Goodwin, A., & Hoffman, P. S. (2009). Characterization of the NAD(P)H oxidase and metronidazole reductase activities of the RdxA nitroreductase of *Helicobacter pylori*. *The FEBS Journal*, *276*(12), 3354–3364. https://doi.org/10.1111/j.1742-4658.2009.07060.x

Onderdonk, A. B., Louie, T. J., Tally, F. P., & Bartlett, J. G. (1979). Activity of metronidazole against *Escherichia coli* in experimental infra-abdominal

sepsis. *Journal of Antimicrobial Chemotherapy*, *5*(2), 201–210. https://doi.org/10.1093/jac/5.2.201

O'Toole, P. W., Lane, M. C., & Porwollik, S. (2000). Helicobacter pylori motility. *Microbes and Infection*.

Pal, P., Khan, M. Y., Sharma, S., Kumar, Y., Mangla, N., Kaushal, P. S., & Agarwal, N. (2023). ResR/McdR-regulated protein translation machinery contributes to drug resilience in Mycobacterium tuberculosis. *Communications Biology*, *6*(1), 708. https://doi.org/10.1038/s42003-023-05059-8

Park, J. Y., Georges, D., Alberts, C. J., Bray, F., Clifford, G., & Baussano, I. (2025). Global lifetime estimates of expected and preventable gastric cancers across 185 countries. *Nature Medicine*, *31*(9), 3020–3027. https://doi.org/10.1038/s41591-025-03793-6

Parrish, J. R., Yu, J., Liu, G., Hines, J. A., Chan, J. E., Mangiola, B. A., Zhang, H., Pacifico, S., Fotouhi, F., DiRita, V. J., Ideker, T., Andrews, P., & Finley, R. L. (2007). A proteome-wide protein interaction map for Campylobacter jejuni. *Genome Biology*, *8*(7), R130. https://doi.org/10.1186/gb-2007-8-7-r130

Patole, S., Rout, M., & Mohapatra, H. (2021). Identification and validation of reference genes for reliable analysis of differential gene expression during antibiotic induced persister formation in Klebsiella pneumoniae using qPCR. *Journal of Microbiological Methods*, *182*, 106165. https://doi.org/10.1016/j.mimet.2021.106165

Pavlou, A., Cinquemani, E., Pinel, C., Giordano, N., Mathilde, V. M.-G., Mihalcescu, I., Geiselmann, J., & De Jong, H. (2025). Single-cell data reveal heterogeneity of investment in ribosomes across a bacterial population. *Nature Communications*, *16*(1), 285. https://doi.org/10.1038/s41467-024-55394-5

Perez Aldana, L., Kondo, T., Zheng, R., Sugiyama, T., Asaka, M., Kato, M., Nakagawa, S., & Kwon, D. H. (2005). In vitro induction of resistance to metronidazole, and analysis of mutations in rdxA and frxA genes from Helicobacter pylori isolates. *Journal of Infection and Chemotherapy*, *11*(2), 59–63. https://doi.org/10.1007/s10156-004-0370-Y

Perez-Perez, G. I., Rothenbacher, D., & Brenner, H. (2004). Epidemiology of *Helicobacter pylori* Infection. *Helicobacter*, *9*(s1), 1–6. https://doi.org/10.1111/j.1083-4389.2004.00248.x

Phuc, B. H., Tuan, V. P., Binh, T. T., Tung, P. H., Tri, T. D., Dung, H. D. Q., Thuan, N. P. M., Fauzia, K. A., Tshibangu-Kabamba, E., Alfaray, R. I., Saruuljavkhlan, B., Matsumoto, T., Akada, J., & Yamaoka, Y. (2023). Comparative genomics of two Vietnamese *Helicobacter pylori* strains, CHC155 from a non-cardia gastric cancer patient and VN1291 from a duodenal ulcer patient. *Scientific Reports*, *13*(1), 8869. https://doi.org/10.1038/s41598-023-35527-4

Piir, K., Paier, A., Liiv, A., Tenson, T., & Maiväli, Ü. (2011). Ribosome degradation in growing bacteria. *The EMBO Reports*, *12*(5), 458–462. https://doi.org/10.1038/embor.2011.47

Polikanov, Y. S., Blaha, G. M., & Steitz, T. A. (2012). How Hibernation Factors RMF, HPF, and YfiA Turn Off Protein Synthesis. *Science*, *336*(6083), 915–918. https://doi.org/10.1126/science.1218538

Pontes, M. H., Yeom, J., & Groisman, E. A. (2016). Reducing Ribosome Biosynthesis Promotes Translation during Low Mg 2+ Stress. *Molecular Cell*, *64*(3), 480–492. https://doi.org/10.1016/j.molcel.2016.05.008

Porwollik, S., Noonan, B., & O'Toole, P. W. (1999). Molecular Characterization of a Flagellar Export Locus of *Helicobacter pylori*. *Infection and Immunity*, *67*(5), 2060–2070. https://doi.org/10.1128/IAI.67.5.2060-2070.1999

Prossliner, T., Skovbo Winther, K., Sørensen, M. A., & Gerdes, K. (2018). Ribosome Hibernation. *Annual Review of Genetics*, *52*(1), 321–348. https://doi.org/10.1146/annurev-genet-120215-035130

Puri, P., Eckhardt, T. H., Franken, L. E., Fusetti, F., Stuart, M. C. A., Boekema, E. J., Kuipers, O. P., Kok, J., & Poolman, B. (2014). *L actococcus lactis* YFIA is necessary and sufficient for ribosome dimerization. *Molecular Microbiology*, *91*(2), 394–407. https://doi.org/10.1111/mmi.12468

Qin, D., & Fredrick, K. (2013). Analysis of Polysomes from Bacteria. In *Methods in Enzymology* (Vol. 530, pp. 159–172). Elsevier. https://doi.org/10.1016/B978-0-12-420037-1.00008-7

Rader, B. A., Campagna, S. R., Semmelhack, M. F., Bassler, B. L., & Guillemin, K. (2007). The Quorum-Sensing Molecule Autoinducer 2 Regulates Motility and

Flagellar Morphogenesis in *Helicobacter pylori*. *Journal of Bacteriology*, *189*(17), 6109–6117. https://doi.org/10.1128/JB.00246-07

Rafil, F., Franklin, W., Heflich, R. H., & Cerniglia, C. E. (1991). Reduction of nitroaromatic compounds by anaerobic bacteria isolated from the human gastrointestinal tract. *Applied and Environmental Microbiology*, *57*(4), 962–968. https://doi.org/10.1128/aem.57.4.962-968.1991

Reier, K., Liiv, A., & Remme, J. (2023). Ribosome Protein Composition Mediates Translation during the Escherichia coli Stationary Phase. *International Journal of Molecular Sciences*, *24*(4), 3128. https://doi.org/10.3390/ijms24043128

Reshetnyak, V. I., & Reshetnyak, T. M. (2017a). Significance of dormant forms of *Helicobacter pylori* in ulcerogenesis. *World Journal of Gastroenterology*, *23*(27), 4867. https://doi.org/10.3748/wjg.v23.i27.4867

Reshetnyak, V. I., & Reshetnyak, T. M. (2017b). Significance of dormant forms of *Helicobacter pylori* in ulcerogenesis. *World Journal of Gastroenterology*, *23*(27), 4867. https://doi.org/10.3748/wjg.v23.i27.4867

Rhen, M., Eriksson, S., Clements, M., Bergström, S., & Normark, S. J. (2003). The basis of persistent bacterial infections. *Trends in Microbiology*, *11*(2), 80–86. https://doi.org/10.1016/S0966-842X(02)00038-0

Ribardo, D. A., Bingham-Ramos, L. K., & Hendrixson, D. R. (2010). Functional Analysis of the RdxA and RdxB Nitroreductases of *Campylobacter jejuni*

Reveals that Mutations in *rdxA* Confer Metronidazole Resistance. *Journal of Bacteriology*, *192*(7), 1890–1901. https://doi.org/10.1128/JB.01638-09

Rittershaus, E. S. C., Baek, S.-H., & Sassetti, C. M. (2013). The Normalcy of Dormancy: Common Themes in Microbial Quiescence. *Cell Host & Microbe*, *13*(6), 643–651. https://doi.org/10.1016/j.chom.2013.05.012

Rocha, G. R., Lemos, F. F. B., Silva, L. G. D. O., Luz, M. S., Correa Santos, G. L., Rocha Pinheiro, S. L., Calmon, M. S., & De Melo, F. F. (2025). Overcoming antibiotic-resistant *Helicobacter pylori* infection: Current challenges and emerging approaches. *World Journal of Gastroenterology*, *31*(10). https://doi.org/10.3748/wjg.v31.i10.102289

Rodnina, M. V. (2018). Translation in Prokaryotes. *Cold Spring Harbor Perspectives in Biology*, *10*(9), a032664. https://doi.org/10.1101/cshperspect.a032664

Rowe, D. C. D., & Summers, D. K. (1999). The Quiescent-Cell Expression System for Protein Synthesis in *Escherichia coli*. *Applied and Environmental Microbiology*, *65*(6), 2710–2715. https://doi.org/10.1128/AEM.65.6.2710-2715.1999

Russo, S., Luján, A. P., Fraaije, M. W., & Poelarends, G. J. (2025). Flavin-Dependent Nitroreductases: Privileged Enzymes for Chemical and Photochemical Synthesis. *ChemCatChem*, *17*(5), e202401304. https://doi.org/10.1002/cctc.202401304

Sagoo, J., Abedrabbo, S., Liu, X., & Ottemann, K. M. (2024). *Helicobacter pylori cheV1* mutants recover semisolid agar migration due to loss of a previously

uncharacterized Type IV filament membrane alignment complex homolog. *Journal of Bacteriology*, *206*(4), e00406-23. https://doi.org/10.1128/jb.00406-23

Sakamoto, K. (2012). The Pathology of *Mycobacterium tuberculosis* Infection. *Veterinary Pathology*, *49*(3), 423–439. https://doi.org/10.1177/0300985811429313

Samatova, E., Daberger, J., Liutkute, M., & Rodnina, M. V. (2021). Translational Control by Ribosome Pausing in Bacteria: How a Non-uniform Pace of Translation Affects Protein Production and Folding. *Frontiers in Microbiology*, *11*, 619430. https://doi.org/10.3389/fmicb.2020.619430

Saracino, I. M., Fiorini, G., Zullo, A., Pavoni, M., Saccomanno, L., & Vaira, D. (2020). Trends in Primary Antibiotic Resistance in H. pylori Strains Isolated in Italy between 2009 and 2019. *Antibiotics*, *9*(1), 26. https://doi.org/10.3390/antibiotics9010026

Sasichai Kangsadalampai. (2021). Expression of Helicobacter pyloriVirulence Genesunder Atmospheric Condition. *Science & Technology Asia*, *26*, 210219. https://doi.org/10.14456/SCITECHASIA.2021.40

Sause, W. E., Castillo, A. R., & Ottemann, K. M. (2012). The Helicobacter pylori Autotransporter ImaA (HP0289) Modulates the Immune Response and Contributes to Host Colonization. *Infection and Immunity*, *80*(7), 2286–2296. https://doi.org/10.1128/IAI.00312-12

Sawyer, E. B., Phelan, J. E., Clark, T. G., & Cortes, T. (2021). A snapshot of translation in Mycobacterium tuberculosis during exponential growth and nutrient starvation revealed by ribosome profiling. *Cell Reports*, *34*(5), 108695. https://doi.org/10.1016/j.celrep.2021.108695

Schmeing, T. M., & Ramakrishnan, V. (2009). What recent ribosome structures have revealed about the mechanism of translation. *Nature*, *461*(7268), 1234–1242. https://doi.org/10.1038/nature08403

Schmid, C., Trinkler, S. N., Vittori, E. T., Oborská-Oplová, M., Panse, V. G., & Hilbi, H. (2026). Regulation of ribosome hibernation controls *Legionella* survival, infection, antibiotic tolerance, and phenotypic heterogeneity. *mBio*, *17*(3), e03762-25. https://doi.org/10.1128/mbio.03762-25

Schoenfeld, D. P. (2024). ACG Guideline on Treatment of *Helicobacter pylori*: New Recommendations... Will Practice Change? *American College of Gastroenterology*.

Schoenhofen, I. C., Lunin, V. V., Julien, J.-P., Li, Y., Ajamian, E., Matte, A., Cygler, M., Brisson, J.-R., Aubry, A., Logan, S. M., Bhatia, S., Wakarchuk, W. W., & Young, N. M. (2006). Structural and Functional Characterization of PseC, an Aminotransferase Involved in the Biosynthesis of Pseudaminic Acid, an Essential Flagellar Modification in Helicobacter pylori. *Journal of Biological Chemistry*, *281*(13), 8907–8916. https://doi.org/10.1074/jbc.M512987200

Schulz, C., Liou, J.-M., Alboraie, M., Bornschein, J., Campos Nunez, C., Coelho, L. G., Quach, D. T., Fallone, C. A., Chen, Y.-C., Gerhard, M., Gisbert, J. P., Jung,

H.-Y., Katelaris, P. H., Kim, J. G., Lu, H., Macke, L., Mahachai, V., Moss, S. F., Remes Troche, J. M., … Malfertheiner, P. (2025). *Helicobacter pylori* antibiotic resistance: A global challenge in search of solutions. *Gut*, *74*(10), 1561–1570. https://doi.org/10.1136/gutjnl-2025-335523

Schwarz, A., Mueller, M., Will, H., Dietrich, L., Giandomenico, S. L., Tushev, G., Bartnik, I., Khusainov, I., Fusco, C. M., & Schuman, E. M. (2026). Ribosomal RNA expansion segments mediate the oligomerization of inactive animal ribosomes. *Science*, *391*(6787), eadr4287. https://doi.org/10.1126/science.adr4287

Secka, O., Berg, D. E., Antonio, M., Corrah, T., Tapgun, M., Walton, R., Thomas, V., Galano, J. J., Sancho, J., Adegbola, R. A., & Thomas, J. E. (2013). Antimicrobial Susceptibility and Resistance Patterns among Helicobacter pylori Strains from The Gambia, West Africa. *Antimicrobial Agents and Chemotherapy*, *57*(3), 1231–1237. https://doi.org/10.1128/AAC.00517-12

Seffouh, A., Nikolay, R., & Ortega, J. (2024). Critical steps in the assembly process of the bacterial 50S ribosomal subunit. *Nucleic Acids Research*, *52*(8), 4111–4123. https://doi.org/10.1093/nar/gkae199

Serena, P., Mare, R., Miutescu, B., Bende, R., Popa, A., Aragona, G., Seclăman, E., Serena, L., Barbulescu, A., & Sirli, R. (2025). Resistance to Clarithromycin and Fluoroquinolones in Helicobacter pylori Isolates: A Prospective Molecular Analysis in Western Romania. *Antibiotics*, *14*(12), 1223. https://doi.org/10.3390/antibiotics14121223

Sergeeva, O. V., Prokhorova, I. V., Ordabaev, Y., Tsvetkov, P. O., Sergiev, P. V., Bogdanov, A. A., Makarov, A. A., & Dontsova, O. A. (2012). Properties of small rRNA methyltransferase RsmD: Mutational and kinetic study. *RNA*, *18*(6), 1178–1185. https://doi.org/10.1261/rna.032763.112

Shah, S. C., Iyer, P. G., & Moss, S. F. (2021). AGA Clinical Practice Update on the Management of Refractory Helicobacter pylori Infection: Expert Review. *Gastroenterology*, *160*(5), 1831–1841. https://doi.org/10.1053/j.gastro.2020.11.059

Sharma, C. M., Hoffmann, S., Darfeuille, F., Reignier, J., Findeiß, S., Sittka, A., Chabas, S., Reiche, K., Hackermüller, J., Reinhardt, R., Stadler, P. F., & Vogel, J. (2010). The primary transcriptome of the major human pathogen Helicobacter pylori. *Nature*, *464*(7286), 250–255. https://doi.org/10.1038/nature08756

Shih, C.-A., Shie, C.-B., Tai, W.-C., Chuah, S.-K., Lee, H.-C., & Hsu, P.-I. (2023). Update on the second-line treatment of *Helicobacter pylori* infection: A narrative review. *Therapeutic Advances in Gastroenterology*, *16*, 17562848231192750. https://doi.org/10.1177/17562848231192750

Shoji, S., Dambacher, C. M., Shajani, Z., Williamson, J. R., & Schultz, P. G. (2011). Systematic Chromosomal Deletion of Bacterial Ribosomal Protein Genes. *Journal of Molecular Biology*, *413*(4), 751–761. https://doi.org/10.1016/j.jmb.2011.09.004

Shore, D., & Albert, B. (2022). Ribosome biogenesis and the cellular energy economy. *Current Biology*, *32*(12), R611–R617. https://doi.org/10.1016/j.cub.2022.04.083

Sisson, G., Jeong, J.-Y., Goodwin, A., Bryden, L., Rossler, N., Lim-Morrison, S., Raudonikiene, A., Berg, D. E., & Hoffman, P. S. (2000). Metronidazole Activation Is Mutagenic and Causes DNA Fragmentation in *Helicobacter pylori* and in *Escherichia coli* Containing a Cloned *H. pylori rdxA*$^{+}$ (Nitroreductase) Gene. *Journal of Bacteriology*, *182*(18), 5091–5096. https://doi.org/10.1128/JB.182.18.5091-5096.2000

Smeets, L. C., Bijlsma, J. J. E., Boomkens, S. Y., Vandenbroucke-Grauls, C. M. J. E., & Kusters, J. G. (2000). *comH* , a Novel Gene Essential for Natural Transformation of *Helicobacter pylori*. *Journal of Bacteriology*, *182*(14), 3948–3954. https://doi.org/10.1128/JB.182.14.3948-3954.2000

Smith, M. A., & Edwards, D. I. (1995). The influence of microaerophilia and anaerobiosis on metronidazole uptake in *Helicobacter pylori*. *Journal of Antimicrobial Chemotherapy*, *36*(3), 453–461. https://doi.org/10.1093/jac/36.3.453

Snider, J., & Houry, W. A. (2006). MoxR AAA+ ATPases: A novel family of molecular chaperones? *Journal of Structural Biology*, *156*(1), 200–209. https://doi.org/10.1016/j.jsb.2006.02.009

Song, S., & Wood, T. K. (2020). ppGpp ribosome dimerization model for bacterial persister formation and resuscitation. *Biochemical and Biophysical Research Communications*, *523*(2), 281–286. https://doi.org/10.1016/j.bbrc.2020.01.102

Spížek, J., & Řezanka, T. (2017). Lincosamides: Chemical structure, biosynthesis, mechanism of action, resistance, and applications. *Biochemical Pharmacology*, *133*, 20–28. https://doi.org/10.1016/j.bcp.2016.12.001

Starosta, A. L., Lassak, J., Jung, K., & Wilson, D. N. (2014). The bacterial translation stress response. *FEMS Microbiology Reviews*, *38*(6), 1172–1201. https://doi.org/10.1111/1574-6976.12083

Subsomwong, P., Doohan, D., Fauzia, K. A., Akada, J., Matsumoto, T., Yee, T. T., Htet, K., Waskito, L. A., Tuan, V. P., Uchida, T., Matsuhisa, T., & Yamaoka, Y. (2022). Next-Generation Sequencing-Based Study of *Helicobacter pylori* Isolates from Myanmar and Their Susceptibility to Antibiotics. *Microorganisms*, *10*(1), 196. https://doi.org/10.3390/microorganisms10010196

Suerbaum, S., & Ailloud, F. (2023). Genome and population dynamics during chronic infection with Helicobacter pylori. *Current Opinion in Immunology*, *82*, 102304. https://doi.org/10.1016/j.coi.2023.102304

Sun, Y., Zhu, M., Yue, L., & Hu, W. (2022). Multiple Bismuth Quadruple Therapy Containing Tetracyclines Combined with Other Antibiotics and Helicobacter pylori Eradication Therapy. *Journal of Clinical Medicine*, *11*(23), 7040. https://doi.org/10.3390/jcm11237040

Sycuro, L. K., Pincus, Z., Gutierrez, K. D., Biboy, J., Stern, C. A., Vollmer, W., & Salama, N. R. (2010). Peptidoglycan Crosslinking Relaxation Promotes *Helicobacter pylori's* Helical Shape and Stomach Colonization. *Cell*, *141*(5), 822–833. https://doi.org/10.1016/j.cell.2010.03.046

Talebi Bezmin Abadi, A. (2017). Strategies used by *helicobacter pylori* to establish persistent infection. *World Journal of Gastroenterology*, *23*(16), 2870. https://doi.org/10.3748/wjg.v23.i16.2870

Tanih, N. F., Ndip, L. M., & Ndip, R. N. (2011). Characterisation of the genes encoding resistance to metronidazole (*rdxA* and *frxA*) and clarithromycin (the 23S-rRNA genes) in South African isolates of *Helicobacter pylori*. *Annals of Tropical Medicine & Parasitology*, *105*(3), 251–259. https://doi.org/10.1179/136485911X12899838683485

Tankovic, J., Lamarque, D., Delchier, J.-C., Soussy, C.-J., Labigne, A., & Jenks, P. J. (2000). Frequent Association between Alteration of the *rdxA* Gene and Metronidazole Resistance in French and North African Isolates of *Helicobacter pylori*. *Antimicrobial Agents and Chemotherapy*, *44*(3), 608–613. https://doi.org/10.1128/AAC.44.3.608-613.2000

Teh, X., Khosravi, Y., Lee, W. C., Leow, A. H. R., Loke, M. F., Vadivelu, J., & Goh, K. L. (2014). Functional and Molecular Surveillance of Helicobacter pylori Antibiotic Resistance in Kuala Lumpur. *PLoS ONE*, *9*(7), e101481. https://doi.org/10.1371/journal.pone.0101481

Terry, K., Williams, S. M., Connolly, L., & Ottemann, K. M. (2005). Chemotaxis Plays Multiple Roles during *Helicobacter pylori* Animal Infection. *Infection and Immunity*, *73*(2), 803–811. https://doi.org/10.1128/IAI.73.2.803-811.2005

Thompson, L. J., Merrell, D. S., Neilan, B. A., Mitchell, H., Lee, A., & Falkow, S. (2003). Gene Expression Profiling of *Helicobacter pylori* Reveals a Growth-Phase-Dependent Switch in Virulence Gene Expression. *Infection and Immunity*, *71*(5), 2643–2655. https://doi.org/10.1128/IAI.71.5.2643-2655.2003

Tishchenko, S., Nikonova, E., Kljashtorny, V., Kostareva, O., Nevskaya, N., Piendl, W., Davydova, N., Streltsov, V., Garber, M., & Nikonov, S. (2007). Domain I of ribosomal protein L1 is sufficient for specific RNA binding. *Nucleic Acids Research*, *35*(21), 7389–7395. https://doi.org/10.1093/nar/gkm898

Tissieres, A. (1958). *Ribonucleoprotein particles from* Escherichia coli.

Tittsler, R. P., & Sandholzer, L. A. (1936). The Use of Semi-solid Agar for the Detection of Bacterial Motility. *Journal of Bacteriology*, *31*(6), 575–580. https://doi.org/10.1128/jb.31.6.575-580.1936

Tobin, C., Mandava, C. S., Ehrenberg, M., Andersson, D. I., & Sanyal, S. (2010). Ribosomes Lacking Protein S20 Are Defective in mRNA Binding and Subunit Association. *Journal of Molecular Biology*, *397*(3), 767–776. https://doi.org/10.1016/j.jmb.2010.02.004

Tollerson, R., & Ibba, M. (2020). Translational regulation of environmental adaptation in bacteria. *Journal of Biological Chemistry*, *295*(30), 10434–10445. https://doi.org/10.1074/jbc.REV120.012742

Tomb, J.-F., White, O., Kerlavage, A. R., Clayton, R. A., Sutton, G. G., Fleischmann, R. D., Ketchum, K. A., Klenk, H. P., Gill, S., Dougherty, B. A., Nelson, K., Quackenbush, J., Zhou, L., Kirkness, E. F., Peterson, S., Loftus, B., Richardson, D., Dodson, R., Khalak, H. G., … Venter, J. C. (1997). The complete genome sequence of the gastric pathogen Helicobacter pylori. *Nature*, *388*(6642), 539–547. https://doi.org/10.1038/41483

Tong, C., Liang, Y., Zhang, Z., Wang, S., Zheng, X., Liu, Q., & Song, B. (2023). Review of knockout technology approaches in bacterial drug resistance research. *PeerJ*, *11*, e15790. https://doi.org/10.7717/peerj.15790

Tsai, A., Petrov, A., Marshall, R. A., Korlach, J., Uemura, S., & Puglisi, J. D. (2012). Heterogeneous pathways and timing of factor departure during translation initiation. *Nature*, *487*(7407), 390–393. https://doi.org/10.1038/nature11172

Tuchscherr, L., & Löffler, B. (2016). *Staphylococcus aureus* dynamically adapts global regulators and virulence factor expression in the course from acute to chronic infection. *Current Genetics*, *62*(1), 15–17. https://doi.org/10.1007/s00294-015-0503-0

Ueta, M., Ohniwa, R. L., Yoshida, H., Maki, Y., Wada, C., & Wada, A. (2008). Role of HPF (Hibernation Promoting Factor) in Translational Activity in

Escherichia coli. *The Journal of Biochemistry*, *143*(3), 425–433. https://doi.org/10.1093/jb/mvm243

Ueta, M., Wada, C., Daifuku, T., Sako, Y., Bessho, Y., Kitamura, A., Ohniwa, R. L., Morikawa, K., Yoshida, H., Kato, T., Miyata, T., Namba, K., & Wada, A. (2013). Conservation of two distinct types of 100 S ribosome in bacteria. *Genes to Cells*, *18*(7), 554–574. https://doi.org/10.1111/gtc.12057

Ueta, M., Wada, C., & Wada, A. (2010). Formation of 100S ribosomes in *Staphylococcus aureus* by the hibernation promoting factor homolog *Sa* HPF. *Genes to Cells*, *15*(1), 43–58. https://doi.org/10.1111/j.1365-2443.2009.01364.x

Vakil, N., Lanza, F., Schwartz, H., & Barth, J. (2004). Seven-day therapy for *Helicobacter pylori* in the United States. *Alimentary Pharmacology & Therapeutics*, *20*(1), 99–107. https://doi.org/10.1111/j.1365-2036.2004.02029.x

Valada, P., Mata, A., Brito, R. M. M., Gonçalves, T., Medeiros, J. A., & Nogueira, C. (2025). Detection of *Helicobacter pylori* and the Genotypes of Resistance to Clarithromycin, Fluoroquinolones, and Metronidazole in Gastric Biopsies: An In Silico Analysis to Help Understand Antibiotic Resistance. *Current Issues in Molecular Biology*, *47*(3), 187. https://doi.org/10.3390/cimb47030187

Valiauga, B., Bagdžiūnas, G., Sharrock, A. V., Ackerley, D. F., & Čėnas, N. (2024). The Catalysis Mechanism of E. coli Nitroreductase A, a Candidate for Gene-Directed Prodrug Therapy: Potentiometric and Substrate Specificity Studies.

International Journal of Molecular Sciences, *25*(8), 4413. https://doi.org/10.3390/ijms25084413

VanNice, J., Gregory, S. T., Kamath, D., & O'Connor, M. (2016). Alterations in ribosomal protein L19 that decrease the fidelity of translation. *Biochimie*, *128–129*, 122–126. https://doi.org/10.1016/j.biochi.2016.07.015

Viasus, D., Gaia, V., Manzur-Barbur, C., & Carratalà, J. (2022). Legionnaires' Disease: Update on Diagnosis and Treatment. *Infectious Diseases and Therapy*, *11*(3), 973–986. https://doi.org/10.1007/s40121-022-00635-7

Wada, A. (1998). Growth phase coupled modulation of *Escherichia coli* ribosomes. *Genes to Cells*, *3*(4), 203–208. https://doi.org/10.1046/j.1365-2443.1998.00187.x

Wada, A., Mikkola, R., Kurland, C. G., & Ishihama, A. (2000). Growth Phase-Coupled Changes of the Ribosome Profile in Natural Isolates and Laboratory Strains of *Escherichia coli*. *Journal of Bacteriology*, *182*(10), 2893–2899. https://doi.org/10.1128/JB.182.10.2893-2899.2000

Wada, A., Yamazaki, Y., Fujita, N., & Ishihama, A. (1990). Structure and probable genetic location of a "ribosome modulation factor" associated with 100S ribosomes in stationary-phase Escherichia coli cells. *Proceedings of the National Academy of Sciences*, *87*(7), 2657–2661. https://doi.org/10.1073/pnas.87.7.2657

Wang, G., Lo, L. F., & Maier, R. J. (2012). A histone-like protein of *Helicobacter pylori* protects DNA from stress damage and aids host colonization. *DNA Repair*, *11*(9), 733–740. https://doi.org/10.1016/j.dnarep.2012.06.006

Wang, X., Xu, W., Yao, F., Liu, S., Zhang, Y., Sourjik, V., & Bi, S. (2025). Discovery of an indole-sensing chemoreceptor in *Helicobacter pylori*. *Current Biology*, *35*(20), 5018-5032.e6. https://doi.org/10.1016/j.cub.2025.09.021

Wells, D. H., & Gaynor, E. C. (2006). *Helicobacter pylori* Initiates the Stringent Response upon Nutrient and pH Downshift. *Journal of Bacteriology*, *188*(10), 3726–3729. https://doi.org/10.1128/JB.188.10.3726-3729.2006

Wen, S., Velin, D., Felley, C. P., Du, L., Michetti, P., & Pan-Hammarström, Q. (2007). Expression of *Helicobacter pylori* Virulence Factors and Associated Expression Profiles of Inflammatory Genes in the Human Gastric Mucosa. *Infection and Immunity*, *75*(11), 5118–5126. https://doi.org/10.1128/IAI.00334-07

WHO Bacterial Priority Pathogens List 2024: Bacterial Pathogens of Public Health Importance, to Guide Research, Development, and Strategies to Prevent and Control Antimicrobial Resistance (1st ed). (2024). World Health Organization.

Williams, M. L., & Ghanem, M. (2022). Evaluation of candidate reference genes stability for gene expression analysis by reverse transcription qPCR in Clostridium perfringens. *Scientific Reports*, *12*(1), 19434. https://doi.org/10.1038/s41598-022-23804-7

Williamson, J. R. (2008). Biophysical studies of bacterial ribosome assembly. *Current Opinion in Structural Biology*, *18*(3), 299–304. https://doi.org/10.1016/j.sbi.2008.05.001

Williamson, K. S., Richards, L. A., Perez-Osorio, A. C., Pitts, B., McInnerney, K., Stewart, P. S., & Franklin, M. J. (2012). Heterogeneity in *Pseudomonas aeruginosa* Biofilms Includes Expression of Ribosome Hibernation Factors in the Antibiotic-Tolerant Subpopulation and Hypoxia-Induced Stress Response in the Metabolically Active Population. *Journal of Bacteriology*, *194*(8), 2062–2073. https://doi.org/10.1128/JB.00022-12

Willumeit, R., Forthmann, S., Beckmann, J., Diedrich, G., Ratering, R., Stuhrmann, H. B., & Nierhaus, K. H. (2001). Localization of the protein L2 in the 50 S subunit and the 70 S E. coli ribosome. *Journal of Molecular Biology*, *305*(1), 167–177. https://doi.org/10.1006/jmbi.2000.4289

Windham, I. H., Servetas, S. L., Whitmire, J. M., Pletzer, D., Hancock, R. E. W., & Merrell, D. S. (2018). Helicobacter pylori Biofilm Formation Is Differentially Affected by Common Culture Conditions, and Proteins Play a Central Role in the Biofilm Matrix. *Applied and Environmental Microbiology*, *84*(14), e00391-18. https://doi.org/10.1128/AEM.00391-18

Wroblewski, L. E., & Peek, R. M. (2013). *Helicobacter pylori* in Gastric Carcinogenesis. *Gastroenterology Clinics of North America*, *42*(2), 285–298. https://doi.org/10.1016/j.gtc.2013.01.006

Wroblewski, L. E., Peek, R. M., & Wilson, K. T. (2010). *Helicobacter pylori* and Gastric Cancer: Factors That Modulate Disease Risk. *Clinical Microbiology Reviews*, *23*(4), 713–739. https://doi.org/10.1128/CMR.00011-10

Wu, J. Y., Kim, J. J., Reddy, R., Wang, W. M., Graham, D. Y., & Kwon, D. H. (2005). Tetracycline-Resistant Clinical *Helicobacter pylori* Isolates with and without Mutations in 16S rRNA-Encoding Genes. *Antimicrobial Agents and Chemotherapy*, *49*(2), 578–583. https://doi.org/10.1128/AAC.49.2.578-583.2005

Wu, W., Yang, Y., & Sun, G. (2012). Recent Insights into Antibiotic Resistance in *Helicobacter pylori* Eradication. *Gastroenterology Research and Practice*, *2012*, 1–8. https://doi.org/10.1155/2012/723183

Xia, H. H.-X. (1999). Clarithromycin resistance in *Helicobacter pylori* and its clinical relevance. *World Journal of Gastroenterology*, *5*(3), 263. https://doi.org/10.3748/wjg.v5.i3.263

Yamagishi, M., Matsushima, H., Wada, A., Sakagami, M., Fujita, N., & Ishihama, A. (1993). Regulation of the Escherichia coli rmf gene encoding the ribosome modulation factor: Growth phase- and growth rate-dependent control. *The EMBO Journal*, *12*(2), 625–630. https://doi.org/10.1002/j.1460-2075.1993.tb05695.x

Yang, J., Wang, M., Wang, Y., Qiang, R., Jin, Q., Zhao, C., Chen, Q., Han, M., Ma, X., & Zhang, H. (2025). Roles of Pho regulon in bacterial pathogenicity. *Virulence*, *16*(1), 2545559. https://doi.org/10.1080/21505594.2025.2545559

Yoshida, H., Nakayama, H., Maki, Y., Ueta, M., Wada, C., & Wada, A. (2021). Functional Sites of Ribosome Modulation Factor (RMF) Involved in the Formation of 100S Ribosome. *Frontiers in Molecular Biosciences*, *8*, 661691. https://doi.org/10.3389/fmolb.2021.661691

Yoshida, H., & Wada, A. (2014). The 100S ribosome: Ribosomal hibernation induced by stress. *WIREs RNA*, *5*(5), 723–732. https://doi.org/10.1002/wrna.1242

You, S., Li, J., Chua, E. G., Tay, A., Benghezal, M., Marshall, B., Tang, H., & Li, H. (2025). Helicobacter pylori outer membrane protein families and related pathogenesis. *Microbial Pathogenesis*, *206*, 107740. https://doi.org/10.1016/j.micpath.2025.107740

Young, D., Hussell, T., & Dougan, G. (2002). Chronic bacterial infections: Living with unwanted guests. *Nature Immunology*, *3*(11), 1026–1032. https://doi.org/10.1038/ni1102-1026

Yu, T., & Zeng, F. (2024). Chloramphenicol Interferes with 50S Ribosomal Subunit Maturation via Direct and Indirect Mechanisms. *Biomolecules*, *14*(10), 1225. https://doi.org/10.3390/biom14101225

Zavialov, A. V., Hauryliuk, V. V., & Ehrenberg, M. (2005). Splitting of the Posttermination Ribosome into Subunits by the Concerted Action of RRF and EF-G. *Molecular Cell*, *18*(6), 675–686. https://doi.org/10.1016/j.molcel.2005.05.016

Zegarra, V., Bedrunka, P., Bange, G., & Czech, L. (2023). How to save a bacterial ribosome in times of stress. *Seminars in Cell & Developmental Biology*, *136*, 3–12. https://doi.org/10.1016/j.semcdb.2022.03.015

Zhang, S., Wang, X., Wise, M. J., He, Y., Chen, H., Liu, A., Huang, H., Young, S., Tay, C. Y., Marshall, B. J., Li, X., & Chua, E. G. (2020). Mutations of *Helicobacter pylori* RdxA are mainly related to the phylogenetic origin of the strain and not to metronidazole resistance. *Journal of Antimicrobial Chemotherapy*, *75*(11), 3152–3155. https://doi.org/10.1093/jac/dkaa302

Zhang, Y., Mandava, C. S., Cao, W., Li, X., Zhang, D., Li, N., Zhang, Y., Zhang, X., Qin, Y., Mi, K., Lei, J., Sanyal, S., & Gao, N. (2015). HflX is a ribosome-splitting factor rescuing stalled ribosomes under stress conditions. *Nature Structural & Molecular Biology*, *22*(11), 906–913. https://doi.org/10.1038/nsmb.3103

Zhou, D., Tanzawa, T., Lin, J., & Gagnon, M. G. (2020). Structural basis for ribosome recycling by RRF and tRNA. *Nature Structural & Molecular Biology*, *27*(1), 25–32. https://doi.org/10.1038/s41594-019-0350-7

Zhu, H., Zhang, H., Xu, Y., Laššáková, S., Korabečná, M., & Neužil, P. (2020). PCR Past, Present and Future. *BioTechniques*, *69*(4), 317–325. https://doi.org/10.2144/btn-2020-0057

Zimmerman, E. H., Ramsey, E. L., Hunter, K. E., Villadelgado, S. M., Phillips, C. M., Shipman, R. T., & Forsyth, M. H. (2024). The *Helicobacter pylori* methylome is acid-responsive due to regulation by the two-component system ArsRS and

the type I DNA methyltransferase HsdM1 (HP0463). *Journal of Bacteriology*, *206*(1), e00309-23. https://doi.org/10.1128/jb.00309-23

Zou, Y., Qian, X., Liu, X., Song, Y., Song, C., Wu, S., An, Y., Yuan, R., Wang, Y., & Xie, Y. (2020). The effect of antibiotic resistance on *Helicobacter pylori* eradication efficacy: A systematic review and meta-analysis. *Helicobacter*, *25*(4), e12714. https://doi.org/10.1111/hel.12714